The role of ischaemia-reperfusion injury and mitochondrial dysfunction in organ transplantation

Jack Lewis Martin

This dissertation is submitted for the degree of Doctor of Philosophy

Department of Surgery
University of Cambridge

MRC Mitochondrial Biology Unit
University of Cambridge

Magdalene College
October 2018

Declaration

This dissertation is the result of my own work and includes nothing which is the outcome of work done in collaboration except as declared in the Preface and specified in the text.

It is not substantially the same as any that I have submitted, or, is being concurrently submitted for a degree or diploma or other qualification at the University of Cambridge or any other University or similar institution except as declared in the Preface and specified in the text. I further state that no substantial part of my dissertation has already been submitted, or, is being concurrently submitted for any such degree, diploma or other qualification at the University of Cambridge or any other University or similar institution except as declared in the Preface and specified in the text.

It was written in partial fulfilment of the requirements for the degree of Doctor of Philosophy during the period from October 2014 to October 2018. Information derived from other sources has been referenced accordingly.

It does not exceed the prescribed word limit for the Degree Committee.

Jack Lewis Martin

October 2018

Summary

The role of ischaemia-reperfusion injury and mitochondrial dysfunction in organ transplantation

Ischaemia and subsequent reperfusion is inherent to solid organ transplantation and contributes to tissue damage, organ dysfunction, and worse recipient outcome. Demand for organs for transplantation in the UK has led to the increasing use of 'less-than-ideal' deceased organs that are less tolerant of ischaemia or have been exposed to greater ischaemic insults. Furthermore, outcomes from clinical transplantation suggest that increasing ischaemia-reperfusion (IR) injury influences not only short-term outcomes but also longer-term outcomes by increasing the rate of chronic organ rejection. Mitochondria are recognised as being integral to IR injury generating a burst of reactive oxygen species that initiates downstream tissue damage. There is emerging evidence that this process is driven by a specific metabolic pathway rather than by a series of random damaging events. A better understanding of this pathophysiology and the mechanisms underpinning IR injury will increase the opportunity for the development of rational therapeutic approaches.

In this work, I have characterised ischaemic metabolism during warm and cold organ storage in murine, porcine and human myocardial tissue. I have demonstrated succinate accumulation to be a conserved signature of ischaemia across species and have demonstrated the ability to moderate metabolic pathways in the mouse heart during organ storage using metabolic inhibitors. In order to investigate the effects of the metabolic changes during ischaemia on reperfusion I developed a novel, small animal model of solid organ transplantation incorporating a warm ischaemic insult. I then used this model to examine the therapeutic efficacy of ameliorating succinate accumulation during ischaemia to reduce organ dysfunction upon reperfusion. Finally, I explored the impact of reperfusion injury on chronic rejection in a previously well characterised model of organ rejection.

Jack Lewis Martin

Acknowledgements

Thank you to my supervisors, Dr Kourosh Saeb-Parsy and Professor Michael Murphy. I feel very privileged to have had the opportunity to work within your outstanding laboratories. Your support, guidance and positivity has been invaluable and inspiring. You have introduced me to new opportunities and encouraged me to develop a passion for science that I hope to continue to explore in the years ahead.

To the numerous collaborators with whom I have worked during the last few years, thank you so much for your time and expertise. None of this would have been possible without you. Thank you to everyone in the Department of Surgery and the Mitochondrial Biology Unit for all your help, patience, insightful discussions, companionship, and most importantly friendship. It has been instrumental in helping me navigate this journey. I look forward with interest to hearing about your successes in the coming years.

Thank you to the staff at Central Biomedical Services past and present who provided excellent technical assistance, support and friendship during the time I spent in their department and thank you to the Medical Research Council for their generous financial support of my studies.

And finally, thank you to my family, Hannah and Matilda for their patience, unconditional love and support.

Table of Contents

Table of Figures

Abbreviations

All abbreviations and standard units, unless listed, are as described in the "Instructions to Authors" of the Biochemical journal (http://biochemj.org)

Δp	proton motive force
ADSS	adenylosuccinate synthetase
AMPK	AMP-activated protein kinases
ANA	antinuclear antibody
ANOVA	analysis of variance
AOA	2-(aminooxy)acetic acid hemichloride
APC	antigen presentation cell
AST	aspartate aminotransferase
AUC	area under the curve
BNP	brain natriuretic peptide
CAC	citric acid cycle
cAMP	cyclic adenosine monophosphate
CAV	chronic allograft vasculopathy
CD	cluster of differentiation
cGAS	cyclic GMP-AMP synthase
CIT	cold ischaemia time
CoA	Co-Enzyme A
CoQ	Co-Enzyme Q
CPB	cardiopulmonary bypass
DAMP	damage-associated molecular patterns
DBD	donation after brainstem death
DC	dendritic cell
DCD	donation after circulatory death
DD	deceased donor (cadaveric donors)
DGF	delayed graft function
DIC	dicarboxylate carrier
DMM	dimethyl malonate
DMS	dimethyl succinate
DMSO	dimethyl sulfoxide
DNA	deoxyribonucleic acid
DZX	diazoxide
ECD	extended criteria donor
ECMO	extracorporeal membrane oxygenation
ELISA	enzyme linked immunosorbent assay
ETC	electron transport chain
ETF	electron transfer flavoprotein
EVG	elastin van Gieson
Fc	fragment crystallizable region
GABA	γ-aminobutyric acid
GAPDH	glyceraldehyde-3-phopshate dehydrogenase
GLUT	facilitated diffusion glucose transporter
H&E	haematoxylin and eosin
HAD	hadacidin
HEp-2	human epithelial type 2
HIF-1α	hypoxia inducible factor 1α
HMGB1	high mobility group box 1
HLA	human leukocyte antigen
$HO^{\bullet}$	hydroxyl radical

HPLC	high pressure liquid chromatography
HSP72	heat shock protein 72
IL	interleukin
IMP	inosinic acid
IR	ischaemia-reperfusion
IRF	interferon regulatory factors
ISG	interferon stimulated genes
IVC	Inferior vena cava
LC-MS	liquid chromatography – mass spectrometry
LN_2	liquid nitrogen
MAS	malate / aspartate shuttle
MAVS	mitochondrial antiviral signaling
MDA5	melanoma differentiation antigen 5
MHC	major histocompatibility complex
MOMP	outer mitochondrial membrane
mtDNA	mitochondrial DNA
mtROS	mitochondrial reactive oxygen species
NF-κB	nuclear factor κ-light chain enhancer of activated B cells
NK	natural killer
NMP	normothermic machine perfusion
NOX	NADPH oxidase
$O^{\bullet-}$	superoxide
$ONOO^-$	peroxynitrite
OPA1	optic atrophy type 1
PAMP	pathogen-associated molecular pattern
PBS	phosphate buffered saline
PCR	polymerise chain reaction
PDH	pyruvate dehydrogenase
PFK-1	phosphofructokinase-1
PGF	primary graft failure
PNC	purine nucleotide cycle
PNF	primary non-function
PPP	pentose phosphate pathway
PRR	pattern recognition receptors
Q-site	ubiquinone binding
RET	reverse electron transport
RIG-I	retinoic acid-inducible gene-1
ROS	reactive oxygen species
ROT	rotenone
SCD	standard criteria donor
SDH	succinate dehydrogenase
SOD	superoxide dismutases
Soltran©	hyperosmolar citrate
STING	stimulator of interferon genes
SVC	superior vena cava
TCA	tricarboxylic acid
TE	Tris EDTA
Th17	T helper 17
TLR	toll-like receptor
TNF	tumour necrosis factor
Treg	regulatory T-cell
TTFA	thenoyltrifluoroacetone
UW	University of Wisconsin solution (ViaSpan®)
XD	xanthine dehydrogenase

XO	xanthine oxidase
XOR	xanthine oxidoreductase

Publications and Prizes

Publications

Martin JL, Gruszczyk AV, Beach TE, Murphy MP, Saeb-Parsy K.
Mitochondrial mechanisms and therapeutics in ischaemia reperfusion injury.
Pediatr Nephrol. 2018 Jun 2. PMID: 29860579

Bundgaard A, James AM, Gruszczyk AV, Martin J, Murphy MP, Fago A.
Metabolic adaptions during extreme anoxia in the turtle heart and their implications for ischaemia-reperfusion injury.
Sci Rep. 2019 Feb 26; 9(1): 2850. PMID 30808950

Prizes

Medawar Medal, British Transplantation Society (2018)

Finalist for Patey Prize, Society of Academic and Research Surgery (2018)

Chapter 1: Introduction

1.1 History of organ transplantation

Significant progress over the last century within the field of organ transplantation has led to it becoming a routine part of clinical practice. Nevertheless, to become the everyday success that it is today, organ transplantation has had to overcome a number of fundamental challenges. These include, developing the technical aspects in anastomosing blood vessels, adequately preserving the organs during transfer from donor to recipient, and preventing rejection of the transplanted organ by the recipient's immune system (1, 2). As clinicians continue to increase the number of lives that can be improved or saved by transplantation and the supply of organs suitable for transplantation dramatically outstrips demand, some of these fundamental problems continue to challenge in the 21st century.

1.1.1 Immunosuppression

There are occasional anecdotal reports and small cases series from attempts at solid organ transplantation dating back to the early part of the 20th century but these were largely unsuccessful with the transplanted organs either demonstrating primary non-function (PNF) or being rapidly rejected within a matter of hours. The modern era of organ transplantation began in 1954 when Joseph Murray successfully transplanted the kidney of one identical twin to another in Boston (1, 3). The transplanted kidney functioned well, and the recipient brother lived for another eight years. The success of this operation lay in the elimination of the risk of immunological rejection. Although successful, this was not an approach that would enable organ transplantation to be introduced to widespread clinical practice. Immunological rejection remained the principal hurdle in the progress of solid organ transplantation until the discovery of chemical immunosuppression, initially with azathioprine and prednisolone, and then then with the introduction of ciclosporin in the mid-1970s. The introduction of these drugs had an immediate effect on outcome and paved the way for widespread transplantation of deceased donor organs (3).

1.1.2 Organ procurement

With the introduction of effective immunosuppression and the associated improvement in outcome, the widespread use of deceased donor organs became a reality. This led to a period of renewed interest in improving organ preservation. Organ procurement is inherently associated with some degree of ischaemic damage, although the extent of this ischaemic injury is greatly dependent on the duration and the temperature of the organ when it is exposed to ischaemia. Warm ischaemia is particularly detrimental to the viability of an organ, something quickly realized during early attempts at transplantation where organs fared far better if cooled.

The concept of brainstem death has had a great impact on organ transplantation. The concept originated in France where the term *coma dépassé* was coined in 1959 by Mollaret and Goulon. A Belgian surgeon, Guy Alexandre, was the first to adopt this to perform the first organ transplant from a brain dead donor in 1963 (4). Prior to this, death in organ donors was declared by cardiopulmonary criteria. In 1968, the Harvard Committee adopted the principle that death was a matter of accepted medical practice and

therefore, patients deemed to be in a state of irreversible coma could be regarded as dead (5). Codes of Practice were introduced in the UK to provide legal and ethical guidance for brain stem death criteria in the late 1970s by the Conference of Medical Royal Colleges in 1979 (5-7). Heart beating donors, later termed donation after brainstem death (DBD) formed the mainstay of organ donors in the UK and internationally for the next two decades. In DBD, the donor continues to receive cardiorespiratory support following the declaration of death by brainstem criteria until the time of donation. At this time, the circulation is stopped by cross clamping the aorta and ice cold preservation solution is flushed through the distal aorta whilst blood is simultaneously drained from the vena cava (1). This technique of *in situ* perfusion, in addition to topical cooling, attempts to minimise 'primary' warm ischaemia during DBD organ retrieval.

The persistent shortage of donors has more recently however, led clinicians to re-examine other potential sources of organs including donors whose death is declared following circulatory arrest (donation after circulatory death; DCD). In the UK, a 5-minute standoff period of observation is required before death can be certified and the organ procurement process commenced. This period of observation varies internationally. The donor is then transferred to the operating theatre, a rapid laparotomy performed with cannulation of the distal aorta, and ice cold perfusion and topical cooling commenced (1)**.** DCD can be classified according to the Maastricht classification. This was first developed in 1995 and has since been revised and expanded from the original four categories (8). The great majority of DCDs in the UK are Maastricht III in which patients die following the planned withdrawal of life-sustaining therapies (9).

In the UK today, deceased donors (DD) account for approximately two thirds of all donors with both DBD and DCD organs used in most areas of solid organ transplantation including kidney, liver, pancreas, lung and heart transplantation (10).

1.1.3 Organ preservation

Since the early era of organ transplantation researchers have explored a variety of techniques to better preserve organs, ranging from topical cooling (11, 12), to perfusion with both cellular and acellular cooled preservation solutions (11), continuous *ex situ* hypothermic, sub-normothermic or normothermic machine perfusion techniques and *in situ* regional perfusion in the donor. Preservation solutions have also formed the focus of much transplant research and undergone numerous refinements over the years.

Early practice adopted techniques reported by Belzer *et al* (13) who demonstrated good outcomes using hypothermic machine perfusion and oxygenated cryoprecipitate plasma (14). This was in the era before brainstem death criteria were widely accepted and therefore, kidneys were often retrieved from donors who had died by cardiopulmonary criteria and had suffered considerable warm ischaemic injury (14). Collins et al (15) demonstrated that kidneys could be preserved for prolonged periods by simple cold storage using a simple solution composed principally of glucose, potassium and phosphate (15). The high concentration of potassium reflected intracellular concentrations and aimed to preserved ion gradients by reducing the loss of intracellular potassium. Cold static storage superseded hypothermic machine

perfusion in organ donation after DBD became common practice and better organ perfusion and cooling was achieved. Cold static storage had the added benefit of not requiring a cumbersome perfusion machine, making organ transport easier, and forms the mainstay of organ preservation today (16).

A number of preservation solutions have been developed. Whilst they have a diverse composition, they retain key constituents that include; an osmotic agent that provides an extracellular oncotic force, a buffer to counter intracellular acidosis, and electrolytes to maintain ion gradients. The two principal approaches to ionic composition in preservation solutions is either to mimic intracellular or extracellular environments (17). In the 1980s, preservation solutions developed at the University of Wisconsin (ViaSpan®) were demonstrated to extend preservation times in a range of organs in animal models (18-21). This has resulted in the widespread adoption of UW into clinical practice today. With the use of DCD and more 'less-than-ideal' donors, there has been renewed interest in other strategies to improve organ preservation. These include, hypothermic machine prefusion, normothermic or sub-normothermic machine perfusion.

1.1.4 Hypothermic machine perfusion

Following Belzer's early experience, there has been renewed interest in hypothermic machine perfusion in both liver and kidney transplantation with particular focus in the use of DCD and marginal donors. It is hypothesized that hypothermic machine perfusion improves preservation by flushing small capillaries and waste metabolites from the organs (1).

1.1.5 Normothermic perfusion

Two of the early pioneers of organ preservation were Charles Lindbergh and Carrel who performed a series of studies into isolated organ perfusion in the 1920s and 30s. Using a perfusion circuit they had developed, they were able to maintain organs in normothermic conditions for a number of days. These early concepts have been re-explored in the UK in recent years following the increased use of DCD organs. There are a number of approaches to normothermic perfusion that continue to be explored. These can be grouped into *in situ* and *ex situ* approaches. *In situ* normothermic perfusion involves the rapid cannulation of the donor circulation following death and the use of cardiopulmonary bypass (CPB) and extracorporeal membrane oxygenation (ECMO) technology and an in-line pump to recover venous blood to perfuse organs *in situ*. After a period of normothermic perfusion the organs can then be retrieved and preserved using any of the techniques used following DBD retrieval. Both abdominal and cardiothoracic organs can be perfused using this approach. If abdominal organs are being retrieved without cardiothoracic organs, abdominal regional perfusion is performed by either placing large-bore canulae peripherally in the femoral vasculature and then limiting reperfusion to abdominal organs with the use of an aortic balloon clamp, or by open cannulation of the abdominal aorta and inferior vena cava (IVC) and clamping the thoracic aorta. Cardiothoracic organs have also been retrieved following *in situ* normothermic perfusion. In this situation, open cannulation following median sternotomy is performed and the patient is placed on cardiopulmonary bypass with exclusion of cerebral flow by clamping of the carotid vessels (22, 23).

Another approach is to retrieve organs immediately and then perfuse the organs *ex situ* using similar technology. In this setting organs can be assessed and reconditioned. There is evidence to suggest that in some circumstances normothermic machine perfusion (NMP) can itself recondition organs against some of the deleterious effects of reperfusion injury. Increasingly it is also being explored as a potentially platform for the delivery of therapeutic agents (24).

Normothermic perfusion involves delivering adequate oxygen and nutrients to maintain cellular integrity and vascular processes during perfusion. Normothermic perfusion is more complex than cold static storage or hypothermic machine perfusion but potential advantages include; minimizing cold ischaemic injury, the ability to make an assessment of the organ prior to transplantation, and organ reconditioning and the opportunity to administer therapies to improve the condition of the organ (25).

1.2 Current trends in solid organ transplantation

In 2016-2017, 3710 DD transplants and 1043 living donor transplants performed in the UK. The total number of patients on the transplant waiting list peaked in 2009-10 and having started to decrease, now appears to have stabilised to approximately 6400 patients. Despite this, compared to 2015-2016, there was a 4% increase in overall deceased organ donation. DBD donors accounted for the majority of this, increasing by 6% on the previous year whilst DCD donation increased by 1% (10).

1.2.1 Heart transplantation

The heart transplant waiting list has plateaued to the current level of approximately 250 patients a year. Whilst the waiting list is not increasing, in 2016-2017 there were only 198 transplants performed and 25% of patients on the urgent waiting list were removed or died by one year and only 18% of non-urgent recipients received transplants. A DCD heart transplant programme was introduced in 2015-2016. 14 (7%) DCD heart transplants were performed in 2016-2017 (10).

1.2.2 Lung transplantation

Between October 2014 and September 2017, 539 lung transplants were performed in the UK. There has been a slight increase in the number of lung transplants performed in 2016-2017 after a slight decrease in 2015-2016. Approximately 20% of lung transplants are performed with organs from DCD (10).

1.2.3 Kidney transplantation

The kidney transplant waiting list continues to decline year-on-year from its peak in 2009. This represents a decline of approximately 25% from 2009 levels. Deceased donor kidney transplants performed in the UK in 2016-2017 increased by 3% compared to 2015-2016 with the number of both DBD and DCD donors increasing from the previous year. Living donor kidney transplants fell by 2% to 937 in 2016-2017 (10). Median cold ischaemia time has decreased in both DBD and DCD over the last 10 years from a median of 17 (DBD) and 16 hours (DCD) in 2007/2008 to 14 (DBD) and 13 hours (DCD) respectively (10).

1.2.4 Liver transplantation

Over the last decade, the number of patients on the liver transplant waiting list has gradually increased. This is in contrast to the last couple of years where the waiting list has decreased. The waiting list in 2016-2017 decreased by 8% from 2015-2016. The number of liver transplants from deceased donors increased by 8% with transplants from DBD donors increasing by 10% and transplants from DCD donors increasing by 1% (10).

1.2.5 Pancreas transplantation

The number of patients on the pancreas waiting list in 2016-2017 fell by 1% from the previous year. There was also a 1% decrease in the number of pancreas transplants performed in 2016-2017 despite an increase in the total number of deceased donors (10).

1.2.6 Summary

In summary, the number of patients on transplant waiting lists in the UK are either remaining constant or decreasing however, the number of transplants that are being performed continues to increase. Despite this, demand continues to outstrip supply with people continuing to die on the waiting list. In 2016-2017, 457 people died on the waiting list. A further 875 patients were removed from the waiting list. The majority of these were removed due to deteriorating health and ineligibility for transplantation and would likely have died soon after their removal from the waiting list (10). Whilst the overall number of donors have increased over the last decade, the donor demographic has changed substantially. Deceased donors have become older, more obese and less likely to have died following trauma. Furthermore, there has been a large increase in the use of donation after circulatory death (DCD) organs. These changes all have the potential to negatively impact the quality of transplanted organs and consequently recipient outcomes (10).

1.2.7 Standard criteria donors and expanded criteria donors

Standard Criteria Donors (SCD) and Expanded Criteria Donors (ECD) are additional sub-classifications of deceased donors that are used to inform clinicians and patients about potential outcomes and can aid organ allocation. It is derived from factors associated with graft loss and defines ECD as those >60 years, or ≥ 50 years with at least two of the following risk factors; a terminal serum creatinine > 1.5 mg/dL, a cerebrovascular accident as the cause of death, or a donor history of hypertension (26).

1.3 Types of ischaemia during organ transplantation

The transplantation process introduces a range of potential ischaemic insults to the transplanted organ. These are discussed below;

1.3.1 Primary warm ischaemia (Asystolic phase)

An organ is exposed to primary warm ischaemia during the asystolic phase which is defined as the time from circulatory arrest to the start of an organ perfusion procedure. This is most commonly the start of cold perfusion with preservation solution but also includes the commencement of regional *in situ* perfusion or machine perfusion (8).

1.3.2 Functional warm ischaemia

Following the withdrawal of life sustaining treatment in DCD there is a variable period of haemodynamic instability until circulatory arrest. This period is defined as the agonal phase (27). A prolonged agonal phase with a long period of haemodynamic instability potentially increases warm ischaemic injury and negatively impacts organ outcome. Counter to this, a prolonged agonal phase with a short period of haemodynamic instability immediately before asystole can be associated with minimal warm ischaemic injury (2, 28, 29). The term functional warm ischaemia attempts to better define the onset of warm ischaemic injury from the commencement of haemodynamic instability and organ hypoperfusion during the withdrawal phase. A number of haemodynamic parameters have been proposed including; mean arterial pressure ≤ 50 mmHg, systolic blood pressure ≤ 50 mmHg, peripheral oxygen saturations ≤ 60% (29). In the UK, the onset of functional warm ischaemia is arbitrarily defined as a systolic blood pressure of ≤ 50 mmHg (26).

1.3.3 Cold ischaemia

This is the period form the commencement of cooling with cold preservation solution to when the organ is removed from cold storage prior to implantation. During this period, additional techniques may be used in an attempt to better preserve organs including hypothermic machine preservation.

1.3.4 Secondary warm ischaemia

Secondary warm ischaemia is the period from removal of the organ from cold storage to reperfusion in the recipient. This period is defined by the implantation of the organ into the recipient. During this period, the organ is exposed to gradual re-warming and there is emerging evidence to suggest that prolonging this period may be detrimental to outcome (30).

1.4 Overview of aerobic metabolism

The eukaryotic cell is thought to have originated following an endosymbiotic event 2.5 billion years ago. It is theorised that an alpha-proteobacteria that used oxygen to convert organic molecules into energy was phagocytosed by an archaebacterium and the mutually beneficial arrangement of a safe, nutrient rich environment for the alphaproteobacteria and a ready source of energy for the arachaebacterium gave rise to the eukaryotic cell (31, 32). In evolutionary terms, anaerobic metabolism is a more primitive form of metabolism. Whilst sufficient to support simple single cell life, glycolysis alone is unable to support the increased energy requirements of more complex life. Aerobic organisms have evolved to live in oxygen rich environments but are nevertheless, frequently exposed to brief periods of ischaemia whereupon they look to their more primitive metabolism to sustain them.

The tolerance of organs to periods of warm and cold ischaemia differs between organs and to some extent reflects subtle differences in metabolic requirements and metabolism. The human heart is a highly metabolically active organ and is the one of the least tolerant grafts to ischaemia during organ transplantation. UK registry data suggests that recipient outcome is worse if cold ischaemic time (CIT) in heart transplantation is greater than 4 hours (33).

1.5 Cardiac metabolism

The daily energy requirements of the heart are the greatest of any organ in the human body. The complex machinery that converts chemical energy into the mechanical myofibril contraction required to beat 100,000 times a day consists of three main components; substrate utilisation, oxidative phosphorylation, and ATP transfer and utilisation. In order to meet these high energy demands there is a degree of metabolic flexibility and a variety of energy substrates can be utilised to generate ATP if required (34). Nevertheless, under normal physiological conditions, 90-95% of ATP production is generated by mitochondrial oxidative phosphorylation with fatty acid ß-oxidation accounting for 60-80% of this ATP production and the remainder largely accounted by carbohydrate oxidation. The principal function of both pathways under aerobic conditions is to transfer protons and electrons via the reduced forms of flavin adenine dinucleotide ($FADH_2$) and nicotinaminde adenine dinucleotide (NADH) to mitochondria to drive oxidative phosphorylation (35).

1.5.1 Fatty acid oxidation

Fatty acids must undergo esterification in the cytosol prior to further metabolism. This is an ATP-dependent process generating a fatty acyl-CoA moiety. These acyl-CoA molecules are bound to specific proteins and can be used in a variety of cellular processes including, phospholipid synthesis, signal transduction of pathways or ß-oxidation. The inner mitochondrial membrane is impermeable to acyl-CoA and therefore, mitochondrial uptake relies on a complex of proteins using carnitine as a shuttle. Once inside the mitochondria, ß-oxidation results in the sequential two-carbon shortening of the fatty acyl-CoA liberating acetyl-CoA which then enters the citric acid cycle (CAC) whilst also generating NADH and $FADH_2$ in the process. Glycolysis converts glucose to pyruvate. In the heart the majority of this then undergoes pyruvate decarboxylation by pyruvate dehydrogenase (PDH) to acetyl-CoA that then enters the CAC (35).

1.5.2 Glucose utilisation

Glycolysis is the biochemical process that converts glucose to pyruvate. In the process, two moles of ATP are generated for each mole of glucose. Under aerobic conditions, this relatively meagre energy return is dwarfed by the energy generated by the subsequent oxidation through the CAC and mitochondrial oxidative phosphorylation (35, 36).

Glycolysis is regulated at several key steps in the pathway with the principal ones being; glucose uptake and the reactions controlled by phosphofructokinase-1 (PFK-1) and glyceraldehyde-3-phopshate dehydrogenase (GAPDH) (36).

Glucose uptake into cells is restricted to specific transporters. There are two uptake mechanisms that are known to exist in animals, Na^+-dependent co-transport and facilitated diffusion glucose transporters (GLUT). Na^+-dependent co-transport does not occur in myocardium and therefore, myocardial glucose uptake is determined by GLUT. There are six recognised isoforms of the GLUT family of which GLUT-4 is the most abundant on the surface of cardiomyocytes (36, 37). Glucose is rapidly phosphorylated on entry

into myocardium preventing efflux. The rate of glucose phosphorylation in the cytosol by hexokinase is usually faster than glucose transport and therefore under physiological conditions, glucose uptake into myocardium forms the first regulatory step in glycolysis (37).

The next regulatory step is the conversion of fructose-6-phosphate to fructose 1,6-bisphosphate by PFK-1. This process requires ATP and is the first irreversible step that commits glucose to glycolysis. ATP, citrate and protons are all negative effectors of PFK-1 that provide allosteric inhibition (37).

GAPDH is another regulatory step in glycolysis. The oxidation and phosphorylation of glyceraldehyde-3-phosphate is linked to the reduction of NAD^+ to NADH. To ensure flux through GAPDH is not restricted, NADH must be re-oxidised to NAD^+. In the presence of oxygen, NADH is oxidised by the malate/aspartate shuttle (MAS) and the mitochondrial electron transport chain (ETC). Under anaerobic conditions, NADH is reduced by lactate dehydrogenase (see below) (35, 36)

1.5.3 Citric acid cycle (CAC)

The CAC, or tricarboxylic (TCA) cycle, or Krebs cycle, is a series of chemical reactions that occur in the matrix of mitochondria of aerobic organisms to release energy by the oxidation of carbohydrates, fats and proteins. In the process, the cycle generates ATP and NADH which can be fed into oxidative phosphorylation.

1.5.4 Mitochondria and Oxidative Phosphorylation

Mitochondria generate ATP through oxidative phosphorylation. Oxidative phosphorylation is the final step in the aerobic metabolism. This process is performed by a series of large, multi-subunit complexes that are embedded in the inner mitochondrial membrane. These complexes channel electrons generated by the CAC and fatty acid ß-oxidation, along the ETC, down an electron gradient via a series of redox reactions to the final electron acceptor, oxygen. Complex I passes electrons produced by the oxidation of NADH to NAD^+ and $FADH_2$ to FADH to the CoEnzyme Q (CoQ) pool. Electrons can also be passed to CoQ following the oxidation of succinate at complex II. Similarly, electrons from ß-oxidation of fatty acids can also be transferred directly to the CoQ pool via the electron transfer flavoprotein (ETF). Electrons in the CoQ pool are transferred via complex III to cytochrome c and then from cytochrome c to complex IV where they are used to reduce oxygen to water. The energy released as the electrons are transferred from complex I, III and IV are used to pump protons across the inner mitochondrial membrane into the cytosol. This generates an electrochemical gradient across the inner mitochondrial membrane. It is this proton motive force (Δp) that then drives the phosphorylation of ADP to ATP at ATP synthase (complex V) thus generating cellular energy (38-40).

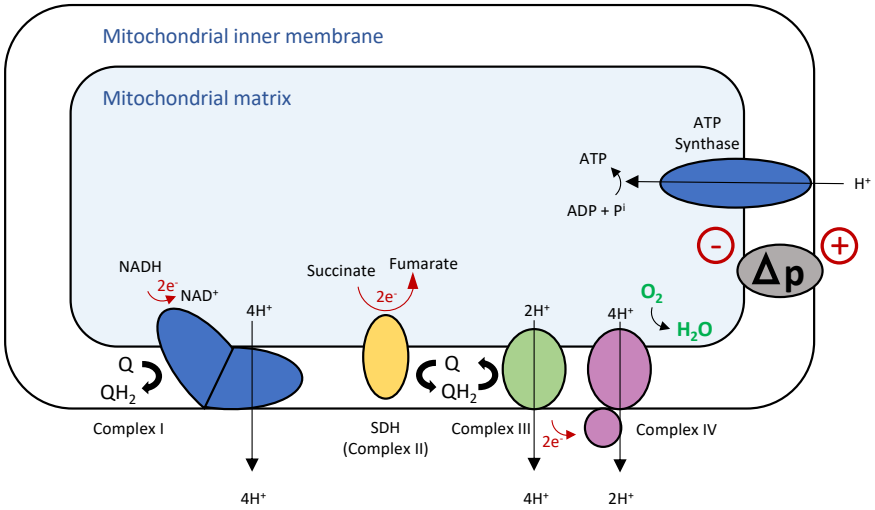

Figure 1: Mitochondria and oxidative phosphorylation.

Electrons generated by the CAC and fatty acid ß-oxidation are channelled along a series of multi-subunit complexes down an electron gradient to the final electron acceptor, oxygen. As a consequence, protons are pumped across the inner mitochondrial membrane into the cytosol generating an electrochemical gradient. This proton motive force (Δp) drives the phosphorylation of ADP by ATP synthase (Complex V) producing ATP.

1.6 Ischaemia

1.6.1 Cardiac ischaemic metabolism

Whenever the arterial supply cannot deliver enough oxygen to meet the metabolic demands of a cell, tissue or organ, it becomes ischaemic. For the majority of organisms that have evolved to exist in oxygen rich environments, ischaemia can only be tolerated transiently and without prompt revascularisation and restoration of blood flow cell death is inevitable.

With the cessation of myocardial blood flow, there is a rapid decrease in tissue oxygen. Studies from animal models have demonstrated that myocardial oxygen tension drops to approximately 75% of baseline values within 8-10 seconds following the onset of ischaemia and exhaustion of tissue oxygen is complete within 30 seconds (41). When oxygen is not available oxidative phosphorylation ceases. Anaerobic metabolism, through glycolysis, is the only available source of energy. This is a more primitive form of energy production but during an episode of ischaemia it can generate limited but sufficient energy to sustain cellular function transiently until revascularisation; however, it is the metabolic changes that occur during anaerobic metabolism that can prime cells and paradoxically lead to reperfusion injury and cellular death on re-oxygenation.

In the first few minutes following the onset of ischaemia there is a paradoxical increase in the rate of glycolysis. This is due to a transient upregulation of key regulatory steps. There is an initial increase in substrate utilisation through an increase in glycogenolysis stimulated in part by ischaemia-induced local catecholamine release and an associated increase in cyclic adenosine monophosphate (cAMP), and also by the reduction in the phosphorylase b inhibition due to a decrease in tissue ATP concentration. The increase in the rate of glycolysis is also the result of increased substrate utilisation through PFK-1 upregulation. Activation of PFK-1 is the result of increased concentrations of the positive effectors, ADP and adenosine monophosphate (AMP), and removal of the inhibition by the negative effector ATP (42). Despite the upregulation of glycolysis during early ischaemia, it is still insufficient to meet energy demands.

After a few minutes of ischaemia, there is a marked reduction in the rate of ATP production and this corresponds to a cessation in contraction. The reduction in ATP generation is likely the result of subsequent inhibition of PFK-1 and GAPDH by the increasing NADH and protons associated with the absence of oxidation and lactate production (42).

Glycolysis cannot continue indefinitely. Studies in animal models were conflicting in identifying the causal mechanisms for the eventual failure of glycolysis (42). Exhaustion of glycolytic substrate or cofactors, or the inhibition or denaturation of glycolytic enzymes have been proposed as potential mechanisms (36, 43). In the absence of coronary flow, lactate and protons accumulate and it is generally understood that this is the causal mechanism that results in the inhibition of glycolysis and ATP production with resultant cell death (36).

1.6.2 Cardioplegia and effects on cardiac metabolism

The early era of open-heart surgery in the 1950s was performed with brief periods of circulatory arrest under whole-body hypothermia that was used to provide protection against hypoxic injury, in particular to the brain. Subsequent development of cardiopulmonary bypass circumvented the hypoxic injury to the brain and other organs, but the extended periods of myocardial ischaemia required to treat more complex cardiac pathologies were increasingly problematic. 'Stone heart' was a previously well-recognised phenomenon in which irreversible ischaemic contracture occurred as a result of exhaustion of ATP. Cardiac surgeons at the time experimented with solutions of high potassium citrate to induce a chemical arrest but the practice was abandoned in the UK for 20 years after it was found to cause focal myocardial necrosis. In the mid-1970's renewed interest in cardioplegic solutions led to the development of St Thomas' Hospital cardioplegic solution by the biochemist, David Hearse and the cardiac surgeon, Mark Braimbridge (44). This solution was based on an extracellular ionic composition. A moderately elevated potassium chloride concentration was used instead of potassium citrate to induce arrest as it was believed that the previous accounts of focal myocardial necrosis resulted from the high citrate concentrations. This cardioplegic solution was first used surgically in 1975 and quickly became the predominant cardioprotective technique used throughout the world (44).

Hyperkalaemic solutions induce a diastolic flaccid arrest by making the resting membrane potential of the myocyte more positive or depolarized compared to normal. This resting potential is more positive than the threshold potential for the voltage dependent Na^+ channel which therefore remain inactivated. This prevents repolarisation, hence the term, 'depolarised' arrest. The cessation of cardiac contraction is thought to provide cardioprotection by reducing myocardial oxygen consumption and ATP depletion (44, 45).

1.7 Reperfusion injury

Reperfusion injury is the pathological exacerbation of tissue injury that occurs on re-oxygenation of an organ that has previously been subjected to a period of restricted or interrupted blood flow (46). The concept of reperfusion injury was first suggested in the 1960s by Jennings *et al* (47). They observed the structural and electrophysiological changes that occurred on coronary reperfusion of canine myocardium, noting that reperfusion actually hastened necrosis (47, 48). Subsequent work by Hearse *et al* (49) demonstrating that intracellular enzymes were released predominantly during reperfusion and not during ischaemia supported this observation. Furthermore, they demonstrated that oxygen was essential for the observed cellular injury and did not occur on anoxic reperfusion (50). This counterintuitive observation that restoration of blood flow and re-oxygenation exacerbates tissue injury is termed, "reperfusion injury" and is recognized as a major contributor to a wide range of pathological entities including; acute coronary syndrome, acute kidney injury, stroke, intestinal ischaemia, multi-organ failure, hypovolaemic shock following trauma and graft dysfunction following solid organ transplantation (46).

It is now known that upon reperfusion, the restoration of oxygen to ischaemic tissues results in the formation of reactive oxygen species (ROS) and that it is ROS that are the effectors of the subsequent tissue injury. ROS are reactive molecules that contain oxygen. They were directly implicated as the central mediators of IR injury using electron spin resonance and spin trapping in the 1980s (50). These studies demonstrated a marginal increase in ROS during ischaemia. ROS remained unchanged during hypoxic reperfusion but rapidly spiked, with a peak at about 20 seconds when the tissues were reperfused with oxygen. The central role of ROS in IR injury was confirmed by studies that demonstrated similar pathophysiological changes to those seen at reperfusion with exogenously administered ROS (50).

1.7.1 Reactive oxygen species

Since ROS were identified as the effectors of reperfusion injury research has focused on the precise source and the mechanism through which they're generated. There are a number of biologically important ROS that include, superoxide ($O^{\bullet -}$), hydrogen peroxide (H_2O_2), nitric oxide ($NO^{\bullet}$), peroxynitrite ($ONOO^-$), hypochlorus acid (HClO), and the hydroxyl radical ($HO^{\bullet}$)(51). The $O^{\bullet -}$ is the predominant ROS generated during ischaemia-reperfusion (IR). Physiological $O^{\bullet -}$ formation occurs at low levels, predominantly as a result of electron leakage within the ETC. During IR there is a burst of $O^{\bullet -}$ formation. There are multiple potential sources of ROS that include, mitochondria, the xanthine oxidase pathway and nicotinamide adenine dinucleotide phosphate (NADPH) oxidase activity. Whilst all sources of ROS contribute, it has been estimated that mitochondria account for the great majority (up to 90%) of the overall oxidative burden (52).

1.7.2 Mitochondria

Mitochondria are frequently referred to as the powerhouses of the cell since their primary function is the transduction of energy into a form that is usable by the cell. Energy is generated through the process of

oxidative phosphorylation and ROS production is a by-product of this process. Mitochondria are important sources of ROS both during physiological and pathophysiological conditions. The principal sources of ROS production are complex I and III. ROS are generated when redox-active prosthetic groups found within these complexes are exposed to oxygen. Antioxidant enzymes are defense mechanisms found both in the mitochondrial matrix and cytoplasm. These superoxide dismutases (SOD) contain copper or manganese metal centers that dismutate $O^{\bullet-}$ to H_2O_2 that can then be further deactivated by catalase to water and oxygen, or by glutathione peroxidases to glutathione disulfide and water (38, 39).

Until recently, mitochondrial ROS generation during IR injury was thought to be a non-specific consequence of the rapid re-oxygenation of a dysfunctional respiratory chain. It has recently been hypothesized that $O^{\bullet-}$ generation during IR injury is, in fact, the product of a specific metabolic process, namely, reverse electron transport (RET) through complex I driven by succinate accumulation during ischaemia (53).

Liquid chromatography – mass spectrometry (LC-MS) analysis of mammalian tissues during ischaemia, demonstrated succinate to be the only CAC metabolite to accumulate in all tissues assessed in the mouse. Under physiological conditions, succinate is generated through a variety of processes including, the oxidation of carbons from glucose, fatty acids, glutamate and the γ-aminobutyric acid (GABA) shunt. During ischaemia however, mitochondria best preserve the electrochemical gradient to enable continued ATP production by reversing the action of succinate dehydrogenase (SDH) to generate succinate from fumarate. The fumarate required for this process is thought to be produced by two pathways, the MAS, and the AMP-dependent activation of the purine nucleotide cycle (PNC) (53). At reperfusion, with the reintroduction of oxygen, the conventional direction of the respiratory chain can resume. The accumulated succinate can be oxidized back to fumarate with complex II donating electrons to CoQ in the standard manner. The sudden generation of electrons through complex II by the oxidation of the accumulated succinate, overwhelms complex III and IV which are running at full capacity. This generates a high Δp. The high Δp may be further exaggerated by the degradation of adenine nucleotides during ischaemia. This limits the availability of ADP for ATP generation by ATP synthase that would normally decrease Δp in the process. In the presence of the high Δp and highly reduced CoQ pool, the bioenergetically favored method to disperse the excess electrons is through RET at complex I which in the process generates $O^{\bullet-}$ (53, 54).

1.7.3 NADPH oxidase

The first member of the NADPH oxidase (NOX) family of transmembrane enzymes was identified in phagocytes. Other members of this family of ROS producing enzymes have since been identified in almost all tissues. They all transport electrons across biological membranes to enable the reduction of oxygen to $O^{\bullet-}$ (55, 56).

The early studies confirming the proximal role of $O^{\bullet-}$ in reperfusion injury also suggested a role for immune activation and ROS production. Experiments in isolated hearts demonstrated a short burst of ROS

production. However, when translated to whole animal studies, this ROS production was shown to remain elevated for over 3 hours. The 'respiratory burst', which is a result of neutrophil infiltration, is an important source of ROS, although whether it has causative or effector role in the pathogenesis of IR injury is uncertain (55, 56).

1.7.4 Cellular xanthine oxidase

The xanthine oxidoreductase (XOR) describes two inter-convertible yet functionally distinct enzymes, xanthine dehydrogenase (XD) and xanthine oxidase (XO) (57). XOR is involved in purine metabolism, catalyzing the conversion of hypoxanthine to xanthine and subsequently uric acid. XD is present *in vivo* and catalyzes the oxidation of hypoxanthine to xanthine by coupling the reaction to the reduction of NAD^+ to NADH. Under certain physiologic and pathophysiologic conditions XD undergoes a post-transcriptional change to XO. XO is unable to couple the oxidation of hypoxanthine to the reduction of NAD^+ instead requiring oxygen, which is reduced in the process producing $O^{\bullet -}$. XOR is found in a variety of tissues including, liver intestine, spleen, kidney and skeletal muscle. In addition, it has been shown to be present in high concentrations on the luminal surface of the microvasculature endothelium of organs including the heart (57).

The XOR system has long been implicated in ROS generation during IR injury. Ischaemia results in modification of XD by proteolytic cleavage to XO. At reperfusion the irreversibly modified XO then generates ROS (50). Unfortunately, the initial positive results in animal studies investigating the role of ROS scavenging with antioxidants or inhibitors of XOR such as allopurinol have not been translated to the clinical setting (57).

1.8 Mitochondria and the immune response

The immune system comprises two complementary and close connected defense mechanisms that enact a response to threatening stimuli. These are the innate and adaptive immune responses. The innate immune response provides the first line of defense generating a non-specific immediate response to invading microorganisms, tissue injury or malignancy. This is an antigen independent response and is not associated with the development of immunological memory. In evolutionary terms, the adaptive immune response is more modern. It is an antigen dependent response that enables the host to develop immunological memory, enabling a heightened immune response if the host encounters the respective pathogen at a later time. mtROS is an upstream effector of the exaggerated tissue injury that occurs during IR injury. The burst of mtROS has the potential to not only impact acute function through potentiation of an innate immune response but also longer-term function through effects on the adaptive immune response.

1.8.1 Sterile Inflammation and the innate immune response

The ROS generated on reperfusion combined with cellular oxidative damage, mitochondrial dysfunction and ischaemic tissue injury initiate an inflammatory response with activation of the innate immune system. This 'sterile inflammation' occurs in the absence of any microorganisms but there are many phenotypical parallels between this, sterile inflammation, and the immune response directed against pathogens.

The innate immune response is characterized by the recruitment of neutrophils, macrophages, the production of pro-inflammatory cytokines, fibroblast proliferation and aberrant collagen accumulation and fibrosis. Microorganisms are recognized through conserved structural moieties found in microorganisms that are collectively known as pathogen-associated molecular patterns (PAMPs). These are recognized by germline encoded pattern recognition receptors (PRR) of which five classes are recognized.

In sterile inflammation, these PRRs are activated by endogenous molecules in the absence of microbial infection. These ligands are termed damage-associated molecular patterns (DAMPs) and when sensed by PRRs initiate an immune response with the production of pro-inflammatory cytokines (58, 59).

1.8.2 Mitochondria and innate immune response

Mitochondria have been shown to be a direct source of DAMPs directly initiating an innate immune response through a number of pathways. Mitochondrial DAMPs include mitochondrial ROS (mtROS) and mitochondrial DNA (mtDNA).

1.8.3 Mitochondrial ROS (mtROS)

mtROS are generated during periods of cellular stress and have been shown to have direct roles as activators or regulators of innate immune signaling pathways. Mitochondrial antiviral signaling (MAVS)

protein is a key protein in a signaling pathway, activating nuclear factor κ-light chain enhancer of activated B cells (NF-κB) and interferon regulatory factors (IRFs) to induce type-I interferons (60). MAVS is localized to the mitochondria and in addition to activation in response to viral replication through (retinoic acid-inducible gene-1) RIG-I and melanoma differentiation antigen 5 (MDA-5) (60), has been shown to be activated by mtROS independent of RNA (32). mtROS have also been shown to have a role in the activation of the NLRP3 inflammasome (32, 61).

1.8.4 Mitochondrial DNA (mtDNA)

The bacterial origins of mitochondria are retained in their DNA. mtDNA is located in close proximity to the respiratory chain and is a circular loop containing 37 genes (62). Like bacterial DNA, mtDNA contains CpG DNA repeats that when liberated into the cytosol or extracellular space by cellular stress or necrosis, can be recognised by the Toll-like receptors (TLRs) and act as a damage associated molecular pattern (DAMP) (63, 64). mtDNA has been shown to activate TLR9 (63), the NLRP3 inflammasome (65), and the STING pathway (66). TLR9 activation leads to activation of the NF-κB signaling pathway with associated induction of proinflammatory genes including those encoding tumour necrosis factor (TNF) (63). Activation of the NLRP3 inflammasome activates caspase-1 which results in the maturation and secretion of IL-1ß and IL-18 (64). Finally, activation of the cytosolic DNA sensor, cGAS, activates the STING pathway culminating in the upregulation of interferon stimulated genes (ISGs) and potentiates type I interferon responses (66). mtDNA is therefore capable of activating an innate immune response through a number of central signaling pathways. Although the innate immune response is not sufficient to itself reject the allograft, this inflammatory milieu may modify the adaptive immune response, upregulating an insidious immune response and thereby potentiating chronic rejection (58).

1.8.5 Mitochondrial regulation of the innate immune response

In addition to the potentiation of an innate immune response directly through the release of these DAMPs described above, in certain settings CAC intermediates such as succinate have been shown to modify the innate immune response by stabilizing hypoxia inducible factor 1α (HIF-1α). This also results in an increase in cytokine production thus providing a separate mechanism through which mitochondria can up regulate the innate immune response at the time of transplantation (58). Finally, mitochondria may also have indirect effects in mediating the innate immune response through additional cellular oxidative damage and the release of other DAMPs.

1.8.6 The adaptive immune response

There is emerging evidence that IR injury has the potential to modulate the adaptive immune response through a number of pathways. High mobility group box 1 (HMGB1) and heat shock protein 72 (HSP72) are both DAMPs. HMGB1 is released following cellular injury and HSP72 is expressed following oxidative stress. Both have been shown to induce dendritic cell (DC) maturation which is associated with the

upregulation in expression of MHC class II, costimulatory molecules and cytokine secretion. Mature DCs can then activate naïve T-cells in secondary lymphoid tissue generating an adaptive alloimmune response.

The cytokines released by the activated innate immune system recruit leukocytes to the inflamed organ, activate the complement cascade facilitating antigen presentation, modify the activation status and permeability of the endothelial cells, upregulate antigen presentation, and stimulate migration of antigen presentation cells (APCs) both into and out of the transplanted organ. These events are all intimately involved in the upregulation of the adaptive immune response (59).

1.8.7 Mitochondria and the adaptive immune response

mtROS have also been shown to be intimately involved in the adaptive immune response. T-cell activation results in a rapid increase in mtROS production that is critical for $CD4^+$ T-cell activation *in vitro* and *in vivo* though CD3 initiated Ca^{2+} signalling; without mtROS, $CD4^+$ T-cells do not express IL-2 (67). Furthermore, mtROS have also been shown to have a role in the fate determination of activated B cells by promoting class switch recombination (68). Together, these observations support a central role for mtROS in the activation and regulation of the adaptive immune response(32).

In addition to direct activation through mtROS, mitochondria are increasingly recognised as a having central role in orchestrating the adaptive immune response. The ancient ancestry of mitochondria underpins the intricate relationship they are increasingly recognised to play in other core metabolic and cellular processes outside of energy synthesis (32, 39). The mammalian immune response requires an intricately coordinated balance of cell activation and inhibition of signaling pathways across a range of cell types. These signaling pathways have traditionally been thought of as linear phosphorylation-based cascades initiated at the cell surface and conveyed to the nucleus. More recent evidence suggests that cellular metabolism not only provides the energy to fuel this process, but also independently moderates these signaling pathways(58). T-cell subsets have dramatically different metabolic profiles that are necessary for T-cell differentiation. Increased glycolytic metabolism has been observed in Th17 cells due to an increase in HIF-1. Inhibiting the effector target of HIF-1 in Th17 cells suppresses Th17 cells and increases Treg formation *in vitro* and *in vivo* models. Similarly, B-cells have also been observed to undergo major transitions in their metabolic requirements during maturation(58). The impact of reperfusion injury mediated mitochondrial dysfunction on these mechanisms is yet to be explored.

1.9 Clinical manifestations of reperfusion injury in organ transplantation

The characterisation of reperfusion injury as a distinct pathological entity and its associated clinical manifestations is confounded by the inherent close association with direct ischaemic injury. There is extensive research supporting the concept that reperfusion injury causes additional myocardial injury, perhaps best evidenced by interventions that can be initiated at the end of ischaemia and still reduce infarct size(69). In organ transplantation, whilst organ injury frequently occurs during the process of transplanting an organ, the precise individual contributions of irreversible ischaemia, and subsequent reperfusion to the overall organ injury are very difficult to isolate and are yet to be definitively defined. Nevertheless, clinical manifestations of IR injury are frequently associated with IR injury in transplantation and include; delayed graft function (DGF) in kidney transplantation, aspartate aminotransferase (AST) rise and the post-reperfusion syndrome in liver transplantation, graft pancreatitis in pancreas transplantation and myocardial dysfunction in heart transplantation.

1.9.1 Clinical impact of ischaemia on short and long-term outcomes

Evidence from *in vitro* and *in vivo* models has identified multiple pathways through which IR injury can impact both short and long-term outcomes in organ transplantation. Data from clinical studies further supports the impact of IR injury on acute organ dysfunction or graft failure, as well as potentially moderating chronic rejection and long-term outcomes.

1.9.2 Outcomes in heart transplantation

Hearts tolerate periods of ischaemia very poorly. The catastrophic complication of irreversible ischaemic injury and primary graft function was all too common to the early pioneers of heart transplantation. Nevertheless, as outcomes quickly improved, the demand for hearts quickly outstripped supply. Clinicians sought ways of expanding the donor pool and one potential source was organs with prolonged ischaemic times (>4 hours). Whilst some studies from single centres have suggested there is no association between ischaemic times and primary graft failure (PGF) (70, 71), the general consensus, supported by recent UK and international data, is that the length of ischaemic time is a strong predictor of PGF and that the risk of PGF increases for ischaemic times beyond 3 hours (33, 72). Whether graft ischaemia impacts mid and long-term outcome in cardiac transplantation is less well defined. Registry data identified ischaemic time as an independent risk factor for 1, 5 and 15-year patient mortality and multivariate analysis demonstrated ischaemic time is likely to be a risk factor for the development of chronic allograft vasculopathy (CAV) at 5 years (73). These findings were at odds with large, single centre cohort studies demonstrating no difference in overall survival with prolonged graft ischaemia(70, 71). In another study, prolonged graft ischaemia was weakly associated with greater incidence of transplant coronary artery disease (74). Furthermore, there was a suggestion that donor age impacted on organ tolerance to

ischaemia: In a subgroup of donors >50 years of age, prolonged graft ischaemia was associated with significantly worse short and long-term outcomes(70, 71).

1.9.3 Outcomes in liver transplantation

Increased cold ischaemia is associated with worse short and long-term outcomes following liver transplantation(75-77). A number of clinical trials have been undertaken in liver transplantation adopting a range of pharmacological strategies to minimise IR injury with limited success(78).

1.9.4 Outcomes in kidney transplantation

The relationship between cold ischaemia time and outcomes in kidneys from DBD has proved difficult to define and there are conflicting results from registry studies (79). Some authors have suggested that there are threshold values below which CIT has no impact on outcome, whilst others have suggested that it should be considered as a continuous risk factor (79).

Prolonged CIT (>24 hours) has been shown to be a risk factor for PNF, DGF, and increased incidence of acute rejection episodes (80-85). Data from the UK registry demonstrate that increasing cold ischaemic time up to 21 hours is not associated with worse short-term outcomes. However, beyond this the risk of transplant failure was increased by 4% for each additional hour of cold ischaemia(82).

The impact of cold ischaemia on longer-term outcomes is less certain, with studies producing conflicting results. Some studies have shown that prolonged cold ischaemia is associated with worse long-term outcomes (79-81, 83, 86-91), although others have failed to identify any difference in longer-term graft survival (82, 85, 92, 93). There are a number of explanations for the disparity between these studies. The multifactorial aetiology of chronic graft loss, differences in study design and the variation in regional and national retrieval practice, donor types, ischaemic times, immunosuppression and long term follow up, all introduce the potential for considerable bias. A recent analysis of data from the modern era of immunosuppression suggested that prolonged cold ischaemia was detrimental to mid-term outcomes. Moreover, there was also a proportional relationship between CIT and mid-term outcomes with every hour of cold ischaemia increasing the risk of graft failure (79). Recent data from the UK transplant registry also suggests ischaemia may impact long-term graft function. In a study by Summers *et al* organs from deceased donors that were exposed to a more severe ischaemic insult had a worse 5 year survival (9).

1.9.5 Clinical outcomes of DCD compared to DBD

DCD is an invaluable source of organs for transplantation, but concern surrounds the additional period of primary warm ischaemia that can be detrimental to immediate and long-term organ outcome. Kidney and liver transplants comprise the majority of DCD transplanted organs and therefore, the impact of DCD on organ outcome outside single centre experience in other organs is limited.

In kidney transplantation, the general consensus, is that DCD negatively impacts immediate graft function with a greater risk of PNF and DGF (27, 91). This does not, however, translate into worse longer-term

outcomes. UK registry data demonstrates no difference in the 3-year, risk adjusted, graft or patient survival following DCD and DBD (26, 91). Animal models (94) and clinical data have shown that DCD kidneys tolerate subsequent prolonged cold ischaemia worse than DBD kidneys with a higher incidence of PNF, DGF and long-term survival (9, 95-97).

In liver transplantation, DCD organs are also associated with increase in surgical complications including PNF (98, 99). Furthermore, in some series this has been shown to translate into a worse longer-term outcome when compared to DBD organs (98, 100, 101). In contrast, some single centre experience and registry data have demonstrated similar short and long-term outcomes in selected cohorts (98, 102). The additional primary warm ischaemia associated with DCD, rather than simply compounding reperfusion injury as observed in some organs, manifests in liver transplantation as a different spectrum of complications with an increased incidence of ischaemic cholangiopathy. This is characterised by the presence of non-anastomotic biliary strictures in the donor biliary tree that occur in the absence of hepatic artery thrombosis or stenosis. The increased ischaemic cholangiopathy translates into a worse longer-term outcome and an increased rate of re-transplantation in recipients of organs following DCD in liver transplantation (100, 103).

In summary, clinical evidence suggests that DCD are an invaluable source of potential organs and, with appropriate donor and recipient selection outcomes, comparable to DBD organs can be achieved. Nevertheless, the additional period of warm ischaemia introduces an insult the precise mechanisms for which are still to be elucidated.

1.10 Allograft rejection in transplantation

The immune response generated following the transplantation of an organ can be both an innate and an adaptive response. Non-specific injury elicits an innate immune response and whilst this is only rarely able to itself reject a graft it is integral in initiating and amplifying the adaptive immune response that results in rejection of the allograft (59).

Various classifications are used to describe the adaptive immune response that can produce rejection of an allograft. These can be based on pathophysiological changes, severity, response to treatment, presence or absence of organ dysfunction and immunologic mechanisms. Categorized simply according to the time course of rejection, rejection can be divided into hyperacute, acute or chronic (104, 105).

1.10.1 Hyperacute rejection

Hyperacute rejection is now relatively rare in solid organ transplantation due to improvements in pre-operative cross matching and a reduction in HLA panel reactive antibodies in potential recipients. Hyperacute rejection is the result of pre-formed recipient antibodies that bind donor endothelial antigens (ABO, HLA). In kidney transplantation, it causes diffuse haemorrhagic cortical necrosis and vascular thrombosis. Within a few minutes of reperfusion the transplanted organ turns a mottled blue and fails to produce urine. The organ usually has to be explanted (106, 107).

1.10.2 Acute rejection

Acute rejection typically occurs within the first 3 months following transplantation and may be cell or antibody mediated. Cell mediated rejection is driven by T-lymphocytes. Solid organ transplantation produces a unique immunological situation in which recipient T cell recognition of foreign antigen can occur through three distinct pathways. Recipient T cells can recognize the intact MHC on the surface of donor APC such as DC. This is termed direct allorecognition. An alternative process of antigen presentation is indirect allorecognition. This involves the internalisation and processing of the donor alloantigen, which is then re-presented by APCs on self MHC. More recently, a further mechanism for alloantigen presentation has been described. In this semidirect pathway, donor MHC is internalized and is represented intact on the recipient APC surface (59, 108).

Direct pathway allorecognition plays a dominant role in initiating an adaptive immune response in clinical transplantation but its effects are short lived as donor APCs are rapidly cleared by the recipient NK cells due to a lack of recipient MHC class I. The indirect pathway, however, can potentially provide a long-lived immune response as donor antigen will be available for internalization, processing and representation by recipient APCs for as long as the graft remains *in situ*. Whilst there is undoubtedly some crossover between these two pathways in clinical practice, direct allorecognition is thought to dominate during the early stages of transplantation with indirect allorecognition becoming the dominant pathway at later stages (59, 108).

Humoral or antibody mediated rejection accounts clinically for approximately 10% of acute rejection episodes (107). There are a variety of antigenic targets against which antibodies can be generated, including MHC molecules, minor histocompatibility complex molecules, endothelial cells, blood group antigens and autoantigens (59, 109). Antibody-mediated graft damage is primarily the result of complement fixation, although direct activation of natural killer cells and macrophages by binding of the antibody Fc region to cell surface receptors expressed on these cells may also contribute to graft damage through antibody-dependent cellular cytotoxicity (59).

There have been significant improvements in the overall management of acute rejection with 1 year survival of organs now over 90% (107).

1.10.3 Chronic rejection

The array of terminology used to describe the insidious decline in function of a transplanted organ reflects the complexity of the pathophysiological processes that undermine it.

Chronic graft dysfunction is a functional definition that does not differentiate the underlying pathophysiological process whereas chronic rejection is used to imply an ongoing immunological response. Histologically, the decline in graft function is characterized by a progressive replacement fibrosis of the graft parenchyma. While there may be a degree of heterogeneity in the predominant pathological process responsible for this, the most common of these is chronic allograft vasculopathy (CAV), which is universal to all transplanted vascularised organs (104, 110).

Allograft vasculopathy is a progressive, concentric intimal hyperplasia that results in luminal narrowing along the entire length of transplanted arterial vasculature (as opposed to atherosclerosis which produces lipid-rich, discrete, eccentric plaques in epicardial vessels). Histopathologically, the plaques are lipid-poor and composed of smooth muscle cells and extra-cellular matrix. The loss of luminal diameter is predominantly due to intimal hyperplasia, although there may also be a degree of adventitial scarring that results in a restrictive component to the luminal stenosis. Vascular remodeling occurs, to some degree, in all transplanted grafts, although clinically significant chronic vasculopathy only occurs in a small subset of patients. Graft failure is associated with a progressive parenchymal replacement fibrosis of allograft thought to be a result of progressive parenchymal ischaemia (104, 110, 111).

Allograft vasculopathy does not occur in syngeneic grafts in experimental models and is not seen past the suture line or atrial remnant in human recipients. This provides strong evidence that the process is driven by an alloimmune response (104, 110, 111).

Although the alloimmune response underlies the pathogenesis of chronic allograft vasculopathy, ongoing allogeneic stimulation is not necessarily required (112-115). This poses the question as to whether an initial activation of an alloimmune response can upregulate the secondary response sufficient for subsequent alloantigen-independent vasculopathy (112).

The aetiology of chronic rejection in kidney allografts is less certain and parenchymal fibrosis is occasionally seen without significant vasculopathy (chronic parenchymal cell rejection). Nonetheless, allograft vasculopathy is still commonly seen in failing renal allografts (112).

1.10.4 Impact of chronic rejection

Chronic graft dysfunction remains a major clinical challenge in transplantation and currently occurs in approximately 3-5% of transplanted grafts per year. This has remained largely unchanged despite considerable progress in other areas of transplantation. In addition to the direct consequences and increased mortality associated with losing a graft for the individual patient, chronic graft loss has a direct impact on the fundamental problem of organ shortage (116).

Chronic graft dysfunction is a complex multifactorial process with an aetiology that likely involves some or all of: the alloimmune response, ischaemia reperfusion injury, toxicity from immunosuppressive agents, as well as recurrence of the original disease (111, 116).

1.11 Protective strategies for treating IR injury

There are multiple opportunities during the transplant process that are theoretically amenable to therapeutic intervention in ameliorating ischaemia and or reperfusion. The use of agents prior to the confirmation of death with the implicit purpose of improving donor organ outcome is controversial. In the UK, the use of interventions that are not of direct benefit to the donor are prohibited pre-mortem.

There is a potential window in DBD during which agents could be administered to the donor prior to the onset of ischaemia. However, DCD organs comprise a significant proportion of all organs transplanted in the UK today and with the increased incidence of IR injury associated with these organs it would be preferable to target interventions during the stages of organ storage and reperfusion.

Pharmacological therapies have been used experimentally to target all aspects of IR injury; pre-ischaemia, during organ storage, and on reperfusion.

1.11.1 Targeting mitochondria

Ameliorating IR injury has previously been explored and the use of the antioxidant scavenger superoxide dismutase demonstrated some efficacy in improving outcomes in kidney transplantation (117). The increasing recognition of the fundamental role of mitochondria in mediating IR injury has increased interest in developing strategies to target the mitochondrial mechanisms that underpin IR injury (39, 118). Therapeutic strategies targeting mitochondria can be grouped into a number of areas including; limiting oxidative stress and mitochondrial ROS generation, reducing tubular cell death through necrosis and apoptosis, moderating mitochondrial dynamics and mitochondrial immunomodulation (118).

1.11.2 Limiting oxidative stress and mitochondrial ROS

The fundamental role of oxidative stress in IR injury has been extensively reported and has provided a strong rationale for the use of antioxidants in this setting. Paradoxically, however, the translation of these therapies to clinical practice has been disappointing. This can be interpreted in one of two ways. Either ROS do not have a role in the pathophysiology of these diseases, or the antioxidants are not adequately delivered to the appropriate region of the cell or at an appropriate time during reperfusion to prevent the cellular damage. Dimethyl malonate (DMM) is a competitive inhibitor of succinate dehydrogenase. As discussed above, reversal in the conventional direction of this enzyme during ischaemia results in the generation of succinate from fumarate. DMM competitively inhibits this process and has been shown *in vivo* to ameliorate succinate accumulation and subsequent IR injury in a variety of animal models (53) and is an appealing therapeutic approach in organ transplantation (118).

1.11.3 Reducing tubular death

Mitochondria are central to necrosis and apoptosis. Apoptosis is initiated by two major but interconnected pathways; mitochondria and death receptors. Increased permeability of the outer mitochondrial membrane (MOMP) releases pro-apoptotic factors such as cytochrome c and other

proteins leading to the formation of the apoptosome. This activates caspase-activation pathways resulting in apoptosis. Therapies designed to target this pathway have demonstrated early promise in other areas of IR injury and are currently in phase II human clinical trials (118-120).

1.11.4 Mitochondrial dynamics

Mitochondria are not solitary, isolated entities but exist as complex interconnected networks that are in constant flux through fusion, fission and the selective removal of individual units by autophagy, a process termed mitophagy. Altered mitochondrial dynamics may contribute to changes in cellular injury and repair following IR injury. A variety of proteins have been identified as regulators of mitochondrial fusion and fission including the pro-fusion proteins, mitofusin 1 and 2, OPA1, and the pro-fission protein dynamin-related protein 1. Pharmacological inhibition or unpregulation of these processes has been shown to have protective effects in models of IR injury, though these findings are yet to be translated to clinical trials (121-124).

1.11.5 Mitochondrial Immunomodulation

Mitochondria are increasingly recognized as being central to the activation and regulation of both the innate and adaptive immune response as discussed above. These emerging pathways may be amenable to pharmacological intervention in the future. The conversion of M1 inflammatory macrophages to M2 anti-inflammatory cells has been shown to be facilitated by both metformin and rotenone. This switch is thought to be initiated through actions on complex I by reducing RET and the generation of ROS. Furthermore, inhibition of SDH using DMM has also been shown to limit a pro-inflammatory response and boost anti-inflammatory responses whilst the metabolite itaconate has also been shown to inhibit SDH and has anti-inflammatory actions (32, 125-127).

1.11.6 Improving short and long-term outcomes

Evidence from animal models supports the role of reperfusion injury in a variety of diseases including organ transplantation. The translation of therapies from animal models to clinical transplantation has been met with limited success however.

1.12 Translation of transplantation research and rationale for project

Early research in transplantation identified and developed methods to preserve organs and these have proved largely successful allowing the widespread introduction of transplantation programmes. IR injury is inherent to organ transplantation. However, with the current need to continue to expand the donor pool to meet demand, the organs that are being transplanted today are increasingly exposed to more significant ischaemic insults and are less tolerant of ischaemia. The recognition of specific metabolic pathways that underpin IR injury may help to explain the paradoxically poor translation of findings from previous small animal models to clinical practice and provides a new opportunity for therapeutic intervention. The demonstration of conserved metabolic pathways across species is, however, fundamental if therapeutic efficacy is to be realized in clinical practice. Registry data and case series support the association of increased IR injury and a worse short-term graft and recipient outcome providing a rationale for the development of therapies to mitigate IR injury and improve short term outcomes.

In addition to the association with a worse short-term outcome, data from registries and case series also supports a role for IR injury mediating longer term outcomes in transplantation. Mechanistically, connecting a distinct, acute event such as IR injury and the insidious process of chronic rejection at the outset may seem contrived. However, the emergence of immunometabolism and the integral role of mitochondria in this process provides a potential link between these two events and supports the development of models that would enable further work and the development of therapeutic strategies for chronic rejection.

1.13 Aims of this work

The success of organ transplantation has led to it becoming a routine part of clinical practice. Nevertheless, demand for organs in the UK continues to outstrip supply and people continue to die on the waiting list. The persistent demand for organs has driven an expansion of the donor pool and the use of organs from DCD donors and other 'less than ideal' organs are fundamental to increasing the number of organs for transplantation. DCD organs provide a vital source of organs in the UK but have been exposed to an additional period of warm ischaemia that can impact outcomes. In addition, less-than-ideal organs (from extended criteria or marginal donors) may be less tolerant of additional warm and prolonged cold ischaemia than organs from SCD. The worse outcomes associated with periods of warm ischaemia and the relative intolerance of ischaemia that may be associated with 'less-than-ideal' organs are potentially routed in the pathological exacerbation of tissue injury that occurs on re-oxygenation that is termed reperfusion injury. Mitochondria are increasingly recognised as initiators of this process generating a burst of ROS upon reperfusion that drives downstream pathways and organ dysfunction. Therapies that ameliorate IR injury could therefore both improve outcome and further expand the donor pool. In addition to impacting short term outcome, increasing IR injury may also worsen chronic rejection and long-term outcomes. Understanding the biochemical pathophysiology is paramount to the development of rational therapeutic strategies to treat IR injury and improve outcomes.

This thesis sought to address the following hypotheses:

Mitochondrial dysfunction contributes to IR injury during organ transplantation and these mechanisms are amenable to therapeutic intervention.

Mitochondrial dysfunction and the subsequent tissue injury associated with IR injury impacts both short- and long-term allograft outcomes.

The overall objective of this thesis was therefore, to examine the mechanism of IR injury in organ transplantation and the relationship between IR injury and early and late organ dysfunction. Specifically, this work:

1. Investigated the metabolic profile of myocardial tissue during organ storage in mice, pigs and humans and identified key metabolic pathways, including the accumulation of succinate, and demonstrated whether these were conserved across species.

2. Explored the metabolic pathways identified through metabolic profiling and demonstrated efficacy in delivering metabolic inhibitors *in vivo* to moderate these key metabolic pathways.

3. Examined the efficacy of small molecule inhibitors in modifying reperfusion *in vivo* in a small animal model of solid organ transplantation.

4. Examined whether increasing IR injury was associated with an increase in chronic rejection in a validated, small animal model of organ transplantation.

Chapter 2: Methods

2.1 Chemicals and solvents

All chemicals were of analytical grade and obtained from Sigma Aldrich (UK) unless otherwise stated. Solvents used for the preparation of samples for LC-MS were of high pressure liquid chromatography (HPLC) grade (Thermo Fisher Scientific).

Soltran© (hyperosmolar citrate): K^+ 80 mM, Na^+ 84 mM, Mg^{2+} 41 mM, citrate 54 mM, sulphate 41 mM, mannitol 33.8g/l, pH 7.1

University of Wisconsin (UW) solution (Viaspan®, Cold Storage Solution, Bridge to Life Ltd, USA): hydroxyethyl starch 50 g/l, lactobionic acid 105 mM, KH_2PO_4 25 mM, MgSO 5 mM, raffinose 30 mM, adenosine 5 mM, allopurinol 1 mM, glutathione 3 mM, KOH 100 mM, pH 7.4

St Thomas' cardioplegia (Cardioplegic Solution, Harefield Hospital Formulation, Terumo BCT Ltd, UK): Na^+ 147 mM, K^+ 84 mM, Mg^{2+} 80 mM, Ca^{2+} 2 mM, Procaine 5 mM, Chloride 400 mM.

2.2 Animal work

2.2.1 Mouse strains and animal husbandry

C57BL/6 mice were purchased from Charles River Laboratories (Margate, UK). All animal experiments were approved by the UK Home Office under the Animals (Scientific Procedures) Act 1986. Mouse experiments were covered by project license PPL 80/2638.

Bm12.Kd.IE mice were previously created in-house from crosses using Bm12 mice (B6(C)-H2-Ab1bm12/KhEgJ (H-2^{bm12})(128) purchased from Jackson Laboratories (Bar Harbor, ME), B6.Kd mice (C57BL/6-Tg(K^d)RPb that additionally express the H-$2K^d$ gene) gifted by Dr R.P. Bucy (University of Alabama, Birmingham, AL)(129) and ABOIE mice (C57BL/6 mice that lack the expression of I-A^b, but express the I-Eα gene and express I-E on the surface of their APCs) gifted by Prof C. Benoist (Joslin Diabetes Centre, Boston, MA)(130). Initially bm12 were crossed with B6.Kd and the offspring that expressed I-A^{bm12} and H-$2K^d$ but not I-A^b were selected using PCR. These, bm12.Kd animals were then crossed with ABOIE animals and the female off-spring expressing I-A^{bm12}, A-E and H-$2K^d$ (bm12.Kd.IE) on PCR were selected(131).

All mice were maintained in specific-pathogen-free animal facilities with *ad libitum* access to food and water.

2.2.2 Porcine strain and animal husbandry

Large white male (Landrace) pigs (45-55 kg) were supplied by Envigo (Huntingdon, UK) and were acclimatised for a minimum of 7 days prior to experiments, with *ad libitum* access to food and water. All animal experiments were approved by the UK Home Office under the Animals (Scientific Procedures) Act 1986. Pig experiments were performed under project license WRS0001 (Envigo Reference).

2.2.3 Human tissue

Heart biopsies were taken from deceased human organ donors aged 36-69 (Figure 2). Ethical approval for the studies was obtained from NRES Committee East of England – Cambridge South (REC Reference 15/EE/0152). Informed consent was obtained from donor families for use of tissue for this study.

2.3 Murine experiments

2.3.1 Metabolite accumulation in organ storage

Metabolite accumulation during organ storage was measured in whole murine hearts exposed to variable periods of warm or cold ischaemia and compared to baseline normoxic hearts.

The donor animals were anaesthetised with isoflurane (Abbott Laboratories, US) and oxygen at 2 l/min. The animals' rectal temperature was measured continuously using a rectal thermometer and maintained at 37°C ± 1°C using a relayed variable heat mat (Kent Scientific). Heparin 100 µl heparin (100 IU in 100 µl 0.9% w/v sodium chloride Leo Pharma A/S, Ballerup, Denmark) was administered via Inferior Vena Cava (IVC) injection 1 minute prior to exsanguination by division of the IVC and aorta.

To measure metabolite concentrations in the heart under baseline normoxic conditions, as close as possible to those *in vivo*, the still-beating heart of anesthetised mice were rapidly frozen using Wollenberg clamps (manufactured by Josh Firman, LMB Workshop, UK) at liquid nitrogen (LN_2) temperature. This process from division of the great vessels to clamp freezing was performed in $\leq$ 5 seconds. The frozen myocardium was then scraped from the clamps and transferred to a pre-cooled (on dry ice) safe-lock Eppendorf and stored at –80°C until further analysis.

To measure metabolite accumulation in cold ischaemia (CI), hearts were placed directly in 10 ml UW solution (Viaspan®, Cold Storage Solution, Bridge to Life Ltd, USA) pre-cooled on wet ice (1-2°C). The retrieval of the heart by division of the great vessels in all experiments was performed in < 20 seconds. Under these conditions, the cardiac beat would stop within 5 contractions (< 5 seconds). To expose the hearts to warm ischaemia, the excised heart was left in the abdomen of the animal, with the abdominal wound closed and the animal maintained at 37°C on a heat mat. Under these conditions the hearts continued to contract intermittently for up to 90 seconds.

At the end of the period of warm or cold ischaemia, hearts were clamp frozen using Wollenberg clamps as described above. The clamped samples were promptly transferred to a pre-cooled (on dry ice) safe-lock Eppendorf and stored at –80°C until further analysis.

2.3.2 Heart temperature measurements

Myocardial temperature during the retrieval process was measured using a thermocouple (model: EasyLog EL-USB-TC-LCD, Lascar Electronics, UK). The donor animals were anaesthetised with isoflurane (Abbott Laboratories, US) and oxygen at 2 l/min. The animals' rectal temperature was measured continuously using a rectal thermometer and maintained at 37°C ± 1°C by a relayed variable heat mat (Kent Scientific). A laparotomy was performed and St Thomas' cardioplegic solution (Cardioplegic Solution, Harefield Hospital Formulation, Terumo BCT Ltd, UK) was administered systemically to the donor animal by IVC injection resulting in complete cessation of cardiac contraction. The heart was exposed, and a thermocouple inserted into the apex of the heart and secured using 10-0 suture (Bear Medic Corp.,

Tokyo, Japan). The heart was retrieved by either division of the great vessels (< 20 seconds) or using a standard retrieval technique described to enable heterotopic heart transplantation (approximately 8 minutes ± 30 seconds) described below (2.7). The hearts were then transferred into 10 ml UW (Viaspan®, Cold Storage Solution, Bridge to Life Ltd, USA) kept on wet ice (1-2°C). Temperature measurements were recorded every 5 seconds.

2.3.3 Administration of cardioplegia

Following division of the great vessels the normothermic mouse hearts continued to beat in isolation for up to 90 seconds. Immersion of a beating mouse heart in UW (Viaspan®, Cold Storage Solution, Bridge to Life Ltd, USA) solution kept on wet ice (1-2°C) produced rapid arrest of cardiac contraction. In order to ensure myocardial contraction was comparable under conditions of cold and warm ischaemia, systemic administration of cardioplegia (Cardioplegic Solution, Harefield Hospital Formulation, Terumo BCT Ltd, UK) via a central vein was used to produce rapid cessation of cardiac contraction (< 5 seconds). After administration of heparin (100 IU in 100 µl 0.9% w/v sodium chloride Leo Pharma A/S, Ballerup, Denmark) 500 µl of St Thomas' cardioplegia was administered by IVC injection using a 1 ml syringe attached to a 31-gauge needle. The apex beat was used to confirm cessation of cardiac contraction (less than 5 seconds). To minimise passive diffusion of the cardioplegia out of the heart and prevent spontaneous return of cardiac contraction, the abdominal aorta and IVC were not divided. The heart was retrieved by either division of the great vessels (< 20 seconds) and then stored in CI or WI as described above or using a standard retrieval technique described to enable heterotopic heart transplantation (approximately 8 minutes ± 30 seconds) described below. Spontaneous return of cardiac contraction was not observed after administration of cardioplegia in any hearts.

2.4 Porcine experiments

Pigs were sedated and received narcotic analgesia (ketamine 10 mg/kg, midazolam 0.1 mg/kg, medetomidine 0.02 mg/kg). General anaesthesia was induced using intravenous propofol (10 mg/ml) and remifentanil (6 µg/ml) through a peripheral vein. Animals were intubated and ventilated with intermittent positive pressure ventilation. Heart rate, blood pressure and O_2 saturation was monitored throughout the procedure. The pigs were exsanguinated and, at the time of exsanguination, the thoracic cavity was accessed through the diaphragm and the apex of the heart (~ 20 - 30 g) was amputated with a scalpel. A full thickness tissue sample (~ 100 mg) was immediately clamped frozen using Wollenberger clamps at LN_2 temperature, taking < 10 seconds from cessation of aortic pulse to freezing. The remaining tissue was divided in half, one half transferred to cold storage solution and then further cut into smaller pieces (~ 100 mg) which were then stored in UW (Viaspan®, Cold Storage Solution, Bridge to Life Ltd, USA) storage solution at ~ 2˚C. The other half of the heart tissue was also cut into sections (~ 100 mg) which were stored in a humidified atmosphere at 37˚C by suspension above saline in sealed Eppendorf tubes maintained using a heat block (Thermo Fisher Scientific, UK). At various times the tissues were then frozen using Wollenberger clamps at LN_2 temperature and stored at -80˚C until analysis.

2.5 Human experiments

Deceased human organ donors, undergoing donation after brainstem death (DBD) abdominal multi-organ procurement, but for whom cardiothoracic organs had been declined for transplantation were identified (Figure 2). Appropriate consent for research was obtained from the donor families. A thoracotomy was performed as a routine part of the abdominal organ retrieval procedure, thus allowing a sample (~ 20-30 g) of myocardium from the apex of the still-beating heart to be removed at the same time as exsanguination of the donor as part of the organ procurement procedure. The heart tissue was frozen in Wollenberg clamps, taking < 5 seconds to go from the beating oxygenated heart to frozen sample. After this base line sample, further samples (~ 100 mg) were removed, maintained at either 37˚C or 2˚C as described for the pig tissue, and at various times frozen and stored at -80˚C.

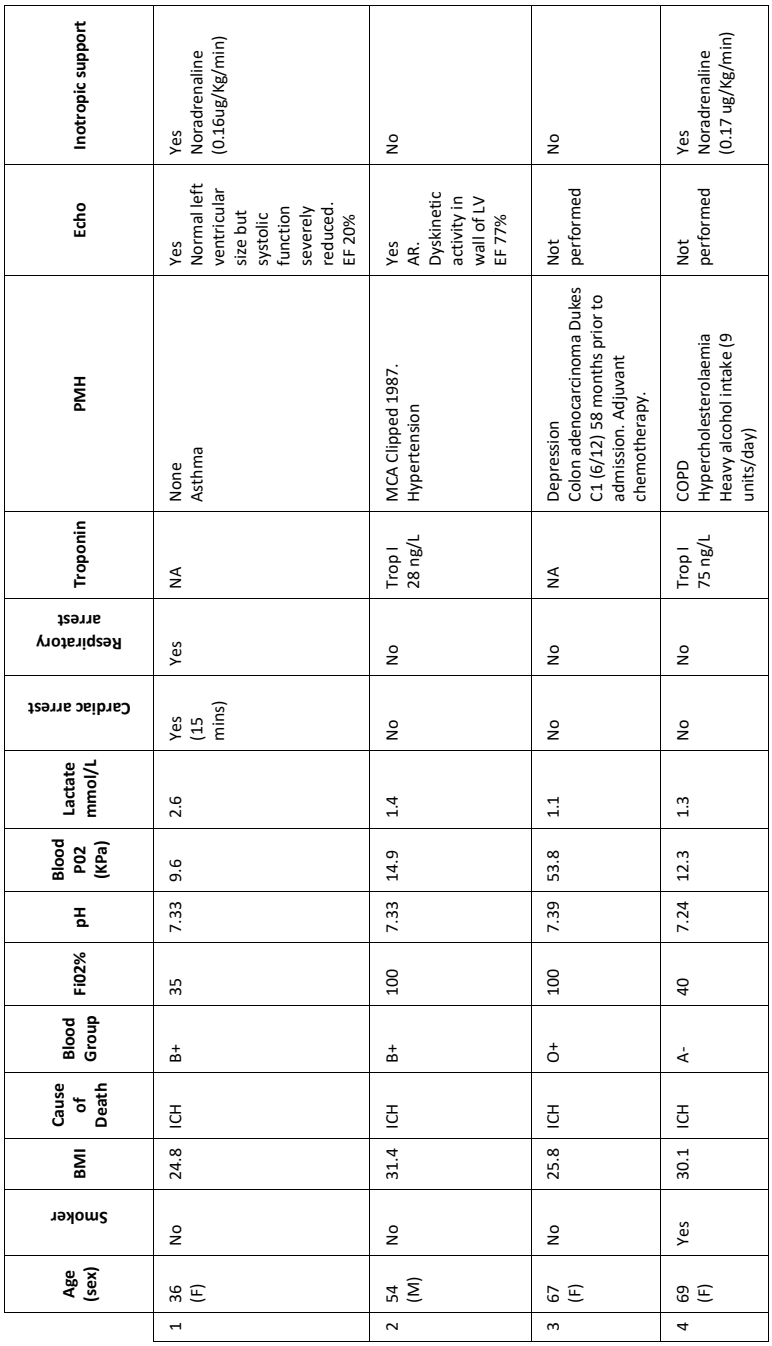

	Age (sex)	Smoker	BMI	Cause of Death	Blood Group	FiO2%	pH	Blood P02 (KPa)	Lactate mmol/L	Cardiac arrest	Respiratory arrest	Troponin	PMH	Echo	Inotropic support
1	36 (F)	No	24.8	ICH	B+	35	7.33	9.6	2.6	Yes (15 mins)	Yes	NA	None Asthma	Yes Normal left ventricular size but systolic function severely reduced. EF 20%	Yes Noradrenaline (0.16ug/kg/min)
2	54 (M)	No	31.4	ICH	B+	100	7.33	14.9	1.4	No	No	Trop I 28 ng/L	MCA Clipped 1987. Hypertension	Yes AR. Dyskinetic activity in wall of LV EF 77%	No
3	67 (F)	No	25.8	ICH	O+	100	7.39	53.8	1.1	No	No	NA	Depression Colon adenocarcinoma Dukes C1 (6/12) 58 months prior to admission. Adjuvant chemotherapy.	Not performed	No
4	69 (F)	Yes	30.1	ICH	A-	40	7.24	12.3	1.3	No	No	Trop I 75 ng/L	COPD Hypercholesterolaemia Heavy alcohol intake (9 units/day)	Not performed	Yes Noradrenaline (0.17 ug/Kg/min)

Figure 2: Human donor characteristics.

2.6 Tissue extraction and analysis

2.6.1 Liquid chromatography coupled to mass spectrometry (LC-MS)

Frozen tissue samples, obtained from murine, porcine and human experiments outlined above, were weighed into Precellys tubes prefilled with ceramic beads (Stretton Scientific Ltd., Derbyshire, UK), and an exact volume of extraction solution (30% acetonitrile, 50% methanol and 20% water) was added to obtain 40 mg specimen per ml of extraction solution. Samples were lysed using a Precellys®24 tissue homogeniser (Bertin Corp, Rockville, MD 20850, USA. 5500 rpm 15 seconds x 2) and then centrifuged (16,162 x g for 10 min at 4°C). The supernatant was transferred to glass vials (Microsolv Technology Corp., Leland, NC 28451, USA) and stored at -80°C until LC-MS analysis.

LC-MS analyses were performed on a Q Exactive Orbitrap (Thermo Scientific) mass spectrometer coupled to an Ultimate 3000 RSLC system (Dionex). The liquid chromatography system was fitted with either a Sequant ZIC-HILIC column (150 mm × 4.6 mm) or a ZIC-pHILIC column (150 mm × 2.1 mm) and respective guard columns (20 mm × 2.1 mm) (all Merck Millipore, Germany). The metabolites were eluted with previously described gradients (132). The mass spectrometer was operated in full MS and polarity switching mode. Samples were randomised in order to avoid bias due to machine drift and processed blindly. The acquired spectra were analysed using Xcalibur Quan Browser and XCalibur Quan Browser software (Thermo Scientific) by referencing to an internal library of compounds. Absolute quantification of selected metabolites was performed by interpolation of the corresponding standard curve obtained from serial dilutions of commercially available standards (Sigma Aldrich) run with the same batch of samples. When calculating relative change in metabolites with undetectable ion counts, half the lowest detectable ion count for that metabolite was used. LC-MS was analysis performed by Dr Ana S.H. Costa.

2.6.2 ATP/ADP ratio

ATP and ADP concentrations were measured using a Luciferase based assay (133). Frozen tissue samples were homogenised in ice-cold perchloric acid extractant (3% v/v $HClO_4$, 2 mM Na_2EDTA, 0.5% Triton X-100). The supernatant was diluted to a concentration of 1 mg frozen tissue/ml. Samples, ATP and ADP standards (400 µl) were pH neutralized using a potassium hydroxide solution (2 M KOH, 2 mM Na_2EDTA, 50 mM MOPS), vortexed until formation of a white precipitate ($KClO_4$), then centrifuged (17, 000 X g for 1 min at 4°C). For ADP measurements, 250 µl neutralised sample supernatant was mixed with 250 µl ATP sulfurylase assay buffer (20 mM Na_2MoO_4, 5 mM GMP, 0.2 U ATP sulfurylase (New England Biolabs), in Tris-HCl buffer (100 mM Tris-HCl, 10 mM $MgCl_2$ (pH 8.0) to 250 µl), incubated for 30 min at 30°C with shaking (500 rpm), heated at 100°C for 5 min and then cooled on ice. Standards (100 µl), samples for ATP measurement (100 µl) or samples for ADP measurement (200 µl) (in duplicate) were added to 400 µl Tris-acetate (TA) buffer (100 mM Tris, 2 mM Na_2EDTA, 50 mM $MgCl_2$, pH 7.75 with glacial acetic acid) in luminometer tubes. 10 µl pyruvate kinase solution (100 mM PEP, 6 U pyruvate kinase suspension (Sigma #

P1506)) were added to one set of samples for ADP measurement and incubated for 30 min at 25^{o}C in the dark to convert ADP to ATP. The other duplicate tube (without addition of pyruvate kinase solution) served as an ATP 'blank' value. The samples were then all assayed for ATP content in a Berthold AutoLumat Plus luminometer by addition of 100 µl Luciferase/Luciferin Solution (7.5 mM DTT, 0.4 mg/ml BSA, 1.92 µg luciferase/ml (SIGMA #L9506), 120 µM D-luciferin (SIGMA # L9504), made in TA buffer (25% v/v glycerol)), delivered via auto injection, protected from light. Bioluminescence of the ATP- dependent luciferase activity was measured 3 x for 1 min post injection and the data quantified against standard curves. The luciferase based assay was performed by Ms A Gruszczyk.

2.6.3 Glycogen assay

Animals were anaesthetised and donor hearts rapidly excised using the technique described above (2.3.1). The apex of the mouse heart was immediately transected (~ 10 mg) and clamp frozen to provide a baseline, normoxic control. The heart was then returned to warm or cold storage. Intermittently the heart was removed at variable times (6, 12, 30, 60 or 240 minutes) from storage and further myocardial axial sections (~ 10 mg) were excised and clamp frozen. After each sample was excised the heart was returned to organ storage and the process repeated to enable up to 4 separate time points to be taken. Tissue glycogen was measured using a standard assay and relative change in tissue glycogen compared against baseline normoxic values (134). The glycogen assay was performed by Ms F Allen (MRC Mitochondiral Biology Unit).

2.7 Heterotopic heart transplant models of IR injury

2.7.1 Murine heterotopic heart transplantation

The murine heterotopic heart transplant model is a vascularised solid organ transplant model. It was originally described by Corry et al(135) and the operations used in this work were performed using modifications of this original technique. The basic procedure is described below with subsequent variations on this technique described in detail later.

Operations were performed using an operating microscope (M651, Leica, UK) at 6 x to 40 x magnification. The total operative time for the combined donor and recipient procedures was approximately 50 minutes with an operative mortality of less than 5%.

2.7.2 Donor operation

Donor animals were anaesthetised with isoflurane (Abbott Laboratories, US) and oxygen at 2 l/min and the skin at the operative site shaved. Animals were then transferred from the anaesthetic room to the operation table and positioned in a supine position and secured using adhesive tape (Durapore™, 3M™, UK). The animals' rectal temperature was measured continuously using a rectal thermometer and maintained at 37°C ± 1°C using a relayed variable heat mat (Kent Scientific, UK). The depth of anaesthesia was adjusted as necessary to ensure complete absence of a response to a surgical stimulus.

A midline laparotomy incision was performed and 100 IU heparin (Leo Pharma A/S, Ballerup, Denmark) in 100 µl 0.9% w/v sodium chloride was administered via central vein injection using a 1 ml syringe attached to a 31-gauge needle. Animals were exsanguinated by division of the IVC and aorta. In experiments requiring cardioplegia administration, 500 µl cardioplegia (Cardioplegic Solution, Harefield Hospital Formulation, Terumo BCT Ltd, UK) was administered via the IVC using a 1 ml syringe attached to a 31-gauge needle. Cessation of cardiac contraction was observed before progression to thoracotomy but IVC and aorta were not transected to prevent passive diffusion of the cardioplegic solution and associated return of spontaneous contraction.

The thoracic cavity was entered by dividing the diaphragm and adequate exposure achieved by dividing the ribs laterally up to the thoracic inlet and retracting the anterior rib cage cranially. The IVC or caudal caval vein, left SVC or cranial caval vein and right SVC or cranial caval vein were ligated with silk ties(136). The fat and connective tissue was dissected between the aorta and pulmonary artery prior to division of the ascending aorta at the level of the innominate artery. If the heart were to be flushed (chapter 6), the innominate, right carotid and right brachiocephalic artery were ligated and divided. The descending aorta was then divided. The left and right pulmonary arteries were divided adjacent to their bifurcation and the connecting vessel wall divided to create a single opening. During dissection and ligation of vessels the heart was topically cooled intermittently with 0.9% w/v sodium chloride kept on ice. If the donor heart was flushed, 500 µl Soltran® (Baxter Healthcare) was injected via a fine bore (0.28 x 0.165 mm) polyethene tube (Portex tubing, Smith Medical International Ltd, UK) after ligation of the pulmonary artery in a

retrograde fashion into the descending aorta resulting in antegrade coronary perfusion. Adequate antegrade coronary flushing was confirmed visually by extrusion of blood from the pulmonary artery. Following ligation of the pulmonary artery blood remaining in the ventricles was manually expressed. The pulmonary veins were ligated *en masse* and the heart excised and stored in UW (Viaspan®, Cold Storage Solution, Bridge to Life Ltd, USA) until implantation.

2.7.3 Recipient operation

The donor heart was transplanted heterotopically into the abdomen of the recipient animal using a modified microsurgical techniques previously described by Lui *et al* (137). The recipient mouse was weighed before being anaesthetised with isoflurane (Abbott Laboratories, US) and oxygen at 2 l/min. The skin at the operative site was shaved and prepped with HibiScrub® (chlorhexidine gluconate 4% w/v, Mölnlycke Health Care, UK). Analgesia was administered by subcutaneous injection of 100 µl Temgesic (Indivior, UK) diluted in 500 µl 0.9% w/v sodium chloride to the nape of the animal. The animal was transferred to the operating table, secured in a supine position using adhesive tape (Durapore™, 3M™, UK) and the animal's rectal temperature was measured continuously using a rectal thermometer and maintained at 37°C ± 1°C using a relayed variable heat mat (Kent Scientific, UK). A midline laparotomy was performed and adequate exposure achieved using an abdominal self-retaining retractor. The urinary bladder was emptied by gentle pressure using sterile cotton buds. The small bowel and colon were reflected superiorly and a small strip of connective tissue divided to facilitate this manoeuvre. The abdominal viscera were retracted and covered with moistened sterile gauze to provide adequate exposure to the abdominal aorta and IVC and adequate moisture maintained throughout the procedure by periodic topical irrigation.

The connective tissue overlying the abdominal aorta and IVC was divided by a combination of sharp and blunt dissection. The posterior lumbar vessels were identified and ligated using 7-0 silk ties.

Non-crushing vascular clamps were applied to the vessels distal to the renal vessels and proximal to their bifurcation. The IVC was emptied via a venotomy created with a 31-gauge needle. An arteriotomy was then made in the aorta and this was extended using micro-surgical scissors to match the diameter of the donor aorta. The lumen was flushed with 0.9% w/v sodium chloride to remove any remaining blood and clots.

The donor heart was then retrieved from cold storage and placed into the right side of the recipient's abdomen with the remnant ascending aorta adjacent to the arteriotomy. A small piece of gauze moistened with cold (1-2°C) 0.9% w/v sodium chloride was placed over the heart to minimise warming and periodic topical application of (1-2°C) 0.9% w/v sodium chloride was applied to the donor heart during the procedure. Cranial and caudal stay sutures were placed between the donor and recipient vessels using 10-0 nylon Bear™ surgical suture on a round bodied 4 mm (3/8) needle (Bear Medic Corp., Tokyo, Japan). A continuous end-to-side anastomosis run in a counter clockwise direction was then

constructed from the caudal stay suture. After completing one side of the anastomosis, the heart was turned to the animal's left side to enable access and completion of the anastomosis.

The venotomy on the IVC was then extended in a cranial direction. The pulmonary artery was anastomosed in a similar fashion using 10-0 nylon Bear™ surgical suture. Over tightening of sutures was minimised to ensure there was no constriction of the anastomosis. Cut pieces of Surgicel® (Ethicon, Johnson and Johnson, US) were applied around the anastomosis. The distal clamp was removed followed by the proximal clamp. Satisfactory perfusion was indicated by a bright red heart displaying strong rhythmic contractions and warmed topical 0.9% w/v sodium chloride was applied to the heart to expedite this process. The abdominal fascia and skin were closed in two layers with continuous 5-0 vicryl™ (Ethicon, Johnson and Johnson, UK).

Following reperfusion and closure of the midline wound 500 µl of 0.9% sterile saline was injected subcutaneously.

Animals were recovered in an incubator at 28°C overnight on soft, dry bedding with food and water. Animals that developed post-operative hind limb paralysis were killed immediately. The next day animals were returned to standard cages with standard rodent diets and kept for up to 100 days.

2.7.4 Prolonged Cold Ischaemia

In order to develop a model of vascularised solid organ transplant IR injury it was necessary to modify the original procedure of Correy et al(135) to introduce an ischaemic insult. A model of mild and severe IR injury had previously been established and validated by Dr Kourosh Saeb-Parsy (Department of Surgery, Cambridge) and Dr Anna Dare (Mitochondrial Biology Unit, Cambridge)(138). This model introduced a period of prolonged cold ischaemia as the ischaemic insult. The "mild" IR injury group was performed using the standard technique and the heart was implanted and reperfused as quickly as is technically feasible. To introduce a more severe ischaemic insult the period in which the donor heart was stored in cold storage solution was extended from 30 minutes (as for the standard operation) to 4 hours. Previous work by Dr Kourosh Saeb-Parsy had demonstrated 4 hours to be the maximum tolerated period of ischaemia (personal communication) that was reliably associated with a return of spontaneous contraction upon reperfusion.

2.7.5 Prolonged Warm Ischaemia

Data from LC-MS of donor tissue following variable periods of warm and cold ischaemia demonstrated more profound metabolic changes during warm ischaemia. This provided a rationale for the development of a solid organ reperfusion model that introduced a warm ischaemic insult to the period of ischaemia.

The donor animal was anaesthetised and prepared using the standard technique described above and positioned on a variable temperature heat mat (Kent Scientific, US) linked to a rectal thermometer. After

administration of heparin the animal was exsanguinated by division of the IVC and aorta. Hearts were then either immediately retrieved with no additional warm ischaemia or left for 6 or 12 minutes prior to performing the standard retrieval operation. Spontaneous return of contraction was observed with hearts following both 6 and 12 minutes however, there was no significant difference in the 24-hour recipient serum troponin between recipients of hearts control hearts (no additional warm ischaemia) or those exposed to warm ischaemia (Figure 3.1).

To reduce variability in ischaemic injury, cardioplegia was administered to the donor heart at the time of retrieval. Using this technique it was necessary to proceed immediately to the retrieval operation to avoid passive diffusion of cardioplegia and a return of spontaneous contraction. During the retrieval operation, topical ice cold (2°C) saline was periodically applied to the heart. An additional period of warm ischemia was introduced by transferring the prepared donor heart to the abdominal compartment of the carcass maintained at 37°C with a heat mat for the duration of the additional warm ischaemia. After the period of warm ischaemia the heart was transferred to cold static storage as above.

2.7.6 Metabolic inhibitors

The effect of metabolic inhibitors on ischaemic metabolism was examined using two approaches. Metabolic inhibitors were either administered to the donor 10 minutes prior to retrieval as an infusion administered via a central vein or at the precise time of retrieval in cardioplegia (Cardioplegic Solution, Harefield Hospital Formulation, Terumo BCT Ltd, UK). The metabolic inhibitors used in these experiments are listed below;

Dimethyl malonate (DMM) (Sigma-Aldrich, UK)

Dimethyl succinate (DMS) (Sigma-Aldrich, UK)

Diazoxide (DZX) (Sigma-Aldrich, UK)

Hadacidin (HAD) (ACC Corporation, US)

2-(aminooxy)acetic acid hemichloride (AOA) (FluoroChem, UK)

Thenoyltrifluoroacetone (TTFA) (Sigma-Aldrich, UK)

Rotenone (ROT) (Sigma-Aldrich, UK)

2.7.7 Administration of small molecule inhibitors as infusion

Agents were administered as an infusion over 10 minutes via a central vein by microinfusion pump (Kd Scientific, Holliston, MA, USA) via a fine bore (0.28 x 0.165 mm) polyethene tube (Portex tubing, Smith Medical International Ltd, UK). Control animals were infused with 0.9% w/v sodium chloride by microinfusion pump (Kd Scientific, Holliston, MA, USA). On completion of the infusion, 100 µl heparin (Leo Pharma A/S, Ballerup, Denmark) was administered via central vein injection. Mice were divided into 2 groups; metabolic inhibitor (DMM; 16 $mgKg^{-1}min^{-1}$)

2.7.8 Administration of small molecule inhibitors with cardioplegia

Donor animals were prepped and draped as previously described and a midline laparotomy performed. 100 μl heparin (Leo Pharma A/S, Ballerup, Denmark) was administered via central vein injection. Metabolic inhibitors were administered in 500 μl of cardioplegic solution (Cardioplegic Solution, Harefield Hospital Formulation, Terumo BCT Ltd, UK) via a central vein. Retrieval proceeded immediately upon administration of cardioplegic solution. Mice were divided into 2 groups; metabolic inhibitor (DMM, DMS, AOA, DZX, HAD, TTFA, or ROT) or control (cardioplegia alone). Metabolic inhibitors were infused in a 500 μl bolus via the abdominal inferior vena cava in cardioplegic solution (Cardioplegic Solution, Harefield Hospital Formulation, Terumo BCT Ltd, UK) in the following doses; AOA; 20 μM, 200 μM, 2 mM, 20 mM, and 50 mM, DMM; 12 μM, 48 μM, 97 μM, 302 μM and 757 μM (concentrations of DMM were based on the equivalent total volume of DMM that would have been administered during a 40 minute infusion at the following rates; 1 $mgKg^{-1}min^{-1}$, 4 $mgKg^{-1}min^{-1}$, 8 $mgKg^{-1}min^{-1}$, 25 $mgKg^{-1}min^{-1}$, 62.5$mgKg^{1}min^{-1}$), DMS; 87.6 μM (the DMS concentration was based on the equivalent total volume of DMS that would have been administered during a 40 minute infusion of DMS at 8 $mgKg^{-1}min^{-1}$), HAD; 20 μM, 200 μM, 2 mM, 20 mM, and 50 mM, DZX; 100 μM and 1 mM, TTFA; 10 10uM, 100 μM, 1 mM, and 10 mM, and ROT; 6 μM and 60 μM. TTFA and rotenone were dissolved in 5% w/v DMSO in cardioplegia (Cardioplegic Solution, Harefield Hospital Formulation, Terumo BCT Ltd, UK).

2.8 Outcome markers of IR injury

To assess the tissue metabolomic profile on reperfusion of the graft, heart grafts were transplanted heterotopically into a syngeneic (C57BL/6) recipient using the technique described above (2.7.3). The recipient was recovered and the graft subsequently removed under terminal anaesthesia at 24 hours. At the time of harvest the animal was anaesthetised with isoflurane, a midline laparotomy performed. The heart was examined and the beat of the graft scored, a venous blood sample was taken from the IVC, and the heart was then excised by division of the anastomosed great vessels. The atria were removed and discarded. Axial sectioning of the remaining ventricular tissue was performed and specimens snap frozen in liquid nitrogen.

2.8.1 Troponin-I

Non-heparinised IVC blood samples were taken immediately prior to graft harvest. Samples were left for 30 minutes at room temperature to ensure adequate clot propagation, centrifuged (2000 x g for 10 minutes) and serum apportioned into aliquots and stored at -80°C. Serum was analysed for troponin-I and a panel of pro-inflammatory cytokines.

Troponin-I was measured using a mouse cardiac troponin-I ELISA (KT-470, Kamiya Biomedical Company, Seatlle, WA, USA) by the Core Biomedical Analysis Laboratory, Addenbrooke's Hospital, Cambridge.

The panel of inflammatory cytokines included IL-1ß, IL-6, IL-γ and was measured using a 10-plex electrochemical luminescence immunoassay for mouse cytokines (MesoScale Discovery) by the Core Biomedical Analysis Laboratory, Addenbrooke's Hospital, Cambridge.

2.8.2 Tissue mitochondrial DNA amplification

Mitochondrial DNA damage blocks progression of amplification of DNA polymerase during PCR and this enables the quantification of mitochondrial DNA damage using the technique described by Santos *et al* 2006 (107). This assumes that mitochondrial oxidative damage occurs at random and therefore, amplification of a long target (~ 10kb) will be interrupted with increasing oxidative damage as compared to a control short target (~ 120b).

Tissues were snap frozen and stored at -80°C prior to DNA extraction. DNA was isolated from tissues using the Qiagen DNeasy Blood and Tissue kit (Qiagen, UK). Briefly, approximately 20 mg tissue (heart apex) was transferred to an Eppendorf. The tissue was lysed with tissue lysis buffer (ATL) and 20 µl proteinase K, at 70°C in a shaking water bath until the tissue had been completely lysed. 200 µl proprietary buffer (AL) and 210 µl ethanol (96-100%) were added and the sample centrifuged (16 160 x g). Two washing steps (500 µl AW1 and AW2) were performed prior to elution. The eluted DNA was then quantified using the PicoGreen assay.

Primers were previously designed by Logan *et al*. for mice based on the sequence from Santos *et al*(107) and purchased from Sigma Aldrich.

The forward and reverse sequences for the short and long targets are detailed below:

	Tm° (°C)	GC%	Sequence
Forward primer	71.3	54.1	GCCAGCCTGACCCATAGCCATAAT
Long target reverse primer	67.0	44	GAGAGATTTTATGGGTGTAATGCGG
Short target reverse primer	68.8	54.5	GCCGGCTGCGTATTCTACGTTA

Each sample was amplified in duplicate. Each PCR reaction was 50 µl consisting of; 5 µl DNA sample (3 ng/µl, total DNA template [15 ng]) or standard, 35 µl mastermix (5 µl 10 X LA PCR Buffer II (without Mg^{2+}), 0.5 µl bovine serum albumin (10 mg/ml), 2 µl 25 mM $MgCl_2$, 1 µl dNTP Mixture (2.5 mM each dNTP), 2 µl forward primer [20 pmol], 2 µl reverse primer [20 pmol], 22.5 µl nuclease free water) and 10 µl Taq polymerase (1 U) in NFW.

The PCR conditions were chosen so that amplification occurred in a linear fashion with the amount of PCR product amplified from a 5 ng sample of undamaged control DNA was 50% (range 40-60%) that of a 10ng sample when quantified using the PicoGreen assay. To determine this, PCR was performed with increasing cycles of annealing and extension until a reaction that met the above criteria identified. For each experimental specimen a blank control (nuclease free water), 50% dilution of a control sample and a control sample reaction were performed. The PCR was started using a manual hot start with the parameters described below:

Short target		
Hot Start	70°C 3 minutes	
Denaturation	94°C 30 seconds	15 cycles
Annealing	64°C 45 seconds	
Elongation	72°C 45 seconds	
Final elongation	72°C 10 minutes	

Long target		
Hot Start	70°C 3 minutes	
Denaturation	94°C 30 seconds	20 Cycles
Annealing and elongation	64°C 12 minutes	
Final elongation	72°C 10 minutes	

2.8.3 Gel Electrophoresis

To confirm the products amplified by PCR were the long and short targets gel, electrophoresis was performed. 10 µl of the amplified DNA samples were suspended in 2 µl loading buffer (6x stock: 0.25% (w/v) bromophenol blue, 0.25% (w/v) xylene cyanol FF, 30% (w/v) glycerol in H_2O) were loaded on to a 0.8% (w/v) agarose gel in 1% TBE buffer supplemented with 1 µl GelRed™. Two separate ladders were run with the gel. A 1 Kb ladder (Invitrogen) and λ DA/HindIII digest (500 ng, New England Biolabs). The samples were separated by running the gel in TBE buffer for approximately 45 minutes at 100 V. The gel was visualised on a UV transilluminator and photographed with Genesnap software.

2.8.4 DNA Quantification

Quantification of the purified genome and the PCR products was performed using PicoGreen fluorimetric analysis. The samples were analysed in triplicate using the Quant-iT™PicoGreen®dsDNA Assay Kit (Invitrogen, ThermoFisher Scientific). DNA was quantified against a standard curve run with each plate. Samples were then diluted in TE to provide final concentrations of 3 ng/ml.

2.9 Outcome markers of chronic rejection

2.9.1 Collection of blood

Animals were warmed at 37°C to dilate tail veins. Tail vein blood samples were taken (20 – 30 µl) from animals. Samples were stored at 4°C to encourage clot formation. After centrifugation (16 162 x g for 7 min) serum was aspirated and aliquoted. Complement was inactivated by heating at 56°C for 30 min. Samples were stored at -20°C until they were analysed.

2.9.2 Quantification of anti-MHC class I antibody (H-K^d) by ELISA

Serum samples were collected weekly from recipient animals. An ELISA was used to quantify the production of anti-H-$2K^d$ antibody. 96 well plates were coated with recombinant conformational H-$2K^d$ (generated in-house(139)) at 5 µg/ml in Na_2CO_3-$NaHCO_3$ buffer (pH 9.6) and incubated overnight at 4°C. Non-specific binding was blocked with 200 µl/well Marvel (Premier International Foods, UK) dried skimmed milk powder (1 %) in PBS for 2 hours at 37°C. After washing (6 x 0.05% Tween in PBS), 50 µl 1:9 dilutions (in Marvel/PBS) of samples were added to wells of the top row. Triplicate serial dilutions (1/n) were performed down the plate. The plate was incubated for 1 h. After washing (Tween/PBS) 50 µl/well of biotinylated Rabbit F(ab')2 anti-mouse IgG (STAR11B, AbD Serotec, Oxford, UK) at 1 µg/ml in Marvel was added to all wells and the plate incubated for 1 h at 37°C. After washing (Tween/PBS) 50 µl of ExtrAvidin peroxidase conjugate (Sigma, Poole, UK) at 1 µg/ml in Marvel/PBS was added and incubated at room temperature for 1 h. Plates were washed (Tween/PBS) and TMB microwell peroxidase substrate (Kirkegaard & Perry Laboratories, Gaithersburg, MD, USA) was added. The colour change was observed for 5 min before the reaction was stopped with 50 µl 0.2M H_2SO_4 and the absorbance at 450 nm measured using a FLUOstar OPTIMA plate reader (BMG Labtech, Aylesbury, UK). For each sample, the area under the curve of an absorbance versus dilution curve was calculated. On each plate a serial dilution positive (pooled hyperimmune serum from C57BL/6 recipients of BALB/c cardiac allograft collected at 5 weeks post-transplant) and negative (pooled serum from a naïve C57BL/6 mouse) control was run. The AUC of each experimental sample was expressed as a percentage of the AUC of the positive control (pooled hyperimmune) serum(140).

2.9.3 Quantification of autoantibody level by HEp-2 indirect immunofluorescence

The relative antinuclear antibody (ANA) was quantified using a commercially available human epithelial type 2 (HEp-2) indirect immunofluorescence kit (NOVA Lite®, Inova Diagnostics, Inc. San Diego, CA 92131, US). This technique was developed for detecting autoimmune responses in human patients but murine autoantibody has also been shown to bind the target nuclear antigens and has been previously validated for the detection of autoantibody production in transplant models of chronic rejection(131, 141, 142).

Serum samples were diluted 1 in 40 with dilute PBS and incubated for 30 minutes on slides coated with HEp-2 cell line. Bound autoantibody was detected with fluorescein labelled conjugated goat anti-mouse

IgG (STAR70; AbD Serotec, Oxford, UK) by fluorescence microscopy. The intensity of staining of 3 random photomicrographs was measured by morphometric analysis using MetaMorph software (Molecular Devices, Downington, PA, USA). Monospecific positive and negative controls were used according to the manufactures instructions to ensure all reagents and procedures performed appropriately. Serial two-fold dilutions (1 in 10 to 1 in 2560) of pooled hyperimmune serum from TCRKO mice injected IV with 5 x 10^6 purified bm12 CD4 T cells was used to generate a standard curve (Figure 3). This has previously been demonstrated to generate an ANA response(142). Serial dilutions were assigned arbitrary values of 1000 autoantibody units for the 1 in 10 dilution, 500 units for the 1 in 20 dilution etc. The presence of autoantibody in samples was then interpolated using the relative fluorescence intensity compared to a rectangular hyperbola calculated using the standard control values (Figure 3).

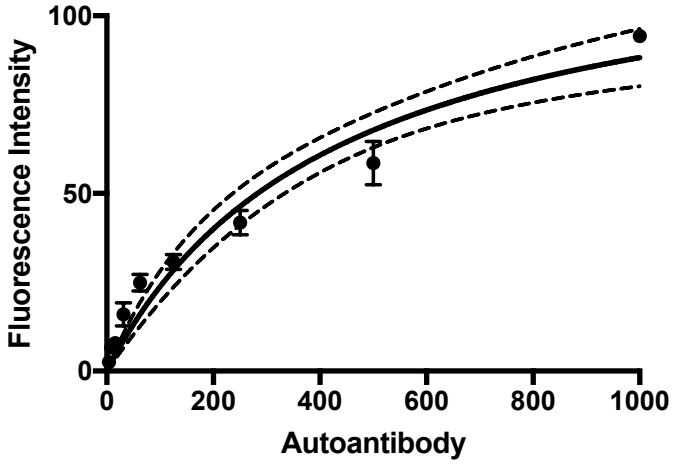

Figure 3: Human epithelial cell line (HEp-2) standard dilution curve.

The relative fluorescence intensity of serial two-fold dilutions of pooled hyperimmune serum (1 in 10 to 1 in 2560) from TCRKO mice injected i.v. with 5 x 10^6 purified bm12 CD4 T cells was measured by morphometric analysis to generate a standard curve that was used to interpolate relative fluorescence of samples.

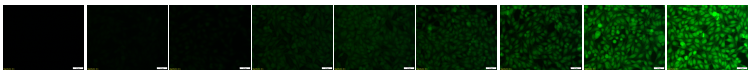

Antibody dilution	1 in 2560	1 in 1280	1 in 640	1 in 320	1 in 160	1 in 80	1 in 40	1 in 20	1 in 10
Arbitrary value	3.906	7.181	15.63	31.12	62.5	125	250	500	1000

Figure 4: Representative immunofluorescence photomicrographs of hyperimmune serum at increasing dilutions.

Control serum samples at increasing dilutions (1 in 2560 to 1 in 10) were diluted 1 in 40 with dilute PBS and incubated for 30 minutes on slides coated with HEp-2 cell line. Bound autoantibody was detected with fluorescein labelled conjugated goat anti-mouse IgG (STAR70; AbD Serotec, Oxford, UK) by fluorescence microscopy.

2.9.4 Rejection kinetics

Rejection of the grafts was assessed by abdominal palpation. Rejection was defined as the complete cessation of a palpable contraction.

2.9.5 Chronic allograft vasculopathy

Donor hearts were stored in 10% formalin in PBS. Paraffin embedded slides were prepared and stained with haematoxylin and eosin (H&E) or elastin van Gieson (EVG) by the Department of Pathology, Papworth Hospital, Cambridge, UK.

Chronic allograft vasculopathy was assessed using CellR digital imaging software. Luminal stenosis was calculated in elastin positive vessels in each section. The measured cross-sectional area of the lumen was subtracted from the cross-sectional area of the internal elastic lamina. This area was then measured as a percentage of the internal elastic lamina cross-sectional area giving a percentage luminal stenosis (%) (Figure 5).

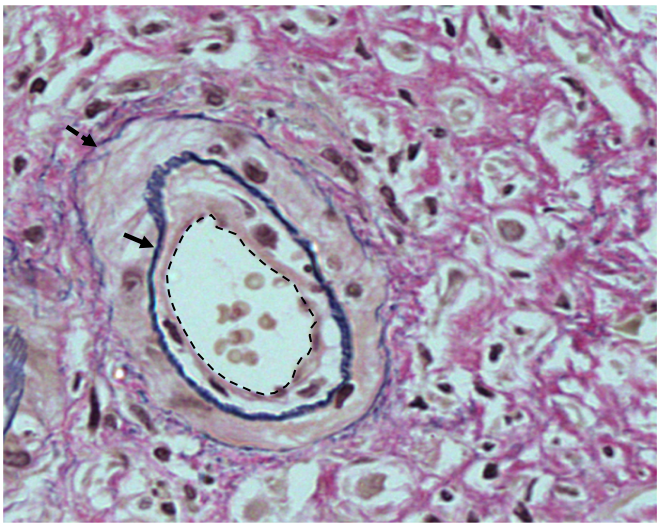

Figure 5: Representative section of a coronary vessel with evidence of vasculopathy.

Donor hearts were formalin fixed, paraffin embedded and slides prepared and stained with elastin van Gieson (EVG). The cross-sectional area of arteries and luminal stenosis was estimated from the cross-sectional area of the lumen and internal elastic lamina using CellR digital imaging software. External elastic lamina (dashed arrow); internal elastic lamina (solid arrow); lumen (dashed line).

2.9.6 Statistics analysis

All data in figures are presented as mean values ± SEM nless otherwise stated. Statistical analysis was performed between two groups using Student's t-test and between multiple groups by one-way analysis of variance (ANOVA) or two-way ANOVA with Bonferroni's multiple comparison testing. A p value of less than 0.05 was considered significant.

To calculate relative concentrations of metabolites that were not detected in all time points by mass spectrometry, half the minimal detectable ion intensity (AU) was used.

2.9.7 Collaborative experiments

A number of experiments were performed in collaboration with other experimenters. Dr Ana S.H. Costa. (MRC Hutchinson/MRC Research Centre, UK) was responsible for LC-MS analysis of tissues and generated the heat maps. The luciferase-based assay was performed by Ms A Gruszczyk (MRC Mitochondrial Biology Unit, UK). The glycogen assay was performed by Ms F Allen (MRC Mitochondrial Biology Unit, UK). Dr Alan Robinson (MRC Mitochondrial Biology Unit, UK) assisted in the analysis of metabolomic data and generated the volcano plots presented.

Chapter 3: The metabolic profile of cardiac tissue during warm and cold ischaemia

3.1 The metabolic profile of cardiac tissue during warm and cold ischaemia

3.1.1 Introduction

Hypothermia has long been recognised to have therapeutic potential in a range of clinical scenarios and has formed the mainstay of organ preservation for the great majority of the modern era of organ transplantation (143). During a transplant procedure, the transplanted organ is subjected to ischaemic conditions across a range of temperatures for varying periods of time. The potential permutations of warm and cold ischaemia to which an organ is subjected has increased with the greater use of DCD organs and renewed interest in hypothermic and normothermic machine perfusion techniques.

The general principle commonly assumed to account for these observed protective effects is stipulated by the Arrhenius equation, the foundation for which lies in the Van't Hoff equation. A generalisation of these formulae is that most enzymatic reactions have a Q_{10} temperature coefficient of approximately 2 and therefore, for every 10°C increase in temperature, the metabolic rate doubles. This is also true in the reverse and therefore there is a halving in the metabolic rate with every 10°C decrease in temperature (143, 144). Anecdotal observations would suggest that the mechanism of hypothermic protection may, however, be more complex and could vary between tissue types(143).

3.1.2 Temperature changes during organ storage

To examine the metabolic changes that occur *in vivo*, mouse, pig and human models of organ storage were developed to measure the changes in a range of metabolites using an untargeted mass spectrometry approach. The mouse model was based on the modified retrieval procedure used for the heterotopic heart transplantation model reported by Dare *et al* (138) and used to investigate IR injury in organ transplantation. To characterise the metabolic profile of mouse hearts during warm and cold ischaemia a simplified model was first devised. In this model, the heart was rapidly excised by division of the great vessels and placed in warm or cold ischaemic conditions for variable periods. Cold ischaemia was induced by placing the heart in UW cooled on ice. Using this technique, hearts were rapidly cooled to 10 °C within 12 seconds of immersion, reaching 3°C after 1 minute and 2°C after 2 minutes (Figure 6(a)). Warm ischaemic conditions were designed to replicate the clinical environment of DCD donation and therefore, the excised hearts were placed in the abdominal compartment of the carcass of the animal whose core rectal temperature was maintained at 37°C. After the period of ischaemia had elapsed the heart was rapidly frozen using Wollenberg clamps and the metabolic profile analysed by untargeted LC-MS. Comparative analyses of the changes in myocardial tissue were also performed using pig and human hearts. In these models, the apex of the heart was rapidly divided. Full thickness sections of myocardium were then placed in warm or cold storage and the changes in metabolites compared to a baseline, normoxic control sample from the same heart.

During the retrieval process for mouse heterotopic heart transplantation, the animal was exsanguinated by division of the IVC or caudal caval vein and aorta and rendered hypoxic by division of the diaphragm and subsequent clamshell thoracotomy. The necessary ligation and division of various great vessels in preparation for subsequent implantation took approximately 7 - 8 minutes. During this period, the heart was intermittently topically cooled with ice cold saline. Topical cooling of the heart results in brief periods of cooling to approximately 12°C and subsequent rewarming to 24°C (Figure 6 (b)). The cooling resulted in marked bradycardia or intermittent brief periods of asystole and rewarming was associated with restitution of ventricular contraction (personal observation).

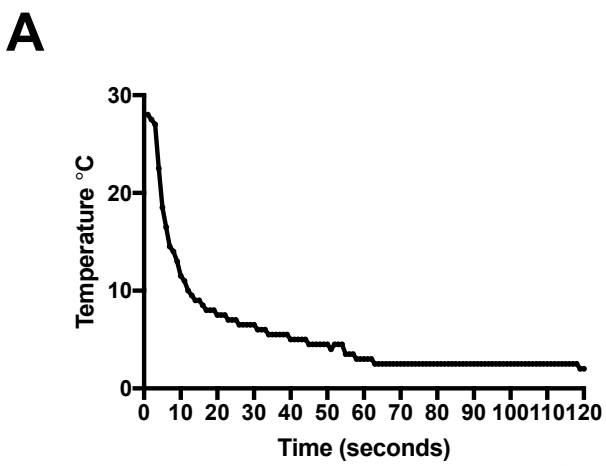

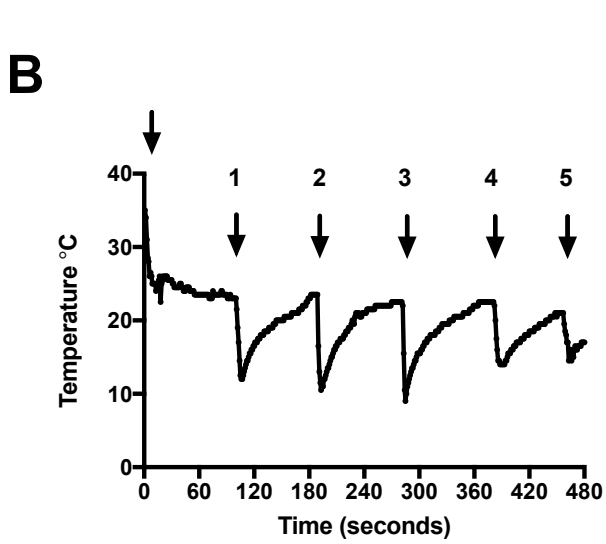

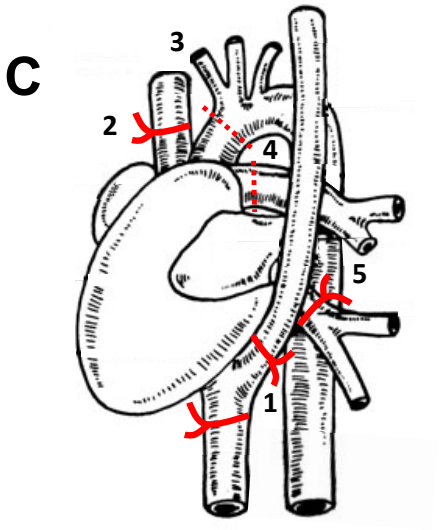

Figure 6 (a - c): Temperature profile of the myocardial apex during cold storage and retrieval in murine heart transplantation.

The temperature of the apex was measured using a thermocouple placed into the myocardium. (**A**) Hearts were either rapidly excised and placed in cold storage or (**B**) retrieved using a technique with the necessary surgical preparation of the great vessels required for heterotopic heart transplantation. During this process topical saline was applied at the start of the retrieval process and then at regular intervals thereafter (arrows). (**C**) demonstrates the murine cardiac anatomy and the great vessels that were ligated (red) and divided (dashed red line) in preparation for transplantation; 1. ligation and division of the IVC or caudal caval vein and left superior vena cava (SVC) or left cranial caval vein (CCV), 2. ligation and division of the right SVC (right CCV), 3. preparation and division of the ascending aorta, 4. preparation and division of the pulmonary artery, 5. ligation and division of the pulmonary veins (145).

3.2 Changes in energy stores

Changes in tissue energy stores are recognised as important determinants of cell integrity and viability and previous work into the mechanism of hypothermic organ protection has focused on the ATP/ADP ratio as this determines the driving force for reactions (146). Two techniques were used to analyse the changes in myocardial ATP and ADP concentration in the mouse heart tissue in this model; Ms A Gruszczyk (Department of Surgery and MRC Mitochondrial Biology Unit) used a luciferase-based assay, and Dr Ana S.H. Costa (Hutchinson/MRC Research Centre) used LC-MS. The luciferase-based assay has been well validated and estimates absolute tissue concentrations of ADP and ATP which can then be used to estimate relative change compared to the normoxic baseline tissues if required. We have less experience measuring ATP with LC-MS. Estimates of tissue concentrations could be inferred from ion counts that could then be used to calculate relative change compared to normoxic baseline tissues. There was concern that there would be degradation of phosphate groups during analysis however, the luciferase-based analysis enabled validation of the LC-MS ATP and ADP data. There was a more rapid decrease in the ATP/ADP ratio in warm ischaemia than in cold ischaemia consistent with the hypothesis that cold storage provides organ protection, at least in part, through preservation of the ATP/ADP ratio (Figure 7). Mammalian cytosolic ATP/ADP ratio estimates in the literature range from 1 to > 100. The wide range is likely due to the inherent problems in measuring tissue concentrations of these nucleotides *in vivo*. Changes in tissue metabolite concentrations were calculated as relative change to normoxic control hearts using LC-MS. The luciferase-based assay provided an estimate of the absolute tissue concentrations of ATP and ADP.

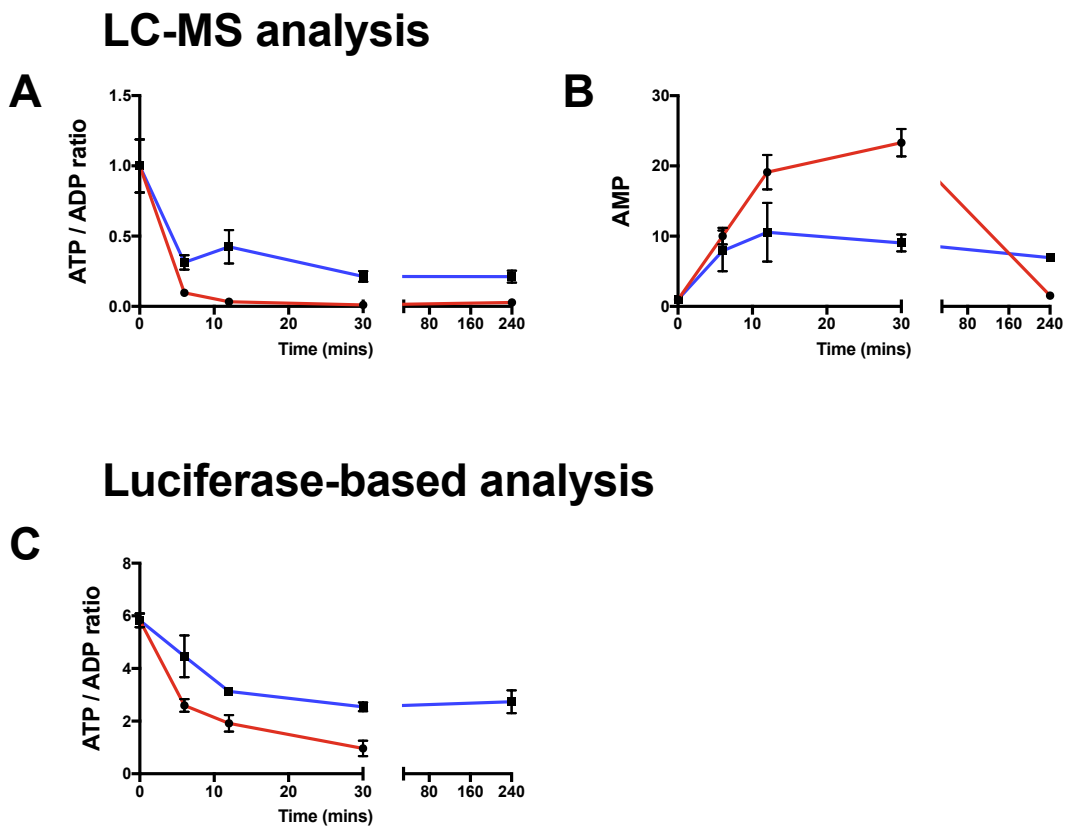

Figure 7 (a – c): ATP/ADP ratio and tissue AMP concentrations in the mouse heart during warm and cold ischaemia.

(a) ATP/ADP ratio in the mouse heart during warm (red) and cold (blue) ischaemia measured by LC-MS. Mouse hearts were rapidly excised and exposed to either warm (red line) or cold (blue line) ischaemia (n = 4-5). Tissue abundance of ATP and ADP was analysed by LC/MS and used to calculate the relative change of each nucleotide in tissue abundance compared to normoxic control hearts (n = 11). The ATP/ADP ratio was calculated from the derived relative change for each heart.

(b) AMP concentration in the mouse heart during warm and cold ischaemia measured by LC-MS. Relative tissue concentrations of AMP estimated by LC-MS (n = 4-5) during warm (red line) and cold (blue line) ischaemia and compared to normoxic control hearts (n = 11)

(c) ATP/ADP ratio in the mouse heart during warm and cold ischaemia measured by luciferase-based assay. Absolute tissue concentrations of ATP and ADP (nmol) were calculated using the luciferase-based assay for each heart (n = 4-13) and used to generate a mean ATP/ADP ratio of mouse heart tissue during warm and cold ischaemia.

There was a rapid decrease in the ATP/ADP ratio within 6 minutes of ischaemia that was more pronounced during warm ischaemia compared to cold ischemia. This trend was observed using both techniques. There was a discrepancy between the two techniques with detectable tissue ATP and ADP concentrations declining more rapidly when calculated using LC/MS. When calculated using LC-MS, this translated to detectable ATP/ADP ratios that rapidly approached zero during warm ischaemia when compared to normoxic baseline control tissue. The ATP ion count was detected in tissue during cold storage, however, which translated into an ATP/ADP ratio that remained at approximately 20% of normoxic control tissue after the initial rapid decline. The changes in nucleotides that contributed to the differences in the ATP/ADP ratio determined by LC-MS differed in warm and cold ischaemia. The relative tissue ATP was better preserved during cold ischaemia, remaining at approximately 80% of baseline until 30 minutes compared to warm ischaemia where relative ATP rapidly approached zero. ADP relative tissue concentrations increased more rapidly and remained better preserved in cold ischaemia compared to warm ischaemia. In warm ischaemia, ADP concentrations increased less rapidly when compared to the baseline, normoxic controls and achieved lower peak concentrations at 12 minutes. Relative tissue concentrations then decreased to near undetectable levels at 30 minutes (Figure 8).

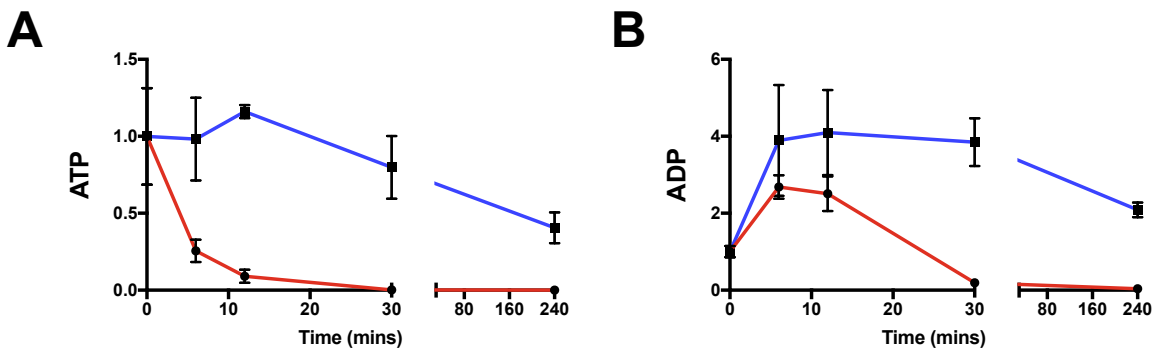

Figure 8: Changes in tissue concentrations of (a) ATP, and (b) ADP during warm (red) and cold (blue) ischaemia in the mouse heart measured by LC-MS.

Mouse hearts were rapidly excised and exposed to either warm or cold ischaemia (n = 4-5). Tissue abundance of ATP and ADP was analysed by LC/MS and used to calculate the relative change of each nucleotide in tissue abundance compared to normoxic control hearts (n = 11).

These findings from the LC-MS analysis were in contrast to the changes demonstrated by the luciferase-based assay. Here the ATP/ADP ratio was largely determined by ATP tissue concentrations which decreased more rapidly during warm as compared to cold ischaemia with ADP concentrations remaining constant (Figure 7 (c)). In addition to the rapid decrease in the ATP/ADP ratio, the overall consumption of nucleotides was faster during warm ischaemia when compared to cold ischaemia as indicated by the sum of ATP and ADP (Figure 9(a)). Although the relative changes in ATP/ADP ratio and AMP were largely conserved across species, it was interesting to observe the marked differences in the baseline levels of ATP and ADP between the mouse, and the pig and human myocardium (Figure 9 (c)(i) – (vi)). This may reflect differences in the experimental technique, however accurate understanding of baseline energy stores across species is

surprisingly sparse within the literature. It will be important to examine these apparent discrepancies in more detail in future studies. Understanding these differences will be paramount in translating findings from animal models to clinical trials and the conserved absolute concentrations of ATP and ADP between the pig and human tissue would support the need for validation of findings from small animal models in such large animal models.

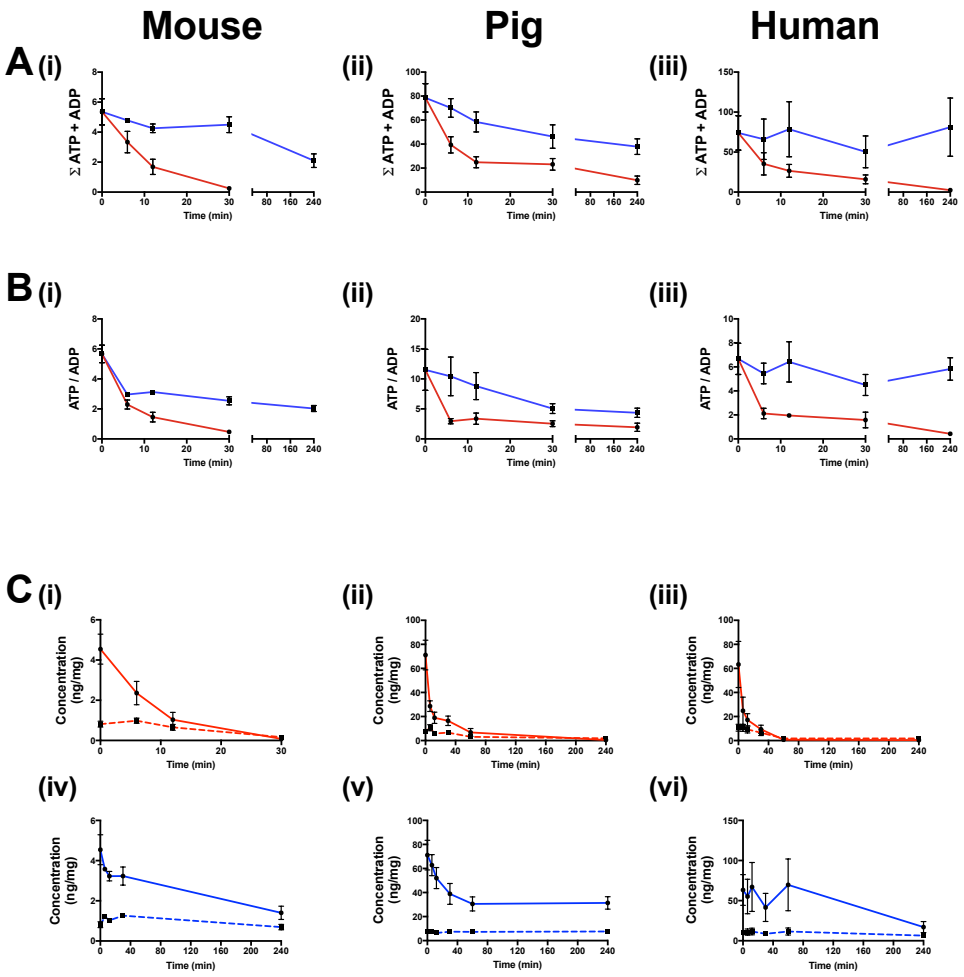

Figure 9: ATP and ADP concentrations during warm and cold ischaemia in the mouse, pig and human heart.

Mouse hearts were rapidly excised and exposed to either warm or cold ischaemia (n = 3-4). For the pig (n = 5) and human (n = 4) assays, the apex was excised from normoxic hearts and rapidly divided into multiple full thickness sections and exposed to either warm (red line) or cold (blue line) ischaemia (n = 5). The ATP and ADP concentrations were calculated using a luciferase-based assay and are presented in columns for the mouse, pig and human. The total nucleotides (ΣATP + ADP) (a(i)- (iii)), the ATP/ADP ratio (b (i) – (iii)), and the absolute tissue concentrations of both ATP (solid line) and ADP (dashed line) for warm (red line) and cold (blue line) (c (i)- (vi)) are presented for mouse, pig and human.

AMP-activated protein kinases (AMPK) play a crucial role in regulating cellular ATP during periods increased demand such as hypoxia. During periods of ATP depletion, adenylate kinase is activated converting two molecules of ADP to ATP and AMP (147, 148). In these experiments, tissue AMP concentrations increase rapidly until 6 minutes in both warm and cold ischaemia relative to normoxic

control hearts. After this time, the relative tissue concentrations then diverge as AMP levels during cold ischaemia plateau, whereas AMP concentrations in warm ischaemia continue to rise until 30 minutes of warm ischaemia (Figure 7). The findings in this analysis are consistent with these previous studies that propose activation of adenylate kinase as a cardioprotective mechanism to maintain cellular ATP during periods hypoxia (148).

The changes in nucleotides were also analysed in pig and human heart tissue. The ATP/ADP ratio was calculated using the luciferase-based assay and tissue AMP relative abundance was calculated using LC-MS. Similar relative changes to those in the mouse were observed in pig and human heart tissue during warm and cold ischaemia (Figure 10).

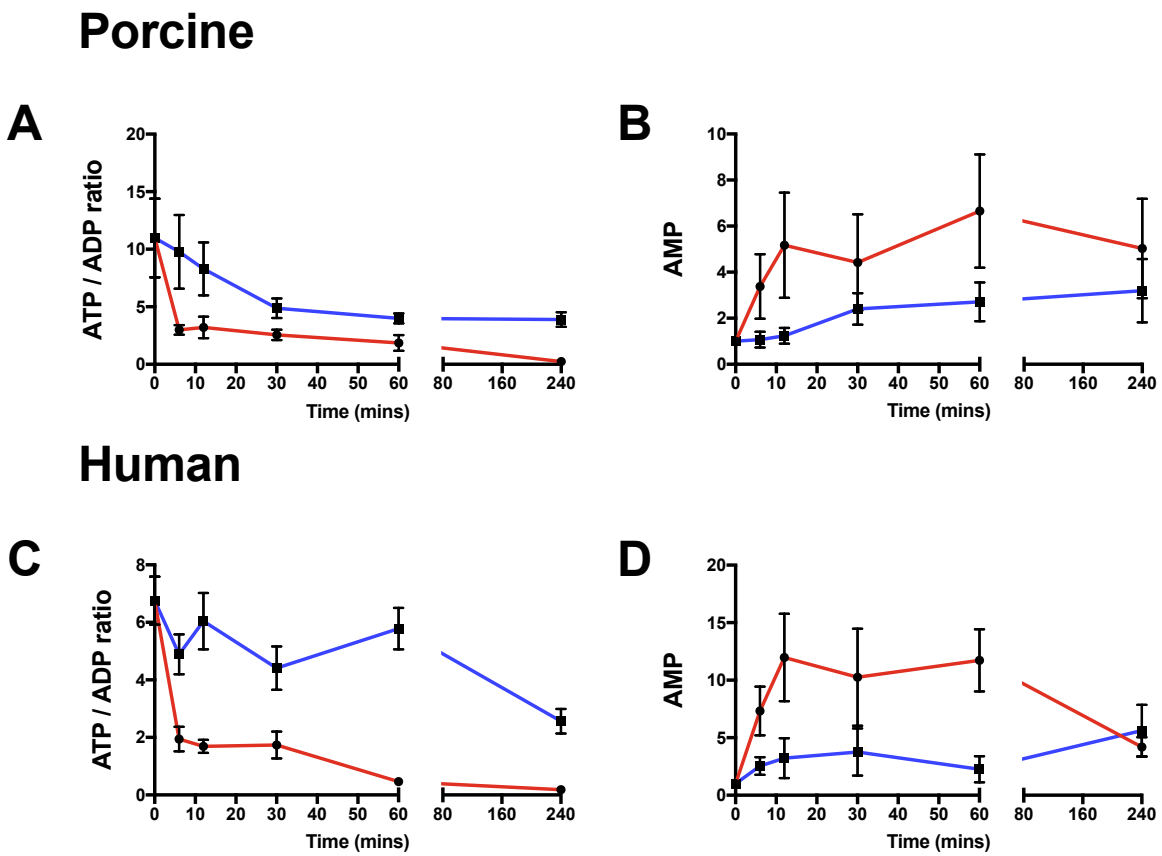

Figure 10 (a – d): ATP/ADP ratio and tissue AMP concentration in the pig and human heart during warm (red) and cold (blue) ischaemia.

(a) The apex was from excised from normoxic pig hearts and rapidly divided into multiple full thickness sections and exposed to either warm (red line) or cold (blue line) ischaemia (n = 5). The ATP/ADP ratio was calculated using a luciferase-based assay. **(b)** Tissue abundance of AMP was analysed in the same samples by LC/MS and the relative change in tissue abundance compared to the normoxic control tissue for each pig heart (n = 5).

The same method was used to process human hearts (n = 4). **(c)** The ATP/ADP ratio was calculated using a luciferase-based assay. **(d)** Tissue abundance of AMP was analysed in the same samples by LC/MS and the relative change in tissue abundance compared to the normoxic control tissue for each human heart (n = 4).

3.2.1 Summary of changes in energy stores

Warm ischaemia is associated with a more rapid decrease in the nucleotides ATP and ADP than during cold ischaemia. This was paralleled by an accumulation of AMP and a more rapid loss of the ATP/ADP ratio during warm ischaemia compared to cold ischaemia and is consistent with the protective effect of cold storage during organ ischaemia. These changes were observed in myocardium from mice, pigs and humans.

3.3 Changes in metabolites during warm ischaemia and cold ischaemia

LC-MS-based metabolomic analysis of tissue allows the simultaneous measurement of a range of metabolites. Subsequent LC-MS analyses reported in the following chapters were all performed with Dr Ana S.H. Costa (Hutchinson/MRC Research Centre). Myocardial tissue of mouse, pig and human hearts was exposed to varying periods of warm and cold ischaemia. In total 54 metabolites were analysed in all samples in mouse, pig and human myocardial tissue. These data are presented as heat maps generated with these data by Dr Ana S.H. Costa (Hutchinson/MRC Research Centre) (Figure 11). Qualitatively, it was observed that similar metabolic changes were present in mouse, pig and human heart tissue during warm and cold ischaemia.

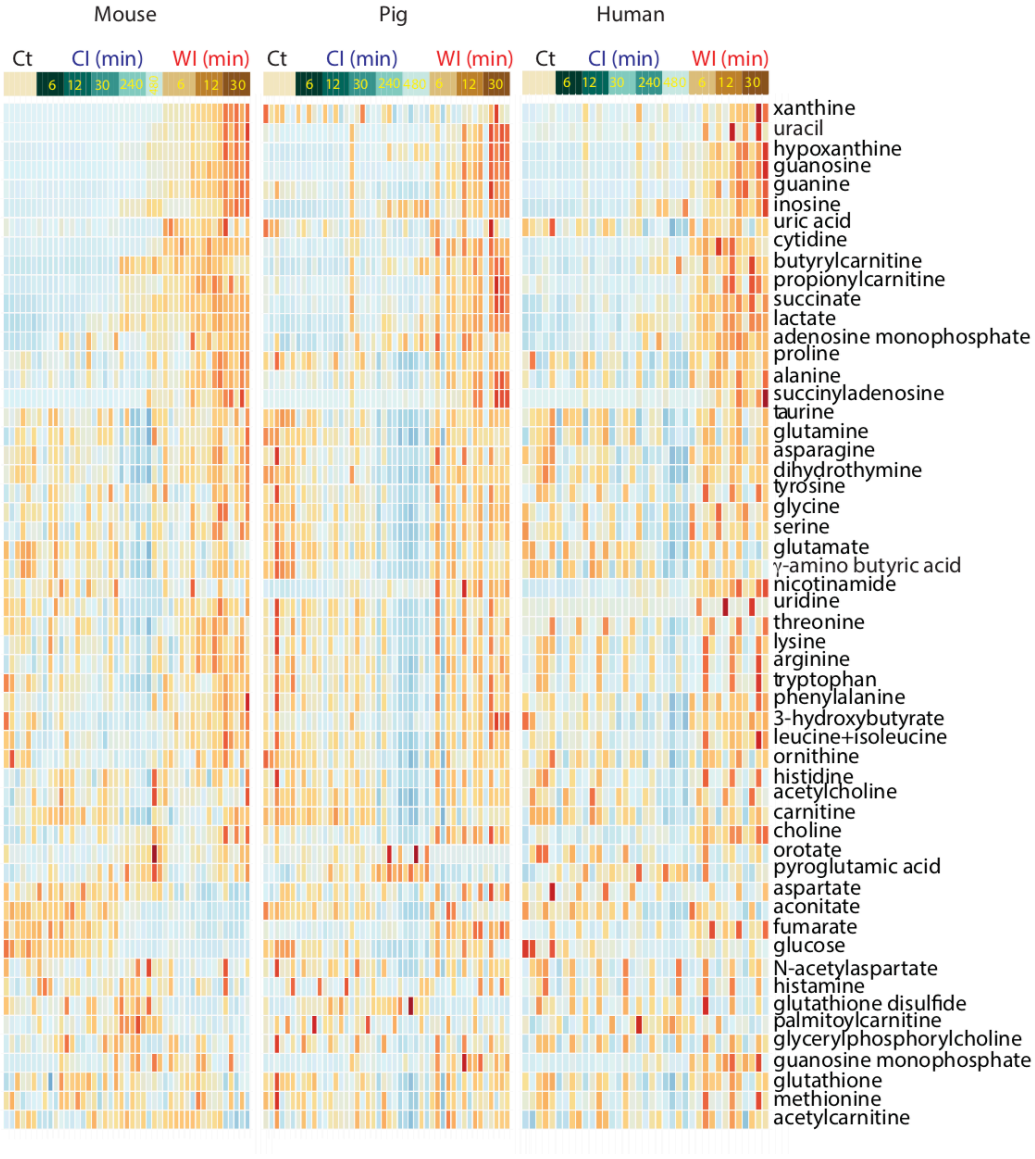

Figure 11: Extended analysis of metabolic changes in the mouse, pig and human during warm and cold ischaemia.

Heat maps showing the relative change in metabolite abundance of 107 different metabolites during warm ischaemia (WI) and cold ischaemia (CI) in mouse (n = 4-11), pig (n = 5) and human (n = 4) heart tissue. The data are from 3-6 independent biological replicates and relative change was compared to normoxic controls (Ct). Colour corresponds to relative change compared to normoxic control heart tissue. Blue labelled metabolites are less abundant, orange-red labelled metabolites are more abundant. Heat maps were constructed by Dr Ana SH Costa.

To facilitate a quantitative comparison of the metabolites that significantly changed between warm and cold ischaemia, I determined the fold change for each metabolite between warm and cold ischaemia at various times. Using the adjusted p value and the fold change, volcano plots were constructed with Dr A Robinson (MRC Mitochondrial Biology Unit) (Figure 12). Using this analysis, metabolites that changed in the same way between warm and cold ischaemia in all three species were identified and have been

annotated in red. Metabolites that changed in the same way in two of the species have been annotated in green. An extended metabolic analysis was performed for the mouse heart tissue. This MS analysis was performed using a second column and increased the total number of metabolites analysed to 107. The metabolites that were shown to differ significantly between warm and cold ischaemia in the additional analysis performed in the mouse heart have been annotated in blue.

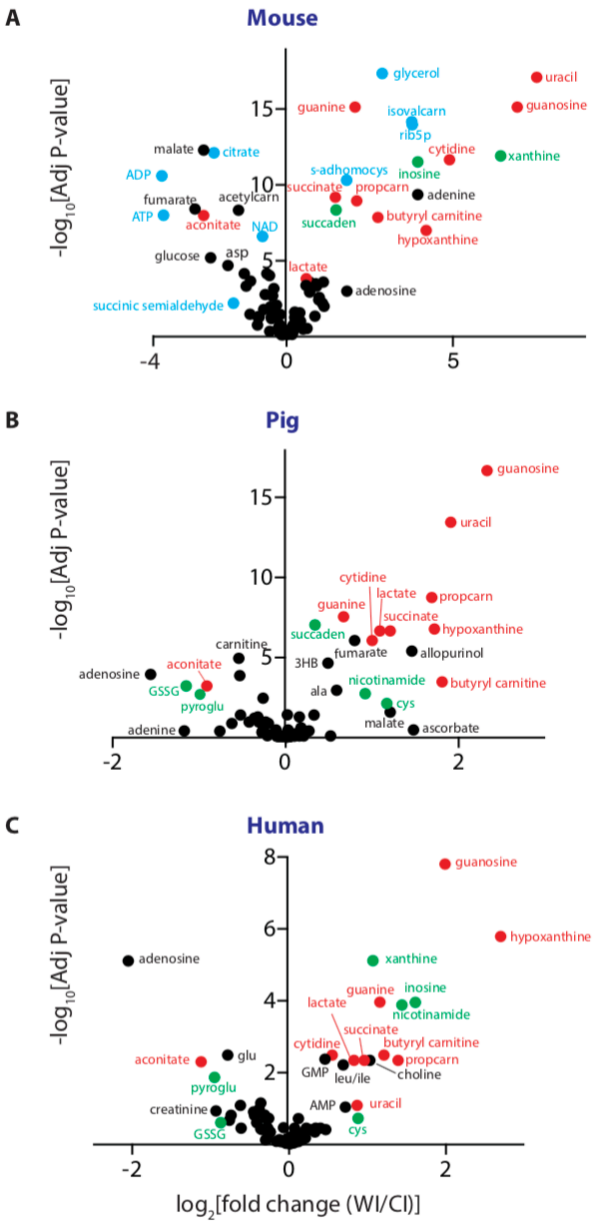

Figure 12: Volcano plots of metabolites analysed by LC/MS.

Volcano plots of the analysed metabolites that demonstrated significant fold change in warm iscahemia compared to cold ischaemia after 30 minutes of organ storage in the (a) mouse (n = 5 - 6), (b) pig (n = 5) and (c) human (n = 4). Volcano plots were constructed by plotting the $-\log_{10}$ of the adjusted p-value against the $\log_2$ of the fold-change in metabolite abundance between 30 mins WI and 30 mins CI. Fold-changes and p-values were calculated using the Limma package with R. Isovaleryl carnitine, isovalcarn; ribulose-5-phosphate, rib5p; proprionylcarnitine, propcarn; S-adenosyl homocysteine, S-adhomocys; acetyl carnitine, acetylcarn; succinyl adenosine;, succaden; 3-hydroxybutyrate, 3HB; pyroglutamic acid, pyroglu; glutathione disulphide, GSSG. Those metabolites that changed in the same way in all three species are annotated in red, metabolites that changed in the same way in two of the species have been annotated in green and the additional metabolites that changed in the expanded analysis performed in mouse heart tissue are annoted in blue.

The analyses in (Figure 11 and Figure 12) highlighted metabolites that should be further analysed. A more detailed analysis of individual metabolites with respect to different metabolic pathways was also considered. The time course of detected metabolites in glycolysis, the citric acid cycle, the pentose phosphate pathway, the urea cycle, free fatty acids, selected acyl carnitines, and amino acids are discussed below.

3.4 Glycolytic intermediates

The heart is a highly metabolically active organ. In regional ischaemia models of myocardial ischaemia there is a rapid decrease in myocardial oxygen concentrations following the cessation of coronary flow. Tissue oxygen decreases to 75% baseline values within seconds 8-10 seconds and to 10% of baseline values at 11-52 seconds (41, 149). With exhaustion of myocardial oxygen, fatty acid oxidation and oxidative phosphorylation will cease and the only source of energy available to the myocardium will come from anaerobic metabolism. Glycogen stores fuel glycolysis during anaerobic metabolism. Glycogen stores in the mouse heart were analysed using a glycogen assay. Glycogen was depleted more rapidly in warm compared to cold ischaemia. After an initial rapid depletion in glycogen stores during warm ischaemia, tissue glycogen levels plateaued. In contrast, during cold ischaemia the glycogen stores continued to decrease until they were completely exhausted (Figure 13).

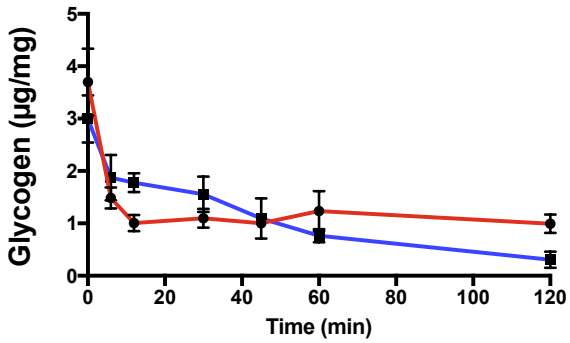

Figure 13: Glycogen stores in the mouse heart during warm and cold ischaemia.

Mouse hearts were rapidly retrieved and the apex excised. This apical section was then rapidly clamp frozen to provide a baseline normoxic control glycogen concentration. Sequential axial sections were taken after variable periods of warm (red line) or cold (blue line) storage and tissue concentrations of glycogen were calculated relative to the control sample (n = 3). The glycogen assay was performed by Ms F Allen (MRC Mitochondrial Biology Unit).

3.4.1 Glycolytic substrate utilisation during ischaemia

To further analyse glycolysis during ischaemia, comparative changes in glycolytic intermediates were analysed by LC-MS in the mouse heart. Consistent with the findings from glycogen assays, glucose consumption demonstrated different trends during warm and cold organ storage. During cold organ storage, there was a more gradual decrease in myocardial glucose compared to warm ischaemia (Figure 14). This was in contrast to the metabolic profile of glucose 6-phosphate and fructose 6-phosphate which demonstrated no difference between warm and cold ischaemia up to 12 minutes. After the early period of ischaemia, both glucose 6-phosphate and fructose 6-phosphate demonstrated similar trends with a divergence in the myocardial concentrations observed when hearts were stored in warm or cold ischaemic conditions. The product of PFK-1 phosphorylation, fructose 1,6 bisphosphonate, was very

poorly detected in this analysis in all heart specimens including the control hearts despite discernible changes in tissue concentrations of metabolites up and downstream of it.

Tissue concentrations of glyceraldehyde-3-phosphate remained approximately at baseline tissue concentrations in hearts stored under cold ischaemic conditions to 30 minutes of ischaemia and then decreased to a fraction of baseline concentrations by 240 minutes of cold ischaemia. In contrast to hearts stored in cold ischaemia, hearts stored in warm ischaemia demonstrated a slight increase in glyceraldehyde 3-phosphate tissue concentrations above baseline concentrations during early time points until 12 minutes. Beyond 30 minutes, tissue concentrations then appeared to decline. However, the decrease in tissue concentration were less exaggerated in warm ischaemia compared to hearts stored in cold ischaemia. The glycolytic intermediates downstream of glyceraldehyde-3-phosphate, 3-phosphoglycerate and phosphoenolpyruvate were detected in only 20% of control hearts. This step in glycolysis generates ATP and therefore proceeds rapidly during ischaemia and would account for the limited detection even in control hearts. During cold ischaemia, there was a greater rate of detection of 3-phosphoglycerate and phosphoenolpyruvate but these intermediates were still not detected in all samples. These data support existing evidence that glycolysis continues throughout cold organ storage at a slower rate compared to hearts maintained at normothermia and that glycolytic failure may be the result of inhibition of GAPDH. (Figure 14).

Pyruvate is the end product of glycolysis. There are a number of potential pathways through which is it metabolised (Figure 16). During anaerobic respiration, reduction to lactate is the predominant pathway and can be used to assess flux through anaerobic glycolysis. Glycolytic flux in mouse hearts during organ storage was examined at prolonged periods of cold ischaemia. These periods of cold storage were outside the limits of viability for transplantation (Dr K Saeb-Parsy, personal communication). Lactate appeared to plateau during cold ischaemia and did not achieve peak tissue concentrations greater than those observed during warm ischaemia. Glucose tissue concentrations decreased to 10% of baseline tissue concentrations by 4 hours and then remained at this level even after extended periods of cold organ storage remaining at approximately 14% of baseline tissue concentrations. Tissue lactate increased to approximately 5 times baseline tissue concentrations demonstrating a reciprocal relationship with glucose. The peak tissue concentrations of lactate achieved during cold storage were lower than those during warm ischaemia (Figure 15). This supports the observations from glycogen assays that glycolysis is not inhibited by a lack of substrate during cold ischaemia.

3.4.2 Pyruvate metabolism in warm and cold ischaemia

Pyruvate tissue concentrations demonstrated a rapid decrease to approximately 20% of baseline tissue concentrations within 6 minutes of warm or cold storage and there was no significant difference in the profiles between warm or cold storage (Figure 14). Pyruvate can be metabolised by a number of pathways (Figure 16) that include; reduction to lactate, transamination to alanine, carboxylation to oxaloacetate or conversion to acetyl-CoA following transfer across the mitochondrial inner membrane.

During warm ischaemia, there was an increase in tissue alanine above baseline concentrations that plateaued after 12 minutes. This was not observed during cold organ storage where tissue concentrations remained unchanged from baseline. Although oxaloacetate was not detected by LC-MS, the products of oxaloacetate metabolism, malate and aspartate, were detected. Aspartate demonstrated a slight initial increase above baseline concentrations during cold storage and then remained constant. This was in contrast to warm ischaemia where tissue concentrations were observed to have a reciprocal relationship to alanine tissue concentrations initially declining to 50% of baseline concentrations, and then plateauing during continued warm ischaemia. Contrasting trends during warm and cold ischaemia were also observed in malate tissue concentrations. Malate was better preserved by cold storage compared to warm ischaemia where tissue concentrations rapidly decreased and were 25% of baseline tissue abundance by 12 minutes and 10% by 30 minutes of warm ischaemia (Figure 16).

Ischaemia makes oxidative decarboxylation of pyruvate to acetyl CoA and subsequent carboxylation to oxaloacetate unfavourable. Reduction of pyruvate to lactate generates NAD^+ and is employed during anaerobic metabolism to maintain the NADH/NAD^+ ratio but cannot continue indefinitely as the lactate cannot be metabolised further and the associated cellular acidosis is toxic to the cell.

An alternative pathway involves the transamination of pyruvate and glutamate to alanine and α-ketoglutarate (Figure 16). Alanine also demonstrates rapid accumulation during the first 12 minutes of warm ischaemia. This is not observed during cold ischaemia where relative tissue concentrations remain at normoxic baseline levels. After 12 minutes of warm ischaemia however, relative tissue concentrations plateau. This coincides with the plateau seen in lactate and would be in keeping with flux through this pathway during anaerobic metabolism with transamination of the rapidly accumulating pyruvate and glutamate to alanine and α-ketoglutarate.

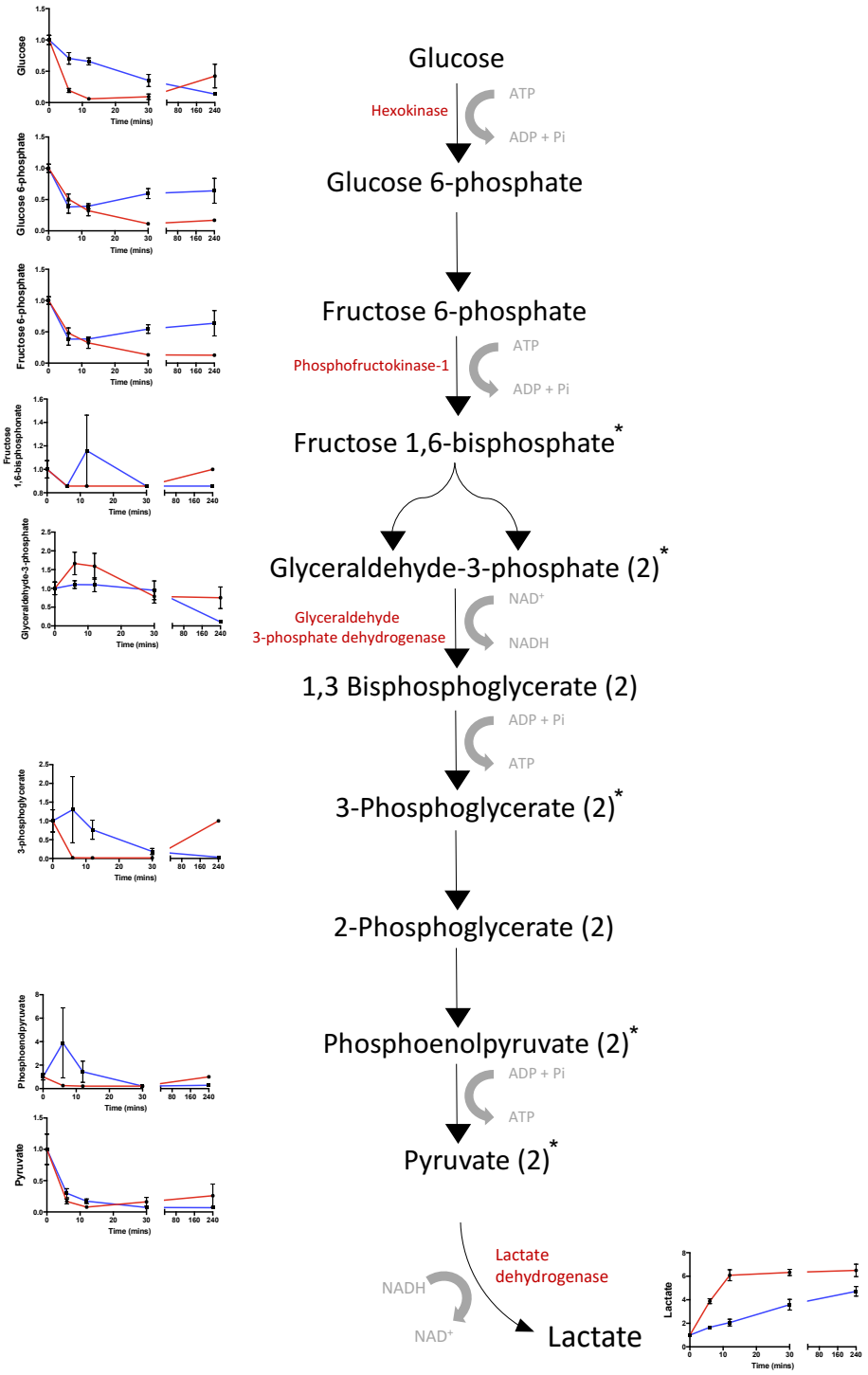

Figure 14: The metabolic profile of glycolytic intermediates during warm (red) and cold (blue) ischaemia in the mouse heart.

Mouse hearts were rapidly excised and exposed to either warm (red line) or cold (blue line) ischaemia (n = 4-5). Tissue abundance of glycolytic intermediates was analysed by LC-MS and used to calculate relative change in tissue abundance compared to normoxic control hearts (n = 11). When metabolites were not detected a value of half the minimum recorded ion count from that dataset was used to enable calculations of relative change (*metabolites with at least one sample demonstrating undetectable ion counts).

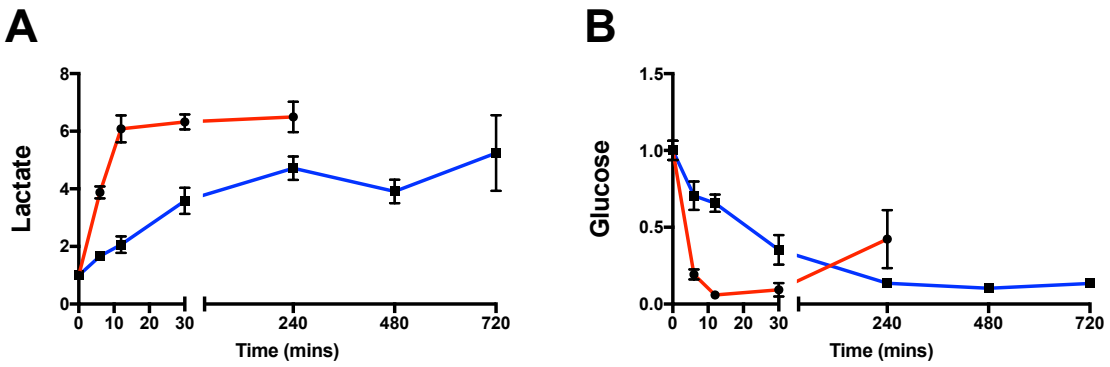

Figure 15 (a and b): Metabolic profile of lactate and glucose during cold organ storage extended to 12 hours.

Mouse hearts were rapidly excised and exposed to cold (blue line) ischaemia (n = 4-5) for variable lengths of time up to 720 minutes and compared to hearts exposed to warm ischaemia (red line) up to 30 minutes (n = 5). Tissue abundance of lactate (A) and glucose (B) was analysed by LC-MS and compared to normoxic baseline control hearts (n = 6-11).

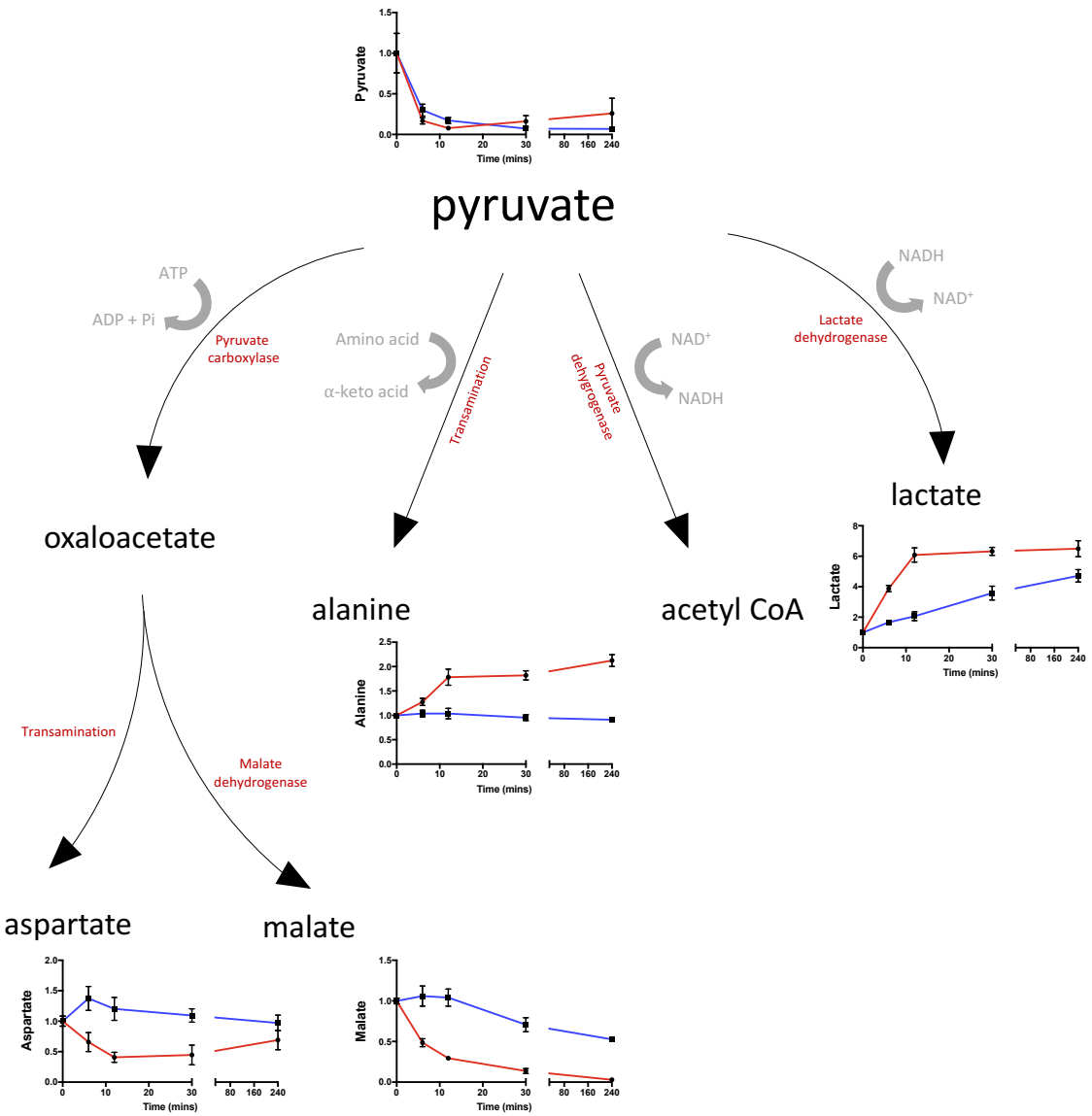

Figure 16: Pyruvate metabolism during warm (red line) and cold (blue line) ischaemia in the mouse heart.

Mouse hearts were rapidly excised and exposed to either warm (red line) or cold (blue line) ischaemia (n = 4-5). Tissue abundance of metabolic intermediates was analysed by LC-MS and used to calculate relative change in tissue abundance compared to normoxic control hearts (n = 11).

3.4.3 GAPDH constrains glycolysis during warm but not cold ischaemia

The divergence observed between warm and cold organ storage in glucose and lactate tissue concentrations was not replicated in all other glycolytic intermediates. This supports the presence of key regulatory steps controlling glycolysis. Key regulatory steps previously identified include those catalysed by PFK-1 and GAPDH. A reduction in flux through any particular reaction can be implied by the accumulation of upstream intermediates however, an increase in flux will not be observed in this analysis unless substrate is limited. The cellular conditions required to increase flux through PFK-1 such as the depletion in ATP were demonstrated however, direct evidence with conclusive changes in up and downstream intermediates of PFK-1 were not identified.

One key regulatory step in glycolysis is the metabolism of glyceraldehyde-3-phosphate by GAPDH. GAPDH is inhibited by an elevated NADH/NAD^+ ratio. The lactate/pyruvate ratio reflects the tissue NADH/NAD^+ ratio. During warm ischaemia there was a more rapid increase in both the lactate/pyruvate ratio and the NADH/NAD^+ ratio compared to cold ischaemia (Figure 17). The lactate/pyruvate ratio is also observed to peak at 12 minutes whereas during cold ischaemia it continues to rise until 240 minutes. These data are consistent with a rapid increase in glycolysis that initially sustains ATP production during warm ischaemia but then ceases as the elevated NADH/NAD^+ ratio inhibits GAPDH. In contrast, during cold ischaemia glycogenolysis and glycolysis continue until tissue stores have been exhausted. This supports the hypothesis that during cold ischaemia, the NADH/NAD^+ ratio is never high enough to inhibit glycolysis.

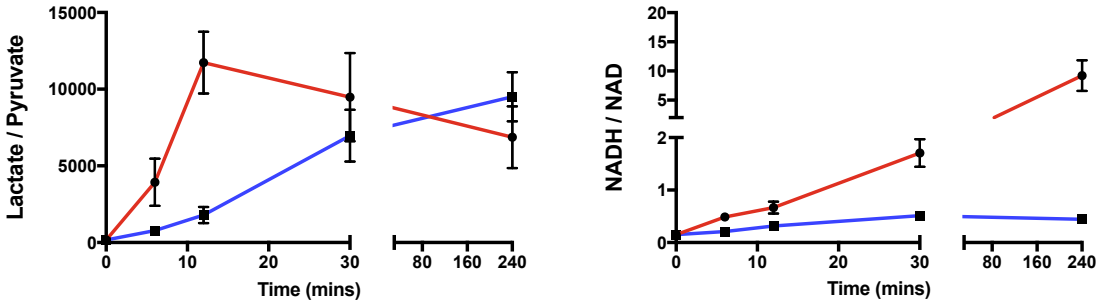

Figure 17: Changes in lactate/pyruvate ratio and NADH/NAD$^+$ ratio during warm (red line) and cold (blue line) organ storage in the mouse heart.

Mouse hearts were rapidly excised and exposed to either warm (red line) or cold (blue line) ischaemia (n = 4-5). Tissue abundance of glycolytic intermediates was analysed by LC-MS and used to calculate relative change in tissue abundance compared to normoxic control hearts (n = 11). When metabolites were not detected a value of half the minimum recorded ion count from that dataset was used to enable calculations of relative change. Pyruvate was not detected in both warm and cold stored hearts. NADH was not detected in 2 control hearts.

3.4.4 Summary of glycolytic metabolites during ischaemia

The rapid onset of anaerobic metabolism from the commencement of organ storage was confirmed by the immediate increase in tissue concentrations of lactate observed in these experiments. Furthermore, consistent with the proportional decline in metabolic rate with decreasing temperature, this data supports a slowing of anaerobic respiration in hearts subjected to cold storage evidenced by the reciprocal relationship between glucose and lactate tissue concentrations over periods of organ storage consistent with organ viability. Whilst anaerobic metabolism cannot continue indefinitely, the exact reason for the failure of glycolysis has been previously debated, with exhaustion of substrates and inhibition of key regulatory pathways both proposed as potential causes (36, 150). The data presented in this thesis would not support the exhaustion of glucose as the principal mechanism of myocardial glycolytic failure during warm ischaemia since glycogen stores persist after lactate concentrations have plateaued. In contrast, during cold ischaemia, glycogen stores are depleted to lower tissue concentrations than those observed during warm ischaemia. Lactate accumulation also mirrors these findings, supporting cessation of glycolysis due to an exhaustion of glycogen stores.

3.5 Generation of NAD^+ during ischaemia

Energy in the form of ATP is generated by glycolysis in the steps that occur downstream of GAPDH. Generating NAD^+ becomes vitally important for the continued generation of ATP during anaerobic respiration. The principal pathway for this involves the reduction of pyruvate to lactate by lactate dehydrogenase, although alternative pathways may have a role in the regeneration of NAD^+ during ischaemia. Alanine has previously been observed to increase during ischaemia, demonstrating a stoichiometric relationship with aspartate (151). A similar relationship was observed in these experiments. During warm ischaemia there was an increase in alanine during the early period of warm ischaemia until 12 minutes before tissue concentrations plateaued. This was reciprocated in aspartate tissue concentrations. In contrast, during cold organ storage tissue concentrations of both remained largely unchanged from baseline. The generation of malate from oxaloacetate by malate dehydrogenase has been proposed to take place during ischaemia (54) and generates NAD^+. The transamination of aspartate to oxaloacetate provides the substrate for this process but it also necessitates a source of α-ketoglutarate. Tissue concentrations of α-ketoglutarate are shown in these data to be rapidly exhausted. The anaplerotic transamination of glutamate and pyruvate to alanine and α-ketoglutarate would therefore provide an additional source of α-ketoglutarate to enable a brief period of additional NAD^+ generation. This would result in no net change in tissue α-ketoglutarate or glutamate as was observed in these data and would be consistent with the reciprocal changes in alanine and aspartate observed (Figure 16). Interestingly, the changes in alanine were not observed during cold organ storage where preserved glycolytic flux was observed.

3.6 Pentose phosphate pathway

The pentose phosphate pathway (PPP) runs parallel to glycolysis in the cytosol (Figure 18). It is primarily catabolic, generating nicotinamide adenine dinucleotide phosphate (NADPH) and ribulose-5-phosphate. It consists of an irreversible oxidative stage that results in the production of ribulose-5-phosphate from glucose-6-phosphate via a series of sequential steps that in the process generate NADPH. The NADPH serves a number of functions in the cell that include; *de novo* fatty acid synthesis, regulation of oxidative stress and cholesterol biosynthesis. The second reversible non-oxidative phase generates ribulose-5-phosphate which serves as a precursor for nucleotide synthesis. In myocardial tissue, however, the PPP is thought to have a very limited metabolic role since, the rate limiting step of the irreversible oxidative phase, glucose-6-phosphate dehydrogenase along with other PPP enzymes, has very low expression and activity in myocardium (152).

PPP metabolites were only detected in the additional LC-MS analysis performed on mouse hearts. There was no measurable ribulose-5-phosphate in the control (normoxic) hearts. Ribulose-5-phosphate was detected at increasing concentrations with prolonged durations of ischaemia. The accumulation of ribulose 5-phosphate was markedly greater in hearts stored in warm ischaemia compared to hearts stored in cold ischaemia and continued to increase for up to 30 minutes during warm ischaemia. Tissue concentrations were observed to be 20-fold higher following 6 minutes of warm ischaemia compared to cold ischaemia (Figure 18). The increase in ribulose-5-phosphate during ischaemia has previously been reported in rat hearts. Inhibition of the oxidative stage of the PPP by the NADPH inhibitor diphenyleneiodonium, was shown in this model to decrease IR injury (153). Changes in flux through the PPP has been reported in other pathophysiological processes such as heart failure (152) however, the significance of the changes in the PPP observed in this data during organ storage are uncertain.

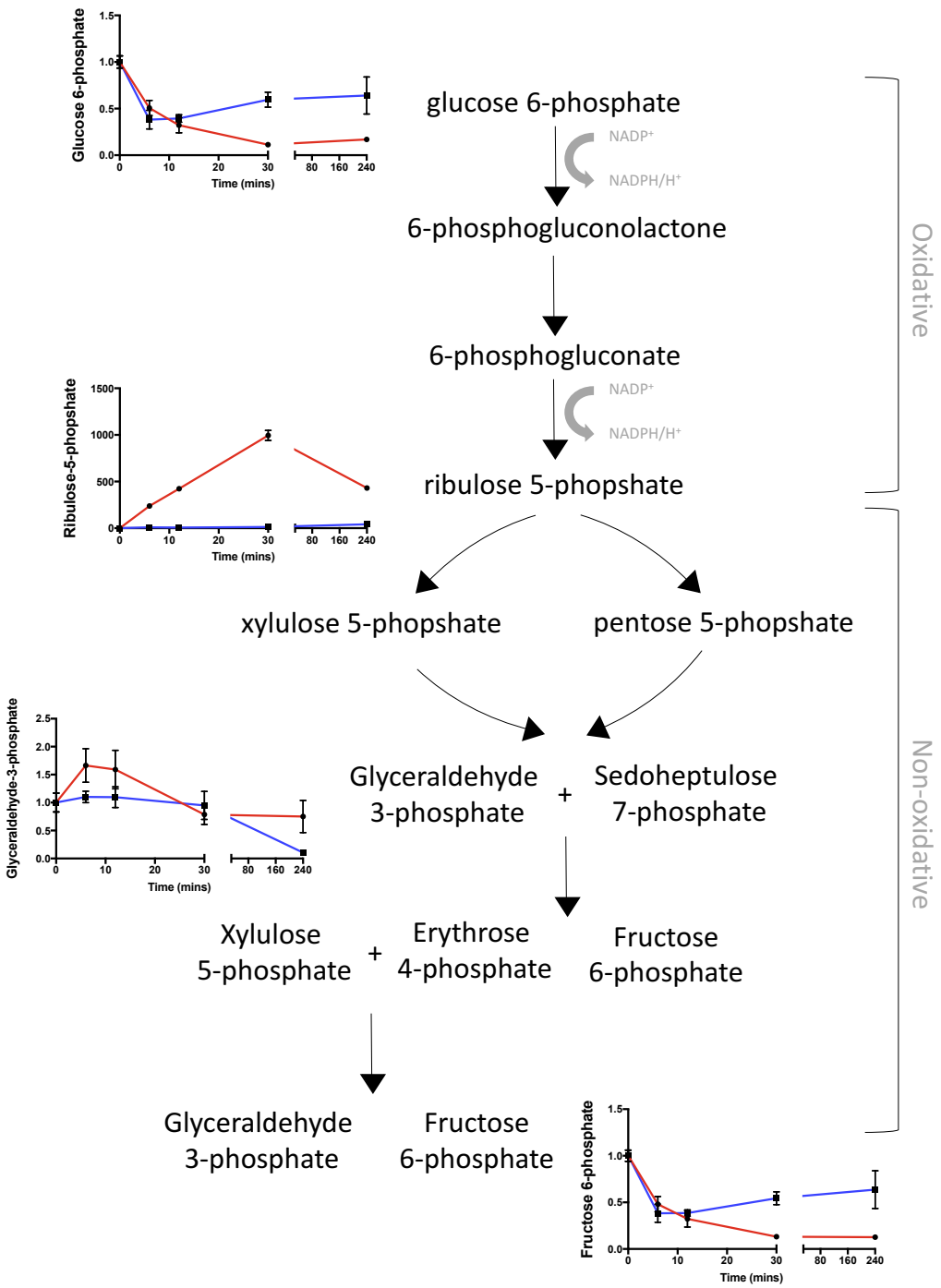

Figure 18: The metabolic profile of pentose phosphate pathway intermediates during warm and cold storage in the mouse heart.

Mouse hearts were rapidly excised and exposed to either warm (red line) or cold (blue line) ischaemia (n=4-5). Tissue abundance of pentose phosphate pathway intermediates was analysed by LC-MS. Relative change compared to normoxic baseline control hearts (n = 5-11) was calculated.

3.7 Citric acid cycle intermediates

At the onset of ischaemia, with rapidly dwindling ATP and increasing concentrations of NADH, the conventional CAC cycling that occurs in aerobic conditions ceases. In this study, mouse hearts exposed to warm and cold ischaemia demonstrated different CAC metabolic profiles. During warm ischaemia, there was a rapid decline in all measured CAC intermediates, except succinate, which demonstrated a reciprocal increase in myocardial tissue concentrations reaching a peak tissue concentration 12-fold above baseline normoxic tissue concentrations by 30 minutes of warm ischaemia. After this rapid increase, tissue succinate levels plateaued. In contrast, during cold ischaemia there was a more gradual, constant increase in tissue succinate concentrations. These failed to achieve the same peak concentrations observed during warm ischaemia. Succinate accumulation during cold ischaemic was also observed to continue beyond viable cold ischaemic times[1]. A linear increase in tissue succinate was observed when hearts were stored in cold storage for 8 and 12 hours (Figure 19). Similar changes in succinate accumulation were also observed in pig and human myocardial tissue (Figure 20 and Figure 21). These relative increases in tissue succinate abundance were highly conserved demonstrating similar absolute, quantified tissue succinate concentrations during warm and cold ischaemia (Figure 22).

In mouse hearts, fumarate, malate and citrate decreased more rapidly for the first 12 minutes of warm ischaemia. In contrast, during cold ischaemia relative tissue abundance remained near baseline. At increasing durations of warm and cold ischaemia beyond 12 minutes, more gradual decline in these metabolites was observed. By 30 minutes of warm ischaemia, tissue concentrations had fallen to less than 20% of baseline tissue levels (Figure 19).

α-ketoglutarate tissue concentrations fell to approximately 5% of baseline normoxic concentrations within 6 minutes ischaemia, demonstrating similar profiles during both warm and cold ischaemia. The oxidative decarboxylation of isocitrate to α-ketoglutarate is an irreversible step in the TCA cycle and highly regulated. A rapid decline in tissue α-ketoglutarate concentrations was observed in mouse hearts stored in both warm and cold ischaemia and the disparity in cellular concentrations of this CAC metabolite compared to the other CAC intermediates in this study is an interesting observation (Figure 19). Rapid termination and reversal of the CAC could partially explain the process, however the discordance in the trends between warm and cold ischaemia observed in the downstream metabolites is not in keeping with this and would suggest flux through an additional catabolic pathway. Oxidative deamination to glutamate is usually unfavourable due to the low physiological NADH/NAD^+ ratio but may occur in some

[1]The viability of a donor organ was assessed by the ability of the heterotopically transplanted heart to spontaneously return to ventricular contraction upon reperfusion. This was achieved regularly following 12 minutes of warm ischaemia (in addition to the ischaemic injury sustained during the retrieval procedure) or following 240 minutes of cold ischaemia (personal observation).

circumstances (154, 155). The high NADH/NAD$^+$ ratio in ischaemia might favour this process and could explain the rapid decline in α-ketoglutarate.

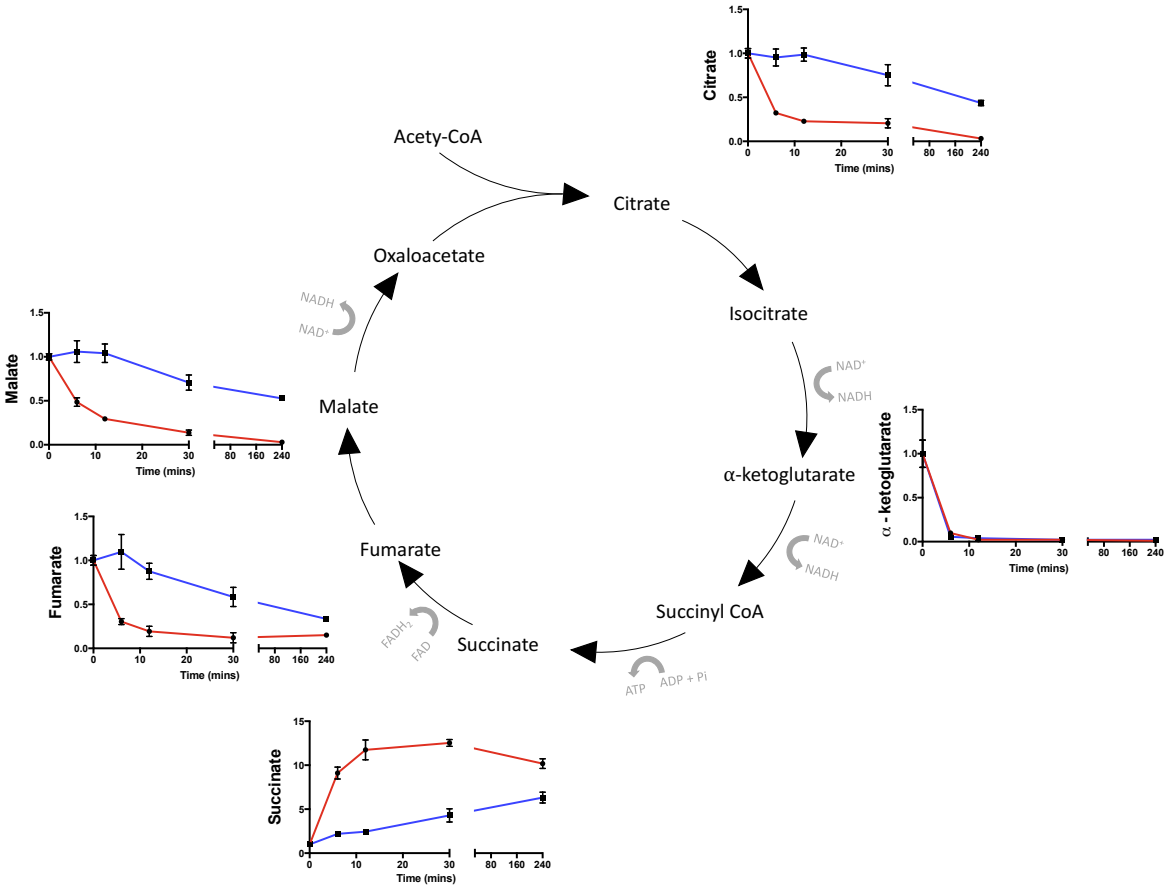

Figure 19: Metabolic profile of CAC intermediates during warm (red line) and cold (blue line) organ storage in the mouse heart.

Mouse hearts were rapidly excised and exposed to either warm (red) or cold (blue) ischaemia (n = 4-5). Tissue abundance was analysed by LC-MS and relative change compared to normoxic baseline control hearts (n = 5-11) calculated.

CAC intermediates were also examined in pig and human heart tissue (Figure 20). As discussed above, these data demonstrated similar trends in succinate accumulation in warm and cold ischaemia. The accumulation of the other CAC intermediates malate and fumarate however, demonstrated contrasting changes during warm ischaemia (Figure 20). In pig and human myocardium, malate and fumarate demonstrated similar trends to succinate during warm ischaemia with a rapid increase in tissue concentrations compared to the normoxic control that plateaued after 12 minutes of ischaemia. In contrast, tissue fumarate and malate remained at a similar concentration to normoxic baseline concentrations throughout cold organ storage. Tissue malate concentrations were only detected in one human heart (Figure 20).

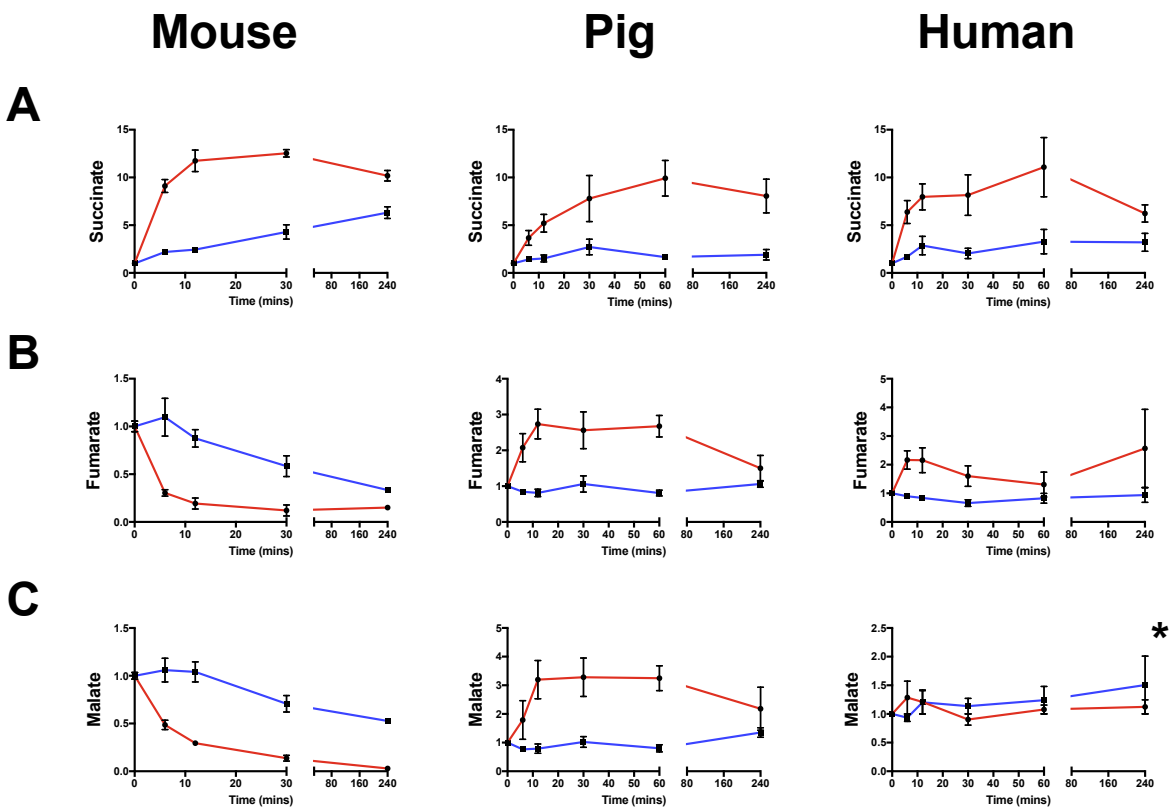

Figure 20: Relative change in the CAC intermediates in mouse, pig and human hearts tissue during warm (red line) and cold (blue line) organ storage.

Relative change in the CAC intermediates (a) succinate, (b) fumarate, and (c) malate in mouse, pig and human hearts tissue during warm (red line) and cold (blue line) organ storage.

Mouse (n = 5 -11), pig (n = 5) and human (n = 4) heart tissue was retrieved and exposed to variable periods of warm (red) or cold (blue) ischaemia. Tissue abundance was analysed by LC-MS and compared to normoxic baseline control tissue (mouse (n = 11), pig (n = 5), human (n = 4)). The succinate/fumarate ratio was calculated from absolute tissue concentrations of metabolites. Absolute quantification was performed by interpolation of the corresponding standard curve obtained from serial dilutions of commercially available standards that were run with the same batch of samples.
*Tissue malate was only detected in one human donor heart.

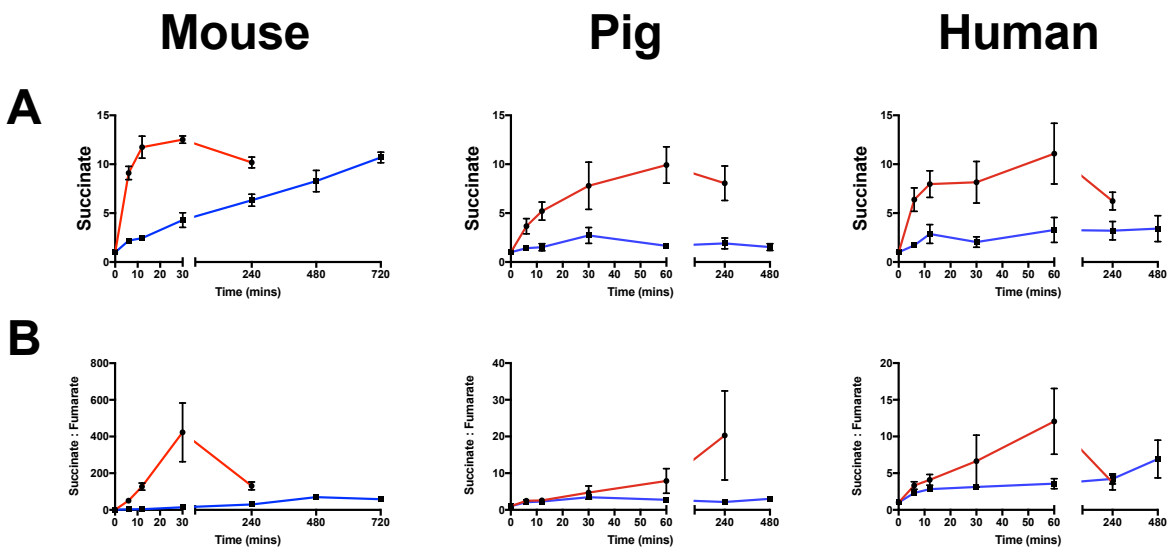

Figure 21 (a and b): Succinate accumulation and the succinate/fumarate ratio during warm (red line) and cold storage (blue line) in the mouse, pig and human heart.

Mouse (n = 3-5), pig (n = 5) and human (n = 3 - 4) heart tissue was retrieved and exposed to variable periods of warm (red) or cold (blue) ischaemia. Tissue succinate abundance was analysed by LC-MS and compared to normoxic baseline control tissue (mouse (n = 15), pig (n = 5), human (n = 3-4)). The succinate/fumarate ratio was calculated from absolute tissue concentrations of metabolites. Absolute quantification was performed by interpolation of the corresponding standard curve obtained from serial dilutions of commercially available standards that were run with the same batch of samples.

It has been hypothesised that upon reperfusion, rapid oxidation of accumulated succinate is responsible for the generation of mtROS through RET at complex I (53). RET in this process is dependent on a reversal of flux through NADH/NAD^+ that can only occur in the presence of a sufficient succinate/fumarate ratio with the amount of mtROS proportional to the total pool of succinate (53, 54). Despite the differences in fumarate accumulation during warm ischaemia between species, the trend in the succinate/fumarate ratio is largely determined by tissue succinate concentrations. Warm ischaemia resulted in a more rapid and greater peak succinate/fumarate ratio compared to cold ischaemia. This trend was more pronounced in mouse hearts compared to the pig and human hearts. In the mouse heart, warm ischaemia resulted in a linear rise in the succinate/fumarate ratio to > 100:1 within 12 minutes, peaking at 30 minutes. Cold ischaemia abrogated this rise with succinate/fumarate ratios 3:1 at 12 minutes and reaching 25:1 at 240 minutes of cold ischaemia (Figure 21). The succinate/fumarate ratio was also examined in tissue stored in cold ischaemia times beyond the limit of organ viability. Despite the continued increase in tissue succinate observed in these hearts a similar increase in tissue the succinate/fumarate ratio was not observed as tissue fumarate concentrations were not decreased to the same extent as observed during warm ischaemia (Figure 21).

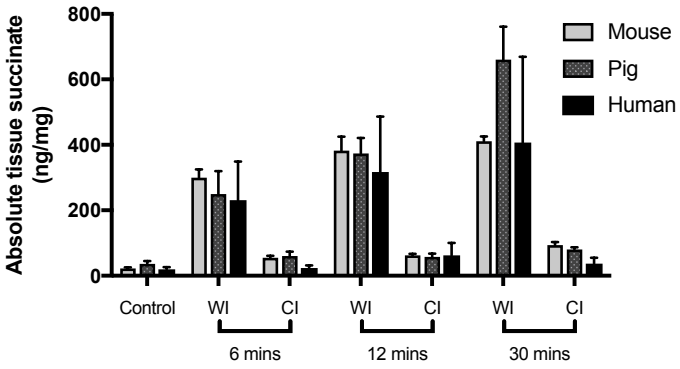

Figure 22: Comparative absolute tissue succinate concentrations during warm and cold organ storage in the mouse, pig and human.

Mouse (n = 3-5), pig (n = 5) and human (n = 3 - 4) heart tissue was retrieved and exposed to variable periods of warm (red) or cold (blue) ischaemia. Tissue abundance was analysed by LC-MS and compared to normoxic baseline control tissue (mouse (n = 15), pig (n = 5), human (n = 3-4)). Absolute quantification was performed by interpolation of the corresponding standard curve obtained from serial dilutions of commercially available standards that were run with the same batch of samples. Absolute tissue succinate concentrations are conserved across species.

3.8 Cardiac contraction and ischaemic metabolism

3.8.1 Cardiac contraction and succinate accumulation in mouse hearts

The principal ATP-utilising process in myocardium is contraction. Contraction can be altered by a variety of conditions. It has previously been shown that there is a rapid loss of contractile activity in localised hypoxia, as occurs during coronary artery occlusion. Severe hypothermia is cardioplegic and the high potassium concentrations of the preservation solution used in these experiments also had a cardioplegic like effect. In this model, hearts subjected to cold ischaemia rapidly ceased to beat within 5 contractions (< 5 seconds) following immersion in UW. However, hearts stored under warm ischaemic conditions continued to contract for approximately 90 seconds. To investigate whether the difference in contractility between the hearts stored in warm and cold storage might have contributed to the different metabolic profiles, St Thomas' cardioplegia was administered to donor animals prior to warm organ storage. St Thomas' cardioplegia is a crystalloid solution based on the extracellular ionic composition. The high potassium concentration induces rapid diastolic arrest (< 5 seconds) following intravenous injection through a central vein.

3.8.2 Contractility and energy stores

Complete cessation of contraction using cardioplegia did not decrease the ATP/ADP ratio in hearts stored in warm ischaemia compared to hearts stored in cold storage. These findings support the hypothesis that the observed changes in the ATP/ADP ratio between hearts stored in warm and cold ischaemia were not the result of changes in contractility.

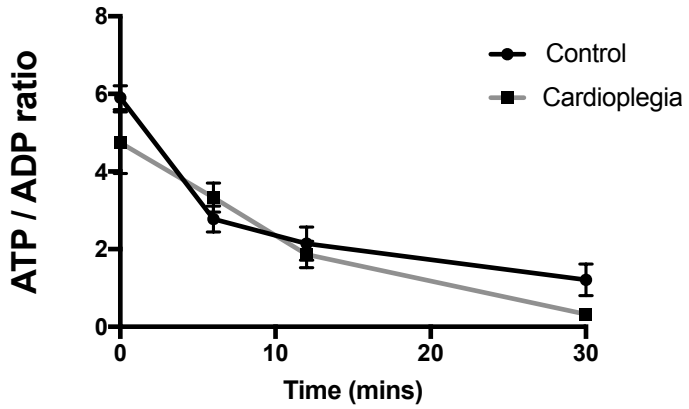

Figure 23: ATP/ADP ratio in mouse hearts from donors treated with (grey line) and without (black line) cardioplegia and stored for variable periods of warm ischaemia.

Donor animals (n = 3) were treated with or without 500 μL St Thomas' cardioplegia before hearts were rapidly excised and stored for variable periods of warm ischaemia. There was no difference in the ATP/ADP ratio measured by luciferase-based assay.

3.8.3 Contractility and metabolite abundance

The administration of St Thomas' cardioplegia had no effect on baseline tissue succinate concentrations. There was a reduction in tissue fumarate concentration immediately following administration of cardioplegia with differences in the baseline tissue concentrations. These changes occurred very rapidly and were not observed in any other detected metabolite (Figure 24).

Succinate accumulation during warm ischaemia was not significantly moderated by the administration of cardioplegia ($F(4, 48) = 2.43$, $p = 0.06$, 2-way ANOVA), although the relative peak succinate tissue concentration after 30 minutes of warm ischaemia was reduced (11.6 vs 13.7 $p = 0.03$, $n = 3 - 5$) when hearts were treated with cardioplegia (Figure 25). The rapid rise in succinate accumulation observed during warm ischaemia persisted with and without cardioplegia administration. In hearts treated with cardioplegia succinate accumulation was significantly greater following warm ischaemia compared to succinate accumulation during cold ischaemia ($F(4, 49) = 15.73$, $p < 0.0001$, 2-way ANOVA). Baseline tissue fumarate concentrations in hearts treated with cardioplegia were lower than those observed when hearts were not treated with cardioplegia (15.2 vs 3.2 ± 3.3, $p = 0.029$, $n = 3$, one-way ANOVA with Tukey's multiple comparisons test) (Figure 26). Tissue fumarate concentrations in hearts treated with cardioplegia then remained constant. This profile was not significantly different to hearts not treated with cardioplegia and stored in warm ischaemia ($F(4, 48) = 1.83$, $p = 0.13$, 2-way ANOVA). In these hearts the initial fumarate concentration was greater but then rapidly decreased to tissue concentrations similar to those in hearts treated with cardioplegia within 12 minutes of warm ischaemia (Figure 25 (b)). Tissue concentrations of fumarate remained constant during more prolonged periods of warm ischaemia in both hearts treated with or without cardioplegia. These findings suggest that there was significant accumulation of succinate during warm ischaemia irrespective of the direct effects of temperature on myocardial contraction. These findings have implications for the application of therapeutic agents in the amelioration of IR injury and application of organ cooling strategies in the prevention of IR injury.

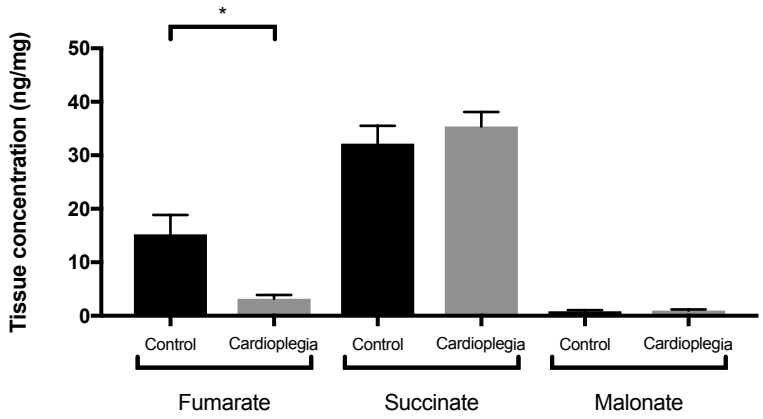

Figure 24: Baseline normoxic metabolite abundance in mouse hearts following treatment with and without St Thomas' cardioplegia.

Donor animals (n = 3) were treated with or without 500 μL St Thomas' cardioplegia. Hearts were rapidly excised and snap frozen within 20 seconds of the onset of ischaemia. Tissue abundance was measured by LC-MS. Absolute quantification was performed by interpolation of the corresponding standard curve obtained from serial dilutions of commercially available standards that were run with the same batch of samples. There was significant decrease in fumarate concentration following the administration of cardioplegia (15.2 vs 3.2 $\pm$ 3.3, $p = 0.029$, $n = 3$). There was no difference in the abundance of other detected metabolites. One-way ANOVA with Tukey's multiple comparisons test (* $p < 0.05$)

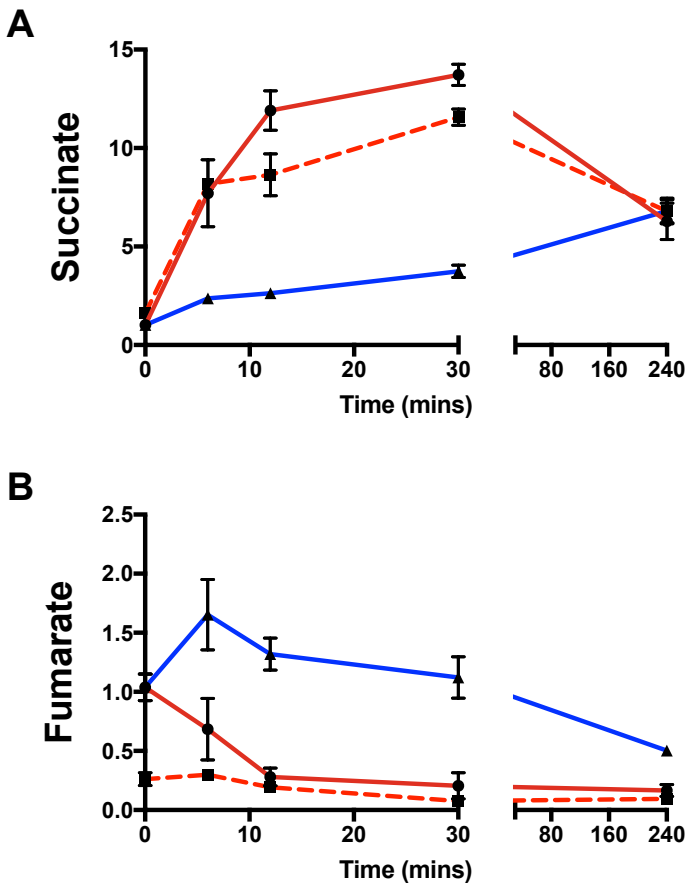

Figure 25 (a and b): Effect of contractility on succinate and fumarate accumulation during warm and cold ischaemia in the mouse heart.

Mouse hearts (n = 3 - 8) were treated with (dashed red line) or without (red line) St Thomas' cardioplegia prior to rapid retrieval and exposed to variable periods of warm (dashed red and red line) or cold ischaemia. (a) Succinate and (b) fumarate abundance was measured by LC-MS and relative change in metabolite abundance was compared to baseline control hearts (n = 17) that were not treated with cardioplegia.

3.9 Temperature and CAC intermediate accumulation

It is generally assumed that a large proportion of the protective effects of hypothermia are the result of changes in the rate of metabolism, as governed by the relatively similar Q_{10} that most biological enzymes exhibit. To investigate whether the difference in succinate accumulation observed between warm and cold ischaemia was a linear phenomenon, tissue succinate and fumarate concentrations were measured after 12 minutes of ischaemia (Figure 26).

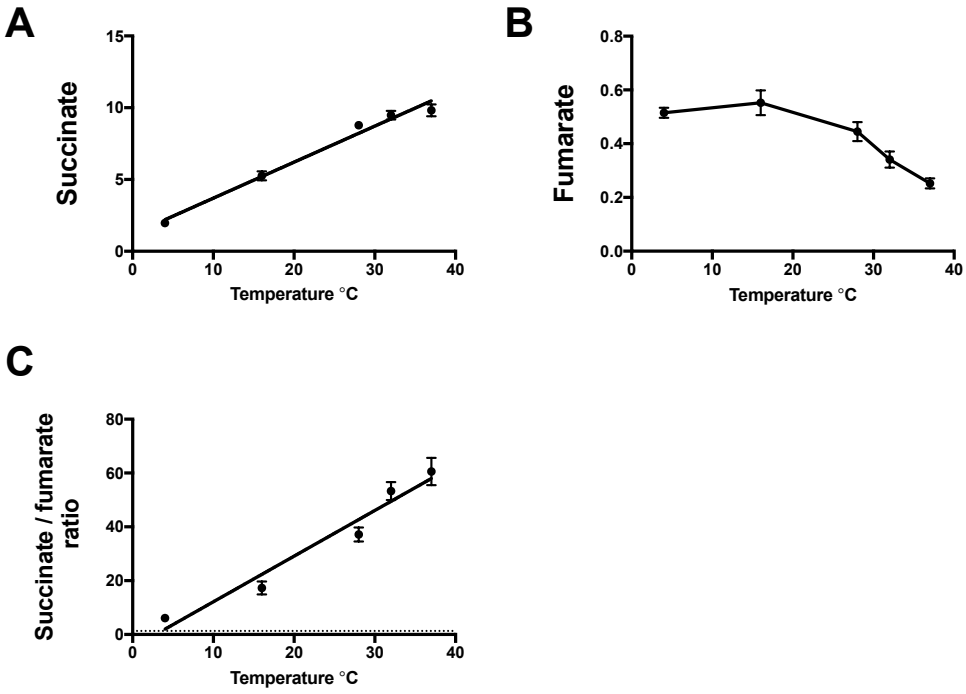

Figure 26 (a – c): Succinate and fumarate tissue concentrations after 12 minutes of ischaemia in mouse hearts stored at different temperatures.

St Thomas' cardioplegia was administered to donor animals. Hearts (n = 4) were rapidly excised and stored for 12 minutes in UW at different temperatures (4, 16, 28, and 32°C). Tissue abundance of succinate (a) and fumarate (b) was measured using LC-MS. Relative change in metabolite abundance was compared to baseline control hearts (n = 9) that were not treated with cardioplegia. Data were compared to hearts treated with St Thomas' cardioplegia and stored in the carcass of the animal maintained at 37°C with the use of a heat mat. To calculate succinate/fumarate ratio absolute quantification of succinate and fumarate was performed by interpolation of the corresponding standard curve obtained from serial dilutions of commercially available standards that were run with the same batch of samples. The mean succinate/fumarate ratio was then calculated from each heart (c).

Succinate accumulated in a linear fashion with increasing temperature during 12 minutes of organ storage ($R^2 = 0.95$) (Figure 26(a)). In addition, the accumulation of succinate occurred rapidly in the mouse heart with significant increases in tissue succinate observed after 12 minutes of organ storage at temperatures as low as 16°C. It was only when hearts were stored at 4°C that succinate tissue concentrations remained at normoxic baseline tissue concentrations after 12 minutes of organ storage (Figure 27). At temperatures

in the range 16°C – 37°C, fumarate also demonstrated a linear trend. There was a significant depletion below baseline in tissue fumarate when mouse hearts were stored for 12 minutes in cold storage at 4°C (Figure 26(b)). This was in contrast to previous data when hearts were not treated with cardioplegia where there was no initial decrease in tissue fumarate compared to normoxic, baseline hearts at 12 minutes of cold storage (Figure 19).

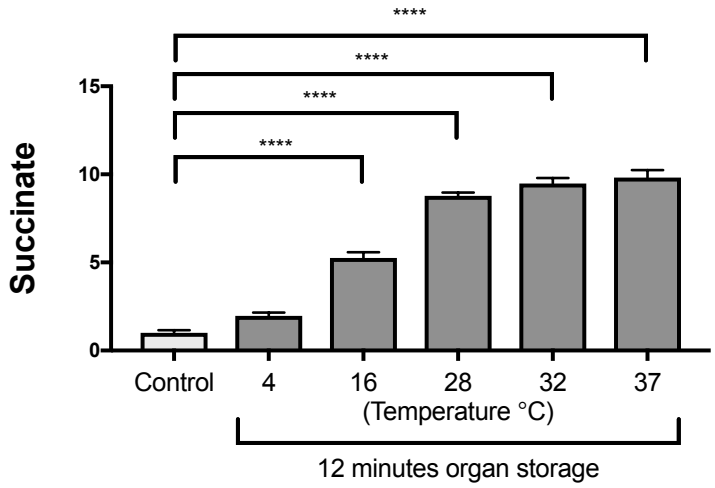

Figure 27: Succinate accumulation in the mouse heart after 12 minutes of organ storage at varying temperatures.

St Thomas' cardioplegia was administered to donor animals. Hearts (n = 4) were rapidly excised and stored for 12 minutes in UW at different temperatures (4, 16, 28, and 32°C). Tissue abundance of metabolites was measured using LC-MS. Relative change in metabolite abundance was compared to baseline control hearts (n = 9) that were not treated with cardioplegia.

One-way ANOVA with Tukey's multiple comparisons test (**** $p < 0.0001$)

Succinate tissue concentrations did not change as a result of cardioplegia administration (Figure 24). The differences in fumarate did not translate to changes in the succinate/fumarate ratio which demonstrated a linear relationship with temperature when hearts stored for 12 minutes ischaemia ($R^2 = 0.89$) (Figure 26(c)). The other detected CAC metabolites malate and citrate also demonstrated reciprocal linear relationships with temperature when hearts were stored for 12 minutes (malate, $R^2 = 0.86$; citrate, $R^2 = 0.86$)There was a weaker correlation between α-ketoglutarate and temperature during 12 minutes of organ storage (α-ketoglutarate, $R^2 = 0.51$) (Figure 28).

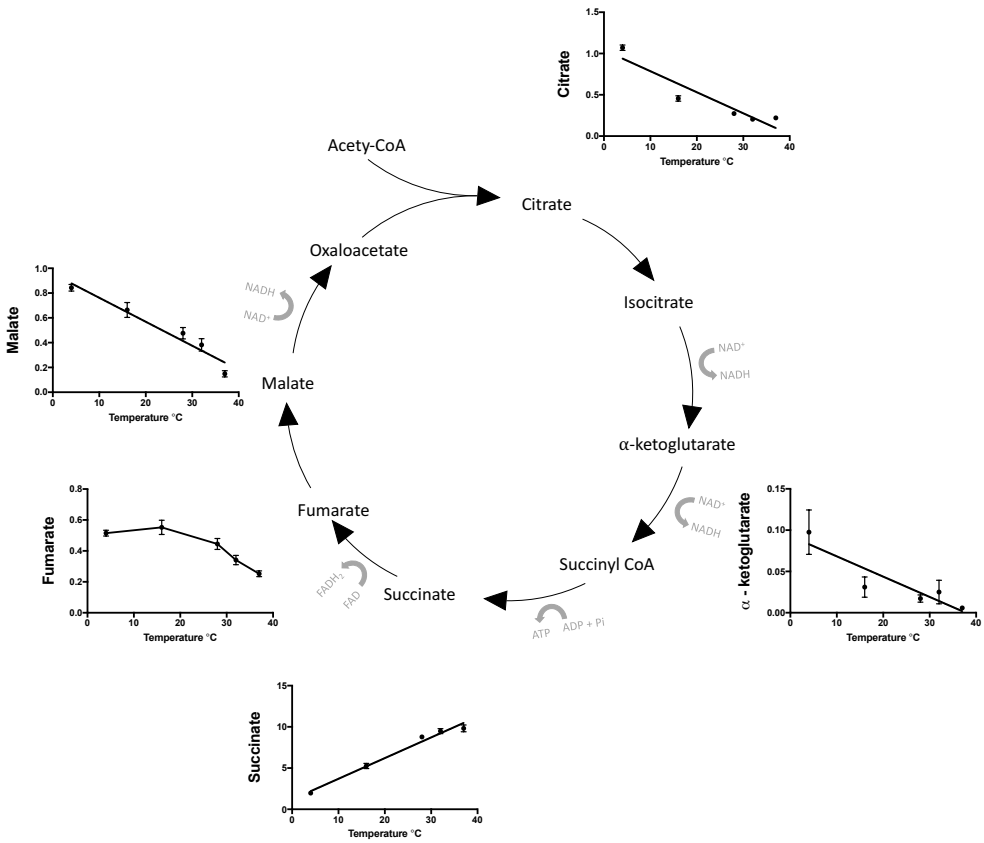

Figure 28: Tissue abundance of CAC metabolites in mouse hearts stored at variable temperatures for 12 minutes.

St Thomas' cardioplegia was administered to donor animals. Hearts (n = 4) were rapidly excised and stored for 12 minutes in UW at different temperatures (4, 16, 28, and 32°C). Tissue abundance of metabolites was measured using LC-MS. Relative change in metabolite abundance was compared to baseline control hearts (n = 9) that were not treated with cardioplegia. Data were compared to hearts treated with St Thomas' cardioplegia and stored in the carcass of the animal maintained at 37°C with the use of a heat mat.

The impact of increasing the temperature of organ storage on the flux through glycolysis was also examined. Lactate accumulation increased in a linear fashion with temperature and there was a reciprocal relationship with glucose suggesting there was increased flux through glycolysis with increasing temperature during 12 minutes of organ storage (Figure 29 (a) and (b)). This linear relationship was observed in the other glycolytic intermediates that were detected (Figure 30) across the temperature range of 4 to 32°C (glucose; $R^2 = 0.91$, glucose 6-phopshate; $R^2 = 0.89$, fructose 6-phopshate; $R^2 = 0.89$, glyceraldehyde 3-phosphate; $R^2 = 0.46$, lactate; $R^2 = 0.99$). Relative tissue lactate after 12 minutes of ischaemia at 37°C was observed to rapidly decrease to 4-fold that of baseline, normoxic tissue concentrations. The hearts stored at 37°C were analysed by LC-MS at a discrete time to the remaining dataset. A 10-fold peak lactate tissue concentration was not previously achieved in hearts not administered cardioplegia and 12 minutes of warm ischaemia was only shown in other analyses to reach 6-fold baseline tissue concentrations. It is unclear whether the late decrease in lactate demonstrated in

these data reflects a pathophysiological process or an error in analysis though the linear relationship observed between other glycolytic intermediates and temperature was also abolished when these data were analysed together. The difference in techniques used to maintain the temperature of organ storage could explain the differences in this analysis however, a similar disparity was not observed in other metabolites.

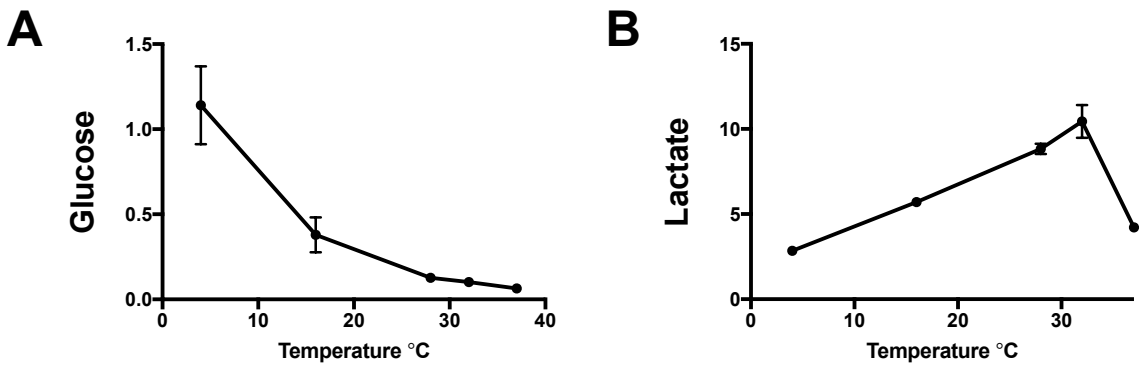

Figure 29: Relationship between glycolysis and temperature in mouse hearts stored for 12 minutes of ischaemia.

St Thomas' cardioplegia was administered to donor animals. Hearts (n = 4) were rapidly excised and stored for 12 minutes in UW at different temperatures (4, 16, 28, and 32°C). Tissue abundance of metabolites was measured using LC-MS. Relative change in metabolite abundance was compared to baseline control hearts (n = 9) that were not treated with cardioplegia.

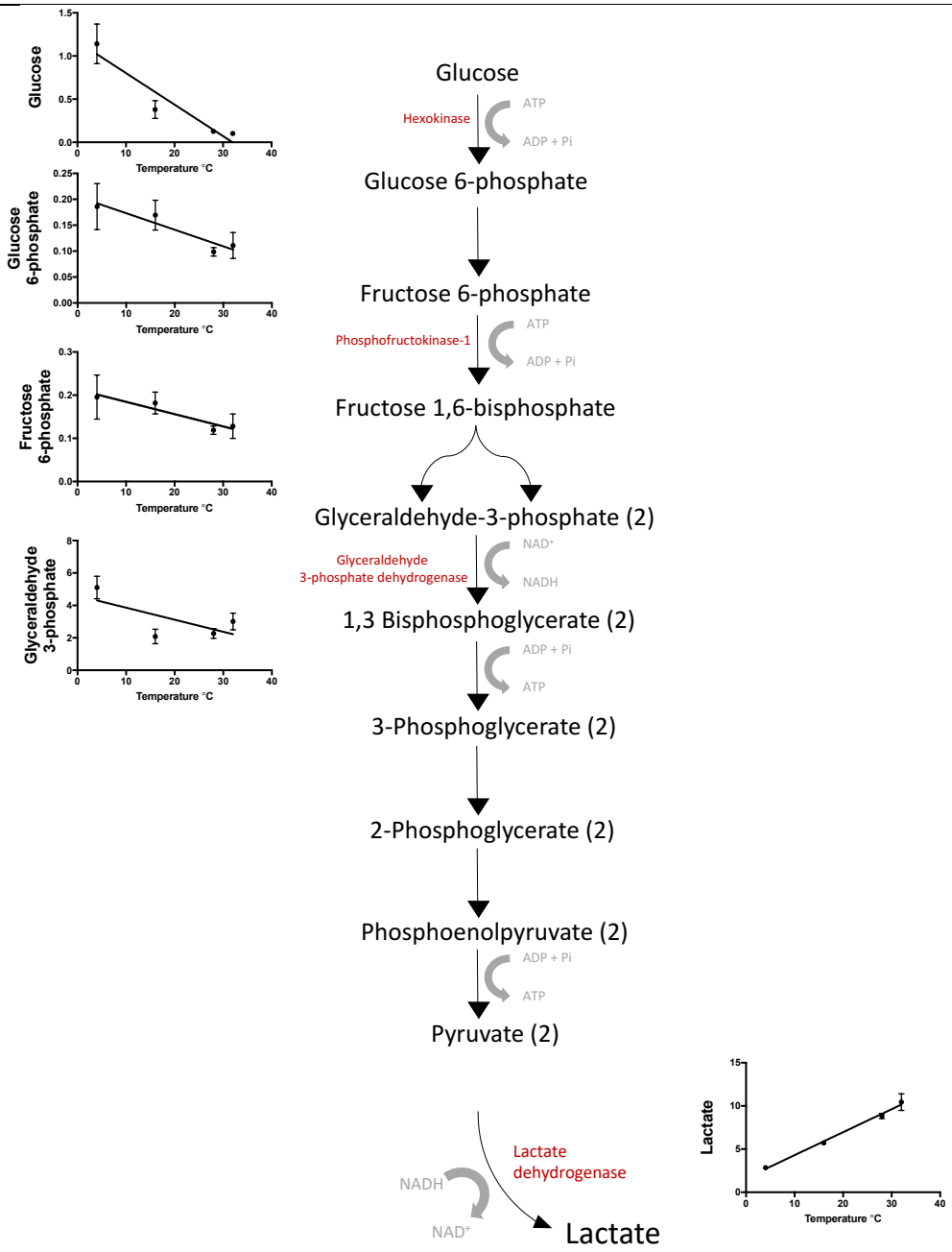

Figure 30: The accumulation of glycolytic intermediates after 12 minutes of ischaemic metabolism with varying temperatures of organ storage in the mouse heart.

St Thomas' cardioplegia was administered to donor animals. Hearts (n = 4) were rapidly excised and stored for 12 minutes in UW at different temperatures (4, 16, 28, and 32°C). Tissue abundance of metabolites was measured using LC-MS. Relative change in metabolite abundance was compared to baseline control hearts (n = 9) that were not treated with cardioplegia.

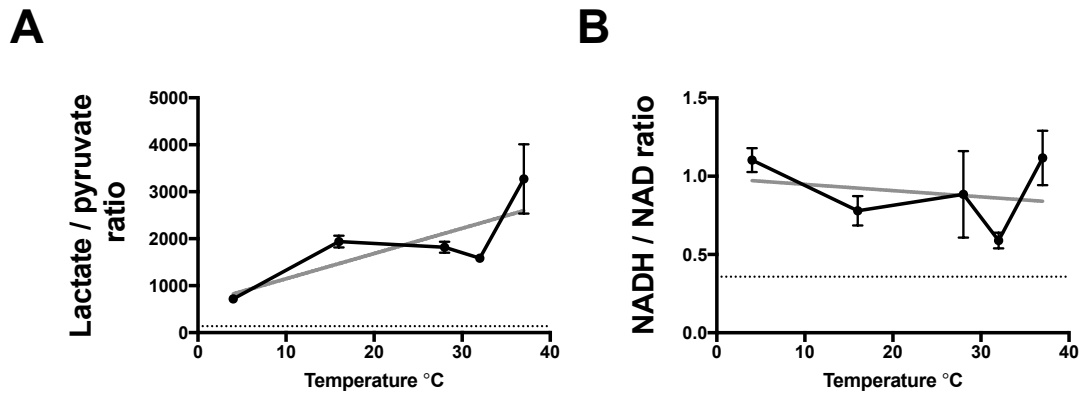

Figure 31: Assessment of tissue NADH/NAD^+ after 12 minutes of ischaemia in mouse hearts stored at difference temperatures.

St Thomas' cardioplegia was administered to donor animals. Hearts (n = 4) were rapidly excised and stored for 12 minutes in UW at different temperatures (4, 16, 28, and 32°C). Tissue abundance of metabolites was measured using LC-MS. Relative change in metabolite abundance was compared to baseline control hearts (n = 9) that were not treated with cardioplegia. Baseline, normoxic lactate/pyruvate ratio and NADH/NAD^+ ratio is indicated by dotted line.

The failure of energy stores during anaerobic metabolism was demonstrated in hearts not treated with cardioplegia to coincide with elevations in the NADH/NAD^+ ratio and the inhibitory effects this may have on GAPDH (Figure 17(a) and (b)). The lactate/pyruvate ratio reflects the tissue NADH/NAD^+ ratio. There was discordance in the trends of these ratios when analysed in these data. The lactate/pyruvate ratio after 12 minutes of ischaemia demonstrated a weak linear trend (R^2 = 0.40) with increasing temperature of organ storage however there was no apparent trend in the NADH/NAD^+ ratio in these data (Figure 31(a) and (b)).

In summary, organ cooling significantly ameliorated the accumulation of succinate during ischaemia and demonstrated a linear relationship with temperature even after only short durations of organ storage. In addition, temperature had a linear relationship with the succinate/fumarate ratio. These findings highlight the need for very effective organ cooling during the early period of ischaemia if mtROS mediated IR injury is to be prevented by organ storage.

3.10 Urea cycle intermediates

The urea cycle converts toxic ammonia into urea. Ammonia is derived primarily from the metabolism of amino acids but has also been shown during ischaemia to be the product of deamination of the purine nucleoside, adenosine (156). Although most tissues can synthesise urea, the greatest amount is produced in the liver. The first step occurs in the mitochondria generating citrulline from ornithine and carbamoyl phosphate. Citrulline is then transported into the cytoplasm by a specific transporter where the remaining three reactions occur. The urea cycle and CAC are connected by the aspartate-arginosuccinate shunt and in certain situations the urea cycle can replenish the CAC cycle with fumarate (32).

During warm ischaemia, ornithine tissue concentrations remained near baseline levels up to 30 minutes but there was a significant difference in the effect of cold ischaemia compared to warm ischaemia on tissue abundance ($F(1, 51) = 16.1$. $p = 0.0002$, two-way ANOVA). Myocardial tissue concentrations of ornithine decreased to < 60% of baseline concentrations at 6 minutes of cold ischaemia and then remained at this level. There was no significant difference between myocardial concentrations of citrulline stored in warm or cold ischaemic conditions. Significant differences in tissue concentrations of the urea cycle intermediate, arginine, was observed between hearts stored in warm and cold ischaemia ($F (1, 51) = 20.9$ $p < 0.0001$, two-way ANOVA). Cold organ storage maintained tissue concentrations of arginine at baseline tissue concentrations. In contrast, warm ischaemia produced a rapid rise in arginine from 6 to 12 minutes of warm ischaemia. After this time tissue concentrations of arginine remained stable. There were significant differences in relative tissue abundance of aspartate ($F (1, 51) = 38.3$, $p < 0.0001$, two-way ANOVA) and fumarate ($F (1, 51) = 61.3$, $p < 0.0001$, two-way ANOVA) between warm and cold organ storage (Figure 32).

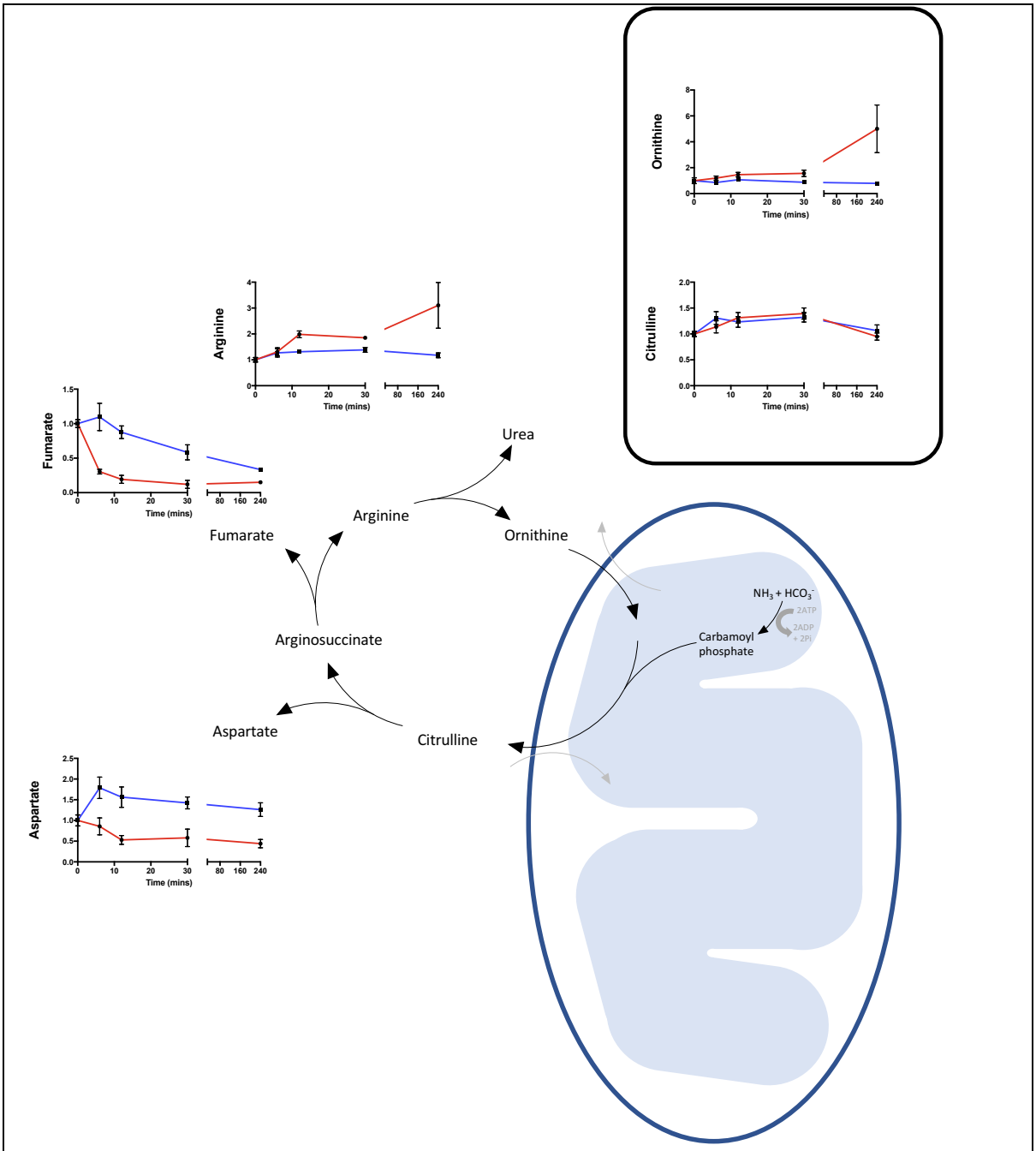

Figure 32: Accumulation of urea cycle intermediates during warm and cold ischaemia in the mouse heart.

Mouse hearts were rapidly excised and exposed to either warm (red) or cold (blue) ischaemia (n = 4-5) for variable periods of time before being clamp frozen. Tissue abundance was analysed by LC-MS and compared to baseline, normoxic control hearts (n = 11).

3.11 Free fatty acids and acyl carnitines

Fatty acid oxidation represents a major substrate for energy metabolism in myocardium and is estimated to account for 60-90% of total oxygen consumption under aerobic conditions (157). Beta-oxidation is, however, highly sensitive to tissue hypoxia and under global ischaemic conditions is rapidly terminated. Inhibition of beta-oxidation is consistent with increasing cytosolic concentrations of long chain acyl-CoA and decreasing acetyl-CoA levels. The increase in long chain acyl-CoA might be expected to increase cytosolic long chain acylcarnitines.

There was a more rapid increase in the short odd chain carnitines isovalerylcarnitine ($F(1, 51) = 82.4$, $p < 0.0001$, two-way ANOVA) and propionylcarnitine ($F(1, 51) = 103.1$, $p < 0.0001$, two-way ANOVA) with warm ischaemia that was not observed with cold ischaemia. This likely represents an increase in amino acid catabolism during warm ischaemia. Butrylcarnitine can also be derived from amino acid metabolism and followed a similar trend to propionylcarnitine and isovalerylcarntine. The long chain carnitines, myristoylcarnitine ($F(1, 51) = 21.5$, $p < 0.001$, two-way ANOVA), stearoylcarnitine ($F(1, 51) = 7.4$, $p < 0.0001$, two-way ANOVA), and palmitoylcarnitine ($F(1, 51) = 81.0$, $p < 0.0001$, two-way ANOVA) demonstrated a different profile with minimal change compared to baseline concentrations both during warm or cold ischaemia during early time points to 30 minutes. There was a late rise in these long chain carnitines in the tissues maintained under cold storage that was accompanied by a minor rise in acetylcarnitine. This was not observed in warm ischaemic myocardium, which at prolonged storage demonstrated an exhaustion of all tissue carnitines (Figure 33).

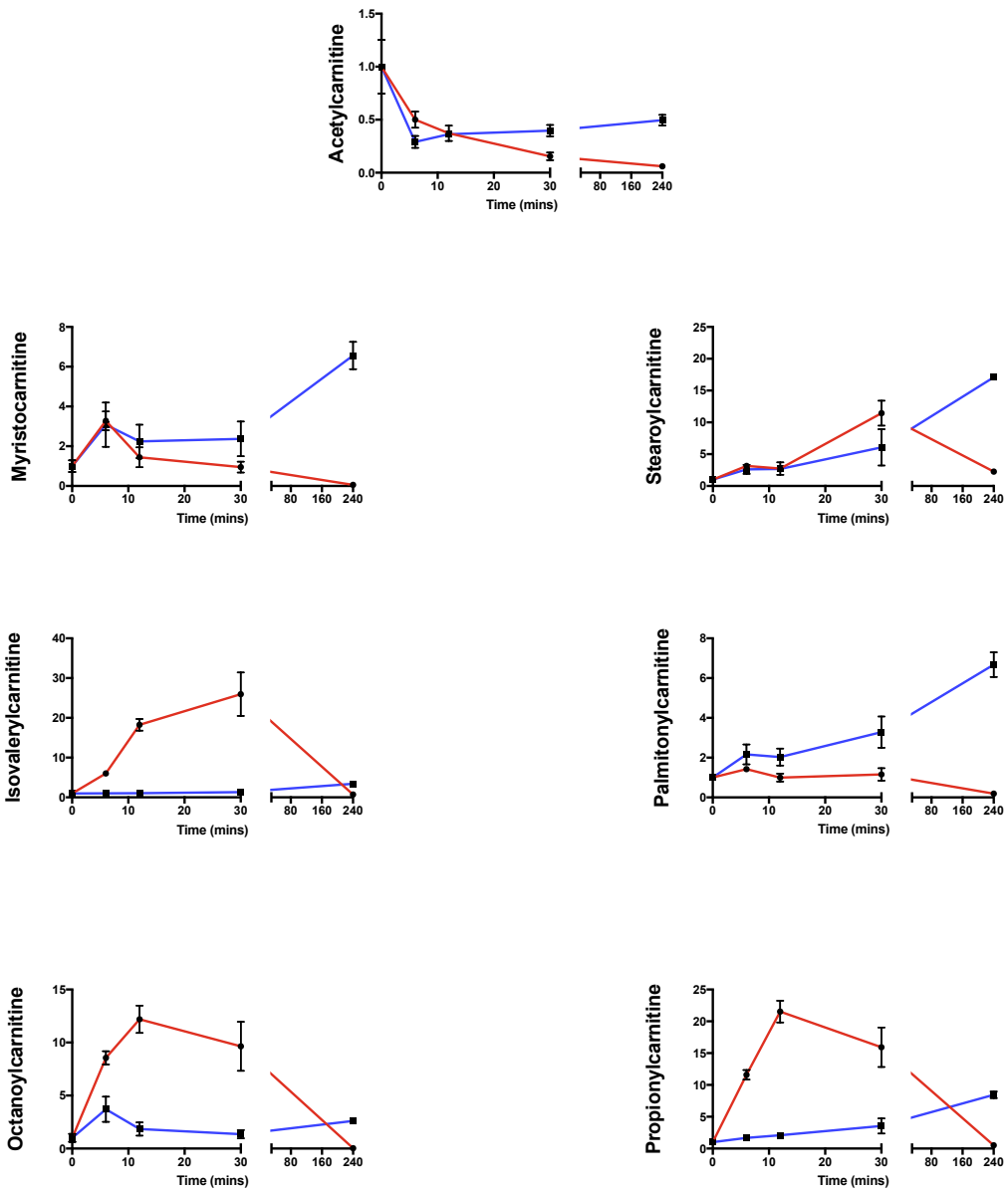

Figure 33: Accumulation of carnitines in the mouse heart during warm and cold ischaemia.

Mouse hearts were rapidly excised and exposed to either warm (red) or cold (blue) ischaemia (n = 4-5) for variable periods of time before being clamp frozen. Tissue abundance was analysed by LC-MS and relative change compared to baseline, normoxic control hearts (n = 11) calculated.

3.12 Amino acid metabolism in ischaemia

Under conditions unfavourable for oxidation such as ischaemia, the heart switches to alternative metabolic substrates in order to meet its energy requirements. Amino acids offer potential advantages to ischaemic myocardial metabolism as they can undergo non-oxidative metabolism and contribute little to cellular acidification (158). For this reason, there is increasing interest in the use of amino acids as cardioprotective substrates during ischaemia. The metabolic changes of some amino acids have already been discussed in relation to other metabolic pathways. The changes in a number of other key metabolites are discussed below. Transamination of glutamate was discussed in relation to the metabolic profile of α-ketoglutarate. There were no significant differences between the tissue concentrations of glutamate or glutamine in hearts stored in warm or cold ischaemia and tissue concentrations remained near baseline tissue concentrations. This profile would not support flux during myocardial ischaemia in this pathway (Figure 34).

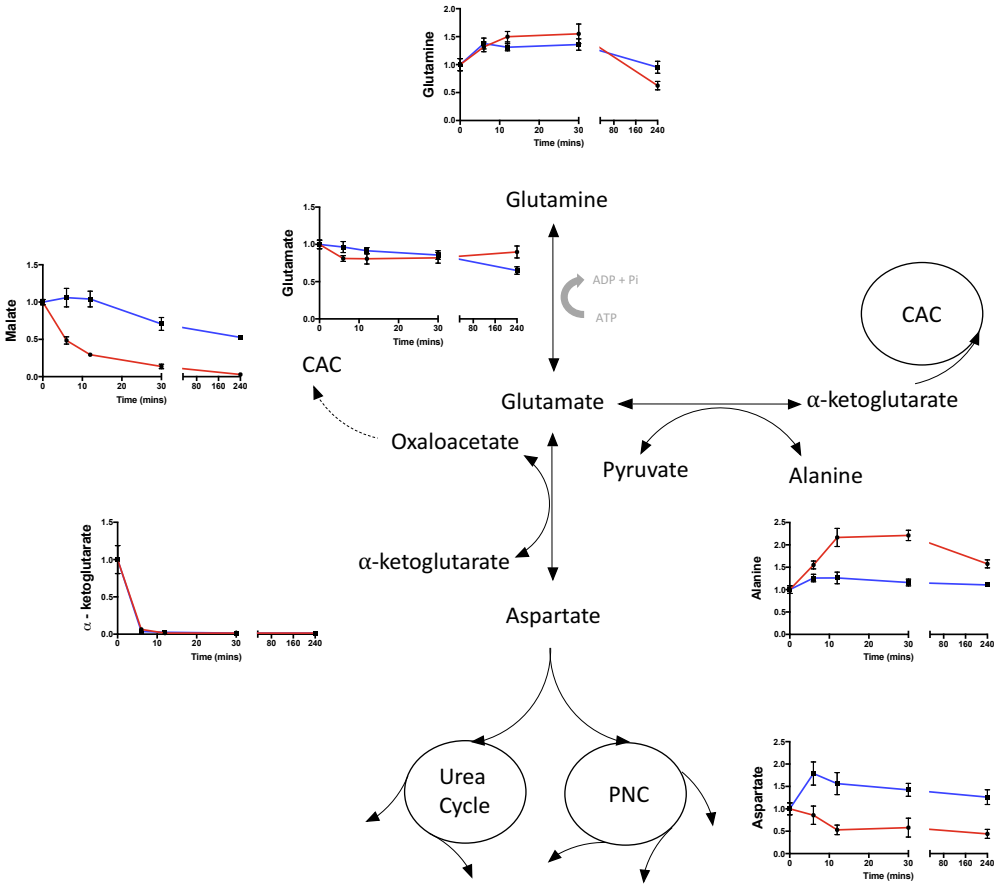

Figure 34: Amino acid and glutamate metabolism during warm and cold ischaemia in the mouse heart.

Mouse hearts were rapidly excised and exposed to either warm (red) or cold (blue) ischaemia (n = 4-5) for variable periods of time before being clamp frozen. Tissue abundance was analysed by LC-MS and relative change compared to baseline, normoxic control hearts (n = 11) calculated.

Alanine is produced and released by the heart in both physiological and pathophysiological conditions. It is thought to be produced by the transamination of pyruvate and has been shown to occur both in aerobic and anaerobic cells, where the availability of the substrate, pyruvate, is the rate limiting step. Alanine has been shown to increase in the hypoxic tissues of diving mammals and during myocardial ischaemia (158).

In this data, alanine concentrations in hearts stored in cold ischaemia remained at baseline tissue concentrations but there was a significant difference in the tissue concentrations during warm ischaemia with a rapid rise during early ischaemia until 12 minutes whereupon tissue concentrations remained constant ($F(1, 51) = 57.0$, $p < 0.0001$, two-way ANOVA) (Figure 16 and Figure 36 (b)). These changes in alanine were also conserved across species (Figure 35).

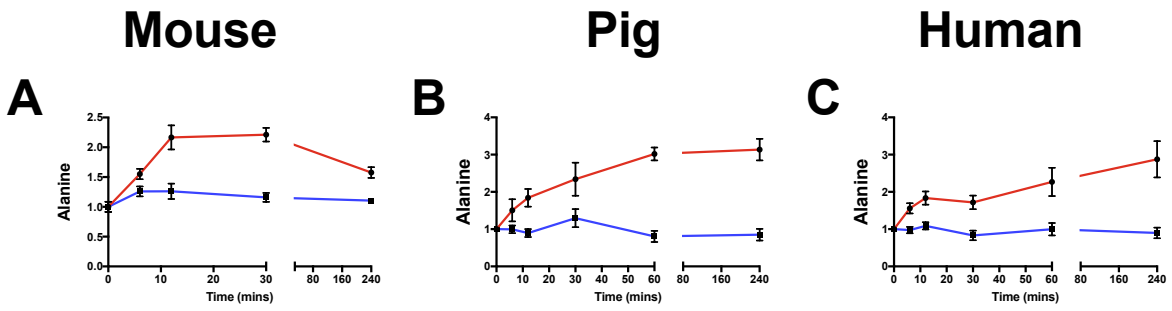

Figure 35: Relative change in tissue alanine during warm and cold storage in the mouse heart.

(a) mouse (n = 5-11), (b) pig (n = 5) and (c) human (n = 4) hearts during warm (red line) and cold (blue line) storage.

Mouse (n = 4 - 11), pig (n = 5) and human (n = 4) heart tissue was retrieved and exposed to variable periods of warm (red) or cold (blue) ischaemia. Tissue abundance was analysed by LC/MS and compared to normoxic baseline control tissue (mouse (n = 11), pig (n = 5), human (n = 4)).

Asparagine can be converted to aspartate which can then be transaminated generating the CAC oxaloacetate (158). Asparagine levels remained near baseline until 30 minutes of ischaemia. Thereafter, there was a divergence in tissue concentrations between warm and cold ischaemia. This translated to a significant difference in asparagine abundance between hearts during warm and cold storage ($F(1, 51) = 11.8$, $p = 0.0012$, two-way ANOVA). There was also a significant difference in tissue aspartate concentrations between warm and cold ischaemia ($F(1, 51) = 38.3$, $p < 0.0001$, two-way ANOVA). (Figure 36 (a)).

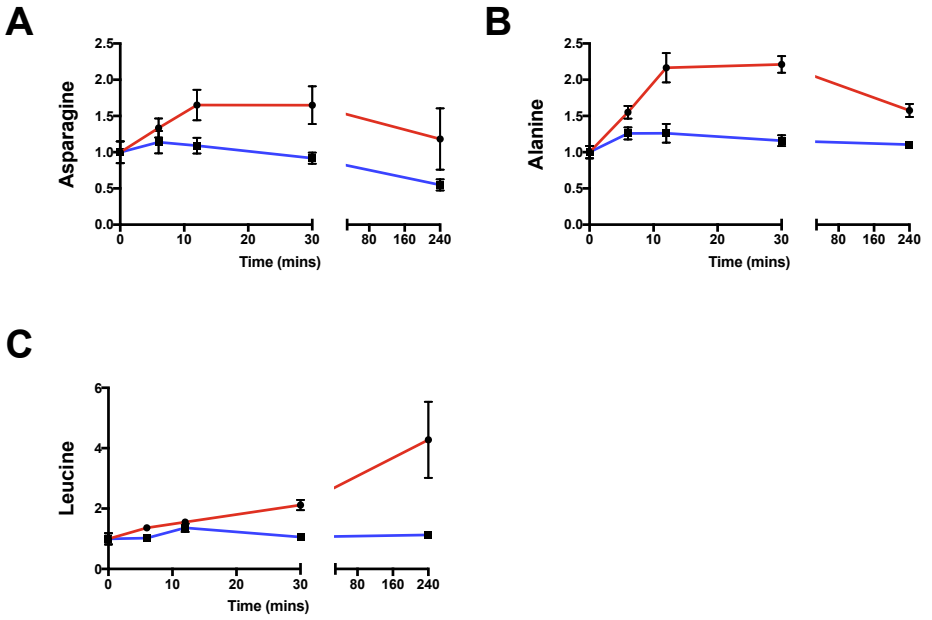

Figure 36: Amino acid tissue concentrations during warm and cold storage in the mouse heart.

Mouse hearts were rapidly excised and exposed to either warm (red) or cold (blue) ischaemia (n = 4-5) for variable periods of time before being clamp frozen. Tissue abundance was analysed by LC-MS and relative change compared to baseline, normoxic control hearts (n = 11) calculated.

In summary, different metabolic profiles between warm and cold ischaemia were identified in certain amino acids, in particular, alanine. The concentrations of other amino acids by contrast were quiescent, remaining at baseline tissue concentrations. Whilst constant flux through these pathways could account for such findings, the absence of dynamic changes could be interpreted as a cessation of flux during ischaemia in this model.

3.13 Discussion

Research over the course of the last half century has generated great insights into myocardial metabolism during both normoxia and ischaemia. In view of the great burden that ischaemic heart disease places on Western healthcare, this research has primarily centred around the pursuit to develop cardioprotective strategies and to improve outcomes following myocardial infarcts. In translating our understanding of myocardial ischaemic metabolism to the transplant arena, it is important that the models adequately replicates the clinical setting to ensure accurate extrapolation of data.

There are considerable difficulties exposing cells to periods of hypoxia *in vitro* and findings from studies in cardiomyocytes are often difficult to interpret. A number of *ex vivo* models of myocardial ischaemia have been used to expose myocardium to differing degrees of hypoxia or anoxia in a variety of flow states. There are a number of advantages to using isolated perfused organs to investigate myocardial metabolism. In these models, the heart can be exposed to hypoxia or anoxia in the presence of continued normal coronary perfusion, reduced coronary perfusion or a 'low-flow' state, or in the presence of no coronary flow. Myocardium may also be rendered locally ischaemic by ligation of a coronary artery or globally ischaemic through cessation of coronary perfusion or continued perfusion with anoxic perfusates. *In vivo* localised myocardial ischaemia models, such as the left anterior descending (LAD) coronary artery occlusion model, are also routinely used in the study of myocardial ischaemia. However, it is apparent that any conclusions drawn from a study or translated to another clinical scenario must take into account the true nature of the ischaemic environment to which the model exposes myocardium. For example, there is evidence that coronary occlusion does not completely stop perfusion in myocardial models of regional ischaemia. In animal models, collateral circulation has been shown to maintain flow at 10-20% of baseline flow in the infarct zone (150). This has the potential to significantly impact the ischaemic metabolic environment.

In studying the ischaemic changes that occur during organ storage in the context of organ transplantation I aimed to develop a model that would replicate the clinical scenario of global, no flow ischaemia in a whole organ. Furthermore, upon characterising ischaemic metabolism, I wanted to be able to extrapolate any findings to a reperfusion model in a vascularised solid organ transplant. The murine heterotopic heart transplant model was established at my institution and had previously been used to investigate IR injury. I therefore designed the model used in these experiments around the donor procedure. Cold storage organ preservation was replicated by immersing the heart in cold UW which was shown to rapidly cool myocardium. Hearts were exposed to warm ischaemia by leaving the heart in the carcass of the donor animal maintained at a constant temperature by use of a heat mat. It could be argued that the warm and cold environments to which the hearts were exposed were different and a more appropriate design would have placed the hearts in identical environments with only changes made to temperature. I elected against this approach on the grounds that; (1) this model better replicated the clinically relevant scenario

of primary warm ischaemia in DCD, and (2) previous investigators had used similar techniques and therefore, this enabled better comparison of findings (159).

The descriptive nature of the data generated by this analysis presents challenges for drawing definitive conclusions about the ischaemic metabolism of myocardial tissue during warm and cold ischaemia. Nonetheless, this approach provides a wealth of information that can be used to guide the more detailed examination of individual pathways. Previous studies have examined ischaemic metabolism but this approach examined a wide range of metabolites using an untargeted mass spectrometry approach that included analysis of nucleotides, thereby also enabling estimates of ATP/ADP and NADH/NAD^+ ratios to be made. There are inherent difficulties in measuring nucleotides accurately *in vivo* and therefore, cautious interpretation of the data is necessary. Furthermore, it is important to recognise that the measurement of intermediates reflect whole tissue changes. Using these techniques, for example, I was unable to differentiate between cytosolic or mitochondrial concentrations of these metabolites nor whether NADH or NAD^+ were free or protein bound (160).

I have made a number of assumptions in analysing the LC/MS spectrums of most of the metabolites. Importantly, I have assumed that there is a linear relationship between ion count and tissue concentration. The calculation of ratios such as ATP/ADP and NADH/NAD^+ ratios also assume that these nucleotides were detected at the same frequencies and that there wasn't degradation of these metabolites during analysis. One approach to addressing this issue was to quantify the ion count against standard curves of the metabolite. Tissue concentrations of some metabolites such as succinate and fumarate were quantified confirming a linear relationship between ion count and tissue concentrations of these metabolites at the concentrations observed in these tissues however, this could not be performed for all metabolites. An alternative method of analysing tissue concentrations of ATP and ADP were used and the results of this corroborated the findings of the LC-MS analysis for these nucleotides.

In addition to biological variability, the extraction and analysis of samples was a potential source of variability. The duration across which experiments were performed was minimised and extractions and analyses performed in single batches. Furthermore, baseline controls were used to normalise datasets against, if required.

These results are consistent with a rapid cessation of aerobic respiration at the onset of ischaemia in this model. Flux through glycolysis differed in warm and cold ischaemia. During warm ischaemia, there was evidence of inhibition of glycolysis despite there being detectable stores of tissue glycogen. This inhibition of glycolysis coincided with an elevation in tissue NADH/NAD^+. These data support GAPDH inhibition, due to a high NADH/NAD^+ ratio, as the cause for the cessation of anaerobic respiration during warm ischaemia. During cold ischaemia flux through glycolysis continued at a lower rate with more moderate tissue NADH/NAD^+ increases. As a result, cessation of glycolysis during cold ischaemia coincided with exhaustion of tissue glycogen stores.

In addition to the changes in glycolysis with warm and cold ischaemia I have also demonstrated diverse changes in succinate accumulation between warm and cold ischaemia. In warm ischaemia, succinate accumulated rapidly reaching a maximal succinate tissue concentration by 12 minutes. During organ storage in cold ischaemia, there was a small, early rise until 30 minutes. Thereafter, more prolonged duration of cold storage was associated with a persistent linear increase in succinate accumulation that continued until 12 hours. It is interesting that this rise continued in hearts that were beyond the limit of organ viability. These changes at the extreme durations of cold ischaemia were not observed in myocardial sections of human or porcine heart. In these experiments, further accumulation of succinate ceased.

There was also a marked difference in the succinate/fumarate ratio with warm ischaemia demonstrating a rapid increase in this ratio, not observed with cold ischaemia. The succinate/fumarate ratio is proposed as the driving force behind RET and therefore these findings would suggest a possible mechanism for the detrimental impact of warm ischaemia. The difference in succinate accumulation with prolonged duration of cold ischaemia points towards a possible role for the intact heart in mediating continued succinate accumulation with prolonged cold storage.

Finally, succinate accumulation during ischaemia was observed to be highly conserved across species including humans. This increases the potential for the translation of novel therapeutic agents designed to ameliorate IR injury from animal models into clinical practice.

In contrast to succinate accumulation, there was discordance across species with regards to the accumulation of the other CAC intermediates malate and fumarate. During warm ischaemia, malate and fumarate demonstrated different trends with a rapid decrease observed in the mouse and rapid increases observed in the pig and human hearts.

There is conflicting data within the literature relating to the metabolic profile of hearts during ischaemia. In contrast to the data from this analysis and other publications (53, 54, 161), data from a recent study examining myocardial interstitial, left ventricular metabolite concentrations measured using a microdialysis catheter in isolated, perfused rat hearts with global, no flow ischaemia demonstrated rapid accumulation of all CAC cycle metabolites during ischaemia within 30 minutes (162). The metabolic changes reported in this analysis are similar to those observed in the pig and human data reported here.

The C57BL/6J mouse used in these experiments is known to have a mutation in *Nnt* that has roles in metabolism. NNT is a key protein in the inner mitochondrial membrane and has been shown to impair mitochondrial function (163). Nevertheless, these studies were focused on mitochondrial function within the context of impaired glucose tolerance and diabetes and not within the context of IR injury however, this impaired mitochondrial function is a possible limitation of this work. Examining the metabolic changes during ischaemia in mouse strains with wild type *Nnt* could be considered in the first instance in order to address this concern.

Another explanation could be that these discrepancies reflect subtle differences in experimental models. *Ex vivo* models have a normoxic stabilisation period during which the heart is frequently perfused with glucose as the only substrate (162). Under physiological conditions, fatty acid oxidation provides the majority of substrate for ATP synthesis however, under a variety of conditions including heart failure, metabolic switching has been observed (34). The impact of metabolic switching on subsequent ischaemic episodes following changes in substrate utilisation is not known. In these data, the pig and human heart model used myocardial sections rather than whole hearts. The myocardial sections demonstrate only brief fibrillation as opposed to the whole mouse heart which continues to beat for up to 90 seconds following the onset of warm ischaemia. The impact of this is uncertain and contrasting effects on the direction of CAC cycling would not be impossible. Nevertheless, when mouse hearts were treated with cardioplegia, fumarate was observed to decrease, as opposed to the increase observed in pig and human cardiac sections. This would therefore, not support myocardial contraction as the source of the observed discrepancy in these CAC intermediates.

Succinate accumulation during ischaemia has been suggested to be the result of a reversal in the direction of succinate dehydrogenase and CAC cycling. This occurs in the presence of a highly reduced CoQ pool (54). Succinate accumulation during ischaemia was a conserved finding across species and it might therefore be expected that the changes in other CAC metabolites would also be similar. The different profiles in malate and fumarate could be interpreted as a different cycling of the CAC however, fumarate and malate both have cytosolic and mitochondrial pools and therefore the measured intermediate concentrations might not reflect mitochondrial concentrations. There are also other pathways that generate fumarate and malate such as the urea cycle and the malate-aspartate shunt that could be responsible for the differences observed.

This analysis highlights metabolites that appear to have similar profiles and provides a foundation for future work to elucidate the sources of key metabolites such as succinate and identify the active pathways during ischaemia and potentially provide novel targets for future therapies.

Chapter 4: Exploring the source of succinate accumulation during ischaemia

4.1 Exploring the source of succinate accumulation during ischaemia

4.1.1 Introduction

In the previous chapter, metabolomic profiling of mouse hearts during warm and cold ischaemia demonstrated a rapid accumulation of succinate during warm ischaemia, with a corresponding increase in the succinate/fumarate ratio, that was abrogated by cold organ storage.

Recent studies by our group has theorised the mechanism for this rapid accumulation of succinate during ischaemia to involve the reduction of fumarate at complex II (53, 54). This work demonstrated that the major carbon sources for CAC intermediates during normoxia, fatty acid ß-oxidation, glucose, the GABA shunt, and glutamate, did not contribute to the accumulation of succinate during ischaemia. Rather, two potential sources of fumarate were identified as possible candidates: the malate-aspartate shuttle (MAS)and AMP-dependent activation of the purine nucleotide cycle (PNC) (53).

Elucidating the mechanism of succinate accumulation is central to the development of future therapeutic agents. To further explore the source of succinate proposed from the work using an *ex vivo* model (53), I examined a number of potential pathways were using a variety of metabolic inhibitors in this model of ischaemia during organ retrieval. Metabolic inhibitors were administered in cardioplegic solution administered to the anaesthetised donor animals. Hearts were then stored under warm ischaemic conditions prior to clamp freezing and metabolite accumulation was compared to untreated control hearts that received only cardioplegia prior to warm ischaemia. LC-MS analysis was performed by Dr Ana S.H. Costa (Hutchinson/MRC Research Centre).

4.2 Aminooxyacetate (AOA)

AOA is competitive inhibitor of transaminases such as aspartate aminotransferase which catalyses the transamination of aspartate to oxaloacetate (162, 164, 165). AOA would be hypothesised to inhibit succinate accumulation during ischaemia by limiting the potential fumarate reservoir available for reduction in mitochondria. When AOA was administered at the onset of ischaemia, there was a significant decrease in succinate tissue concentrations after 12 minutes of warm ischaemia compared to the untreated control (one-way ANOVA and Bonferroni multiple comparison testing, $p = 0.001$) (Figure 37). This was also associated with trends towards a decrease in fumarate and for an increase in tissue aspartate, but the differences were not statistically significant ($p= 0.05$ and $p = 0.08$ respectively, one-way ANOVA and Bonferroni multiple comparison testing).

The amelioration of succinate accumulation together with a trend towards an increase in tissue aspartate concentrations would support the theory that the MAS is active in ischaemia and that inhibition of aminotransferases blocks this pathway. It is hypothesised that the cytosolic malate generated in the presence of the high $NADH/NAD^+$ ratio is exchanged for mitochondrial succinate by the dicarboxylate carrier (DIC). In the mitochondria matrix, it can then be converted to fumarate by mitochondrial fumarate hydratase before being reduced to succinate (54). The inhibition of aspartate transaminase is consistent with the observed more rapid decline in concentrations of malate and fumarate since the upstream substrate to this process, oxaloacetate, can no longer be generated.

Interestingly, these findings are at odds with the recent findings from Jespersen *et* al who reported an increase in myocardial interstitial fumarate and malate concentrations during ischaemia, in an *ex vivo*, global ischaemia model in the rat heart (162).

AOA is a non-specific competitive inhibitor of transaminases. This was consistent with a significant decrease in tissue concentrations of alanine in hearts treated with AOA (Figure 38). The accumulation of alanine during ischaemia is well recognised (151). Conceivably, this non-glycolytic, anaplerotic reaction could complement the transamination of aspartate to oxaloacetate by regenerating the α-ketoglutarate required. The decreased tissue concentrations of alanine with inhibition of alanine transaminase suggests that there is flux through this pathway and a potential role in the accumulation of succinate.

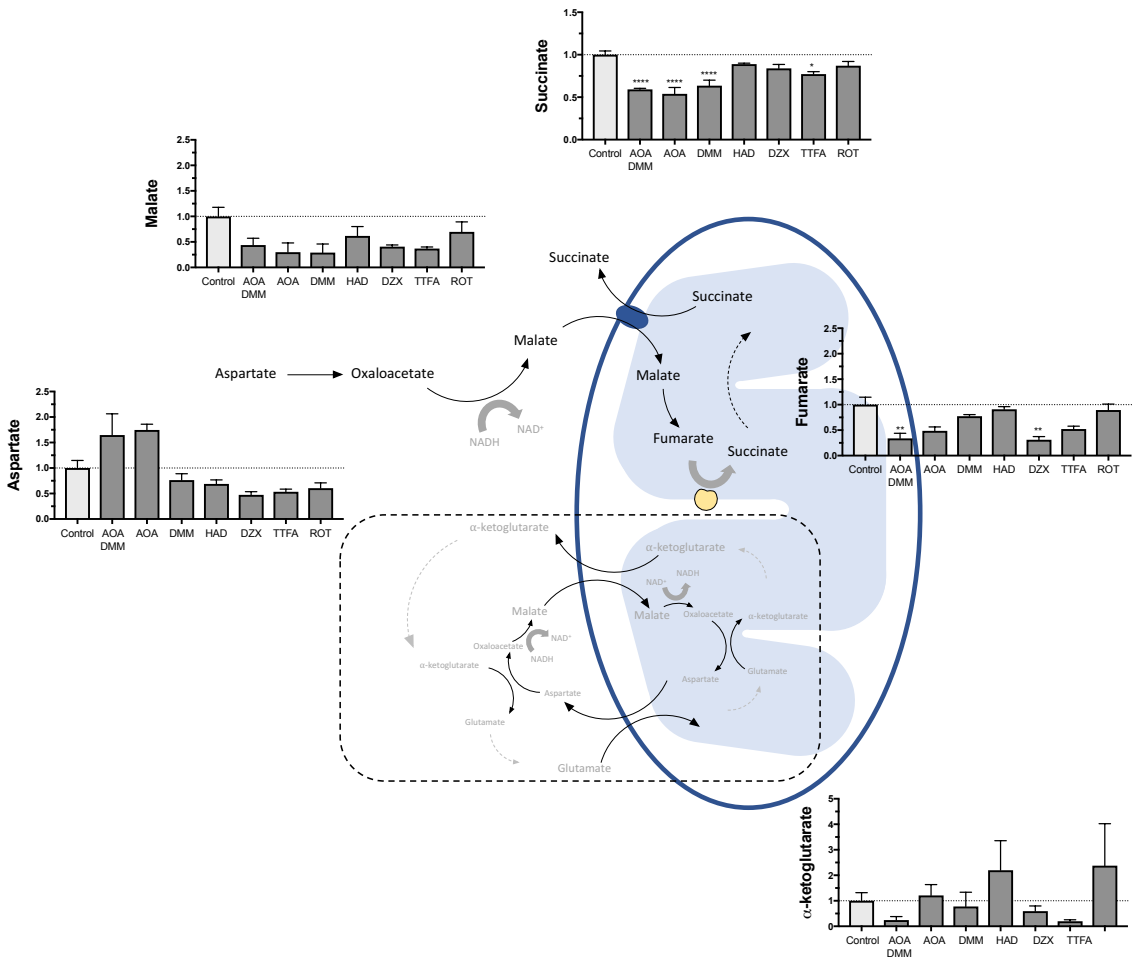

Figure 37: Effect of metabolic inhibitors on MAS intermediates during ischaemia in the mouse heart.

Donor animals (n = 4) received various metabolic inhibitors (2 mM aminooxyacetate (AOA), 3.2 mg dimethyl malonate (DMM), 1 mM diazoxide (DZX), 2 mM hadacidin (HAD), 1 mM thenoyltrifluoroacetone (TTFA) in 5% DMSO, or 60 μM rotenone (ROT) in 5% DMSO) as bolus injections in St Thomas' cardioplegia via a central vein immediately prior to rapid excision and storage in warm ischaemic conditions (12 minutes). Relative metabolite abundance was compared to control hearts that were treated with cardioplegia alone and stored in warm ischaemic conditions for 12 minutes (n = 8). One-way ANOVA with Bonferroni multiple comparisons testing. * $P < 0.05$, ** $P < 0.01$, *** $P < 0.001$, **** $P < 0.0001$.

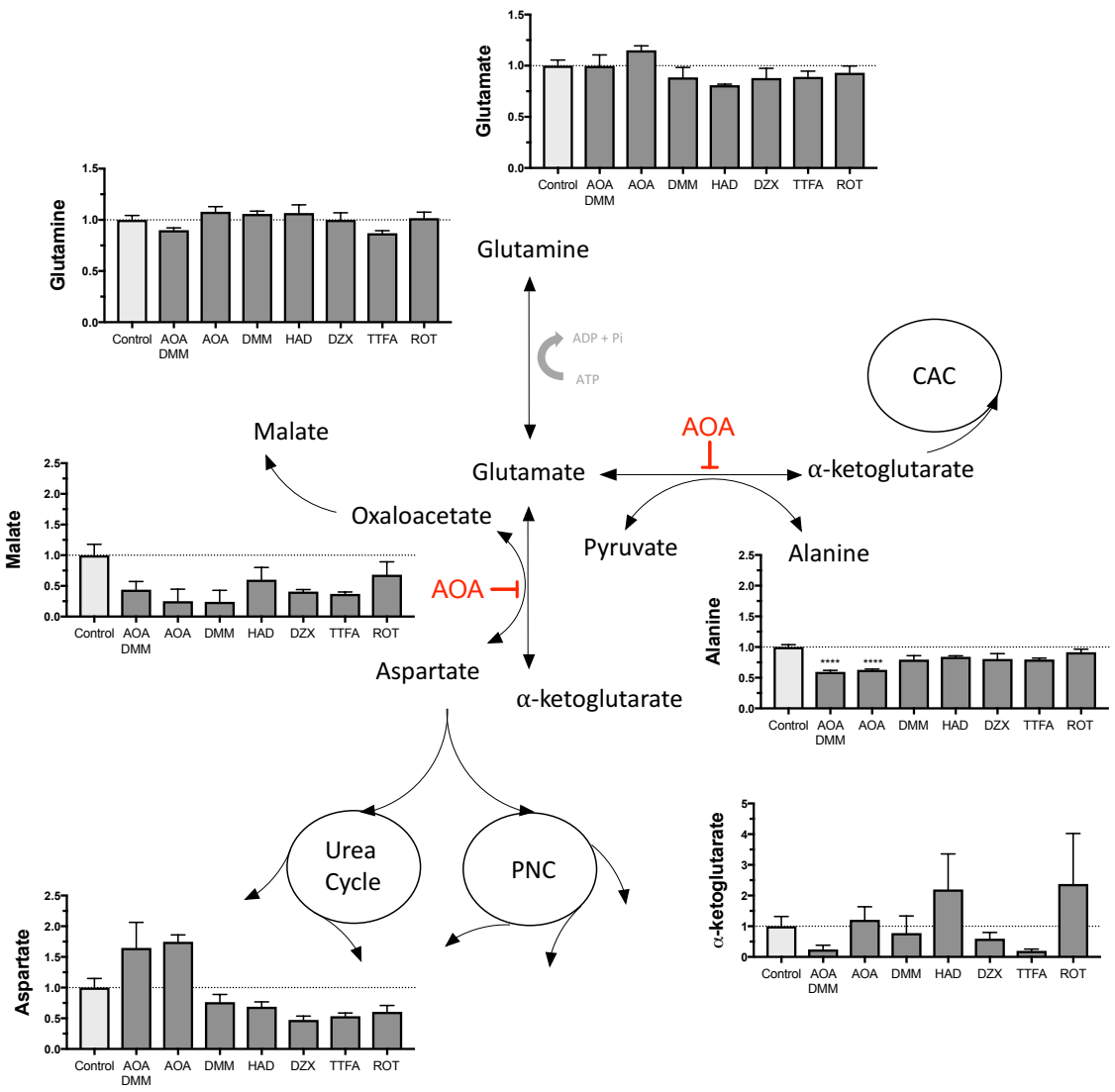

Figure 38: Effect of metabolic inhibitors on transamination in the mouse heart.

Donor animals (n = 4) received various metabolic inhibitors (2 mM aminooxyacetate (AOA), 3.2 mg dimethyl malonate (DMM), 1 mM diazoxide (DZX), 2 mM hadacidin (HAD), 1 mM thenoyltrifluoroacetone (TTFA) in 5% DMSO, or 60 μM rotenone (ROT) in 5% DMSO) as bolus injections in St Thomas' cardioplegia via a central vein immediately prior to rapid excision and storage in warm ischaemic conditions (12 minutes). Relative metabolite abundance was compared to control hearts that were treated with cardioplegia alone and stored in warm ischaemic conditions for 12 minutes (n = 8). One-way ANOVA with Bonferroni multiple comparisons testing. * $P < 0.05$, ** $P < 0.01$, *** $P < 0.001$, **** $P < 0.0001$.

4.3 Dimethyl malonate (DMM)

Dimethyl malonate is hydrolysed *in vivo* to produce the competitive inhibitor of complex II, malonate. DMM has previously been shown to ameliorate succinate accumulation during ischaemia (53, 161). Preliminary dose-response studies demonstrated rapid hydrolysis of DMM *in* vivo with no detectable DMM identified after 12 minutes of warm ischaemia following administration of up to 20 mg of DMM (Figure 39(a)). This was further supported by an associated increase in malonate abundance (Figure 39(b)). In addition, there was an associated significant amelioration of succinate accumulation (one-way ANOVA and Bonferroni multiple comparison testing, $p = 0.002$). There were no significant changes in other detected MAS (Figure 37) or CAC (Figure 40) intermediates after 12 minutes of warm ischaemia. Similar changes in CAC intermediates were demonstrated between baseline normoxic controls and hearts exposed to 12 minutes of warm ischaemia (Figure 41).

These data support the theory that complex II is responsible for the increase in succinate accumulation observed during ischaemia in the mouse heart. Furthermore, I have demonstrated that delivery of DMM at the onset of ischaemia is sufficient to achieve elevated tissue concentrations and effective inhibition of complex II in this model and will investigate this further in Chapter 5.

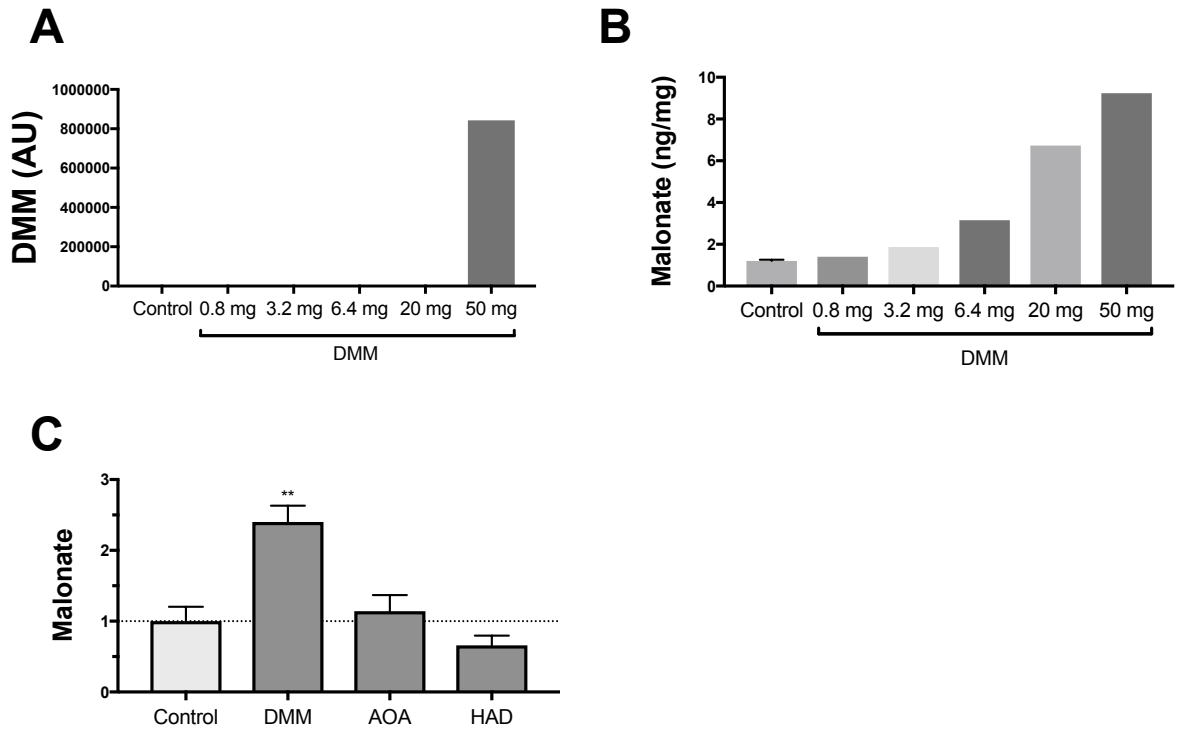

Figure 39 (a – c): DMM undergoes rapid hydrolysis *in vivo*.

A 500 μL inferior vena cava (IVC) bolus injection of St Thomas' cardioplegia was administered to anaesthetised donor animals with varying concentrations of DMM (12 μM (0.8 mg), 48 μM (3.2 mg), 97 μM (6.4 mg), 300 μM (20 mg), 757 μM (50 mg) (n = 1 - 4) or another metabolic inhibitor (2 mM aminooxyacetate (AOA) or 2 mM hadacidin (HAD) (n = 4)). Following the administration of metabolic inhibitor or cardioplegia alone, hearts were stored for 12 minutes of warm ischaemia prior to clamp freezing. Tissue DMM abundance and malonate was quantified by LC-MS and compared to control hearts that were treated with cardioplegia alone and stored in warm ischaemic conditions for 12 minutes (n = 4), ** $p < 0.01$.

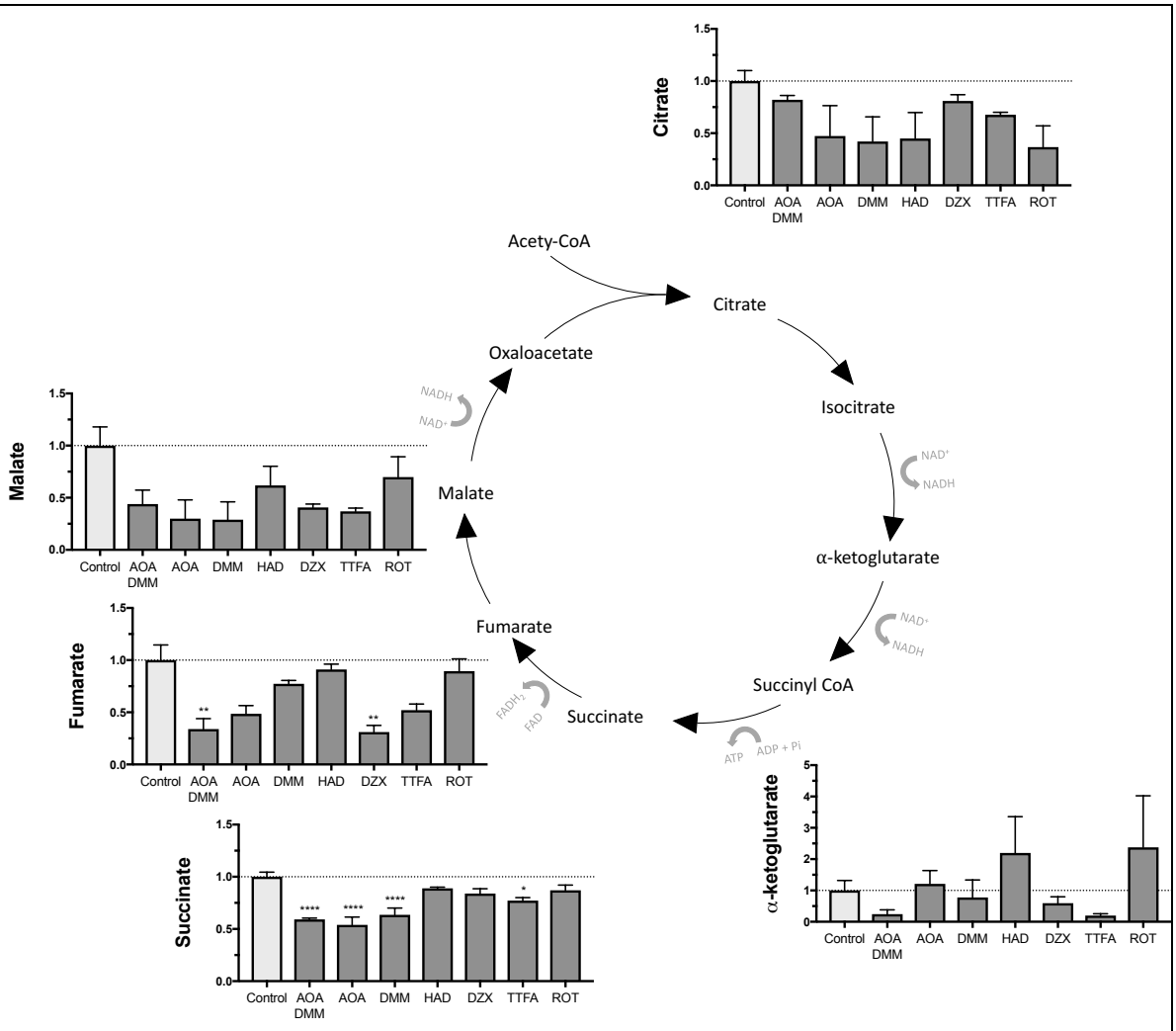

Figure 40: The effect of metabolic inhibitors on CAC metabolite accumulation during warm ischaemia.

Donor animals (n = 4) received various metabolic inhibitors (2 mM aminooxyacetate (AOA), 3.2 mg dimethyl malonate (DMM), 1 mM diazoxide (DZX), 2 mM hadacidin (HAD), 1 mM thenoyltrifluoroacetone (TTFA) in 5% DMSO, or 60 μM rotenone (ROT) in 5% DMSO) as bolus injections in St Thomas' cardioplegia via a central vein immediately prior to rapid excision and storage in warm ischaemic conditions (12 minutes). Relative metabolite abundance was compared to control hearts that were treated with cardioplegia alone and stored in warm ischaemic conditions for 12 minutes (n = 8). Significant changes by one-way ANOVA with Bonferroni multiple comparison testing * $P < 0.05$, ** $P < 0.01$, *** $P < 0.001$, **** $P < 0.0001$.

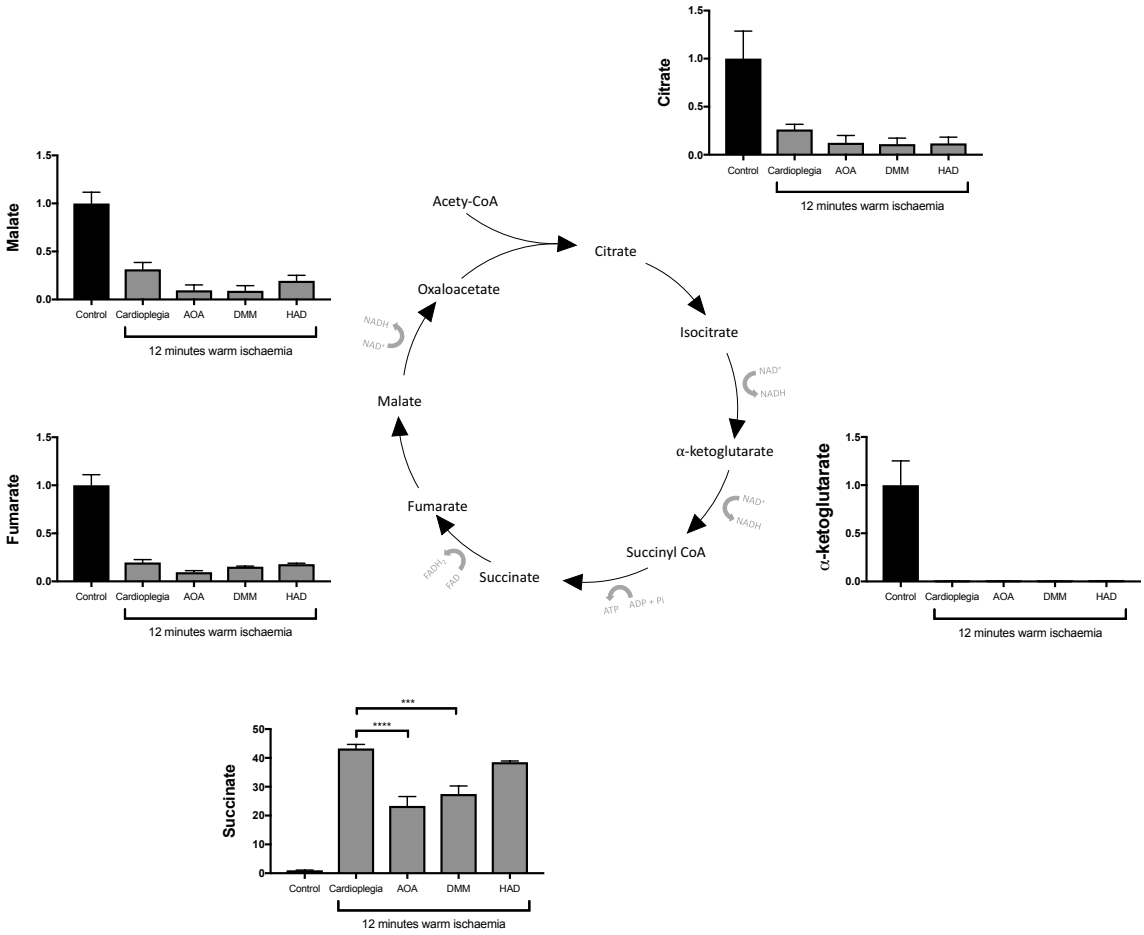

Figure 41: Relative change of CAC metabolites compared to baseline normoxic tissue following the administration of cardioplegia and various metabolic inhibitors or cardioplegia alone.

Donor animals (n = 4) received various metabolic inhibitors (2 mM aminooxyacetate (AOA), 3.2 mg dimethyl malonate (DMM), 2 mM Hadacidin) as bolus injections in St Thomas' cardioplegia via a central vein immediately prior to rapid excision and storage in warm ischaemic conditions (12 minutes). Relative metabolite abundance was compared to control hearts that were rapidly excised and immediately snap frozen (n = 5). Significant changes by one-way ANOVA with Bonferroni multiple comparison testing (**** p<0.0001, *** p<0.001, ** p<0.01, * p<0.05).

4.4 Dimethyl malonate and aminooxyacetate

The data above demonstrate that DMM and AOA moderated ischaemic metabolism in this model, ameliorating the accumulation of succinate when administered in isolation. This was associated with complementary changes in other related metabolites. I next examined the impact of administration of the two compounds together on succinate accumulation and other metabolic intermediates.

Interestingly, there was an additive effect on tissue fumarate when both DMM and AOA were administered concurrently. When administered alone, DMM and AOA significantly reduced tissue succinate compared to controls but there was no significant decrease in tissue fumarate. When administered together the significant reduction in tissue succinate was associated with a significant decrease in tissue fumarate. There were no other significant changes in other measured metabolites when compared to controls (Figure 37).

4.5 Hadacidin

Another proposed source of fumarate during ischaemia was the PNC (53). The net result of the PNC is to convert aspartate and GTP into fumarate and AMP. This is catalysed by adenylosuccinate synthetase (ADSS) and adenylosuccinate lyase. Hadacidin is a specific competitive inhibitor of ADSS (166).

In this study, there was no significant change in the tissue succinate or fumarate concentration when donor hearts were treated with hadacidin. Furthermore, there was no significant change in the tissue abundance of the PNC intermediates, AMP, IMP nor adenosine which have also previously been used as surrogates of PNC activity (Figure 37 and Figure 42) (167).

These findings are at odds with Wu *et al* who demonstrated evidence of inhibition of the PNC by hadacidin during ischaemia in *ex vivo* perfused hearts (167) and would refute the notion that the PNC is a source of fumarate for reduction to succinate at complex II by mitochondria. These data do not, however, differentiate between an inadequate inhibition of ADSS by hadacidin and adequate inhibition in the absence of flux through this pathway during ischemia. Dose-response curves were performed and no response was observed at higher doses despite demonstrating that hadacidin was detectable in mouse hearts after 12 minutes of warm ischaemia (Figure 43). The initial step converting aspartate to adenylosuccinate in the PNC requires energy in the form of GTP. In the ischaemic environment of the cell low concentrations of GTP would make this unfavourable and could explain the failure of hadaciding to change tissue concentrations of succinate in these data.

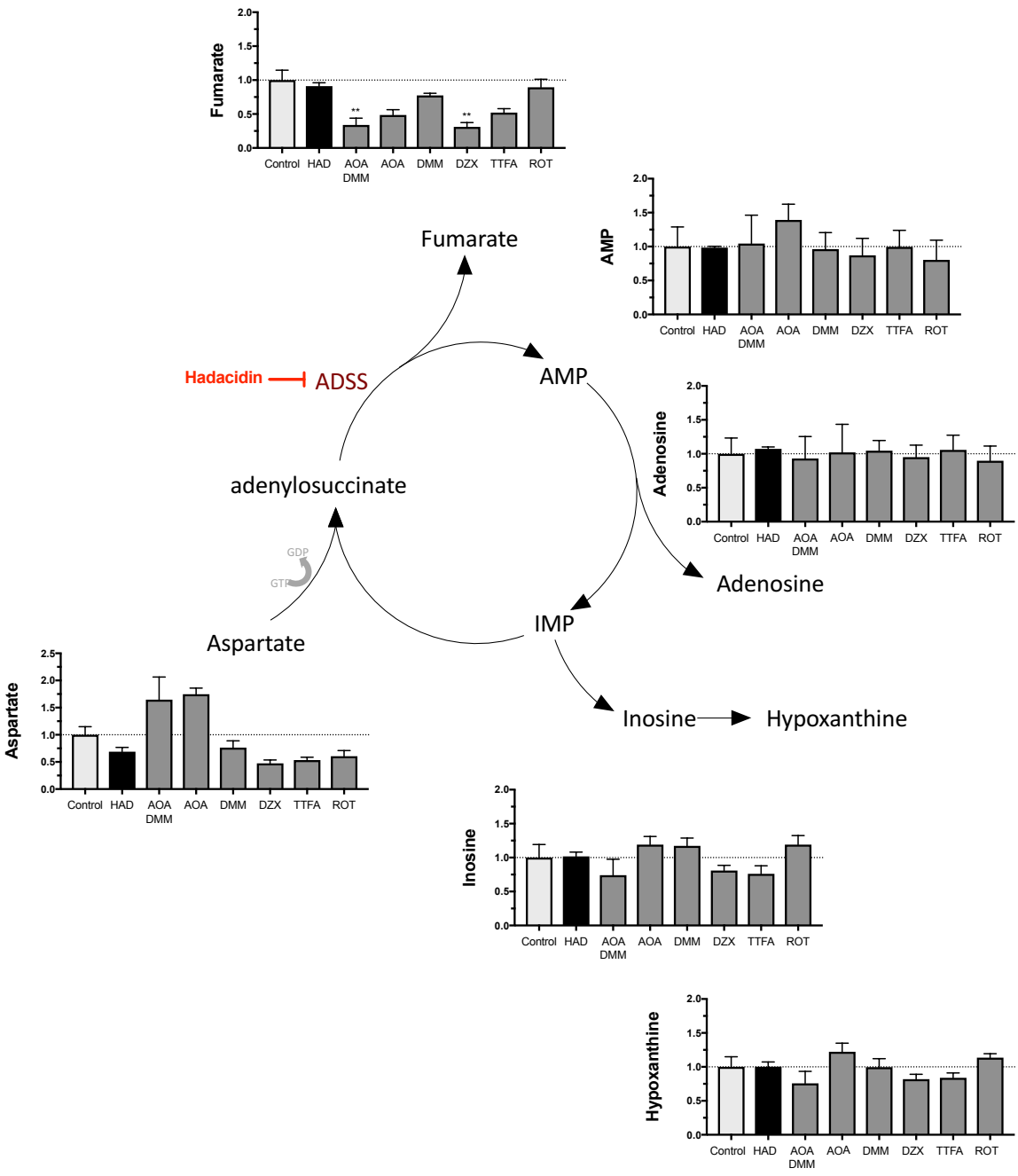

Figure 42: Effect of hadacidin administration on ischaemic metabolism in the mouse heart

Donor animals (n = 4) received various metabolic inhibitors (2 mM aminooxyacetate (AOA), 3.2 mg dimethyl malonate (DMM), 1 mM diazoxide (DZX), 2 mM hadacidin (HAD), or 60 µM rotenone (ROT)) as bolus injections in St Thomas' cardioplegia via a central vein immediately prior to rapid excision and storage in warm ischaemic conditions (12 minutes). Relative metabolite abundance was compared to control hearts that were treated with cardioplegia alone and stored in warm ischaemic conditions for 12 minutes (n = 8). One-way ANOVA with Bonferroni multiple comparison testing. * $P < 0.05$, ** $P < 0.01$. Mean baseline control metabolite abundance denoted by dotted line.

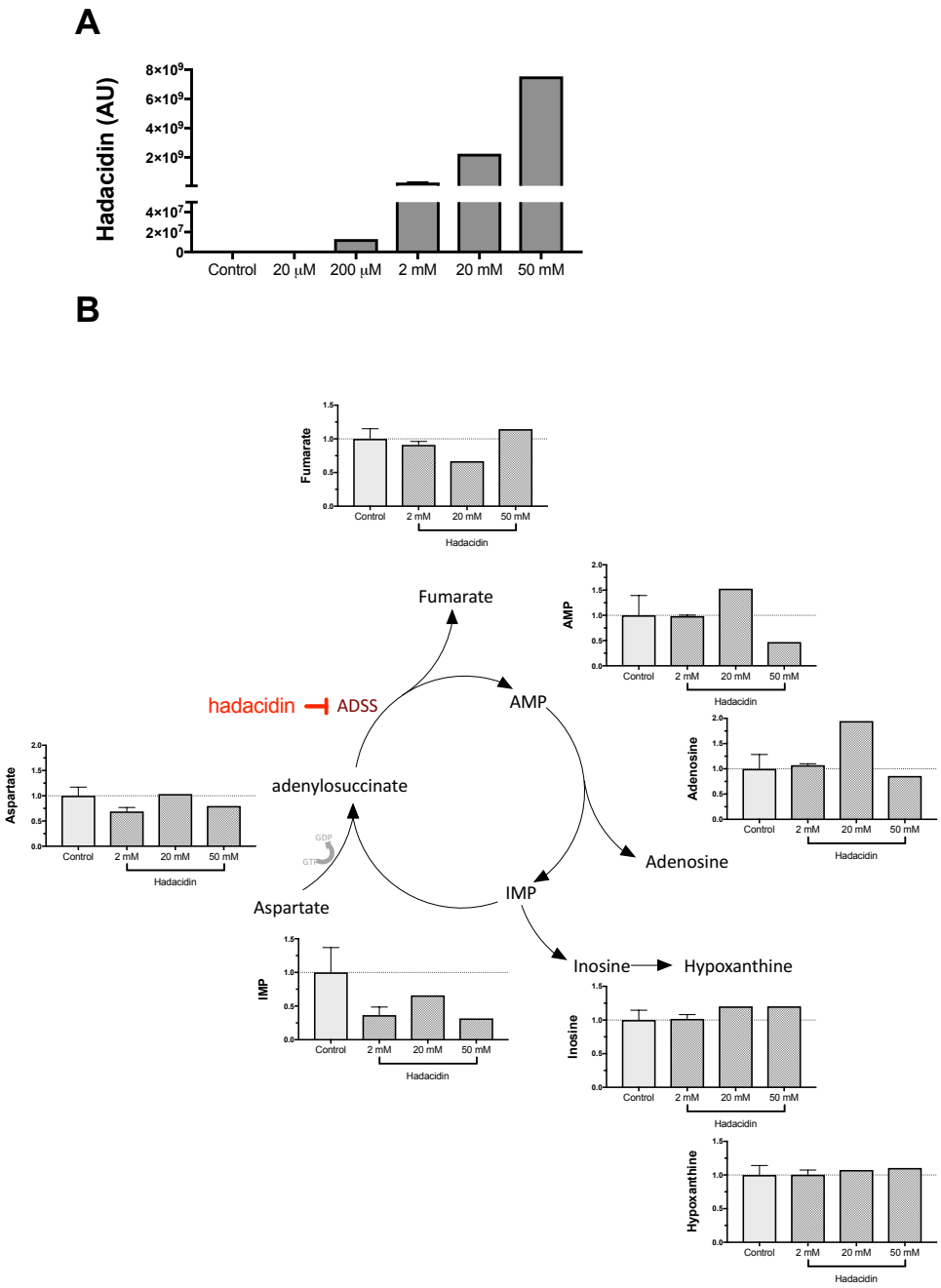

Figure 43 (a and b): The efficacy of hadacidin administration by bolus injection and the impact on PNC intermediate metabolites during warm ischaemia.

Donor animals (n = 1-4) received the metabolic inhibitor Hadacidin at variable concentrations (20 μM, 200 μM, 2 mM , 20 mM, 50 mM) as a bolus injections in St Thomas' cardioplegia via a central vein immediately prior to rapid excision and storage in warm ischaemic conditions (12 minutes). Hadacidin abundance was detected in hearts by LC-MS. Relative metabolite abundance was compared to control hearts that were treated with cardioplegia alone and stored in warm ischaemic conditions for 12 minutes (n = 4). One-way ANOVA with Bonferroni multiple comparison testing. Mean baseline control metabolite abundance denoted by dotted line.

4.6 Thenoyltrifluoroacetone (TTFA) and Diazoxide (DZX)

In addition to competitive inhibition at the dicarboxylate binding site, complex II can also be inhibited at the ubiquinone binding site (Q-site). TTFA is a non-competitive inhibitor of complex II. When bound to the Q-site it prevents the transfer of electrons from the dicarboxylate binding site of complex II (168, 169). Preliminary dose-response studies demonstrated low solubility and tissue delivery at concentrations above 100 μM in cardioplegic solution alone. In order to increase delivery to concentrations that had previously demonstrated a metabolic effect it was necessary to increase solubility. This was achieved with dimethyl sulfoxide (DMSO). When TTFA was administered with 5% DMSO w/v in cardioplegic solution a metabolic effect on succinate accumulation was observed with concentrations of 1 mM TTFA (Figure 44). Succinate accumulation during ischaemia was significantly ameliorated at 12 minutes of warm ischaemia (one-way ANOVA and Bonferroni multiple comparison testing, $p = 0.001$). This was not however, associated with a significant change in fumarate or other CAC and MAS intermediate compared to control (Figure 37 and Figure 40).

DZX has been shown to effect cardiac metabolism through two pathways. DZX is a selective opener of the ATP sensitive-potassium channel that has been shown to have cardioprotective properties and improve preservation of hearts stored in cold storage (170). More recently, however, DZX has also been shown to directly inhibit complex II (171, 172). In contrast to TTFA, DZX administration demonstrated no significant amelioration of succinate accumulation during warm ischaemia, although there was a significant reduction in fumarate abundance. Interestingly, changes in tissue fumarate were not observed with TTFA (Figure 37 and Figure 40). Whilst there were trends towards a reduction in tissue malate with the administration of DZX and TTFA, these were not statistically significant (one-way ANOVA with Bonferroni multiple comparison testing) (Figure 37**).**

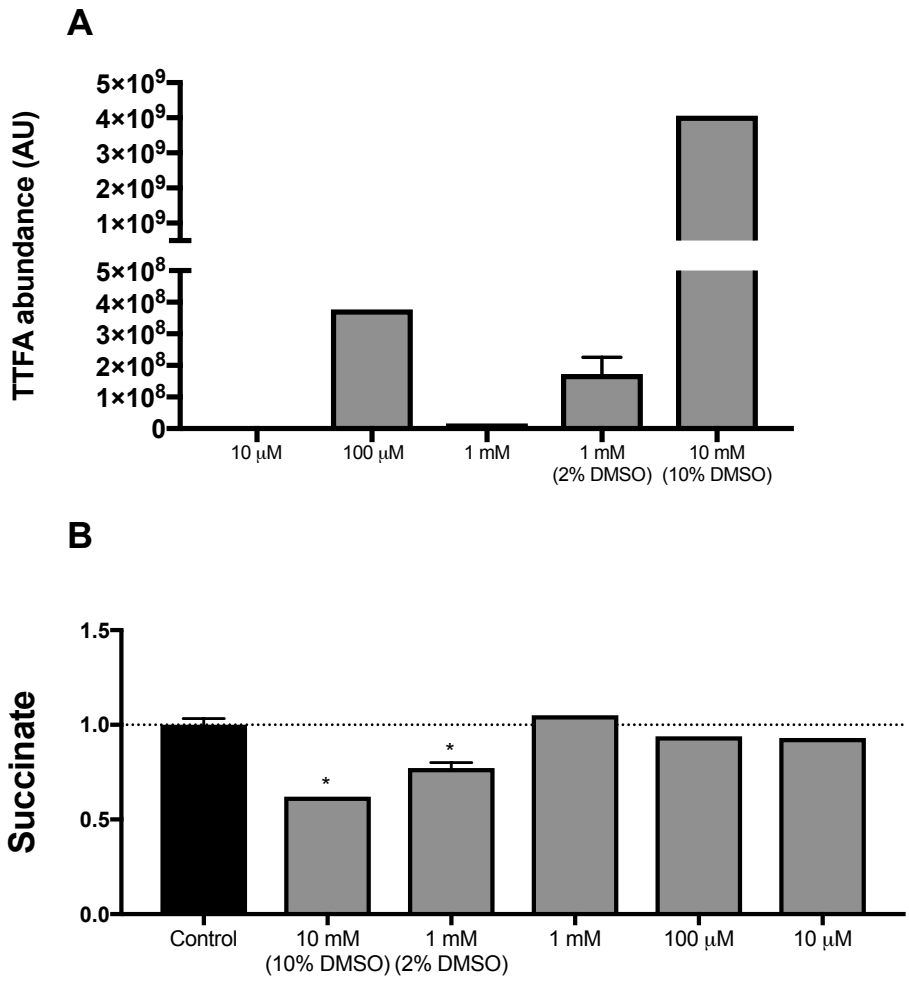

Figure 44: TTFA solubility and delivery to the heart following IVC bolus injection with cardioplegia.

Donor animals (n = 1-4) received the metabolic inhibitor TTFA at variable concentrations (10 μM, 100 μM, 1 mM , 1 mM, 10 mM) as a bolus injections in St Thomas' cardioplegia via a central vein immediately prior to rapid excision and storage in warm ischaemic conditions (12 minutes). Relative metabolite abundance was compared to control hearts that were treated with cardioplegia alone and stored in warm ischaemic conditions for 12 minutes (n = 4). Significant changes by one-way ANOVA with Bonferroni multiple comparison testing. * $P < 0.05$

4.7 Rotenone

Rotenone is a potent, irreversible inhibitor of complex I. In these experiments, it did not have any effect on succinate, fumarate or other metabolites during ischaemia. While this may be due to inadequate delivery *in vivo,* it would equally be consistent with low activity of complex I during ischaemia (Figure 37, Figure 38 and Figure 40)(173). The lack of changes in CAC metabolites would be consistent with the rapid cessation of oxidative phosphorylation at the onset of ischaemia and complex I inhibition would potentially be hypothesised to have a greater impact on reperfusion. Complex I is fundamental to the burst of mtROS on reperfusion and therefore, effectively delivering an agent that could inhibit this process *in vivo* could be invaluable to investigating IR injury. The poor solubility of rotenone *in vivo* however makes this very challenging. Moreover, the central role of complex I to oxidative phosphorylation makes complex I inhibitors highly toxic to the cell and the irreversible nature of complex I inhibition with rotenone will make identifying a therapeutic window *in vivo* difficult. It would nevertheless be interesting to examine the early metabolic changes in the first few minutes following reperfusion in a transplanted heart treated with rotenone however, the toxicity may confound longer term follow up and the interpretation of reperfusion injury and its impact on organ dysfunction. An alternative approach could be to investigate the efficacy of less potent complex I inhibitors such as the biguanide, metformin.

4.8 Discussion

The comparative metabolomics from chapter 3 identified a rapid accumulation of succinate during warm ischaemia that was significantly abrogated by cold storage of organs. The rapid accumulation of succinate and the mechanisms through which it accumulates have previously been explored in an *ex vivo* global ischaemia model(53). In this chapter, I further examined the metabolic processes involved in succinate accumulation during warm ischaemia. Focussing on complex I and II, the PNC and the MAS, I examined the early period of warm ischaemia (12 minutes) when a marked divergence in the metabolomic profiles was apparent between organs preserved in cold and warm storage. Moreover, the untargeted LC-MS approach enabled analysis of multiple metabolic intermediates and pathways in myocardial tissue during ischaemia. To examine the accumulation of succinate during warm ischaemia I used metabolic inhibitors of the PNC, the MAS and 3 different inhibitors of complex II.

4.8.1 Efficacy of metabolic inhibitors in organ storage

Three of these inhibitors, TTFA, DMM and AOA, had a significant effect on succinate accumulation during ischaemia. The Q site inhibitor of complex II, TTFA, reduced the accumulation of succinate during ischaemia. This was not, however, associated with a significant change in fumarate. Fumarate is reduced to succinate in the presence of a highly reduced Q-pool during ischaemia. Inhibition of SDH could potentially produce reciprocal changes in other CAC intermediates. There was a non-significant decrease in tissue fumarate observed with TTFA. Succinate is required for co-transport of malate at the dicarboxylate carrier (DIC) into the mitochondria. The malate exchanged into the mitochondria is converted into fumarate by fumarate hydratase and therefore the decrease in available mitochondrial malate would be consistent with the changes in fumarate concentrations observed with TTFA administration in this study (54). DZX also inhibits complex II. Unlike TTFA however, administration of DZX was not associated with a change in tissue succinate. There was however, a significant decrease in tissue fumarate associated with DZX. Whether the failure to ameliorate succinate accumulation was due to inadequate delivery to the mitochondrial matrix, inadequate concentrations at the onset of ischaemia or a consequence of an off-target effect was not identified. In other studies, the inhibitory effect of DZX was observed to be less efficient than TTFA and malonate (169, 172).

Competitive inhibition of the dicarboxylate binding site of complex II with malonate also demonstrated a significant amelioration of succinate accumulation during ischaemia with no change in fumarate. Interestingly, there was a significant decrease in malate with DMM administration. There was a general trend towards a more rapid decrease in malate with all complex II inhibitors and AOA, but only reached statistical significance in hearts treated with DMM and AOA.

AOA is a competitive inhibitor of aspartate aminotransferase and was also shown to significantly reduce succinate accumulation during warm ischaemia in this model. In addition, administration of AOA was associated with a significant increase in tissue aspartate and a decrease in tissue fumarate compared to the untreated control. The non-specific nature of transaminase inhibition by AOA was highlighted by the

significant reduction in the rise in tissue alanine that was observed during ischaemia. In addition, this further supports flux through a pathway involving alanine during ischaemia. The marked accumulation of alanine during cardiac ischaemia has previously been observed (151). It was observed to increase stoichiometrically to the rate of aspartate degradation. Succinate accumulation in this study was minor in comparison and it was thus proposed that alanine accumulated in ischaemic myocardium through a series of anapleurotic reactions utilising aspartate and CAC intermediates (151). The metabolic changes observed in this study would support flux through a process involving alanine but in contrast to this being isolated from succinate accumulation, it would appear to be intricately involved. It could be proposed that the transamination of pyruvate and glutamate to alanine regenerates α–ketoglutarate in the process enabling the further generation of oxaloacetate. This process would require continued production of pyruvate through glycolysis. Alanine tissue concentrations are observed to increase rapidly during the first 12 minutes of warm ischaemia before remaining constant. This would be consistent with such a mechanism.

4.8.2 Activity of PNC during ischaemia

The PNC has previously been proposed as a source of fumarate during ischaemia. Hadacidin is a specific inhibitor of ADSS which is necessary for the generation of fumarate and AMP from adenylosuccinate. There was no change in succinate associated with ADSS administration. Furthermore, there was no change in any of the downstream metabolites after ADSS. These findings could either be interpreted as a failure in adequate delivery and inhibition of ADSS or as a lack of flux through the PNC during ischaemia in this model. It is interesting that the initial step involving the generation of adenylosuccinate from aspartate and IMP is a GTP-dependent process which is likely to be scarce during ischaemia.

The heart is highly metabolically active and myocardial oxygen reserves are rapidly exhausted following complete cessation of coronary flow. During aerobic respiration myocardium derives energy in the form of ATP primarily from ß-oxidation of fatty acids and the oxidation of glucose (34). In the absence of oxygen, these processes cease and the heart is reliant on glycolysis as the principal source of energy. The heart can demonstrate versatility, however, switching between these different metabolic processes depending on a variety of other conditions including substrate availability and myocardial energy status (34, 36, 174). This has the potential to influence the effects of metabolic inhibitors *in vivo* when investigating their impact on ischaemic metabolism. The technique employed in this model sought to minimise the metabolic effect of administering inhibitors during normoxia by delivering the metabolic inhibitor at the onset of ischaemia without any prior ischaemic insult. The animal was oxygenated throughout anaesthesia prior to the administration of cardioplegia and the metabolic inhibitor being examined. The rapid induction of diastolic asystole was visually confirmed by the cessation of an apex beat and subsequent rapid excision of the heart prevented spontaneous return of contraction.

In examining the effect of a metabolic inhibitor, it is necessary to ensure adequate delivery of the inhibitor at adequate concentrations to its target. All metabolic inhibitors were administered by IVC bolus

injection with cardioplegia. Rapid intracellular or extracellular hydrolysis of the precursor DMM to malonate was confirmed by the presence of significantly elevated tissue malonate and the absence of a DMM LC-MS signal after 12 minutes of ischaemia. The inner mitochondrial membrane is highly impermeable to charged molecules and therefore, transport of intermediates into mitochondria is highly regulated requiring specific transporters. Although malonate has previously been shown to be taken up into mitochondria, direct competitive inhibition could nevertheless not be definitively confirmed. The other metabolic inhibitors used in this study did not undergo modification after administration and, therefore, similar inferences could not be made. LC-MS signals were detectable in tissues after 12 minutes ischaemia following IVC bolus injection. The exact intracellular or extracellular location of these can only be assumed, however significant alterations in the metabolic profile of hearts was observed using some of these which provides a useful surrogate.

Another potential problem in analysing the impact metabolic inhibitors of mitochondrial processes *in vivo* is that the LC-MS analysis cannot differentiate between the exact location of intermediates. The cytosolic compartment constitutes, by volume, a greater proportion of cell mass than the mitochondrial matrix. Small but biologically significant changes in mitochondrial metabolic intermediates could thus not be detected as significant changes in overall tissue concentrations of metabolites in our analysis. Similarly, stoichiometric changes between compartments were also not appreciated using this technique.

4.8.3 Summary

In summary, the amelioration of succinate accumulation by DMM and TTFA supports the hypothesis that succinate accumulation during ischaemia occurs through reduction of fumarate at complex II. The effect of AOA inhibition on aspartate aminotransferase and the reduction in succinate accumulation further supports aspartate as a source of fumarate used to generate this succinate. The observation that AOA inhibition also significantly alters alanine concentrations suggests a possible additional role for alanine in this process.

It has previously been proposed that the PNC is a source of fumarate during ischaemia. The results from these data do not support this. No change in any of the measured PNC metabolites were identified. Adequate intracellular and or mitochondrial delivery of metabolic inhibitors remains a potential concern, however, since the PNC is an energy dependent process requiring GTP. In the energy depleted environment of ischaemic myocardium, although previous data has suggested to the contrary, it would seem paradoxical for it to be activated and therefore, one explanation for these findings is that PNC is inactive during ischaemia.

In addition to providing important additional insights to the existing literature on the mechanism of succinate accumulation during ischaemia, this work also highlights the potential of DMM as a therapeutic agent in the amelioration of IR injury associated with organ preservation and provided a rationale to investigate the efficacy of DMM in a small animal model of IR injury in organ transplantation.

Chapter 5: Moderating IR injury in a model of solid organ transplantation

5.1 Moderating IR injury in a model of solid organ transplantation

5.1.1 Introduction

The murine heterotopic heart transplant is a vascularised model of solid organ transplantation developed by Corry et al(135). It has previously been modified to study the role of ischaemia reperfusion injury in organ transplantation. In this adapted model, a standard (30 minute) or prolonged (240 minute) period of cold ischaemia was used to induce mild or severe ischaemic injury before transplantation(138). The metabolomic data described in chapter 3 identified warm ischaemia as the predominant factor in the accumulation of succinate in a mouse heart model of organ storage. Succinate accumulation has been shown to be a key factor in driving IR injury and a recent clinical study has identified warm ischaemia as a key determinant of graft survival in solid organ transplantation(175). This provided the rationale for the development of a novel model of IR injury within the setting of solid organ transplantation that examined the effect of warm ischaemia in exacerbating IR injury and organ dysfunction.

Outcome markers related to both mitochondrial and organ dysfunction were examined. Mitochondrial dysfunction was assessed by measuring mitochondrial DNA damage. This was done by measuring the relative amplification by PCR of short and long sequences of mitochondrial DNA. Mitochondrial damage interrupts the amplification of the long sequence and is therefore inversely proportional to relative mitochondrial damage. Organ dysfunction was assessed by measuring the recipient serum troponin at 24 hours after transplantation.

5.1.2 Developing a novel and reproducible model of IR injury in organ transplantation

To replicate a DCD scenario, a period of warm ischaemia was introduced by exsanguinating the animal under anaesthesia. A standoff period was observed with the thorax closed to mimic the clinical scenario. During this period the animals core temperature was maintained at 37°C using a heating pad and relayed rectal temperature probe. Initially, hearts were retrieved after a stand-off period of 6 and 12 minutes and compared to hearts retrieved immediately with minimal exposure to additional warm ischaemia.

After a 6-minute delay before proceeding with the standard retrieval all hearts would beat spontaneously on reperfusion. When hearts retrieved with an additional 6 minutes of warm ischaemia were compared to those retrieved immediately with minimal additional warm ischaemia, there was marked variability observed within the warm ischaemia group and no significant difference in serum troponin (control vs 6 mins WI, 12.3 ± 5.3 (n=3) vs 6.9 ± 1.2 (n=7)). (Figure 45). Furthermore, there was no significant difference in mitochondrial dysfunction between groups (Figure 45(a)).

Metabolomic analysis demonstrated that there was a continued rise in succinate accumulation beyond 12 minutes. Since all hearts were observed to contract spontaneously on reperfusion after 6 minutes of additional warm ischaemia, the warm ischaemic period was extended to 12 minutes. Increasing additional warm ischaemia to 12 minutes resulted in a non-significant increase in the mean serum troponin rise at

24 hours when compared to 6 minutes of primary warm ischaemia (16.9 ± 6.4 (n=4) vs 12.3 ± 5.3 (n=3) p = 0.62). As observed with 6 minutes additional warm ischaemia, there was marked variability in organ dysfunction following the reperfusion of hearts exposed to 12 minutes of additional warm ischaemia which led to a failure to demonstrate a difference in either, mitochondrial DNA damage or organ dysfunction between hearts transplanted with and without the additional 12 minutes of primary warm ischaemia (relative amplification of mtDNA (0.41 ± 0.07 (n=4) vs 0.31 ± 0.05, (n = 7) p = 0.35); recipient serum troponin at 24 hours (16.9 ± 6.4 (n = 4) vs 12.3 ± 5.3 (n = 7) p = 0.07) (Figure 46).

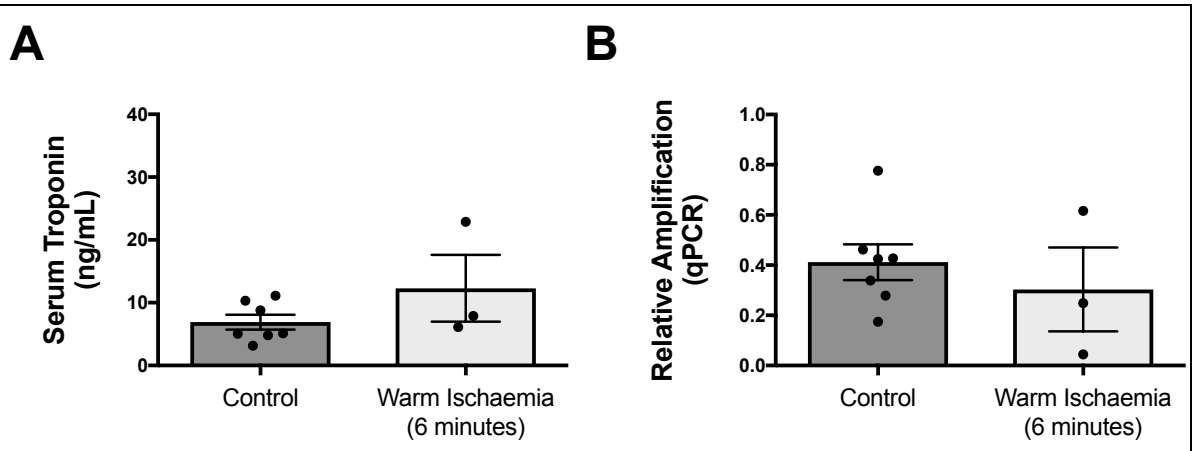

Figure 45: Effect of 6 minutes of warm ischaemia on IR injury following heterotopic heart transplantation in the mouse.

Donor animals (n = 3 - 7) were anaesthetised and exsanguinated by division of the IVC and aorta. A standoff period of 6 minutes was observed with the donor animals core temperature maintained at 37°C. Hearts were heterotopically transplanted after minimal additional cold ischaemia and the reperfusion injury compared to those of a standard transplant without additional warm ischaemia.

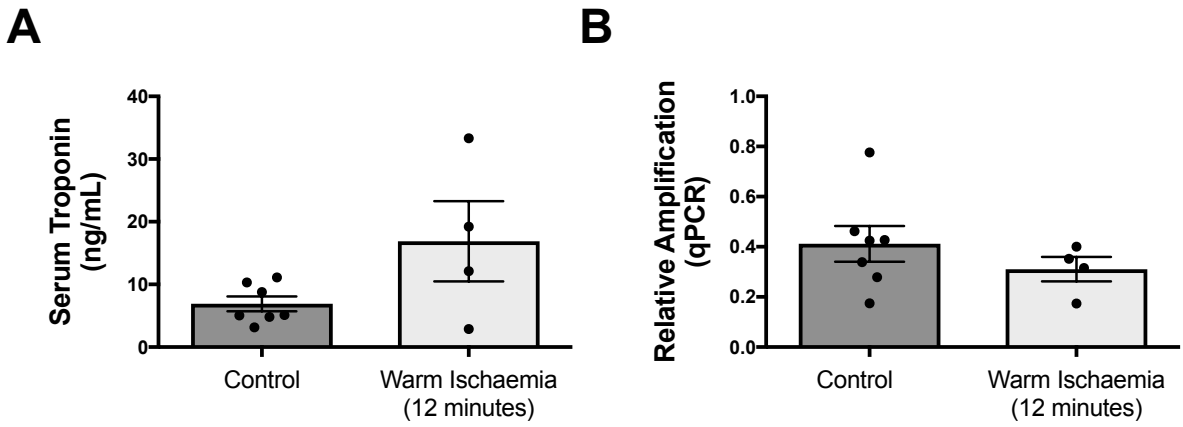

Figure 46: Effect of 12 minutes of warm ischaemia on IR injury following heterotopic heart transplantation in the mouse.

Donor animals (n = 4 - 7) were anaesthetised and exsanguinated by division of the IVC and aorta. A standoff period of 12 minutes was observed with the donor animals core temperature maintained at 37°C. Hearts were heterotopically transplanted after minimal additional cold ischaemia and the reperfusion injury compared to those of a standard transplant without additional warm ischaemia.

During the donor retrieval operation, topical ice-cold saline was regularly applied to the heart. There is inherent variability in the efficacy of myocardial cooling using this technique which is likely to be amplified by the cardioplegic effects of hypothermia and the associated effects on metabolism. To minimise the effects of variable cardiac contraction during warm ischaemia and the retrieval operation a new protocol with administration of cardioplegia to the donor animal at the time of organ harvest was developed.

Cardioplegia has been used in human clinical practice in a variety of situations during cardiac surgery for a number of decades (44). It can be administered directly to the heart as an antegrade or retrograde infusion. Direct cardiac infusion was precluded in this model due to limited access to microsurgical positive pressure ventilation in our institution. Intubation and ventilation would have been necessary if a sternotomy were to be performed allowing access to the mediastinum for appropriate preparation and cannulation of vessels. Systemic, central venous administration via the abdominal IVC provided a reliable alternative approach inducing cardiac arrest within 5 seconds of a bolus injection of 500 µL cardioplegic solution (Cardioplegic Solution, Harefield Hospital Formulation, Terumo BCT Ltd, UK). There was an apparent passive diffusion of cardioplegia following bolus administration that was aided by respiratory effort, evidenced by a return of cardiac contraction within approximately 60 seconds following bolus administration of cardioplegia if there was no additional intervention. By proceeding immediately to retrieval however, a sufficient extracellular potassium concentration was maintained and the heart remained in diastole. The donor heart could then be subjected to an additional period of warm ischaemia at the end of the retrieval procedure before transfer to cold storage solution.

5.1.3 Additional primary warm ischaemia following retrieval with cardioplegia

To examine whether cardioplegia impacted IR injury in this model recipient serum troponin at 24 hours post reperfusion was compared in hearts retrieved with and without cardioplegia. Hearts were retrieved either following donor administration of cardioplegia or without cardioplegia and transplanted heterotopically into recipient animals. Recipient serum troponin at 24 hours post reperfusion was significantly reduced when cardioplegia was administered to the donor animal arresting cardiac contraction (Figure 47(a)). In addition to significantly reducing the mean tissue injury there was also a reduction in variability when cardioplegia was administered prior to retrieval (1.96 ± 0.13 (n=6) vs 6.90 ± 1.17 (n=7), p = 0.0007) (Figure 47). The difference observed in IR injury with the presence or absence of cardiac contraction during retrieval was not observed when hearts were exposed to an additional 12-minute period of warm ischaemia. There was no significant difference in IR injury between hearts exposed to an additional 12 minutes of warm ischaemia following the administration of cardioplegia or when retrieved after exsanguination and a 12-minute standoff time. There was however, a reduction in the variability in serum troponin following the administration of cardioplegia (8.6 ± 1.9 (n = 6) vs 16.8 ± 6.4 (n = 4), p = 0.18). These findings suggested that the administration of cardioplegia to the donor heart during retrieval reduced IR injury but also reduced the variability in IR injury when compared to hearts that continued to contract during the retrieval operation. Importantly, when hearts were retrieved after administration of cardioplegia and subjected to an additional period of warm ischaemia and were compared to hearts transplanted without additional warm ischaemia there was a significant increase in IR injury (1.0 ± 0.13 (n=6) vs 8.6 ± 1.9 (n=6) p = 0.003) (Figure 47(b)). In Section 5.1.2 I demonstrated that mouse hearts could be successfully transplanted following IR injury that resulted in a troponin rise at 24 hours post reperfusion of up to 33 ng/ml (Figure 46(a)). This troponin rise was greater than that observed in any transplant performed when cardioplegia was administered to donor hearts. The greatest serum troponin rise observed in recipients of donor hearts retrieved after cardioplegia administration and exposed to 12 minutes of additional warm ischaemia was 17 ng/ml (Figure 47(b)). The duration of primary warm ischaemia in donor hearts retrieved after cardioplegia administration could theoretically be increased further without compromising successful transplantation. However, the use of 12 minutes of warm ischaemia enabled comparison with metabolomic data and was shown to significantly increase IR injury in this model. Therefore, extending primary warm ischaemia beyond 12 minutes was not explored.

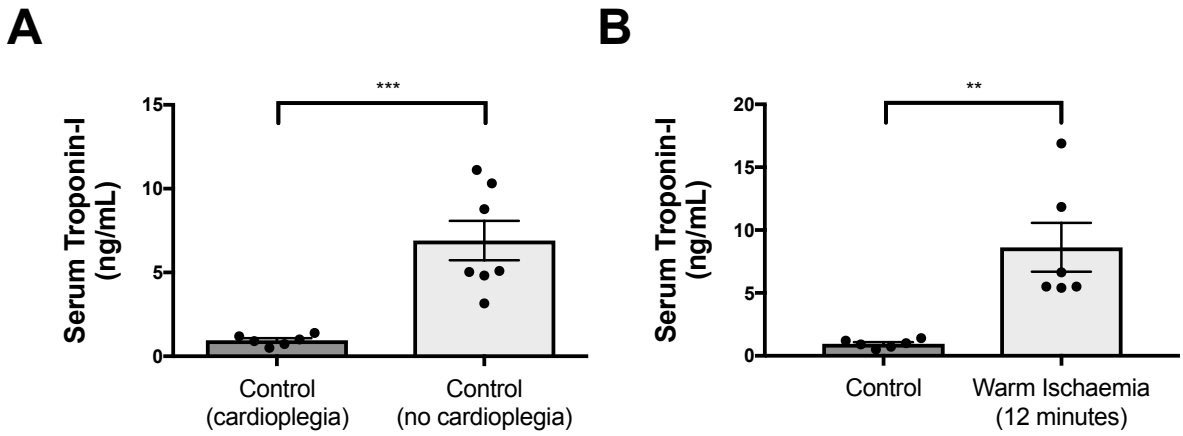

Figure 47: Effect of cardioplegia and 12 minutes of warm ischaemia on reperfusion injury in the heterotopic heart transplant.

(a) Hearts (n = 6-7) were retrieved from anaesthetised donors following IVC administration with cardioplegia or retrieved after standard exsanguination and division of the IVC and aorta. Hearts were heterotopically transplanted after minimal additional cold ischaemia and recipient serum troponin measured at 24 hours. **(b)** Hearts (n = 6) were retrieved from anaesthetised donors immediately following IVC administration of cardioplegic solution. Hearts were either heterotopically transplanted with no additional warm ischaemia or stored for 12 minutes of warm ischaemia in the carcass of the donor maintained at 37°C with a heat mat. Two-tailed, unpaired t-test. * $p < 0.05$, ** $p < 0.01$, *** $p < 0.001$.

5.1.4 Summary

In summary, I have established a reproducible mouse model of ischaemia reperfusion injury in heart transplantation with the ischaemic component comprising an additional 12 minutes of warm ischaemia. There was a reduction in the extent and variability of reperfusion injury observed in all hearts when cardioplegia was administered during the retrieval procedure. This model was then used to investigate the role of IR injury in organ transplantation and the efficacy of therapeutic agents.

5.2 Therapeutic efficacy of agents in ameliorating IR injury in organ transplantation

The metabolomic data presented in chapter 3 demonstrated that succinate accumulates in the mouse heart during organ storage to a greater extent during warm ischaemia. In other models of IR injury, the accumulation of succinate during ischaemia was shown to be responsible for driving ROS production and organ dysfunction upon reperfusion. Succinate accumulation during ischaemia has also been shown to be attenuated with inhibitors of various steps in this pathway providing not only a testable hypothesis but also therapeutic potential in this setting.

During organ transplantation, there are multiple opportunities during which therapeutic agents could potentially be administered to the donor organ or recipient. Chouchani *et al* demonstrated a cardioprotective effect of DMM in the *in situ* LAD occlusion model. In this model, DMM (4 $mgKg^{-1}min^{-1}$, total dose 3.2 mg) was administered as a continuous infusion 10 minutes prior to the onset of ischaemia and continued throughout the proceeding 30 minutes of ischaemia. In a solid organ transplant model, continuous infusion during the ischaemic phase is not feasible in a small animal model. An equivalent dose of DMM was therefore infused into the donor animal 10 minutes prior to retrieval.

The efficacy of DMM in ameliorating reperfusion injury was examined following a donor DMM infusion for 10 minutes (0.32 $mgmin^{-1}$) immediately prior to ischaemia. Donor hearts were subjected to an additional 12 minutes of warm ischaemia after retrieval. All hearts contracted spontaneously following reperfusion and were beating at 24 hours. Reperfusion injury, denoted by recipient serum troponin concentration at 24 hours, was significantly decreased in hearts from donors that received the DMM infusion immediately prior to retrieval (Figure 48).

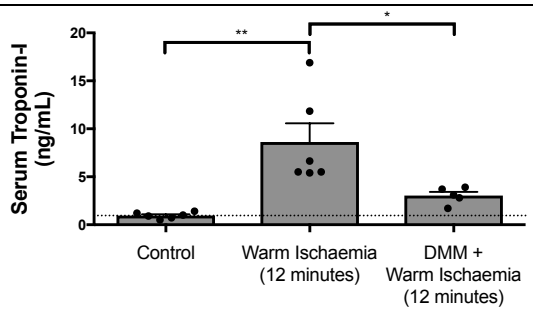

Figure 48: DMM ameliorates IR injury in a mouse heart transplant model.

Anaesthetised donors were either treated with an infusion of DMM (n =5) or saline control (n=6) 10 minutes prior to retrieval. Donor hearts were retrieved following IVC administration of cardioplegia and exposed to either 12 minutes of warm ischaemia or no additional warm ischaemia. Donor hearts were then transplanted heterotopically in to recipient animals and compared to control transplants (n = 6). Control hearts were retrieved from donor animals after administration of cardioplegia and were not exposed to any additional warm ischaemia. Following retrieval hearts were heterotopically transplanted after minimal additional cold ischaemia and recipient serum troponin measured at 24 hours. One-way ANOVA with Bonferroni's multiple comparison testing. * $p < 0.05$, ** $p < 0.01$.

In chapter 4, I demonstrated that the same total dose of DMM used in this experiment administered as a bolus with cardioplegia significantly reduced tissue succinate concentrations after 12 minutes of warm ischaemia. These findings were consistent with previous reports (53). In this model, DMM administered as an infusion during normoxia prior to the onset of ischaemia did not ameliorate succinate accumulation (Figure 49) despite its abrogation of IR injury and organ dysfunction (Figure 48).

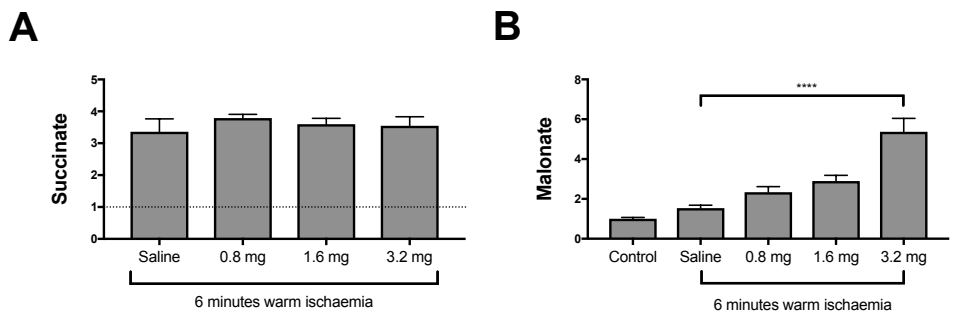

Figure 49: The effect of DMM infusion on tissue malonate and succinate concentrations.

Anaesthetised donor animals (n = 5 per group) received an infusion of DMM at increasing concentrations (total DMM infusion 0.8 mg, 1.6 mg or 3.2 mg) or a saline control for 10 minutes prior to retrieval. Hearts were retrieved following exsanguination and exposed to an additional 6 minutes warm ischaemia prior to clamp freezing and metabolomic analysis by LC-MS. One-way ANOVA with Bonferroni's multiple comparison testing. **** $p < 0.0001$

There was a discrepancy between the metabolic effect on succinate accumulation of DMM administered at subtly different stages of organ retrieval and the observed amelioration of IR injury with DMM. When DMM was administered as an infusion prior to retrieval there was a significant reduction in serum troponin. In contrast, when DMM was administered as a bolus with cardioplegic solution the significant reduction in serum troponin was no longer observed (Figure 50). The limited study period and resources precluded further examination of this disparity however, one explanation could be insufficient numbers to adequately power statistical analysis.

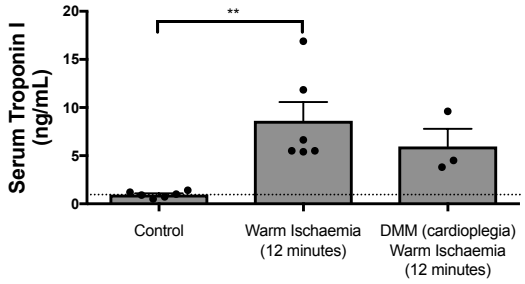

Figure 50: DMM administered as a bolus did not significantly ameliorate IR injury in a mouse heart transplant model.

Anaesthetised donors were retrieved immediately after a receiving a bolus of DMM (3.2 mg) in cardioplegic solution (n = 3) or cardioplegia alone (n= 6). Hearts were exposed to either 12 minutes of warm ischaemia. Donor hearts were transplanted heterotopically in to recipient animals and compared to control transplants that were not exposed to any additional warm ischaemia (n = 6). Allograft dysfunction was assessed by recipient serum troponin measured at 24 hours. One-way ANOVA with Bonferroni's multiple comparison testing. ** $p < 0.01$.

5.2.1 Modifying succinate accumulation and exacerbating IR injury in the mouse heart during organ transplantation

Chouchani et al. demonstrated exacerbation of IR injury following the administration of dimethyl succinate (DMS) (53). To investigate whether exogenous succinate could be delivered to myocardial tissue in this model I examined whether a bolus administration of DMS with cardioplegia would significantly elevate tissue concentrations of succinate. Tissue concentrations of DMS, succinate and fumarate were measured by LC-MS after 12 minutes of warm ischaemia.

In contrast to DMM, there was a detectable DMS signal after 12 minutes of warm ischaemia suggesting hydrolysis of the precursor, DMS, to succinate was less rapid than DMM *in vivo* (Figure 51(a)). Furthermore, there was no significant increase in tissue succinate ($p = 0.25$) nor significant decrease in tissue fumarate ($p = 0.07$) following administration of DMS to donor hearts. This failure to demonstrate a metabolic effect with DMS translated into a failure of DMS to exacerbate injury; a DMS (0.64 $mgmin^{-1}$) infusion administered over 10 minutes prior to retrieval failed to exacerbate IR injury when compared to a standard transplant (Figure 52).

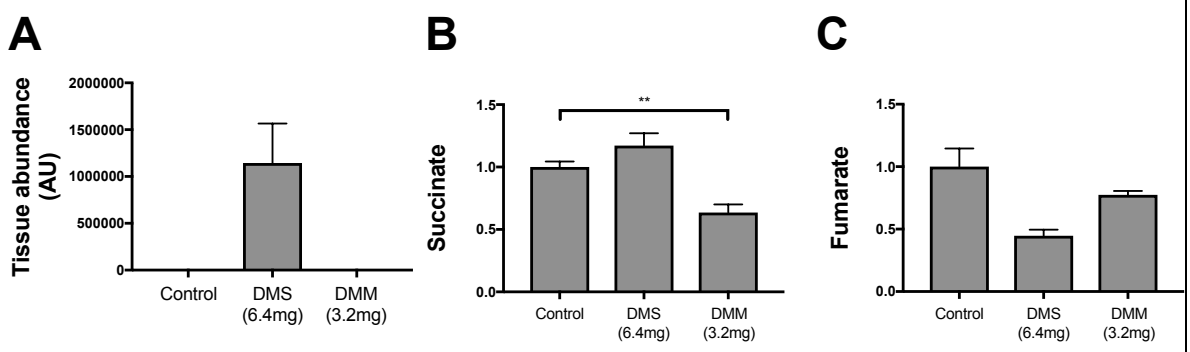

Figure 51: DMS delivery following IV bolus with cardioplegia and the associated metabolomic effect.

Donor animals (n = 4) received DMM (3.2 mg) or DMS (6.4 mg) as bolus injections in St Thomas' cardioplegia via a central vein immediately prior to rapid excision and storage in warm ischaemic conditions (12 minutes). Relative metabolite abundance was compared to control hearts that were treated with cardioplegia alone and stored in warm ischaemic conditions for 12 minutes (n = 8). One-way ANOVA with Bonferroni's multiple comparison testing. ** $p < 0.01$.

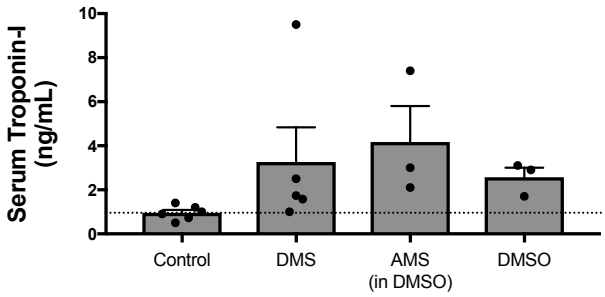

Figure 52: DMS, AMS (in 5% w/v DMSO) or 5% DMSO administered to donor hearts prior to ischaemia did not significantly exacerbate reperfusion injury in a mouse heart transplant model.

Anaesthetised donors received an infusion of DMS (6.4 mg) (n = 5), acetoxymethyl succinate (AMS) in 5% w/v DMSO (n = 3), 5% DMSO (n = 3), or a saline control (n = 6) 10 minutes prior to retrieval. Cardioplegia was administered immediately prior to retrieval. Donor hearts were transplanted heterotopically into recipient animals. Allograft dysfunction was assessed by recipient serum troponin measured at 24 hours.

The presence of DMS in donor hearts after 12 minutes of ischaemia (Figure 51(a)), and the failure to exacerbate tissue injury could be explained by inadequate hydrolysis of the DMS *in vivo* in this model. To improve delivery of succinate to tissues alternative compounds were examined. Acetoxymethyl succinate is rapidly hydrolysed *in vitro* (176). It is poorly soluble in saline and 5% w/v DMSO was used to increase solubility. 5% w/v DMSO was not demonstrated to be detrimental when administered to donor hearts however, acetoxymethyl succinate also failed to significantly exacerbate tissue injury in this model (Figure

52). Unfortunately, due to limited availability of the compound I was unable to examine the effect of acetoxymethyl succinate on tissue succinate concentrations during ischaemia. It will be important to examine this in the future.

5.3 Discussion

In this chapter, a novel, vascularised, small animal model of IR injury in solid organ transplantation was developed. Previous metabolomic data identified warm ischaemia as the predominant driver of succinate accumulation in organ storage. To investigate the effect of succinate accumulation on reperfusion injury in organ transplantation it was necessary to develop a small animal model of solid organ transplantation in which the additional ischaemic injury was a period of warm ischaemia. This was in contrast to previous models that used prolonged cold ischaemia to introduce a severe ischaemic component. The addition of a period of warm ischaemia has clinical relevance in the UK where the use of DCD organs is increasing and recent evidence from registry data has identified increased primary warm ischaemia to be associated with worse graft outcomes(175).

When primary warm ischaemia was introduced in this model by means of a standoff period similar to that used in DCD donors marked variability in the extent of IR injury was observed. To reduce the variability of the ischaemic injury, cardioplegia was administered to donor animals. With the introduction of cardioplegia the variability in the model was reduced. A reproducible ischaemic insult of 12 minutes of primary warm ischaemia translated into significant exacerbation of organ dysfunction as measured by recipient serum troponin at 24 hours post reperfusion when compared to organ dysfunction following transplantation without any additional warm ischaemia.

Having developed a novel model of IR injury in organ transplantation, the therapeutic efficacy of metabolic inhibitors and compounds in modifying tissue succinate was examined. The relatively controlled onset of ischaemia and reperfusion in organ transplantation makes it appealing for the development of therapeutic interventions. In the model used in these experiments there are a number of potential opportunities to administer therapies. Chouchani *et al* demonstrated efficacy of DMM in a non-recovery LAD occlusion mouse model. In this model DMM was administered as an infusion 10 minutes prior to the onset of ischaemia and then continued throughout the subsequent 30 minutes of ischaemia(53).

When a similar approach was used to deliver DMM in the organ transplant model, an infusion of DMM prior to the onset of ischaemia significantly reduced reperfusion injury. Further studies confirmed adequate delivery of malonate to tissues was achieved with this DMM regime however, a significant reduction in succinate accumulation was not observed. When DMM was administered as a bolus with cardioplegia, adequate delivery of malonate was again observed. In contrast to DMM administration as an infusion, this also translated into a significant reduction in tissue succinate. This did not however, translate into a significant reduction in organ dysfunction on reperfusion as observed when DMM was administered as an infusion. These differences in the metabolic effects following subtly different techniques of DMM administration could be explained by the direction in which the CAC is operating at the time of DMM administration. The absence or presence of oxygen is a critical determinant of the direction of the CAC. During administration of DMM as an infusion the CAC will be operating in a forward

direction and rapid oxidation of succinate may explain the failure of it to significantly change tissue concentrations of succinate. Malonate has been shown to be protective against reperfusion injury when administered both before or during hypoxia (53, 161). In the organ transplant model, DMM was shown to protect against reperfusion injury when administered as an infusion and whilst DMM administration was not shown to be protective when administered as a bolus with cardioplegia at the onset of ischaemia, the numbers in this group (n = 3) may have been insufficiently powered to demonstrated significance.

To test the hypothesis that succinate accumulation drives reperfusion injury, I sought to examine the effect of increasing tissue succinate concentrations. DMS was administered as a bolus with cardioplegia. DMS remained detectable after 12 minutes of ischaemia and did not significantly increase tissue succinate concentrations. The detection of DMS but not DMM in mouse hearts after minutes of organ storage is consistent with a reduced rate of hydrolysis of DMS *in vivo* compared to DMM and could explain the failure of DMS to increase tissue succinate concentrations. Acetoxymethyl succinate (AMS) is more rapidly hydrolysed *in vitro* and has previously been shown to have therapeutic efficacy in modifying mitochondrial complex II function (176). There was a limited supply of AMS during the period of these studies preventing analysis of the metabolic effects during ischaemia in this model. The effect of administration of AMS to donor hearts on organ dysfunction following reperfusion was however examined. Both AMS and DMS failed to exacerbate organ dysfunction when administered to donors as an infusion during normoxia prior to the onset of ischaemia.

In summary, this chapter has demonstrated therapeutic efficacy of DMM in ameliorating reperfusion injury during organ transplantation in a novel small animal model but there were inconsistencies between data relating to levels of injury and succinate accumulation across the models. The development of a reproducible model provides a foundation for future work to further examine the therapeutic efficacy of metabolic inhibitors and the mechanisms through which reperfusion injury is ameliorated.

Chapter 6: Examining the role of IR injury in a model of chronic rejection

6.1 The role of ischaemia reperfusion injury in chronic allograft vasculopathy

6.1.1 Introduction

Despite improvements in short-term outcomes, most transplanted organs suffer an insidious decline in function. This process involves progressive allograft vasculopathy that leads to gradual fibrosis of graft parenchyma and eventual graft failure. This 'chronic rejection' or chronic graft dysfunction remains a major problem and is observed in a significant proportion of allografts within 5 years following transplantation. The aetiology of chronic rejection is likely multifactorial with contributions from, the alloimmune response, IR injury, toxicity from immunosuppressive agents, and recurrence of the underlying disease (116, 177).

A better understanding of the role of IR injury and its contribution to chronic rejection is fundamental if therapies or protective strategies are to be developed to ameliorate this process. To investigate this further I examined whether increasing IR injury augments the alloimmune response, exacerbates allograft vasculopathy and reduces allograft survival in a model of chronic rejection that has been well characterised in our laboratory (131).

6.2 Prolonged cold ischaemia and chronic rejection of the allograft

The Bm12.Kd.IE strain was developed in house by Dr Jason Ali (Department of Surgery, Cambridge, UK) and kindly gifted for this work. The strain was created through two crosses. First, Bm12 mice were crossed with B6.Kd. Offspring expressing I-A^{Bm12} and H-$2K^{d}$ but not I-A^{b} were selected using PCR. These Bm12.Kd mice were then crossed with ABOIE animals (gifted by Prof C Benoist (Joslin Diabetes Center, Boston, MA)). Flow cytometry was used to confirm the presence of H-$2K^{d}$ and I-E on peripheral blood mononuclear leukocytes. When Bm12.Kd.IE hearts were heterotopically transplanted into a C57BL/6J recipient they are chronically rejected with a median survival time of > 100 days. The mechanism of rejection has been well characterised and is the result of an alloimmune response directed against both MHC class I and II, and an autoimmune response (131). An additional mismatch can be achieved in this model by transplanting hearts from donors into a recipient of the opposite sex. This results in the indirect allorecognition of minor H-Y antigens. There is literature to suggest a gender difference in tolerance to ischaemia and therefore only female donor-recipient pairs were used in these experiments. Hearts from female Bm12.Kd.IE donors were transplanted heterotopically into female C57BL/6 recipients after either a standard (30 minutes) or a prolonged (240 minutes) period of cold static storage. The alloimmune response to the allograft was assessed by serum anti-H-$2K^{d}$ alloantibody production and allograft survival assessed by weekly abdominal palpation. Histological assessment of chronic allograft vasculopathy (CAV) was performed at 100 days by quantifying the mean luminal stenosis of intra-myocardial vessels in the donor heart (Figure 53).

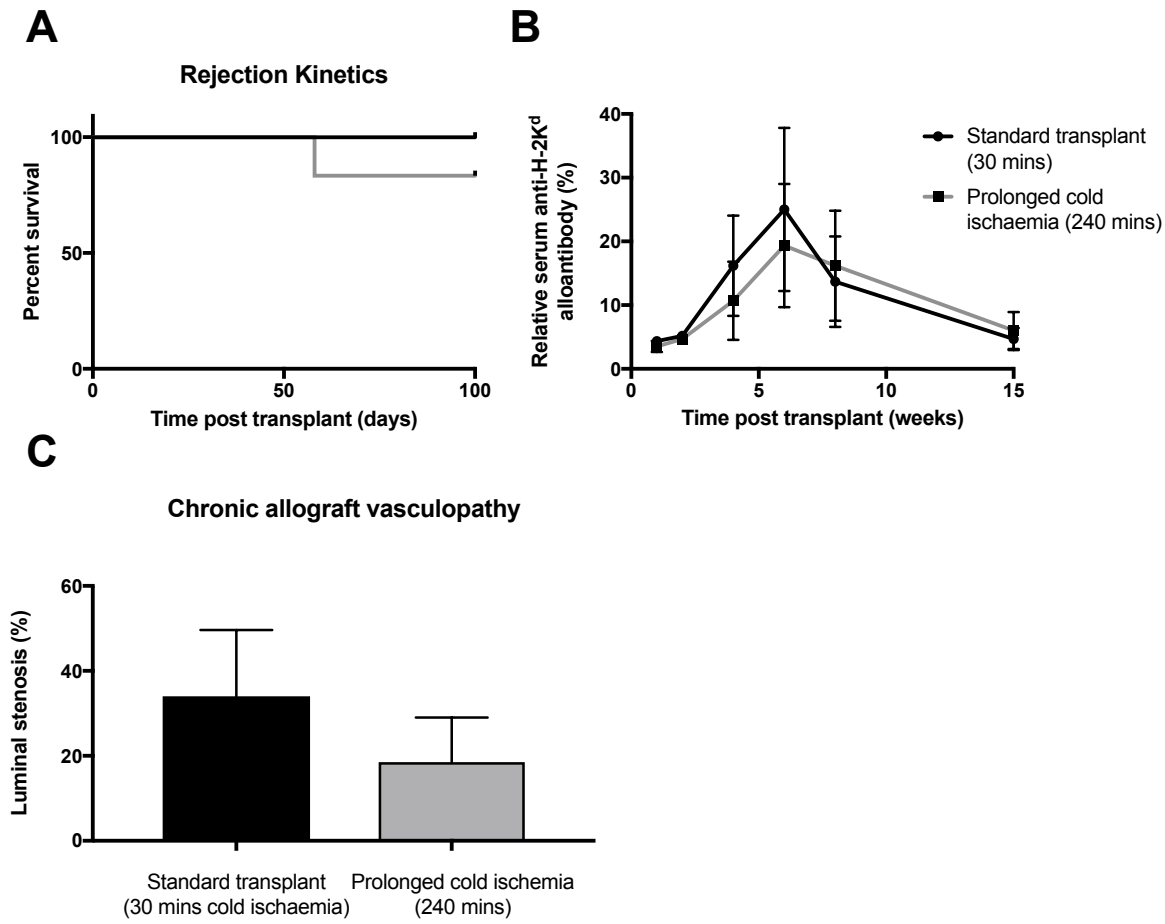

Figure 53 (a – c): Chronic rejection of the bm12.Kd.IE cardiac allograft following transplantation into a C57BL/6 recipient after standard or prolonged cold static storage.

Female Bm12.Kd.IE donor hearts were flushed with 0.5 mL Soltran and then subjected to 30 minutes of cold static storage (n = 6) or 240 minutes (n = 6) of cold static storage before being transplanted into female C57BL/6 recipients; (a) Rejection kinetics of transplanted allografts was assessed by weekly abdominal palpation (n = 6 per group), p = 0.32 by Log-rank (Mantel-Cox) test. (b) Recipient anti-H-2K^d alloantibody production in weekly serum samples assessed by ELISA (n = 6 per group), p = 0.98 by two-way ANOVA. (c) Allograft vasculopathy as assessed on elastin van Gieson stained paraffin sections (n = 2-3*) p = 0.53 by unpaired t-test. *Some allografts were lost during processing.

Consistent with previous reports, an alloimmune response with evidence of chronic allograft vasculopathy and graft loss was demonstrated in this model. There was, however, no difference in the allograft survival, CAV or the recipient alloimmune response against donor hearts that were exposed to prolonged cold storage when compared to hearts transplanted using a standard technique. The vasculopathy observed in this model has been shown to be the result of both an alloimmune and autoimmune response. Assessment of the autoantibody production was not performed due to a lack of available serum.

It is noteworthy that the alloimmune response and allograft vasculopathy observed in both groups was lower than that previously reported by Ali *et al* (131). This global reduction in the immune response and allograft rejection could prevent a significant difference between the control and treatment groups being

observed. This difference in chronic rejection could be explained by both the flushing of the donor heart and the use of female donor allografts. Flushing of the donor allograft more closely replicates practice in clinical transplantation and also provides a unique opportunity to administer therapeutic agents to isolated organs during transplantation. However, donor CD4 T cells are responsible for the generation of both the alloimmune and autoimmune response in this model and flushing of the donor allograft has been shown to remove a modest proportion of donor leucocytes (Dr J Ali, personal communication). By removing the CD4 T cells, flushing of the allograft could result in the abrogation of the alloimmune response and CAV. Another potential mechanism for the reduction in the rate of chronic rejection is the absence of indirect allorecognition of minor H-Y antigen due to the transplantation of female rather than male allografts into female recipients. There is literature to suggest that there is a gender difference in tolerance to IR injury and in these studies female donors and recipients were used throughout to remove this potential confounder (178, 179). The absence of minor H-Y antigen could however, also explain the amelioration of allograft vasculopathy observed in these data.

Modifying the period of cold storage has previously been shown to be a reproducible method of introducing a modifiable ischaemic injury to hearts during murine heterotopic heart transplantation. Dare *et al* demonstrated that a prolonged period of cold ischaemia increased mitochondrial dysfunction and IR injury in a syngeneic model and that this translated into measurable differences in outcome markers of myocardial tissue damage at 3 and 24 hours post reperfusion (138). The same model of ischaemic injury was used in this experiment but the difference in ischaemic injury did not translate to an increase in chronic rejection. When compared to the heterotopic heart transplantation technique described by Corrie *et* al, the operation used in this experiment requires additional steps to ligate branches of the aorta to enable allograft flushing. These result in the heart being exposed to an additional period (approximately 50% of the operative time) of moderate warm ischaemia. Hearts were topically cooled, intermittently during this period however their core temperature cycled between 10°C and approximately ambient room temperature (Figure 6). The accumulation of succinate in mouse hearts was shown in chapter 3 (Figure 25 and Figure 26**)** to have a linear relationship with temperature and to plateau at a threshold concentration. In the mouse heart this peak succinate accumulation occurs after approximately 12 minutes of (37 degree) warm ischaemia (Figure 19). One explanation for the failure of additional, prolonged cold ischaemia to impact organ dysfunction and as a result chronic rejection is that even in the standard transplant, succinate accumulation was significantly elevated and the relative difference introduced by the additional period of warm ischaemia was insufficient to translate into a difference in chronic rejection.

In order to reduce the initial inherent injury to the heart and examine whether flushing was responsible for a reduction in chronic allograft rejection I examined the effect of prolonged cold ischaemia on chronic rejection in a heterotopic heart transplant without flushing of the donor heart.

6.3 Flushing of the donor heart and chronic rejection of the allograft

Mouse hearts were transplanted heterotopically after retrieval without flushing. The alloimmune response, CAV and allograft rejection of standard transplants exposed to minimal cold ischaemia was compared to that of allografts exposed to prolonged cold ischaemia (240 mins). Assessment of the autoantibody production was again not performed in this experiment due to a lack of available serum.

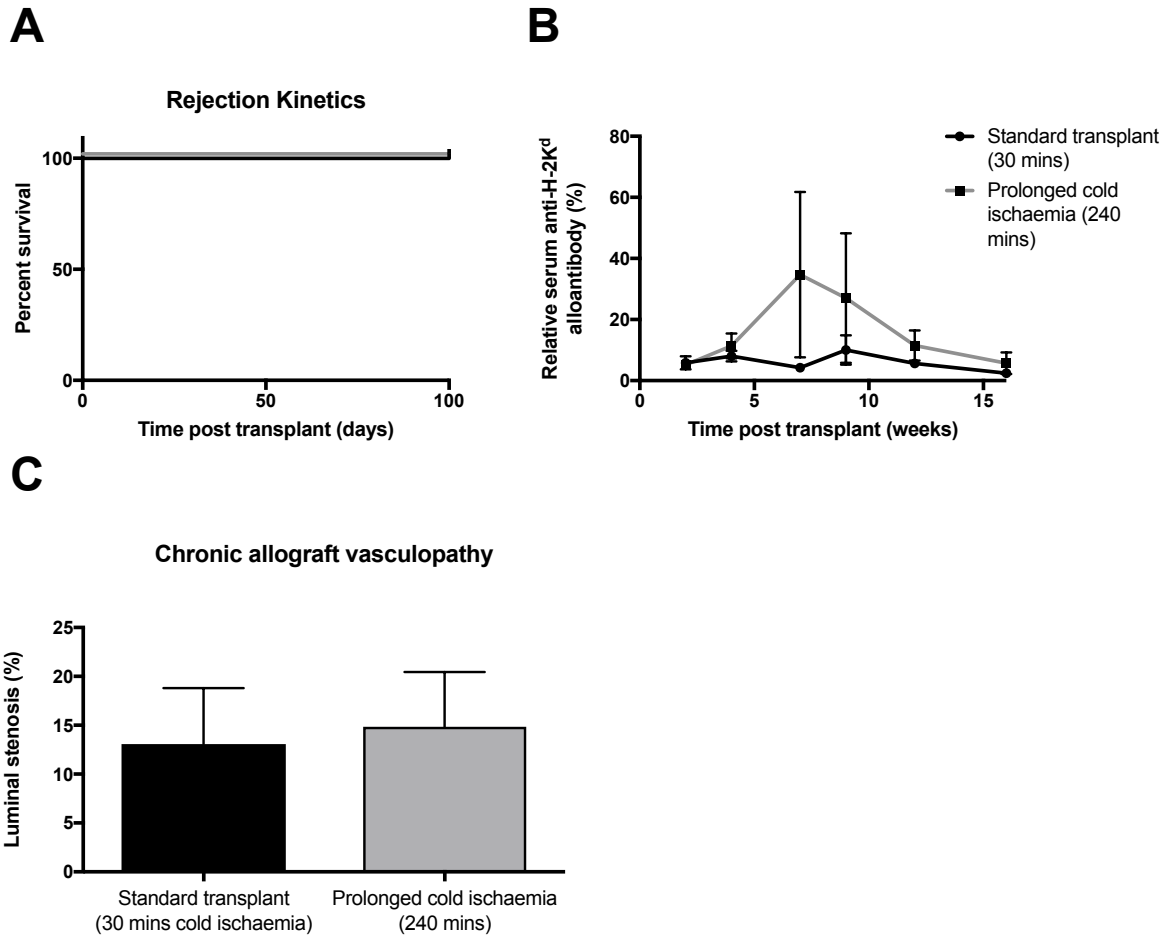

Figure 54 (a - c): Chronic rejection of the bm12.Kd.IE cardiac allograft prepared without flushing of the allograft during retrieval and transplanted into a C57BL/6 recipient after standard or prolonged cold static storage.

Female Bm12.Kd.IE donor hearts were retrieved without flushing of the allograft and subjected to 30 minutes (n = 5) of cold static storage or 240 minutes (n = 6) of cold static storage before transplantation into female C57BL/6 recipients. (a) Rejection kinetics of transplanted allografts was assessed by weekly abdominal palpation, $p > 0.99$ by Log-rank (Mantel-Cox) test. (b) Recipient anti-H-$2K^d$ alloantibody production in weekly serum samples assessed by ELISA, $p = 0.75$ by two-way ANOVA. (c) Allograft vasculopathy as assessed on elastin van Gieson stained paraffin sections, $p = 0.91$ by unpaired t-test.

There was again no significant difference in any measures of chronic rejection when hearts were retrieved without flushing and stored for standard or prolonged periods of cold static storage. Furthermore, allograft vasculopathy was similar to that reported when hearts were flushed and lower than that observed in historical analyses. These findings do not support the hypothesis that flushing of the heart during the retrieval process significantly abrogates the alloimmune response to the allograft. In addition, although there was a reduction in allograft vasculopathy compared to historical controls these experiments did not examine the cause for this nor the role of indirect allorecognition of minor H-Y antigen in amplifying the alloimmune and autoimmune response in this model.

Interestingly, reduction in the ischaemic injury inherent to the retrieval operation again failed to translate into differences in acute or chronic allograft survival previously observed using additional periods of cold ischaemia. No allografts were rejected in this experiment and the lack of overt rejection limits the potential for any treatment condition to have a significant effect on outcome markers.

6.4 Warm ischaemia and chronic rejection of the allograft

During the course of these experiments, the metabolic profile of succinate accumulation during warm and cold ischaemia was better characterised. The difference in the profile of succinate accumulation during warm and cold ischaemia together with the potential for manipulation of succinate accumulation by small molecule inhibitors of SDH supported the development of a model of chronic rejection that introduced an additional warm ischaemic insult during retrieval of the donor heart rather than using prolonged cold static storage. Such a model also has clinical relevance to DCD donors which form a significant proportion of donors used in UK clinical transplantation.

Donor animals were exsanguinated and then left for a standoff period of 6 minutes before proceeding to retrieval. Allografts were not flushed during the retrieval operation and were heterotopically transplanted into the abdomen of the recipient animal.

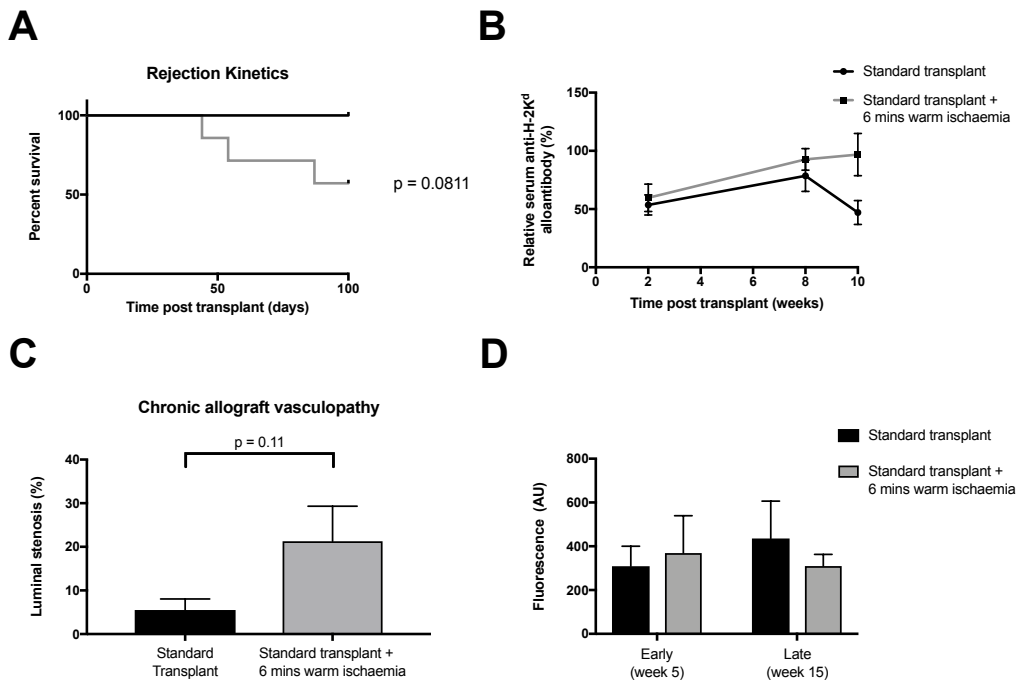

Figure 55 (a – d): Chronic rejection of the bm12.Kd.IE cardiac allograft prepared without flushing of the allograft during retrieval and transplanted into a C57BL/6 recipient following a standard retrieval or with an additional 6 minutes of warm ischaemia.

Female Bm12.Kd.IE donor animals were exsanguinated and the hearts left in the carcass of donor animal for 6 minutes (donor animal maintained at 37 degrees with a heat mat) and then retrieved without flushing of the allograft (n = 7). Control donor hearts underwent standard retrieval (n = 6). (a) Rejection kinetics of transplanted allografts was assessed by weekly abdominal palpation, p = 0.08 by Log-rank (Mantel-Cox) test. (b) Recipient anti-H-2K^d alloantibody production in weekly serum samples assessed by ELISA, p = 0.21 by two-way ANOVA. (c) Allograft vasculopathy as assessed on elastin van Gieson stained paraffin sections, p = 0.11 by unpaired t-test. (d) Recipient autoantibody production at early (5 weeks) and late (15 weeks) time points assessed by HEp-2 indirect immunofluorescence, p = 0.48 by two-way ANOVA.

The introduction of an additional period of warm ischaemia to the transplant procedure did not significantly impact the recipient alloimmune response, autoantibody production or chronic rejection of the allograft when compared to the standard heart transplant (Figure 55). Allograft vasculopathy was again abrogated when compared to historical data however, a non-significantly increased rate of clinical rejection was observed in the warm ischaemic group. This again supports a possible role of the indirect allorecognition of minor H-Y antigen in mediating allograft rejection in this model. The alloimmune response appears to be stronger in both the control and treatment groups when compared to other experiments (Figure 53 and Figure 54) but this did not translate to a difference in CAV. An alternative explanation for the observed difference in the alloimmune response could be experimental variation in the standard pooled hyperimmune sera. Alloantibody was calculated as a relative change compared to a standard pooled hyperimmune sera and variation in the concentration or affinity of this could impact the relative observed change in serum alloantibody. Recipient production of autoantibody was assessed at late and early time points by HEp-2 indirect immunofluorescence. This confirmed the generation of autoantibody against the allografts in recipients at both early and late time points. There was no difference in the levels of autoantibody between groups at either early or late time points.

6.5 Increased IR injury and its impact on chronic rejection

Further characterisation of the metabolic profile of murine heart tissue and in particular succinate during warm and cold ischaemia highlighted the rapidity and sensitivity to temperature of these pathways. To translate this to the mouse heart transplant model it was clear that further refinement of the retrieval process would be required to reduce variability in the ischaemic insult.

To minimise variability and enable therapies to be administered to the allograft at the time of retrieval, cardioplegia was administered to the recipient to prevent continued contraction during the retrieval operation and the warm ischaemic period. Following administration of cardioplegia it was necessary to immediately proceed to retrieval rather than leave the animal for a stand-off period. Whilst this does not directly replicate the clinical scenario, a stand-off period risked passive diffusion of cardioplegia from the heart, aided by changes in intrathoracic pressure, that would result in a spontaneous restoration of cardiac contraction. It was therefore necessary to immediately perform the retrieval operation and then introduce an additional warm ischaemic period to the treatment group. In previous experiments, flushing of the donor heart was not demonstrated to have a significant impact on chronic rejection and therefore allografts were flushed with a view to future administration of mitochondria-targeted therapies.

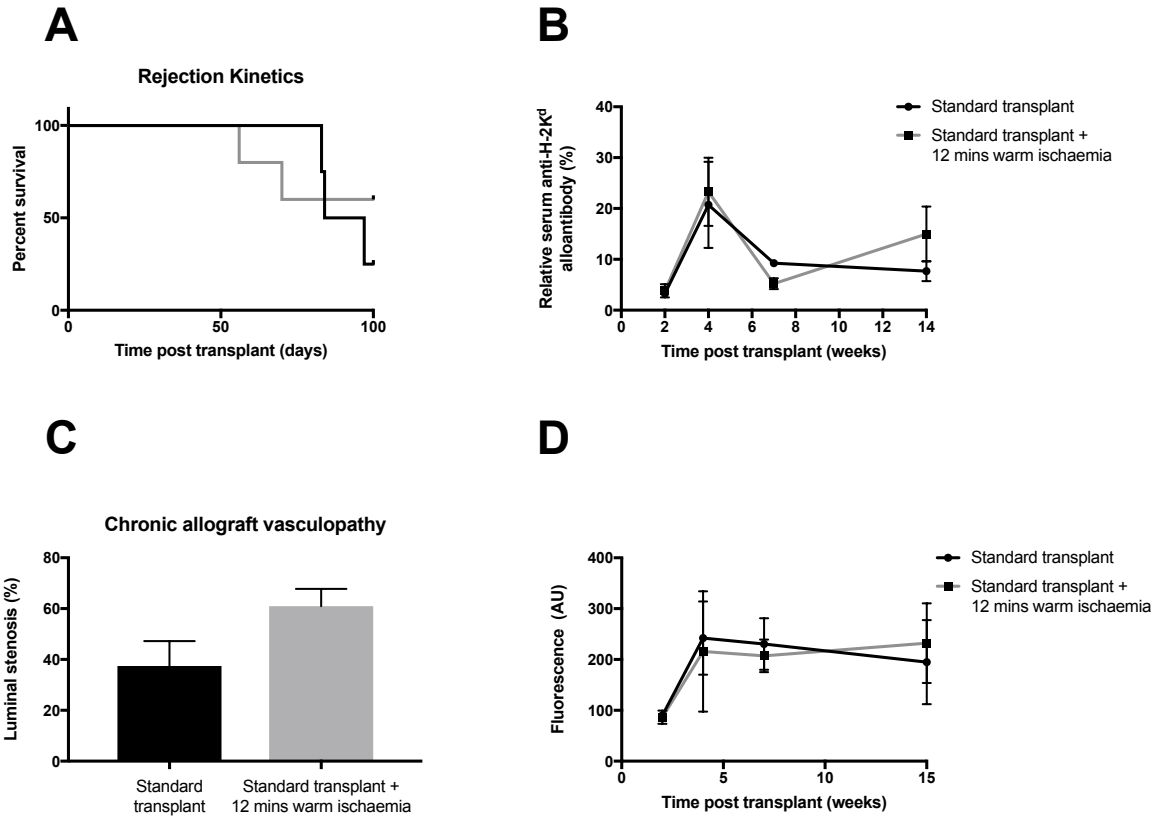

Figure 56 (a - d): Chronic rejection of the bm12.Kd.IE cardiac allograft following either no additional warm ischaemia or 12 minutes warm ischaemia prior to transplantation into a C57BL/6 recipient.

Female Bm12.Kd.IE donor hearts were retrieved after systemic administration of St Thomas' cardioplegia to the donor and flushed with 0.5 mL Soltran. Donor hearts were then exposed to an additional 12 minutes warm ischaemia or no additional warm ischaemia and transplanted using the standard technique. (a) Rejection kinetics of transplanted allografts was assessed by weekly abdominal palpation, p = 0.32 Log-rank (Mantel-Cox) (b) Recipient anti-H-2K^d alloantibody production in weekly serum samples assessed by ELISA, p = 0.64 by two-way ANOVA. (c) Allograft vasculopathy as assessed on elastin van Gieson stained paraffin sections p = 0.08 by unpaired t-test. (d) Recipient autoantibody production in serum samples at intervals following transplant assessed by HEp-2 indirect immunofluorescence, p = 0.97 by two-way ANOVA.

Chronic rejection of the allografts was observed in both groups. This occurred in the presence of a demonstrable recipient alloimmune and autoimmune antibody production, and chronic allograft vasculopathy. There was no significant difference in the rejection of allografts exposed to an additional period of warm ischaemia when compared to a standard transplant (Figure 56). The relative alloantibody and autoantibody concentrations were similar to those demonstrated in previous experiments.

6.6 Discussion

In this chapter, the impact of a defined period of additional ischaemic injury on the chronic rejection of a vascularised allograft was examined. The impact of additional warm ischaemia and prolonged cold ischaemia were both examined in these experiments. No significant difference in chronic rejection was observed between the standard and severe ischaemia groups as assessed by; alloantibody, autoantibody allograft vasculopathy or rate of chronic rejection of the allografts. The work presented in this chapter therefore does not demonstrate that IR injury exacerbates chronic graft dysfunction.

These data have demonstrated some of the challenges of working with this model of chronic rejection. I have been able to demonstrate evidence of chronic allograft rejection in the Bm12.Kd.IE to C57BL/6J heterotopic heart transplant model and demonstrated that production of both alloantibody and autoantobody but it was not possible to introduce a reproducible, modifiable difference in the rate of this chronic rejection.

A recipient alloimmune response against class I alloantigen and an autoimmune response were both demonstrated in these studies with the corresponding development of CAV and rejection. The absence of indirect allorecognition of minor H-Y antigen due to the use of female donors and recipients may have had an impact on the observed vasculopathy and chronic rejection. Chronic allograft vasculopathy and rejection was abrogated when compared to historical analyses, but these observations were not definitively investigated and could be explained by other factors such as genetic drift in strains. In these data, flushing of the allografts did not have any significant impact on chronic rejection.

Chronic rejection remains a major clinical problem and improvements in rates and the treatment of acute allograft rejection have not been replicated in longer-term allograft survival. The alloimmune and autoimmune response appear integral to the process of chronic rejection and an immune-mediated response is necessary for hearts to be chronically rejected in the murine heterotopic heart transplant model (131). IR injury itself is a short-lived phenomenon but these early events in the transplant process are frequently hypothesised to set in motion a series of events either through increased tissue damage and the generation of a heightened inflammatory milieu, or through direct immunomodulatory effects on specific immune components associated with the alloimmune or autoimmune response. A role for IR injury negatively impacting longer-term outcome in solid organ transplantation is supported by clinical data from registries and case series (79-81, 86). Nevertheless, the underlying pathophysiology that links IR injury to late outcomes and chronic rejection is very poorly understood and lacks definitive experimental evidence to support these observed associations. How best to answer these questions however, remains to be seen.

To definitively investigate these mechanisms robust models are required. The multifactorial aetiology of chronic rejection makes the development of such animal models very challenging. The model used in these experiments was designed to overcome some of the recognised problems of other models by

creating a more clinically relevant immune mediated chronic rejection. The immune response in this model has been well characterised but inherent shortfalls remain. It is important to remember that there are significant differences between the development, activation, and response to challenge of the murine and human immune systems. Whilst the immune response is likely integral to the process of chronic rejection there are other aetiologies that have also been implicated and these are not examined by this model.

One problem observed in these experiments was the difficulty in generating a reproducible, measurable, significant difference in the ischaemic insults between the control (standard transplant) and treatment (severe ischaemia) groups. There is inherent, operator variability associated with technically demanding procedures such as heterotopic heart transplantation and this is associated with a long learning curve (approximately 300 transplants). Minimising background IR injury and the variability associated with the procedure itself is essential if additional warm or cold ischaemic insults are to impact outcome. Refinements of the technique such as the introduction of cardioplegia had a significant effect in reducing the variability and minimising background ischaemic injury (Figure 48). Other measures to objectively assess the IR injury such as recipient serum troponin 24 hours after transplantation could enable better correlation between IR injury and long-term outcome. In addition, whilst allograft rejection remains the clinically relevant outcome measure, a biochemical measure of rejection and allograft failure such as brain natriuretic peptide (BNP) might provide a more sensitive tool for allograft assessment however, this has not been characterised in this model.

An alternative, more targeted approach to examining the role of IR injury in chronic rejection could build on evidence that donor CD4 T cells augment both the alloimmune and autoimmune response. This provides a potential mechanism through which IR injury could upregulate immune mediated chronic rejection. One approach would involve a model of chronic rejection in which CD4 T cell deplete allografts were transplanted into recipients who were reconstituted on the day of transplantation with donor CD4 T cells. These donor CD4 T cells could be exposed in vitro to variable periods of ischaemia. Exposing cells *in vitro* to true anoxia is notoriously difficult however and may limit this approach. Moreover, an understanding of how ischaemia upregulates donor CD4 T cell antigen recognition or activation and a mechanism to demonstrate cell viability following exposure to ischaemia would be required to interpret any results. Future research into chronic rejection

Basic scientific research into chronic solid organ rejection remains paramount. Nevertheless, this work has highlighted some of the potential difficulties in studying the role of IR injury in chronic rejection. In the first instance developing a robust, reproducible model that can be used to explore the mechanisms underpinning chronic rejection remains the principal problem preventing progress in this area. The models that have formed the mainstay of *in vivo* transplant immunological research in the past have not routinely employed immunosuppression. This is contrary to clinical practice and it is important to recognise this limitation if findings from these studies are to be extrapolated into clinical transplantation.

An alternative approach would be to use a fully mismatched model (eg. Balb/c to C57BL/6J) with recipient animals receiving immunosuppression. The chronic rejection associated with these models will still be inherently variable and therefore, increased numbers in each group may be required to demonstrated sufficient power within groups. Furthermore, this approach does not address the inherent significant differences between murine and human immune system development, activation and response challenge with antigen (180).

Basic research into the pathophysiology and mechanism through which IR injury exacerbates chronic rejection may conversely be better directed towards ameliorating acute graft dysfunction rather than focusing directly on chronic rejection. It would seem counterintuitive that any IR injury therapy would fail to demonstrate efficacy in ameliorating acute graft dysfunction yet improve long-term outcomes. Therefore, actively pursuing the translation of agents with therapeutic efficacy in ameliorating IR injury and acute graft dysfunction to well-designed clinical trials that enable the concurrent examination of short and long-term outcomes might be a more rewarding longer-term approach in answering the question of whether IR injury exacerbates chronic rejection in human solid organ transplantation. This approach would avoid potential problems associated with extrapolating findings from small animal chronic rejection models to clinical practice however, it is only relevant to IR injury where the pathophysiology is a short-lived phenomenon. Ongoing research into the allo- and autoimmune response would likely complement and provide avenues for further research in the future and remains fundamental to understanding the multitude of mechanisms that underpin chronic graft dysfunction.

Chapter 7: Discussion

7.1 General discussion

Mitigating the effects of the inevitable period of organ ischaemia is fundamental to the success of solid organ transplantation. Over the past seven decades, a number of approaches have been explored in order to better preserve organs during storage. Cold storage has been central to this for much of the history of organ transplantation but organs are inevitably exposed to variable periods of both warm and cold ischaemia during organ retrieval. Whilst some of the metabolic changes during organ storage have been explored in a range of species, significant gaps in our understanding remain.

7.1.1 Metabolic profile of ischaemia

In this work, models were designed to mimic transplantation and used to assess the metabolic changes in mice, pig and human hearts. To investigate these metabolic changes, it was important to have a reliable baseline, normoxic control value to which metabolic changes could be compared. Following the onset of hypoxia, the switch to ischaemic metabolism is rapid in mammalian metabolism, occurring within a few seconds. Rapid organ retrieval and freezing of tissue specimens were therefore paramount and initial results demonstrated an increased variability during the retrieval process due to operator factors. This variability was reduced following multiple, incremental, refinements in the retrieval technique. These included; changes to the induction of anaesthesia, the introduction of intra-operative rectal temperature monitoring, the use of cardioplegia, and changes to aspects of the operation to improve economy of movement and reduce operative times without impacting outcome. In addition, variability in the processing of specimens was further reduced with the use of more efficient tissue homogenising techniques.

For efficient translation of clinical therapies, it is essential to ensure metabolic pathways are conserved across species from the experimental model to the patient at the outset. The difficulties in replicating metabolism and hypoxia both *in vitro* and *ex vivo* means research is, at present, reliant on *in vivo* models. Mouse models are well established in basic science research, have formed the backbone of transplant immunology research, and provided a versatile model to initially investigate the hypotheses in this work. The rate of organ cooling and therefore the kinetics of warm and cold ischaemia is however, critically affected by the size of organs. Corroborating findings from the small animal model in organs that were a similar size to human organs provided a foundation for the development of the pig model. This methodological approach, designed to enable concurrent investigation of hypotheses across both small and large animal models simultaneously, is different from the more traditional stepwise approach of drug development and has the potential to identify problems in the translation of therapies earlier and to stream line the process.

There are a number of factors that must be taken into consideration when drawing conclusions from this data. The models used to understand ischaemic metabolism in organs storage did not directly reflect the clinical scenario of organ transplantation. The complexity of clinical organ transplantation introduces multiple variables and therefore the models used to examine ischaemic metabolism were designed to

simplify the process and examine warm and cold ischaemia in isolation. This approach was carried through to the pig and human models. To enable direct comparison of metabolomic analyses of the mouse, pig and human data I looked to replicate the model as far as technically feasible. Due to the size and cost of large animal models, it was not possible to use multiple hearts for each time point. To resolve this issue, the initial apical section served as a control for all remaining time points. However, any variability in the sampling of the baseline control specimen had the potential to influence all remaining time points to a greater extent than in the mouse experiments where the normoxic control was calculated from the mean of replicates. Further differences between the small and large animal models were the result of differences in the available animal facilities. The pig experiments were performed on a separate site under a different animal license and this study plan precluded entering the thorax or mediastinum of the animal prior to death. In addition, the pigs were anaesthetised with a different anaesthetic regime to the mouse. The human model used a similar approach to the pig model with each heart providing multiple time points due to the reasons discussed above. In contrast to the pig model however, the human organ donation routinely permitted access to the thorax and thus to the heart at the time of retrieval. Finally, in contrast to the human donors, the animals in the mouse and pig model were not exposed to brainstem injury. Brain death results in a large catecholamine release and changes in the donor's haemodynamic status. This has the potential to affect the procured organs and human donors receive a variety of medications to manage this and optimise the haemodynamic status of the donor prior to organ procurement. Other groups have used models that introduce significant brain injury, but these were not available in our facilities. In general, despite the variation in the techniques and the potential confounders described above the metabolomic data demonstrated a conserved process across the species examined.

Energy stores in these models were shown to be better preserved by cold ischaemia when compared to warm ischaemia. The principal means of sustaining energy stores in the absence of oxidative phosphorylation is through glycolysis. Interestingly, there were differences in the apparent rate limiting components of glycolysis in warm and cold ischaemia. During cold ischaemia exhaustion of glycogen stores limited glycolysis however, during warm ischaemia the elevated $NADH/NAD^+$ ratio was the limiting factor (Chapter 3). A comparative metabolomic approach was then used to examine metabolic changes in this heart tissue during warm and cold ischaemia (Chapter 3). Succinate accumulation during ischaemia has been shown to be integral to reperfusion injury and mitochondrial dysfunction (53). In this analysis, the accumulation of succinate during organ storage was also present. Furthermore, it was shown to be conserved across species and was more rapid during warm compared to cold ischaemia. The accumulation of succinate has been hypothesised to be due to reversal of SDH(54). Whilst succinate accumulation was a conserved finding in this analysis it was interesting to observe that tissue concentrations of the other CAC intermediates fumarate and malate demonstrated disparate changes during ischaemia between the mouse, and the pig and human data. Fumarate and malate demonstrated similar profiles to that of succinate in the pig and human tissue. In contrast to the data from mouse

hearts, Wistar rat hearts in an isolated *ex vivo* organ perfusion model have also been reported to demonstrate metabolic changes during ischaemia that were similar to the profiles from pig and human tissue in these analyses (162). The selective accumulation of succinate over other CAC metabolites during ischaemia may be a consequence of multiple metabolic reactions converging on succinate which, in contrast to other CAC metabolites, cannot be metabolised further. The disparities in the accumulation of fumarate and malate during ischaemia between species is difficult to interpret and may be a consequence of these multiple converging pathways. Nevertheless, the conserved nature of succinate accumulation across species remains reassuring for the translation of future therapeutic interventions targeting succinate accumulation and reperfusion injury.

The protective effects of cold organ storage are generally attributed to a reduction in global metabolic rate. In this analysis, a linear relationship with temperature was observed in the accumulation of a range of metabolites in the mouse heart, including succinate, supporting this theory. Accumulation of succinate was however, observed to be a rapid phenomenon with significant increases in succinate relative to baseline tissue concentrations still occurring after 12 minutes of organ storage at 16°C. In comparison to the mouse heart, human organs cool more slowly even with the use of cold perfusion techniques (181). These findings therefore suggest; the accumulation of succinate is likely to feature in both DBD and DCD transplantation, the reliance on cold storage to abrogate succinate accumulation is unlikely to be effective, and there is therapeutic potential for additional clinical therapies that target this process.

The comparative metabolomic approach was then used to explore the source of succinate accumulation in this model. Metabolic inhibitors were administered in a bolus of cardioplegia prior to organ retrieval and 12 minutes of warm ischaemic storage. This technique delivered the inhibitor to tissues at the onset of ischaemia in an organ that, until this time, had been perfused in normoxic conditions *in vivo*. This is in contrast to other *ex vivo* organ perfusion models that frequently require a stabilisation period. The perfusate used during a period of stabilisation can itself result in changes to the metabolism of these organs and this can potentially affect subsequent ischaemic metabolism (34, 36, 174). Adequate intracellular and mitochondrial delivery of metabolic inhibitors using intravenous administration with cardioplegia was a concern however, LC/MS analysis enabled simultaneous assessment of both metabolic intermediates and tissue concentrations of metabolic inhibitors (AOA, DMM, HAD and TTFA). Furthermore, in the case of DMM where hydrolysis of the precursor to malonate was required the kinetics of this reaction could also be assessed. Amelioration of succinate accumulation was observed with inhibitors of both SDH and transamination. The corresponding changes in other CAC intermediates were more variable and further experiments would be required to elucidate the underlying pathophysiology. The non-specific inhibition of transaminases by AOA not only prevents transamination of aspartate to oxaloacetate but also the transamination of pyruvate to alanine. There is evidence that some marine animals (eg *Mytilus edulis*) undergo periods of facultative anaerobic respiration and generate energy through the transamination of pyruvate to alanine and that this process is coupled to aspartate transamination and its further conversion to oxaloacetate and then to succinate. In these

preliminary data, AOA administration demonstrated an increase in aspartate, a reduction in alanine and a reduction of succinate tissue accumulation that was consistent with actions on both pathways. These preliminary data require future work to examine the role of these pathways in the accumulation of succinate during warm and cold ischaemia and IR injury. Previous data has suggested the PNC may contribute to succinate accumulation during ischaemia (53). In these data administration of the PNC inhibitor, ADSS, failed to result in any changes to tissue metabolite concentrations including succinate accumulation. Hadacidin was detected in tissue after 12 minutes of warm ischaemia supporting adequate delivery however, the failure to change tissue metabolite concentrations does not confirm the absence of flux through this pathway. These data do not definitively identify the source of succinate however, they demonstrate this model to be effective in delivering inhibitors and manipulating metabolism during organ storage. Further experiments with compounds to increase tissue concentrations of metabolites would provide a greater understanding of some of these pathways. In addition, understanding the changes in both mitochondrial and cytoplasmic metabolite concentrations would also aid the elucidation of pathways in the future.

7.1.2 Examining IR injury *in vivo* in organ transplantation

The identification of rapid succinate accumulation in donor organs during warm ischaemia and the adequate delivery of metabolic inhibitors at the time of organ harvest provided the background for the development of a novel small animal model of solid organ transplantation to investigate the effect of reperfusion injury in organ transplantation. The heterotopic heart transplant model has previously been invaluable in exploring a range of different questions within the context of solid organ transplantation and transplant immunology. A well validated small animal transplant reperfusion model with robust markers of acute organ dysfunction would expand the potential applications considerably into the field of transplant IR injury and explore areas that have not been investigated in the current models. In this work, troponin was used a surrogate of organ dysfunction. Although a specific marker of myocardial injury it provides limited information on the upstream pathophysiology or organ function. This could in the future be addressed through the use of assays examining the actual burst of mtROS, or downstream sequelae of the ROS production that support the role of mitochondrial dysfunction in IR injury such as; isoprostanes, protein carbonyl formation, or mtDNA damage. Furthermore, pressure-volume loops could also be used to characterise the effect of reperfusion injury on cardiac function.

In Chapter 5 a transplant model was developed with a reproducible warm ischaemic insult and the therapeutic efficacy of DMM in ameliorating reperfusion injury was examined. When DMM was administered to the donor as an infusion immediately prior to hypoxia, DMM ameliorated reperfusion injury. Interestingly, when DMM was administered with cardioplegia, at the onset of hypoxia, there was only a non-significant trend towards a reduction in reperfusion injury. Furthermore, the different methods of administering DMM had differing effects on succinate accumulation on donor hearts during ischaemia with an infusion of DMM having no effect on succinate accumulation and bolus administration with cardioplegia significantly reducing tissue succinate concentrations. This disparity could simply be due

to insufficiently powered experiments. An alternative explanation is the differing effect of exogenous malonate on the CAC in the presence and absence of oxygen. When malonate was administered as an infusion in the presence of oxygen the CAC would have been cycling in the standard direction and might not affect tissue succinate concentrations until the heart was retrieved. When DMM was administered as a bolus at the onset of hypoxia malonate would have been delivered to the CAC cycling in reverse, potentially inhibiting succinate accumulation.

Malonate is hypothesised to inhibit the pathological oxidation of succinate to fumarate upon reperfusion (53). Despite the differing effects of malonate administration described above, a reduction in reperfusion injury could theoretically be achieved either, by reducing the initial succinate concentration, or by sufficiently elevating tissue malonate concentrations relative to tissue succinate concentrations at the time of reperfusion. This interpretation provides an explanation for the apparently contrasting data described above and is supported by data demonstrating the efficacy of malonate in reducing reperfusion injury when administered at the time of reperfusion (161).

7.1.3 Examining IR injury and chronic organ rejection

In Chapter 6, the novel model of reperfusion injury in organ transplantation developed in Chapter 5 was used to examine whether reperfusion injury would translate to measurable differences in the rate of allograft rejection in a well-established model of chronic allograft vasculopathy. No difference was observed in the immune response or the long-term outcome of allografts when donor hearts were exposed to additional ischaemic insults. Chronic rejection remains a major problem in organ transplantation and there is clinical data supporting a detrimental effect of reperfusion injury on long term outcome (80, 81, 86). A better understanding of the pathophysiological process would enable development of specific therapies however, the multifactorial nature of chronic rejection makes research challenging. Reproducible small animal models are yet to be developed for this precise purpose and their translational potential given the known limitations of some of these models should be taken into consideration (180). The Bm12KdIE to BL/6 model of chronic rejection has been well validated and provided an opportunity to examine the key pathways in chronic rejection; the direct alloimmune response, the indirect alloimmune response, and the autoimmune response. Nevertheless, the approach was reliant on creating a modifiable reproducible IR injury. The steep learning curve associated with the technique, the incremental refinements that had to be made, and the long duration of follow up were all potential confounders and could explain the failure of these data to demonstrate the exacerbation of chronic rejection reported in clinical data.

An alternative approach to the translation of basic research to clinical practice in the management of chronic rejection in organ transplantation focusing on the longer-term outcomes of trials whose primary outcomes were designed to examine the efficacy of treatments ameliorating reperfusion injury and acute graft dysfunction may be a more efficient approach.

The metabolic changes during organ storage have been demonstrated in this work to be amenable to therapeutic intervention and have the potential to ameliorate ischaemia reperfusion. This approach, using a model that is directly relevant and translatable to the clinical environment has provided a wealth of data that could provide the foundation of future work. Reperfusion injury is inherent to organ transplantation and a better understanding of the pathophysiological processes will enable the develop of future therapies and potentially improve both short and long-term transplant outcomes.

In summary, this thesis examined the mechanism of IR injury in organ transplantation and the relationship between IR injury and early and late organ dysfunction. This work has examined the metabolic profile of myocardial tissue during warm and cold organ storage in mice, pigs, and humans and demonstrated that succinate accumulation was a conserved process during ischaemia across species. Moreover, this work has demonstrated the potential to moderate this process during organ storage. To investigate whether the amelioration of succinate accumulation during organ storage would translate to a reduction in reperfusion injury, a small animal model of IR injury in organ transplantation was developed. The efficacy of DMM, a small molecule inhibitor of SDH, in ameliorating reperfusion injury following organ transplantation was then confirmed. Finally, the effect of IR injury on chronic rejection was examined in a well characterised model of chronic rejection. In this model, an increase in IR injury failed to translate into an exacerbation of late organ dysfunction or chronic rejection.

7.2 Future directions

Mitochondrial research has rapidly expanded over the course of the last two decades. This has transformed our understanding of their role within the cell from simple, powerhouses to their now well recognised role in an ever-increasing number of central, cellular functions and disease processes including IR injury. Until recently it had been assumed that the mechanisms underlying IR were imprecise with multiple sources resulting in non-specific cellular and organ dysregulation (54). The identification of a specific, common pathway has provided an opportunity to better understand the process and develop potential therapies. I would propose that future work should focus on two key areas; the pathophysiology of succinate accumulation during ischaemia, and the development of therapies to ameliorate reperfusion injury in organ transplantation.

The source of the succinate that has been shown in this work to accumulate during ischaemia is yet to be conclusively described. In these data there was disparity in the changes in the CAC metabolites, fumarate and malate, in mice and other species during ischaemia despite a conserved accumulation of succinate. It will be important to investigate this further and in the first instance, the ischaemic metabolic changes in rat hearts and other wildtype mouse strains could be examined *in vivo* to enable a direct comparison. The preliminary data presented in this work examining the potential source of succinate demonstrated the efficacy of the technique and adequate delivery of metabolic inhibitors. This technique examined ischaemia in a model that directly reflected normal ischaemic metabolism. This may be more readily translatable to the clinical scenario than other *ex vivo* perfusion models. Further work is required to explore why some metabolic inhibitors failed to have an effect on metabolism and whether this reflects a lack of uptake in the ischaemic environment following bolus injection or is due to a lack of flux through pathways during ischaemia. Previous work demonstrated an exacerbation of reperfusion injury by elevating tissue succinate concentrations (54). DMS was not hydrolysed sufficiently to elevate tissue succinate however, more rapidly hydrolysed versions have been developed by our collaborators and could provide a new approach to exploring this area. Complex I is fundamental to the generation of mtROS. Inhibition *in vivo* is challenging but would also be an important area to explore in the future. Finally, the comparative metabolic analysis highlighted other metabolites such as alanine that had different profiles in warm and cold ischaemia that have not been explored. Understanding the pathophysiology of these processes would provide another interesting area of research.

In moderating succinate accumulation or the rate of succinate oxidation at the time of reperfusion the environment into which metabolic inhibitors are delivered appears to be critical. The relatively controlled onset of ischaemia and subsequent reperfusion provides a wealth of potential opportunities to administer therapies in organ transplantation. Reperfusion injury could be abrogated in transplantation by treating a combination of the donor, the organ, or the recipient. The work presented here suggests moderating metabolism in this setting is critically dependent on the timing of administration and the presence or absence of oxygen. Future work will need to clarify this in more detail and examine the use of metabolic

inhibitors that have been designed to be more rapidly delivered to the cell *in vivo* or selectively targeted to mitochondria using strategies such as by conjugation to lipophilic cations such as triphenylphosphonium. This work has demonstrated that the heterotopic heart transplant mouse model can be used to examine IR injury within the context of transplantation. Further work should look to expand the repertoire of outcome markers used to examine IR injury. Examining ROS, mitochondrial and organ dysfunction at different times during the evolution of reperfusion would improve the under. Markers characterising the severity of the IR injury without the need to sacrifice the animal would enable correlations between early mitochondrial dysfunction and later organ dysfunction and explore the downstream pathways in more details *in vivo.*

In conclusion, since the recognition of IR injury as a pathophysiological process there have been numerous therapeutic avenues that have been explored. The initial optimism with some of these has unfortunately failed to translate to an improvement in clinical outcomes. With the recognition of a specific metabolic pathway underpinning this process there is renewed optimism that rational therapeutic strategies may have greater success in treating IR injury. Collaboration will continue to be instrumental in delivering this success as an increasing number of ever more complex techniques and new *in vivo* or *ex vivo* models may be required to further examine the pathophysiological process. Chronic rejection remains a major clinical problem but with the benefit of hindsight, I do not believe the approach I pursued in this work was the most efficient method of exploring the problem of chronic rejection and its relationship with IR injury. With finite resources, I would suggest that we invest time into better understanding the pathophysiology of IR injury. This would focus and expedite the development of therapies to ameliorate IR injury. With well-designed clinical trials, the efficacy of these therapies in moderating long-term outcomes could then be later examined as secondary outcomes.

Chapter 8: References

1. Watson CJ, Dark JH. Organ transplantation: historical perspective and current practice. British journal of anaesthesia. 2012;108 Suppl 1:i29-42.
2. Rhee JY, Alroy J, Freeman RB. Characterization of the withdrawal phase in a porcine donation after the cardiac death model. American journal of transplantation : official journal of the American Society of Transplantation and the American Society of Transplant Surgeons. 2011;11(6):1169-75.
3. Hakim NS, Papalois VE. History of organ and cell transplantation. London

River Edge, NJ: Imperial College Press ;

Distributed by World Scientific Pub.; 2003. xviii, 444 p. p.
4. Machado C, Kerein J, Ferrer Y, Portela L, de la CGM, Manero JM. The concept of brain death did not evolve to benefit organ transplants. J Med Ethics. 2007;33(4):197-200.
5. Woodcock T, Wheeler R. Law and medical ethics in organ transplantation surgery. Ann R Coll Surg Engl. 2010;92(4):282-5.
6. Hoult JR, Moore PK. Pathways of prostaglandin F2alpha metabolism in mammalian kidneys. Br J Pharmacol. 1977;61(4):615-26.
7. Orr RD, Gundry SR, Bailey LL. Reanimation: overcoming objections and obstacles to organ retrieval from non-heart-beating cadaver donors. J Med Ethics. 1997;23(1):7-11.
8. Thuong M, Ruiz A, Evrard P, Kuiper M, Boffa C, Akhtar MZ, et al. New classification of donation after circulatory death donors definitions and terminology. Transplant international : official journal of the European Society for Organ Transplantation. 2016;29(7):749-59.
9. Summers DM, Johnson RJ, Allen J, Fuggle SV, Collett D, Watson CJ, et al. Analysis of factors that affect outcome after transplantation of kidneys donated after cardiac death in the UK: a cohort study. The Lancet. 2010;376(9749):1303-11.
10. NHS Blood and Transplant. Organ donation and transplantation, 2018, [Available from: https://www.odt.nhs.uk/statistics-and-reports/organ-specific-reports/,.
11. Calne RY. The present position and future prospects of organ transplantation. Ann R Coll Surg Engl. 1968;42(5):283-306.
12. Calne RY, Pegg DE, Pryse-Davies J, Brown FL. Renal Preservation by Ice-Cooling: An Experimental Study Relating to Kidney Transplantation from Cadavers. Br Med J. 1963;2(5358):651-5.
13. Belzer FO, Ashby BS, Dunphy JE. 24-hour and 72-hour preservation of canine kidneys. Lancet (London, England). 1967;2(7515):536-8.
14. Belzer FO, Ashby BS, Gulyassy PF, Powell M. Successful seventeen-hour preservation and transplantation of human-cadaver kidney. The New England journal of medicine. 1968;278(11):608-10.
15. Collins GM, Bravo-Shugarman M, Terasaki PI. Kidney preservation for transportation. Initial perfusion and 30 hours' ice storage. Lancet (London, England). 1969;2(7632):1219-22.
16. Hartley LC, Collins GM, Clunie GJ. Kidney preservation for transportation. Function of 29 human-cadaver kidneys preserved with an intracellular perfusate. The New England journal of medicine. 1971;285(19):1049-52.
17. <Saeb-Parsy 2007 - Organ preservation.pdf>.
18. Jamieson NV, Sundberg R, Lindell S, Claesson K, Moen J, Vreugdenhil PK, et al. Preservation of the canine liver for 24-48 hours using simple cold storage with UW solution. Transplantation. 1988;46(4):517-22.
19. Wahlberg JA, Love R, Landegaard L, Southard JH, Belzer FO. 72-hour preservation of the canine pancreas. Transplantation. 1987;43(1):5-8.
20. Ploeg RJ, Goossens D, McAnulty JF, Southard JH, Belzer FO. Successful 72-hour cold storage of dog kidneys with UW solution. Transplantation. 1988;46(2):191-6.
21. Jeevanandam V, Auteri JS, Sanchez JA, Barr ML, Ott GY, Hsu D, et al. Improved heart preservation with University of Wisconsin solution: experimental and preliminary human experience. Circulation. 1991;84(5 Suppl):III324-8.
22. Hessheimer AJ, Billault C, Barrou B, Fondevila C. Hypothermic or normothermic abdominal regional perfusion in high-risk donors with extended warm ischemia times: impact on outcomes? Transplant international : official journal of the European Society for Organ Transplantation. 2015;28(6):700-7.
23. Page A, Messer S, Large SR. Heart transplantation from donation after circulatory determined death. Ann Cardiothorac Surg. 2018;7(1):75-81.

24. DiRito JR, Hosgood SA, Tietjen GT, Nicholson ML. The future of marginal kidney repair in the context of normothermic machine perfusion. American journal of transplantation : official journal of the American Society of Transplantation and the American Society of Transplant Surgeons. 2018.
25. Hosgood SA, van Heurn E, Nicholson ML. Normothermic machine perfusion of the kidney: better conditioning and repair? Transplant international : official journal of the European Society for Organ Transplantation. 2015;28(6):657-64.
26. Summers DM, Watson CJ, Pettigrew GJ, Johnson RJ, Collett D, Neuberger JM, et al. Kidney donation after circulatory death (DCD): state of the art. Kidney international. 2015;88(2):241-9.
27. van Heurn LW, Talbot D, Nicholson ML, Akhtar MZ, Sanchez-Fructuoso AI, Weekers L, et al. Recommendations for donation after circulatory death kidney transplantation in Europe. Transplant international : official journal of the European Society for Organ Transplantation. 2016;29(7):780-9.
28. Ghorpade MV, Kulkarni SA, Kulkarni AG. Cryptosporidium, Isospora and Strongyloides in AIDS. Natl Med J India. 1996;9(4):201.
29. Coffey JC, Wanis KN, Monbaliu D, Gilbo N, Selzner M, Vachharajani N, et al. The influence of functional warm ischemia time on DCD liver transplant recipients' outcomes. Clinical transplantation. 2017.
30. Heylen L, Pirenne J, Samuel U, Tieken I, Naesens M, Sprangers B, et al. The Impact of Anastomosis Time During Kidney Transplantation on Graft Loss: A Eurotransplant Cohort Study. American journal of transplantation : official journal of the American Society of Transplantation and the American Society of Transplant Surgeons. 2017;17(3):724-32.
31. Butsch JL. A method for preventing inadvertent dislodging of drains. Am Surg. 1973;39(3):186.
32. Mills EL, Kelly B, O'Neill LAJ. Mitochondria are the powerhouses of immunity. Nat Immunol. 2017;18(5):488-98.
33. Banner NR, Thomas HL, Curnow E, Hussey JC, Rogers CA, Bonser RS, et al. The importance of cold and warm cardiac ischemia for survival after heart transplantation. Transplantation. 2008;86(4):542-7.
34. Neubauer S. The failing heart--an engine out of fuel. The New England journal of medicine. 2007;356(11):1140-51.
35. Jaswal JS, Keung W, Wang W, Ussher JR, Lopaschuk GD. Targeting fatty acid and carbohydrate oxidation--a novel therapeutic intervention in the ischemic and failing heart. Biochimica et biophysica acta. 2011;1813(7):1333-50.
36. King LM, Opie LH. Glucose and glycogen utilisation in myocardial ischemia--changes in metabolism and consequences for the myocyte. Mol Cell Biochem. 1998;180(1-2):3-26.
37. Depre C, Rider MH, Hue L. Mechanisms of control of heart glycolysis. Eur J Biochem. 1998;258(2):277-90.
38. Murphy MP, Smith RA. Targeting antioxidants to mitochondria by conjugation to lipophilic cations. Annual review of pharmacology and toxicology. 2007;47:629-56.
39. Smith RA, Hartley RC, Cocheme HM, Murphy MP. Mitochondrial pharmacology. Trends in pharmacological sciences. 2012;33(6):341-52.
40. <Bioenergetics 3.pdf>.
41. Sayen Jj Fau - Sheldon WF, Sheldon Wf Fau - Peirce G, Peirce G Fau - Kuo PT, Kuo PT. Polarographic oxygen, the epicardial electrocardiogram and muscle contraction in experimental acute regional ischemia of the left ventricle. (0009-7330 (Print)).
42. Jennings Rb Fau - Reimer KA, Reimer Ka Fau - Hill ML, Hill Ml Fau - Mayer SE, Mayer SE. Total ischemia in dog hearts, in vitro. 1. Comparison of high energy phosphate production, utilization, and depletion, and of adenine nucleotide catabolism in total ischemia in vitro vs. severe ischemia in vivo. (0009-7330 (Print)).
43. Jennings RB, Reimer KA. The cell biology of acute myocardial ischemia. (0066-4219 (Print)).
44. Chambers DJ, Fallouh HB. Cardioplegia and cardiac surgery: pharmacological arrest and cardioprotection during global ischemia and reperfusion. Pharmacology & therapeutics. 2010;127(1):41-52.
45. Habertheuer A, Kocher A, Laufer G, Andreas M, Szeto WY, Petzelbauer P, et al. Cardioprotection: a review of current practice in global ischemia and future translational perspective. Biomed Res Int. 2014;2014:325725.
46. Eltzschig HK, Eckle T. Ischemia and reperfusion--from mechanism to translation. Nature medicine. 2011;17(11):1391-401.
47. Jennings RB, Sommers HM, Smyth GA, Flack HA, Linn H. Myocardial necrosis induced by temporary occlusion of a coronary artery in the dog. Archives of pathology. 1960;70:68-78.
48. Braunwald E, Kloner RA. Myocardial reperfusion: a double-edged sword? The Journal of clinical investigation. 1985;76(5):1713-9.
49. Hearse DJ, Humphrey SM, Bullock GR. The oxygen paradox and the calcium paradox: two facets of the same problem? Journal of molecular and cellular cardiology. 1978;10(7):641-68.

50. Raedschelders K, Ansley DM, Chen DD. The cellular and molecular origin of reactive oxygen species generation during myocardial ischemia and reperfusion. Pharmacology & therapeutics. 2012;133(2):230-55.
51. Murphy MP. How mitochondria produce reactive oxygen species. The Biochemical journal. 2009;417(1):1-13.
52. Balaban RS, Nemoto S, Finkel T. Mitochondria, oxidants, and aging. Cell. 2005;120(4):483-95.
53. Chouchani ET, Pell VR, Gaude E, Aksentijevic D, Sundier SY, Robb EL, et al. Ischaemic accumulation of succinate controls reperfusion injury through mitochondrial ROS. Nature. 2014;515(7527):431-5.
54. Chouchani ET, Pell VR, James AM, Work LM, Saeb-Parsy K, Frezza C, et al. A Unifying Mechanism for Mitochondrial Superoxide Production during Ischemia-Reperfusion Injury. Cell metabolism. 2016;23(2):254-63.
55. Bedard K, Krause KH. The NOX family of ROS-generating NADPH oxidases: physiology and pathophysiology. Physiological reviews. 2007;87(1):245-313.
56. Land WG. Emerging role of innate immunity in organ transplantation: part I: evolution of innate immunity and oxidative allograft injury. Transplantation reviews. 2012;26(2):60-72.
57. Meneshian A, Bulkley GB. The physiology of endothelial xanthine oxidase: from urate catabolism to reperfusion injury to inflammatory signal transduction. Microcirculation (New York, NY : 1994). 2002;9(3):161-75.
58. Weinberg SE, Sena LA, Chandel NS. Mitochondria in the regulation of innate and adaptive immunity. Immunity. 2015;42(3):406-17.
59. Wood KJ, Goto R. Mechanisms of rejection: current perspectives. Transplantation. 2012;93(1):1-10.
60. Seth RB, Sun L, Ea CK, Chen ZJ. Identification and characterization of MAVS, a mitochondrial antiviral signaling protein that activates NF-kappaB and IRF 3. Cell. 2005;122(5):669-82.
61. Gross CJ, Mishra R, Schneider KS, Medard G, Wettmarshausen J, Dittlein DC, et al. K+ Efflux-Independent NLRP3 Inflammasome Activation by Small Molecules Targeting Mitochondria. Immunity. 2016;45(4):761-73.
62. Schon EA. Mitochondrial genetics and disease. Trends in biochemical sciences. 2000;25(11):555-60.
63. Zhang Q, Raoof M, Chen Y, Sumi Y, Sursal T, Junger W, et al. Circulating mitochondrial DAMPs cause inflammatory responses to injury. Nature. 2010;464(7285):104-7.
64. Nakahira K, Haspel JA, Rathinam VA, Lee SJ, Dolinay T, Lam HC, et al. Autophagy proteins regulate innate immune responses by inhibiting the release of mitochondrial DNA mediated by the NALP3 inflammasome. Nat Immunol. 2011;12(3):222-30.
65. Shimada K, Crother TR, Karlin J, Dagvadorj J, Chiba N, Chen S, et al. Oxidized mitochondrial DNA activates the NLRP3 inflammasome during apoptosis. Immunity. 2012;36(3):401-14.
66. West AP, Khoury-Hanold W, Staron M, Tal MC, Pineda CM, Lang SM, et al. Mitochondrial DNA stress primes the antiviral innate immune response. Nature. 2015;520(7548):553-7.
67. Sena LA, Li S, Jairaman A, Prakriya M, Ezponda T, Hildeman DA, et al. Mitochondria are required for antigen-specific T cell activation through reactive oxygen species signaling. Immunity. 2013;38(2):225-36.
68. Jang KJ, Mano H, Aoki K, Hayashi T, Muto A, Nambu Y, et al. Mitochondrial function provides instructive signals for activation-induced B-cell fates. Nat Commun. 2015;6:6750.
69. Ibanez B, Heusch G, Ovize M, Van de Werf F. Evolving therapies for myocardial ischemia/reperfusion injury. J Am Coll Cardiol. 2015;65(14):1454-71.
70. Morgan JA, John R, Weinberg AD, Kherani AR, Colletti NJ, Vigilance DW, et al. Prolonged donor ischemic time does not adversely affect long-term survival in adult patients undergoing cardiac transplantation. J Thorac Cardiovasc Surg. 2003;126(5):1624-33.
71. Del Rizzo DF, Menkis AH, Pflugfelder PW, Novick RJ, McKenzie FN, Boyd WD, et al. The role of donor age and ischemic time on survival following orthotopic heart transplantation. The Journal of heart and lung transplantation : the official publication of the International Society for Heart Transplantation. 1999;18(4):310-9.
72. Messer S, Ardehali A, Tsui S. Normothermic donor heart perfusion: current clinical experience and the future. Transplant international : official journal of the European Society for Organ Transplantation. 2015;28(6):634-42.
73. Stehlik J, Edwards LB, Kucheryavaya AY, Benden C, Christie JD, Dipchand AI, et al. The Registry of the International Society for Heart and Lung Transplantation: 29th official adult heart transplant report--2012. The Journal of heart and lung transplantation : the official publication of the International Society for Heart Transplantation. 2012;31(10):1052-64.
74. Labarrere CA, Lee JB, Nelson DR, Al-Hassani M, Miller SJ, Pitts DE. C-reactive protein, arterial endothelial activation, and development of transplant coronary artery disease: a prospective study. Lancet (London, England). 2002;360(9344):1462-7.
75. Gao Q, Mulvihill MS, Scheuermann U, Davis RP, Yerxa J, Yerokun BA, et al. Improvement in Liver Transplant Outcomes From Older Donors: A US National Analysis. Ann Surg. 2018.

76. Ruiz de Azua-Lopez Z, Naranjo-Izurieta JR, Lameirao J, Martin-Villen L, Porras-Lopez M, Palomo-Lopez N, et al. Cold Ischemia Time as a Factor in Post-transplantation Complications for Orthotopic Hepatic Transplantation. Transplantation proceedings. 2018;50(2):637-9.
77. Pan ET, Yoeli D, Galvan NTN, Kueht ML, Cotton RT, O'Mahony CA, et al. Cold ischemia time is an important risk factor for post-liver transplant prolonged length of stay. Liver Transpl. 2018;24(6):762-8.
78. Zhai Y, Petrowsky H, Hong JC, Busuttil RW, Kupiec-Weglinski JW. Ischaemia-reperfusion injury in liver transplantation--from bench to bedside. Nature reviews Gastroenterology & hepatology. 2013;10(2):79-89.
79. Debout A, Foucher Y, Trebern-Launay K, Legendre C, Kreis H, Mourad G, et al. Each additional hour of cold ischemia time significantly increases the risk of graft failure and mortality following renal transplantation. Kidney international. 2014.
80. Boom H, Mallat MJ, de Fijter JW, Zwinderman AH, Paul LC. Delayed graft function influences renal function, but not survival. Kidney international. 2000;58(2):859-66.
81. Ojo AO, Wolfe RA, Held PJ, Port FK, Schmouder RL. Delayed graft function: risk factors and implications for renal allograft survival. Transplantation. 1997;63(7):968-74.
82. Johnson RJ, Fuggle SV, O'Neill J, Start S, Bradley JA, Forsythe JL, et al. Factors influencing outcome after deceased heart beating donor kidney transplantation in the United Kingdom: an evidence base for a new national kidney allocation policy. Transplantation. 2010;89(4):379-86.
83. Mikhalski D, Wissing KM, Ghisdal L, Broeders N, Touly M, Hoang AD, et al. Cold ischemia is a major determinant of acute rejection and renal graft survival in the modern era of immunosuppression. Transplantation. 2008;85(7 Suppl):S3-9.
84. Perico N, Cattaneo D, Sayegh MH, Remuzzi G. Delayed graft function in kidney transplantation. Lancet (London, England). 2004;364(9447):1814-27.
85. Marcen R, Orofino L, Pascual J, de la Cal MA, Teruel JL, Villafruela JJ, et al. Delayed graft function does not reduce the survival of renal transplant allografts. Transplantation. 1998;66(4):461-6.
86. Hernandez D, Estupinan S, Perez G, Rufino M, Gonzalez-Posada JM, Luis D, et al. Impact of cold ischemia time on renal allograft outcome using kidneys from young donors. Transplant international : official journal of the European Society for Organ Transplantation. 2008;21(10):955-62.
87. van der Vliet JA, Warle MC, Cheung CL, Teerenstra S, Hoitsma AJ. Influence of prolonged cold ischemia in renal transplantation. Clinical transplantation. 2011;25(6):E612-6.
88. Morris PJ, Johnson RJ, Fuggle SV, Belger MA, Briggs JD. Analysis of factors that affect outcome of primary cadaveric renal transplantation in the UK. The Lancet. 1999;354(9185):1147-52.
89. Opelz G, Dohler B. Multicenter analysis of kidney preservation. Transplantation. 2007;83(3):247-53.
90. Salahudeen AK, Haider N, May W. Cold ischemia and the reduced long-term survival of cadaveric renal allografts. Kidney international. 2004;65(2):713-8.
91. Summers DM, Johnson RJ, Hudson A, Collett D, Watson CJ, Bradley JA. Effect of donor age and cold storage time on outcome in recipients of kidneys donated after circulatory death in the UK: a cohort study. The Lancet. 2013;381(9868):727-34.
92. Kayler LK, Magliocca J, Zendejas I, Srinivas TR, Schold JD. Impact of cold ischemia time on graft survival among ECD transplant recipients: a paired kidney analysis. American journal of transplantation : official journal of the American Society of Transplantation and the American Society of Transplant Surgeons. 2011;11(12):2647-56.
93. Kayler LK, Srinivas TR, Schold JD. Influence of CIT-induced DGF on kidney transplant outcomes. American journal of transplantation : official journal of the American Society of Transplantation and the American Society of Transplant Surgeons. 2011;11(12):2657-64.
94. Hosgood SA, Bagul A, Yang B, Nicholson ML. The relative effects of warm and cold ischemic injury in an experimental model of nonheartbeating donor kidneys. Transplantation. 2008;85(1):88-92.
95. Jochmans I, Darius T, Kuypers D, Monbaliu D, Goffin E, Mourad M, et al. Kidney donation after circulatory death in a country with a high number of brain dead donors: 10-year experience in Belgium. Transplant international : official journal of the European Society for Organ Transplantation. 2012;25(8):857-66.
96. Locke JE, Segev DL, Warren DS, Dominici F, Simpkins CE, Montgomery RA. Outcomes of kidneys from donors after cardiac death: implications for allocation and preservation. American journal of transplantation : official journal of the American Society of Transplantation and the American Society of Transplant Surgeons. 2007;7(7):1797-807.
97. Goldsmith PJ, Ridgway Dm Fau - Pine JK, Pine Jk Fau - Ecuyer C, Ecuyer C Fau - Baker R, Baker R Fau - Newstead C, Newstead C Fau - Hostert L, et al. Sequential transplant of paired kidneys following donation after cardiac death: impact of longer cold ischemia time on the second kidney on graft and patient outcome. (1873-2623 (Electronic)).

98. Mateo R, Cho Y Fau - Singh G, Singh G Fau - Stapfer M, Stapfer M Fau - Donovan J, Donovan J Fau - Kahn J, Kahn J Fau - Fong TL, et al. Risk factors for graft survival after liver transplantation from donation after cardiac death donors: an analysis of OPTN/UNOS data. (1600-6135 (Print)).
99. De Carlis R, Di Sandro S, Lauterio A, Botta F, Ferla F, Andorno E, et al. Liver grafts from donors after cardiac death on regional perfusion with extended warm ischemia compared with donors after brain death. Liver Transpl. 2018.
100. Callaghan CJ, Charman Sc Fau - Muiesan P, Muiesan P Fau - Powell JJ, Powell Jj Fau - Gimson AE, Gimson Ae Fau - van der Meulen JHP, van der Meulen JH. Outcomes of transplantation of livers from donation after circulatory death donors in the UK: a cohort study. (2044-6055 (Electronic)).
101. Jay C, Ladner D Fau - Wang E, Wang E Fau - Lyuksemburg V, Lyuksemburg V Fau - Kang R, Kang R Fau - Chang Y, Chang Y Fau - Feinglass J, et al. A comprehensive risk assessment of mortality following donation after cardiac death liver transplant - an analysis of the national registry. (1600-0641 (Electronic)).
102. Ramirez P, Ferreras D, Febrero B, Royo M, Cascales P, Rodriguez JM, et al. Outcomes of Liver Transplantation Using Older Donors After Circulatory Death and the Super-Rapid Technique: 14 Cases. Transplantation proceedings. 2018;50(2):601-4.
103. Kalisvaart M, de Haan JE, Polak WG, Metselaar HJ, Wijnhoven BPL, JNM IJ, et al. Comparison of Postoperative Outcomes Between Donation After Circulatory Death and Donation After Brain Death Liver Transplantation Using the Comprehensive Complication Index. Ann Surg. 2017;266(5):772-8.
104. Nankivell BJ, Chapman JR. Chronic allograft nephropathy: current concepts and future directions. Transplantation. 2006;81(5):643-54.
105. Nankivell BJ, Alexander SI. Rejection of the kidney allograft. The New England journal of medicine. 2010;363(15):1451-62.
106. Braun WE. Renal transplantation: basic concepts and evolution of therapy. Journal of clinical apheresis. 2003;18(3):141-52.
107. Santos JH, Meyer JN, Mandavilli BS, Van Houten B. Quantitative PCR-based measurement of nuclear and mitochondrial DNA damage and repair in mammalian cells. Methods in molecular biology (Clifton, NJ). 2006;314:183-99.
108. Ali JM, Bolton EM, Bradley JA, Pettigrew GJ. Allorecognition pathways in transplant rejection and tolerance. Transplantation. 2013;96(8):681-8.
109. Win TS, Pettigrew GJ. Humoral autoimmunity and transplant vasculopathy: when allo is not enough. Transplantation. 2010;90(2):113-20.
110. Joosten SA, Sijpkens YW, van Kooten C, Paul LC. Chronic renal allograft rejection: pathophysiologic considerations. Kidney international. 2005;68(1):1-13.
111. Suzuki J, Isobe M, Morishita R, Nagai R. Characteristics of chronic rejection in heart transplantation: important elements of pathogenesis and future treatments. Circulation journal : official journal of the Japanese Circulation Society. 2010;74(2):233-9.
112. Mitchell RN. Allograft arteriopathy. Cardiovascular Pathology. 2004;13(1):33-40.
113. Hullett DA, Geraghty JG, Stoltenberg RL, Sollinger HW. The impact of acute rejection on the development of intimal hyperplasia associated with chronic rejection. Transplantation. 1996;62(12):1842-6.
114. Izutani H, Miyagawa S, Shirakura R, Matsumiya G, Nakata S, Shimazaki Y, et al. Evidence that graft coronary arteriosclerosis begins in the early phase after transplantation and progresses without chronic immunoreaction. Histopathological analysis using a retransplantation model. Transplantation. 1995;60(10):1073-9.
115. Nagano H, Libby P, Taylor MK, Hasegawa S, Stinn JL, Becker G, et al. Coronary arteriosclerosis after T-cell-mediated injury in transplanted mouse hearts: role of interferon-gamma. The American journal of pathology. 1998;152(5):1187-97.
116. Libby P, Pober JS. Chronic rejection. Immunity. 2001;14(4):387-97.
117. Boutilier RG. Mechanisms of cell survival in hypoxia and hypothermia. (0022-0949 (Print)).
118. Martin JL, Gruszczyk AV, Beach TE, Murphy MP, Saeb-Parsy K. Mitochondrial mechanisms and therapeutics in ischaemia reperfusion injury. Pediatr Nephrol. 2018.
119. Titze-de-Almeida R, David C, Titze-de-Almeida SS. The Race of 10 Synthetic RNAi-Based Drugs to the Pharmaceutical Market. Pharm Res. 2017;34(7):1339-63.
120. Demirjian S, Ailawadi G, Polinsky M, Bitran D, Silberman S, Shernan SK, et al. Safety and Tolerability Study of an Intravenously Administered Small Interfering Ribonucleic Acid (siRNA) Post On-Pump Cardiothoracic Surgery in Patients at Risk of Acute Kidney Injury. Kidney Int Rep. 2017;2(5):836-43.
121. Hall AM, Schuh CD. Mitochondria as therapeutic targets in acute kidney injury. Curr Opin Nephrol Hypertens. 2016;25(4):355-62.
122. Chen H, Chan DC. Mitochondrial dynamics--fusion, fission, movement, and mitophagy--in neurodegenerative diseases. Hum Mol Genet. 2009;18(R2):R169-76.

123. Zhan M, Brooks C, Liu F, Sun L, Dong Z. Mitochondrial dynamics: regulatory mechanisms and emerging role in renal pathophysiology. Kidney international. 2013;83(4):568-81.
124. Brooks C, Wei Q, Cho SG, Dong Z. Regulation of mitochondrial dynamics in acute kidney injury in cell culture and rodent models. The Journal of clinical investigation. 2009;119(5):1275-85.
125. Mills EL, Kelly B, Logan A, Costa ASH, Varma M, Bryant CE, et al. Succinate Dehydrogenase Supports Metabolic Repurposing of Mitochondria to Drive Inflammatory Macrophages. Cell. 2016;167(2):457-70 e13.
126. Evanna L. Mills DGR, Hiran A. Prag, Dina Dikovskaya, Deepthi Menon, Zbigniew Zaslona, Mark P. Jedrychowski, Ana S. H. Costa, Maureen Higgins, Emily Hams, John Szpyt, Marah Runtsch, Joanna F. McGouran, Roman Fischer, Benedikt M Kessler, Anne F. McGettrick, Mark M. Hughes, Richard Carroll, Lee M. Booty, Elena V. Knatko, Paul J. Meakin, Michael L.J. Ashford, Louise K. Modis, Gino Brunori, Daniel C. Sévin, Padraic G. Fallon, Stuart T. Caldwell, Edmund R. S. Kunji, Martin S. King, Edward T. Chouchani, Christian Frezza, Albena T. Dinkova-Kostova, Richard C. Hartley, Michael P. Murphy* and Luke A. J. O'Neill. Itaconate is an anti-inflammatory metabolite that activates Nrf2 via alkylation of Keap1 Nature. 2018;In press(In press):in press.
127. Kelly B, Tannahill GM, Murphy MP, O'Neill LA. Metformin Inhibits the Production of Reactive Oxygen Species from NADH:Ubiquinone Oxidoreductase to Limit Induction of Interleukin-1beta (IL-1beta) and Boosts Interleukin-10 (IL-10) in Lipopolysaccharide (LPS)-activated Macrophages. The Journal of biological chemistry. 2015;290(33):20348-59.
128. Mengle-Gaw L, Conner S, McDevitt HO, Fathman CG. Gene conversion between murine class II major histocompatibility complex loci. Functional and molecular evidence from the bm 12 mutant. The Journal of experimental medicine. 1984;160(4):1184-94.
129. Honjo K, Xu XY, Bucy RP. Heterogeneity of T cell clones specific for a single indirect alloantigenic epitope (I-Ab/H-2Kd54-68) that mediate transplant rejection. Transplantation. 2000;70(10):1516-24.
130. Le Meur M, Gerlinger P, Benoist C, Mathis D. Correcting an immune-response deficiency by creating E alpha gene transgenic mice. Nature. 1985;316(6023):38-42.
131. Ali JM, Negus MC, Conlon TM, Harper IG, Qureshi MS, Motallebzadeh R, et al. Diversity of the CD4 T Cell Alloresponse: The Short and the Long of It. Cell Rep. 2016;14(5):1232-45.
132. Mackay GM, Zheng L, van den Broek NJ, Gottlieb E. Analysis of Cell Metabolism Using LC-MS and Isotope Tracers. Methods Enzymol. 2015;561:171-96.
133. Strehler BL. Bioluminescence assay: principles and practice. Methods Biochem Anal. 1968;16:99-181.
134. Zhang P. Analysis of Mouse Liver Glycogen Content. Bio-protocol. 2012;2(10):e186.
135. Corry RJ, Winn HJ, Russell PS. Heart transplantation in congenic strains of mice. Transplantation proceedings. 1973;5(1):733-5.
136. Ciszek B, Skubiszewska D, Ratajska A. The anatomy of the cardiac veins in mice. J Anat. 2007;211(1):53-63.
137. Liu F, Kang SM. Heterotopic heart transplantation in mice. Journal of visualized experiments : JoVE. 2007(6):238.
138. Dare AJ, Logan A, Prime TA, Rogatti S, Goddard M, Bolton EM, et al. The mitochondria-targeted anti-oxidant MitoQ decreases ischemia-reperfusion injury in a murine syngeneic heart transplant model. The Journal of heart and lung transplantation : the official publication of the International Society for Heart Transplantation. 2015.
139. Conlon TM, Saeb-Parsy K, Cole JL, Motallebzadeh R, Qureshi MS, Rehakova S, et al. Germinal center alloantibody responses are mediated exclusively by indirect-pathway CD4 T follicular helper cells. Journal of immunology. 2012;188(6):2643-52.
140. Holmes BJ, Richards AC, Awwad M, Copeman LS, McLaughlin ML, Cozzi E, et al. Anti-pig antibody levels in naive baboons and cynomolgus monkeys. Xenotransplantation. 2002;9(2):135-47.
141. Callaghan CJ, Win TS, Motallebzadeh R, Conlon TM, Chhabra M, Harper I, et al. Regulation of allograft survival by inhibitory FcgammaRIIb signaling. Journal of immunology (Baltimore, Md : 1950). 2012;189(12):5694-702.
142. Win TS, Rehakova S, Negus MC, Saeb-Parsy K, Goddard M, Conlon TM, et al. Donor CD4 T cells contribute to cardiac allograft vasculopathy by providing help for autoantibody production. Circulation Heart failure. 2009;2(4):361-9.
143. Tissier R, Chenoune M Fau - Ghaleb B, Ghaleb B Fau - Cohen MV, Cohen Mv Fau - Downey JM, Downey Jm Fau - Berdeaux A, Berdeaux A. The small chill: mild hypothermia for cardioprotection? (1755-3245 (Electronic)).
144. Olthof PB, Reiniers MJ, Dirkes MC, Van Gulik TM, Heger M, Van Golen RF. Protective mechanisms of hypothermia in liver surgery and transplantation. LID - 10.2119/molmed.2015.00158 [doi]. (1528-3658 (Electronic)).
145. Laboratory TSotJ. Biology of the Laboratory Mouse. 2nd ed ed. Green EL, editor: Dover Publications Inc; 1975. 706 p.

146. Tantama M, Martinez-Francois JR, Mongeon R, Yellen G. Imaging energy status in live cells with a fluorescent biosensor of the intracellular ATP-to-ADP ratio. Nat Commun. 2013;4:2550.
147. Hardie DG. The AMP-activated protein kinase pathway--new players upstream and downstream. J Cell Sci. 2004;117(Pt 23):5479-87.
148. Pucar D, Dzeja PP, Bast P, Gumina RJ, Drahl C, Lim L, et al. Mapping hypoxia-induced bioenergetic rearrangements and metabolic signaling by 18O-assisted 31P NMR and 1H NMR spectroscopy. Mol Cell Biochem. 2004;256-257(1-2):281-9.
149. Jennings RB, Reimer KA. Lethal myocardial ischemic injury. The American journal of pathology. 1981;102(2):241-55.
150. Lloyd SG, Wang P, Zeng H, Chatham JC. Impact of low-flow ischemia on substrate oxidation and glycolysis in the isolated perfused rat heart. Am J Physiol Heart Circ Physiol. 2004;287(1):H351-62.
151. Peuhkurinen KJ, Takala TE, Nuutinen EM, Hassinen IE. Tricarboxylic acid cycle metabolites during ischemia in isolated perfused rat heart. Am J Physiol. 1983;244(2):H281-8.
152. Ussher JR, Jaswal JS, Lopaschuk GD. Pyridine nucleotide regulation of cardiac intermediary metabolism. Circulation research. 2012;111(5):628-41.
153. Zuurbier CJ, Eerbeek O, Goedhart PT, Struys EA, Verhoeven NM, Jakobs C, et al. Inhibition of the pentose phosphate pathway decreases ischemia-reperfusion-induced creatine kinase release in the heart. Cardiovascular research. 2004;62(1):145-53.
154. Sanborn T, Gavin W, Berkowitz S, Perille T, Lesch M. Augmented conversion of aspartate and glutamate to succinate during anoxia in rabbit heart. Am J Physiol. 1979;237(5):H535-41.
155. Hohnholt MC, Andersen VH, Andersen JV, Christensen SK, Karaca M, Maechler P, et al. Glutamate dehydrogenase is essential to sustain neuronal oxidative energy metabolism during stimulation. J Cereb Blood Flow Metab. 2017:271678X17714680.
156. Hacker TA, Renstrom B, Paulson D, Liedtke AJ, stanley WC. Ischemia produces an increase in ammonia output in swine myocardium. Cardioscience. 1994;5(4):255-60.
157. Whitmer JT, Idell-Wenger JA, Rovetto MJ, Neely JR. Control of fatty acid metabolism in ischemic and hypoxic hearts. The Journal of biological chemistry. 1978;253(12):4305-9.
158. Drake KJ, Sidorov VY, McGuinness OP, Wasserman DH, Wikswo JP. Amino acids as metabolic substrates during cardiac ischemia. Exp Biol Med (Maywood). 2012;237(12):1369-78.
159. Jennings Rb Fau - Hawkins HK, Hawkins Hk Fau - Lowe JE, Lowe Je Fau - Hill ML, Hill Ml Fau - Klotman S, Klotman S Fau - Reimer KA, Reimer KA. Relation between high energy phosphate and lethal injury in myocardial ischemia in the dog. (0002-9440 (Print)).
160. Sun F, Dai C, Xie J, Hu X. Biochemical issues in estimation of cytosolic free NAD/NADH ratio. PLoS One. 2012;7(5):e34525.
161. Valls-Lacalle L, Barba I, Miro-Casas E, Alburquerque-Bejar JJ, Ruiz-Meana M, Fuertes-Agudo M, et al. Succinate dehydrogenase inhibition with malonate during reperfusion reduces infarct size by preventing mitochondrial permeability transition. Cardiovascular research. 2016;109(3):374-84.
162. Jespersen NR, Yokota T, Stottrup NB, Bergdahl A, Paelestik KB, Povlsen JA, et al. Pre-ischaemic mitochondrial substrate constraint by inhibition of malate-aspartate shuttle preserves mitochondrial function after ischaemia-reperfusion. J Physiol. 2017;595(12):3765-80.
163. Fontaine DA, Davis DB. Attention to Background Strain Is Essential for Metabolic Research: C57BL/6 and the International Knockout Mouse Consortium. Diabetes. 2016;65(1):25-33.
164. Lofgren B, Povlsen JA, Rasmussen LE, Stottrup NB, Solskov L, Krarup PM, et al. Amino acid transamination is crucial for ischaemic cardioprotection in normal and preconditioned isolated rat hearts--focus on L-glutamate. Exp Physiol. 2010;95(1):140-52.
165. Nielsen TT, Stottrup NB, Lofgren B, Botker HE. Metabolic fingerprint of ischaemic cardioprotection: importance of the malate-aspartate shuttle. Cardiovascular research. 2011;91(3):382-91.
166. Shigeura HT, Gordon CN. The mechanism of action of hadacidin. The Journal of biological chemistry. 1962;237:1937-40.
167. Wu J, Bond C, Chen P, Chen M, Li Y, Shohet RV, et al. HIF-1alpha in the heart: remodeling nucleotide metabolism. Journal of molecular and cellular cardiology. 2015;82:194-200.
168. Quinlan CL, Orr AL, Perevoshchikova IV, Treberg JR, Ackrell BA, Brand MD. Mitochondrial complex II can generate reactive oxygen species at high rates in both the forward and reverse reactions. The Journal of biological chemistry. 2012;287(32):27255-64.
169. Siebels I, Drose S. Q-site inhibitor induced ROS production of mitochondrial complex II is attenuated by TCA cycle dicarboxylates. Biochimica et biophysica acta. 2013;1827(10):1156-64.
170. Kevelaitis E, Oubenaissa A, Mouas C, Peynet J, Menasche P. Ischemic preconditioning with opening of mitochondrial adenosine triphosphate-sensitive potassium channels or Na/H exchange inhibition: which is the best protective strategy for heart transplants? J Thorac Cardiovasc Surg. 2001;121(1):155-62.

171. Liu B, Zhu X, Chen CL, Hu K, Swartz HM, Chen YR, et al. Opening of the mitoKATP channel and decoupling of mitochondrial complex II and III contribute to the suppression of myocardial reperfusion hyperoxygenation. Mol Cell Biochem. 2010;337(1-2):25-38.
172. Drose S, Hanley PJ, Brandt U. Ambivalent effects of diazoxide on mitochondrial ROS production at respiratory chain complexes I and III. Biochimica et biophysica acta. 2009;1790(6):558-65.
173. Lesnefsky EJ, Chen Q, Moghaddas S, Hassan MO, Tandler B, Hoppel CL. Blockade of electron transport during ischemia protects cardiac mitochondria. The Journal of biological chemistry. 2004;279(46):47961-7.
174. Andrienko TN, Pasdois P, Pereira GC, Ovens MJ, Halestrap AP. The role of succinate and ROS in reperfusion injury - A critical appraisal. Journal of molecular and cellular cardiology. 2017;110:1-14.
175. Heylen L, Jochmans I, Samuel U, Tieken I, Naesens M, Pirenne J, et al. The duration of asystolic ischemia determines the risk of graft failure after circulatory-dead donor kidney transplantation: A Eurotransplant cohort study. American journal of transplantation : official journal of the American Society of Transplantation and the American Society of Transplant Surgeons. 2018;18(4):881-9.
176. Ehinger JK, Piel S, Ford R, Karlsson M, Sjovall F, Frostner EA, et al. Cell-permeable succinate prodrugs bypass mitochondrial complex I deficiency. Nat Commun. 2016;7:12317.
177. Dhaliwal A, Thohan V. Cardiac allograft vasculopathy: the Achilles' heel of long-term survival after cardiac transplantation. Curr Atheroscler Rep. 2006;8(2):119-30.
178. Murphy E, Steenbergen C. Estrogen regulation of protein expression and signaling pathways in the heart. Biol Sex Differ. 2014;5(1):6.
179. Murphy E, Steenbergen C. Gender-based differences in mechanisms of protection in myocardial ischemia-reperfusion injury. Cardiovascular research. 2007;75(3):478-86.
180. Mestas J, Hughes CC. Of mice and not men: differences between mouse and human immunology. Journal of immunology (Baltimore, Md : 1950). 2004;172(5):2731-8.
181. Hertl M, Howard TK, Lowell JA, Shenoy S, Robert P, Harvey C, et al. Changes in liver core temperature during preservation and rewarming in human and porcine liver allografts. Liver Transpl Surg. 1996;2(2):111-7.

Chapter 9: Appendix

LC-MS raw data of tissue abundance of analysed metabolites in the mouse, pig and human heart during warm and cold ischaemia. Ion counts were calculated from the spectra of analysed metabolites.

Appendix 1: Mouse LC-MS data

Appendix 1: Mouse LC-MS data

condition	HEPES	2-HG	3-hydroxybutyrate	3-phospho-glycerate	acetate
Control - 1	5.92E+07	136787579.7	83039266.6	2.05E+07	NF
Control - 2	6.11E+07	137173546.6	47580746.17	NF	NF
Control - 3	5.89E+07	174586983.9	24333483.07	NF	NF
Control - 4	5.96E+07	179048227.2	32659346.08	2.78E+06	NF
Control - 5	6.25E+07	166135707	50690052.51	NF	NF
Control - 6	5.96E+07	175343454	59482257.41	1.63E+07	NF
6WI - 1	5.23E+07	143932150.1	36997397.78	NF	NF
6WI - 2	5.38E+07	100897988.7	38596206.59	NF	NF
6WI - 3	4.77E+07	113610544.7	62898893.27	2.20E+05	NF
6WI - 4	4.86E+07	130203847.4	33983848.01	NF	NF
6WI - 5	4.96E+07	108452986.7	36478424.22	NF	NF
12WI - 1	4.07E+07	116411979.3	40789181.89	NF	NF
12WI - 2	4.32E+07	125464359.2	42093209.89	NF	NF
12WI - 3	3.45E+07	102500513.2	53640643.3	NF	NF
12WI - 4	3.93E+07	132403698.5	44170399.64	NF	NF
12WI - 5	4.25E+07	163373616.5	44610861	NF	NF
30WI - 1	4.97E+07	97752940.36	71045310.46	NF	6.59E+07
30WI - 2	3.45E+07	110221210.5	52709117.08	NF	4.79E+07
30WI - 3	3.92E+07	75924801.04	36060703.96	NF	NF
30WI - 4	3.46E+07	117925161.7	68624626.34	NF	4.19E+07
30WI - 5	3.42E+07	148188511.1	81986244.17	NF	3.84E+07
6CI - 1	5.45E+07	135518060.4	34223542.01	NF	NF
6CI - 2	5.50E+07	114577037.1	12538898.5	3.80E+06	NF
6CI - 3	5.36E+07	164530155.2	17746287.15	7.81E+06	NF
6CI - 4	5.55E+07	152014692	35072228.41	NF	NF
6CI - 5	5.50E+07	235130287.7	49601459.94	3.14E+07	NF
12CI - 1	5.59E+07	151377869.9	31972709.54	5.47E+06	NF
12CI - 2	6.02E+07	181515996.7	22126740.77	3.42E+06	NF
12CI - 3	5.26E+07	166259683.5	22478733.33	3.66E+06	NF
12CI - 4	5.62E+07	126905826.8	21643221.43	1.53E+06	NF
12CI - 5	5.57E+07	168159274.2	25706804.97	1.14E+07	NF
30CI - 1	5.33E+07	149467954.8	28850033.97	1.18E+06	NF
30CI - 2	5.24E+07	150507575.3	17389760.47	2.97E+06	NF
30CI - 3	5.54E+07	125507618.1	14378191.61	NF	NF
30CI - 4	5.22E+07	176662034.3	21784281.85	1.83E+06	NF
30CI - 5	5.18E+07	167427024.5	22223348.8	2.30E+07	NF
240CI - 1	4.98E+07	153909786.7	23626489.57	7.15E+05	NF
240CI - 2	4.55E+07	130250962.2	17484437.96	NF	2.13E+07
240CI - 3	4.38E+07	143430319.5	23389936.15	NF	NF
240CI - 4	4.84E+07	105683117.3	18967379.51	NF	NF
240CI - 5	4.81E+07	138038093.7	25829576.82	NF	NF
480CI - 1	5.04E+07	121473948.4	31896595.03	8.13E+05	NF
480CI - 2	4.45E+07	189136086	35110132.72	NF	NF
480CI - 3	4.50E+07	183759905	24174782.22	NF	NF
Control	31671657	160797137	22152241	0	0
Control	30767346	232557663	30165304	0	0
Control	33800942	186093130	16519256	0	0
Control	20437761	217786878	26380142	0	0
Control	31515492	228451998	36179504	0	0
240WI	22580676	178418374	41902221	0	0
240WI	24304349	141025503	42879845	0	0
240WI	31015529	163049513	38281227	0	0
240WI	29934824	123206689	34331616	0	0

Appendix 1: Mouse LC-MS data

condition	acetoacetate	acetyl carnitine	acetylcarnitine	acetylcholine	aconitate
Control - 1	1.96E+07	1.85E+10	4159136147	644540563.8	187183732.6
Control - 2	2.61E+07	1.70E+10	5606607555	410830954.5	263031214.3
Control - 3	9.91E+06	3.15E+10	6332678113	829890884.2	206297422.3
Control - 4	3.54E+06	2.43E+10	2936587513	869261608.9	233425033.4
Control - 5	1.05E+07	3.13E+10	3947587791	692692560.4	229539500.3
Control - 6	8.90E+06	2.90E+10	4295616560	1179878047	144156841.6
6WI - 1	NF	2.87E+10	2640167156	1228236629	56378354.99
6WI - 2	4.74E+06	2.99E+10	7635101026	804257878.5	101931406.8
6WI - 3	4.41E+06	3.14E+10	8009034688	678329459.9	82454093.29
6WI - 4	2.08E+06	3.19E+10	7597391352	843356887.3	55692026.58
6WI - 5	1.78E+06	3.19E+10	6459470401	833208756.3	54202881.99
12WI - 1	1.45E+06	2.96E+10	8106330380	798944595.3	52232281
12WI - 2	NF	2.30E+10	5528450126	686941984.2	48648312.32
12WI - 3	NF	2.54E+10	4282278803	804212515.9	14889828.72
12WI - 4	NF	2.71E+10	2898949369	805120203.1	31279913.24
12WI - 5	NF	2.95E+10	3196346802	1022183065	38478914.43
30WI - 1	NF	1.20E+10	1725897939	739120681.6	56267276.98
30WI - 2	NF	1.38E+10	3879519304	755319438.6	26614570.35
30WI - 3	NF	8.95E+09	1401539911	829545470.2	14467875.35
30WI - 4	NF	1.30E+10	1634650852	699102477.2	11889348.73
30WI - 5	NF	9.65E+09	1347228034	1772631162	15825739.43
6CI - 1	9.55E+06	1.42E+10	2266606102	734255991	171910214
6CI - 2	7.76E+06	1.50E+10	4807970689	603607387.4	222661100.4
6CI - 3	5.04E+06	1.37E+10	2228072765	838856484.3	191808605.4
6CI - 4	NF	2.29E+10	3488125602	856248854.2	207366470
6CI - 5	1.70E+07	1.98E+10	5979439234	1471761059	179495086.9
12CI - 1	1.60E+07	1.74E+10	5126665459	931105095.4	256819938.2
12CI - 2	1.80E+07	1.68E+10	5187299441	1076913547	315942934.9
12CI - 3	1.00E+07	1.92E+10	5134095177	751006282.2	171949583.9
12CI - 4	1.32E+07	1.52E+10	4444866491	777138657.2	216399023.7
12CI - 5	6.29E+06	2.65E+10	3547611437	878657163.3	83622048.62
30CI - 1	4.75E+06	3.45E+10	6119245083	710219208.6	132600164.7
30CI - 2	NF	2.20E+10	3652079962	988924999.2	188067918.9
30CI - 3	4.01E+06	2.84E+10	7335436892	1148684730	250338274.4
30CI - 4	NF	2.44E+10	4447641388	892919276.5	141582878.2
30CI - 5	5.30E+06	2.67E+10	6228702418	893301289	152057034.5
240CI - 1	3.51E+06	2.93E+10	7719517136	683320807	93045726.28
240CI - 2	4.39E+06	3.39E+10	5894083565	910218962.8	77264428.25
240CI - 3	2.17E+06	2.75E+10	6916070319	611298161.8	90442407.43
240CI - 4	3.19E+06	2.52E+10	7414551500	649886541.3	98291642.05
240CI - 5	9.21E+05	2.95E+10	4101896342	693479070.8	41284352.32
480CI - 1	3.58E+06	1.42E+10	2038398598	645241012.8	54168433.21
480CI - 2	NF	2.69E+10	5162818517	1784763830	45976690.91
480CI - 3	NF	2.37E+10	3489605139	974133725.8	34561975.24
Control	11975511	18636465019		748932538	474632479
Control	6896390	35512706268		775400701	532155591
Control	5759903	21702923844		827948406	445545720
Control	4737146	15043627003		857264988	530890958
Control	5400932	23970209111		892006193	486524603
240WI	0	783108060		936458904	14956287
240WI	0	0		986864214	10845848
240WI	0	754523142		608034869	9394300
240WI	0	1204351858		759989654	7650592

Appendix 1: Mouse LC-MS data

condition	adenine	adenosine	adenylo-succinate	ADP	agmatine
Control - 1	3158655.099	61353448.76	NF	6.65E+07	6.96E+04
Control - 2	2369884.749	12128047.6	NF	1.09E+07	1.22E+05
Control - 3	9063740.728	15154714.95	NF	1.45E+07	1.16E+05
Control - 4	30419575.51	94973306.28	NF	5.17E+07	7.53E+04
Control - 5	21997675.7	93292054.43	NF	2.72E+07	9.04E+04
Control - 6	15957001.14	10291678.6	NF	6.24E+07	5.72E+04
6WI - 1	238530896.2	2192314844	1.41E+05	8.71E+07	1.53E+05
6WI - 2	88594079.92	2550156451	NF	6.37E+07	3.00E+04
6WI - 3	109458369.6	2953751000	NF	1.09E+08	5.08E+04
6WI - 4	137336297.1	2797462365	NF	1.03E+08	1.80E+05
6WI - 5	167145196.2	2893416627	5.35E+04	1.30E+08	1.07E+05
12WI - 1	256232037.7	6362769234	NF	8.83E+07	1.62E+05
12WI - 2	265068594.8	7051592776	NF	7.42E+07	1.16E+05
12WI - 3	492397101	14756932725	NF	4.83E+07	1.62E+05
12WI - 4	565901076.5	7947433930	NF	1.02E+08	1.53E+05
12WI - 5	571656361.1	8753728493	8.07E+04	1.48E+08	1.58E+05
30WI - 1	1549504483	9593395682	NF	8.54E+06	1.33E+05
30WI - 2	749322989.7	12383871700	NF	3.87E+06	1.11E+05
30WI - 3	1760568810	11869490175	NF	7.45E+06	1.02E+05
30WI - 4	1565020798	13648945791	NF	3.69E+06	2.35E+05
30WI - 5	1858438811	13672000533	8.46E+03	1.16E+07	7.48E+04
6CI - 1	31524263.01	2397840806	3.07E+04	5.69E+07	8.72E+04
6CI - 2	11502047.75	2734996127	NF	8.70E+07	NF
6CI - 3	47177596.49	3292484626	3.17E+04	1.19E+08	1.70E+05
6CI - 4	42739626.88	1203018852	NF	1.01E+08	1.67E+05
6CI - 5	15098177.74	1392493425	2.44E+06	3.51E+08	8.37E+04
12CI - 1	15352398.57	4040256937	1.57E+05	1.46E+08	1.23E+05
12CI - 2	13568151.98	1036836296	1.74E+04	6.11E+07	7.22E+04
12CI - 3	19937848.89	2374495635	6.95E+04	1.64E+08	1.33E+05
12CI - 4	17062413.39	1322431212	8.85E+04	8.66E+07	8.06E+04
12CI - 5	56214097	3583142494	2.15E+06	2.95E+08	1.23E+05
30CI - 1	43451431.82	2315638884	2.17E+05	1.87E+08	1.12E+05
30CI - 2	55271305.66	3181145412	3.86E+04	1.40E+08	8.20E+04
30CI - 3	38643014.76	2701675813	7.65E+03	1.19E+08	6.49E+04
30CI - 4	95100057.37	4212347380	5.61E+05	1.92E+08	1.42E+05
30CI - 5	28966023.35	1340586602	4.28E+06	3.91E+08	8.46E+04
240CI - 1	164937866.1	9431852397	2.11E+05	9.36E+07	1.23E+05
240CI - 2	226986699	5274387646	2.08E+05	9.09E+07	6.76E+04
240CI - 3	160109856.9	9172571689	1.26E+06	7.44E+07	2.06E+04
240CI - 4	158080018.1	12303490774	2.69E+06	5.55E+07	3.11E+04
240CI - 5	211022393.8	7264747608	4.23E+05	6.86E+07	8.90E+04
480CI - 1	380471016.2	13745246985	2.19E+06	2.36E+07	4.40E+04
480CI - 2	461504322	5770814114	7.36E+05	1.20E+07	1.96E+05
480CI - 3	396461515.6	7065562041	4.06E+05	1.18E+07	6.16E+04
Control	11407628	3291699	0	32582409	0
Control	21793333	3181979	0	41348257	0
Control	14420957	26460539	0	42036859	0
Control	16129244	10788021	0	23304635	0
Control	11413569	8807937	0	31561961	11159
240WI	782446881	255631633	0	1169750	410363
240WI	753591832	244967030	0	1999663	216315
240WI	1253605628	327516484	0	1192677	19025
240WI	806720082	222432552	0	1064837	40479

Appendix 1: Mouse LC-MS data

condition	aKG	alanine	allantoin	AMP	arginine	ascorbic acid
Control - 1	4.30E+07	5184824142	266965860.2	1.26E+08	846607604.7	362672.2
Control - 2	1.38E+07	5251209286	235370948.6	4.80E+07	1362019776	439557.74
Control - 3	1.49E+07	5733682918	220527989.6	2.36E+07	1172558285	1053001.5
Control - 4	1.62E+07	7562331407	272125295	1.93E+08	1108825081	2306877.9
Control - 5	1.73E+07	6326076099	218251307.1	8.11E+07	1033079421	5776302.8
Control - 6	9.80E+06	5457960774	179128634.4	3.66E+07	782585889.5	40189795
6WI - 1	3.35E+06	8270047794	166220710	9.12E+08	1242120554	7913959.4
6WI - 2	1.21E+06	6563988122	137907248.7	7.29E+08	776672816	10513556
6WI - 3	3.01E+06	6710438618	149690072.9	5.70E+08	1006164631	409289.93
6WI - 4	1.38E+06	7405923980	191305099.1	4.42E+08	1594532713	41151358
6WI - 5	NF	8787357512	203076965.1	7.51E+08	1131524661	53502199
12WI - 1	NF	9935955069	201121359.3	1.11E+09	1934831350	150684475
12WI - 2	NF	9988851269	192910762.6	1.15E+09	1566130962	156371429
12WI - 3	NF	7552660628	167068325.1	1.84E+09	1416558290	107498069
12WI - 4	NF	11918391993	207022043.7	8.89E+08	2037490064	76084099
12WI - 5	NF	13329620413	240008148.1	1.50E+09	1739125790	147264647
30WI - 1	NF	9962173588	260616116.5	1.19E+09	1489964461	40280165
30WI - 2	NF	10681946458	159162028.2	1.79E+09	1580958839	218046648
30WI - 3	NF	9363505049	182070312.6	1.34E+09	1763359737	75780797
30WI - 4	NF	12599863443	185786197.5	1.78E+09	1800968681	130854391
30WI - 5	NF	11226786296	190052898.3	1.82E+09	1470250605	97927244
6CI - 1	NF	5721276371	204834590.9	2.20E+08	1160181509	36335801
6CI - 2	8.51E+05	5465687902	179651152.9	3.60E+08	894084258.6	88119623
6CI - 3	NF	7602512071	221164350.3	4.61E+08	1633951464	22592238
6CI - 4	NF	6481042770	229042078.6	3.38E+08	1040533990	54705637
6CI - 5	3.23E+06	5421132990	188546755.7	1.31E+09	839748792.3	157014128
12CI - 1	NF	5583487459	181544657.6	9.19E+08	1209180136	146922617
12CI - 2	2.04E+06	4395014293	159201780.6	1.24E+08	1053413900	101584723
12CI - 3	NF	6235723289	185642900.3	7.22E+08	1383940176	129625416
12CI - 4	NF	6197125796	221922587.6	1.56E+08	1057487495	92808861
12CI - 5	NF	8254760332	202179159.8	1.67E+09	1029931392	130499941
30CI - 1	NF	6257266684	178366629.2	8.70E+08	1170112776	104985750
30CI - 2	NF	6052649639	193453325.9	4.52E+08	1005957992	32702205
30CI - 3	NF	4231533263	111026350.2	6.56E+08	1256143193	192756199
30CI - 4	NF	5871788158	165368647.9	6.69E+08	1494909513	53742114
30CI - 5	NF	7178468173	177433256.8	1.86E+09	831960155	135942664
240CI - 1	NF	5227764081	164103437.3	4.27E+08	971550671.7	87279839
240CI - 2	NF	5882222985	221603832	4.05E+08	1291908788	51625003
240CI - 3	NF	5044521614	146485222.5	5.39E+08	952954023.8	189035839
240CI - 4	NF	4954887731	150831236.4	5.63E+08	797874413.1	234414368
240CI - 5	NF	5777455101	182159230	4.22E+08	1126711154	90207026
480CI - 1	NF	4927278849	91080077.17	8.59E+08	689433420.3	155548402
480CI - 2	NF	7197448908	122091193	9.43E+08	1428190992	148542627
480CI - 3	NF	6415008608	173843137.6	8.47E+08	1479656844	185302558
Control	65958357	3669173071	43690253	45352750	712741071	0
Control	50492833	4188273240	86136337	54147483	732887539	262428
Control	41991782	3443310820	70307252	61507099	648829433	3874887
Control	22296264	3822697569	68740142	35644525	619322242	1357452
Control	26988002	2911057340	41437590	41838827	619100105	13697200
240WI	0	8582527167	62034773	64474179	4517491075	26578548
240WI	0	7134772950	55981973	143955563	3494937847	13189076
240WI	0	8217546686	77657651	110102753	1507474143	0
240WI	0	6716666004	82071224	98584020	1354263063	1950108

Appendix 1: Mouse LC-MS data

condition	asparagine	aspartate	ATP	betaine	butyrylcarnitine
Control - 1	230450645.1	5274482080	7.39E+07	816909129	1.11E+08
Control - 2	240482304.3	2467075818	3.79E+06	888647215	4.29E+07
Control - 3	270964322.4	4058233597	2.58E+07	453545044	5.88E+07
Control - 4	309706865.4	2768734857	2.71E+07	2091698414	2.70E+07
Control - 5	270803503.6	3504289104	2.58E+07	1566407325	4.19E+07
Control - 6	383809246.7	3650660977	1.54E+08	775850933	1.36E+08
6WI - 1	363696726.8	2043719123	7.87E+06	1876595636	1.10E+09
6WI - 2	226554184.8	3882569737	1.56E+06	612299349	1.50E+09
6WI - 3	210641870.8	1281118563	1.82E+07	634009932	2.12E+09
6WI - 4	283246558.8	1175393746	8.60E+06	701293915	1.97E+09
6WI - 5	277155176.8	3521743422	1.48E+07	925216216	1.36E+09
12WI - 1	248722897	1541973396	2.10E+06	809380616	2.10E+09
12WI - 2	269594006.9	825468238.2	8.90E+05	584884987	2.10E+09
12WI - 3	284811894.7	990555150.5	1.17E+06	998136959	2.45E+09
12WI - 4	423370408.3	1489130239	3.94E+06	2563939050	1.99E+09
12WI - 5	456279748.2	2534294066	1.00E+07	1837814166	2.06E+09
30WI - 1	312502654.2	3839270578	7.00E+04	2808837987	1.41E+09
30WI - 2	177910691	974493854.1	NF	933276495	1.50E+09
30WI - 3	285330201.3	773264867.7	NF	3211297561	8.14E+08
30WI - 4	430203667.2	1765878173	9.81E+04	1896798115	1.09E+09
30WI - 5	474538300.4	717162137	NF	3500767973	1.28E+09
6CI - 1	187301810.3	6869223677	1.99E+07	1285139149	8.64E+07
6CI - 2	131446578.9	2616549333	4.25E+07	459184757	5.06E+07
6CI - 3	275919250.7	5336644963	3.43E+07	2032051332	6.21E+07
6CI - 4	300750537	4320335454	2.08E+07	2473844993	4.43E+07
6CI - 5	265872019.3	5724569710	7.85E+07	629696827	1.40E+08
12CI - 1	142204999	3228677994	4.42E+07	808369475	4.33E+07
12CI - 2	229938333.1	3768745240	4.79E+07	541907399	8.96E+07
12CI - 3	279916972.4	4015619396	4.37E+07	793364959	3.91E+07
12CI - 4	217404048.1	7031608529	5.24E+07	824866547	5.07E+07
12CI - 5	240760643.3	3725133710	4.37E+07	2271227740	1.53E+08
30CI - 1	201041597.5	4722751026	3.90E+07	1264344147	2.27E+08
30CI - 2	177212494.6	4182653464	4.61E+07	2298128889	4.45E+07
30CI - 3	203783129.1	2861178317	1.56E+07	575144940	1.23E+08
30CI - 4	222821232.5	4830234458	4.91E+07	2531909779	7.45E+07
30CI - 5	204081894.3	5244117983	5.37E+07	762779977	1.57E+08
240CI - 1	97599420.88	2426261034	3.15E+07	1012510642	2.17E+09
240CI - 2	158975393.4	5070963311	1.32E+07	2695698201	2.17E+09
240CI - 3	105667277.3	2902634844	1.10E+07	855800578	1.71E+09
240CI - 4	65948741.57	3971002229	1.59E+07	835860253	1.27E+09
240CI - 5	131275501.6	3205387146	9.28E+06	1842311806	1.85E+09
480CI - 1	75185655.95	3335913197	7.09E+06	2032403648	1.29E+09
480CI - 2	214025019.1	4263877584	1.41E+06	2436346024	2.39E+09
480CI - 3	125982028.4	4707553260	6.30E+05	2419670883	1.60E+09
Control	126235298	1246306702	25763417	0	31108134
Control	110421456	1356251634	28358930	0	27520992
Control	88835140	1778404111	28208927	0	22303057
Control	88099863	2604030442	12580829	0	15349480
Control	121619062	1896224712	33696777	0	39303180
240WI	474115509	1875564842	0	0	18927089
240WI	267634774	1479553441	0	0	33044293
240WI	108430507	967200442	0	330757388	11228053
240WI	113492574	588470851	0	0	25024865

Appendix 1: Mouse LC-MS data

condition	carbamoyl-phosphate	carnitine	CDP	choline	citrate
Control - 1	1.95E+08	4.78E+10	4.25E+04	1777689505	1.22E+09
Control - 2	2.09E+08	5.22E+10	NF	1850474945	8.21E+08
Control - 3	2.53E+08	5.80E+10	NF	1718503511	9.95E+08
Control - 4	2.56E+08	5.81E+10	1.34E+04	2779530236	1.08E+09
Control - 5	2.37E+08	5.37E+10	1.17E+04	2030059436	1.03E+09
Control - 6	2.39E+08	6.21E+10	1.41E+05	3106914600	1.48E+09
6WI - 1	2.47E+08	5.55E+10	2.05E+04	3032694100	3.68E+08
6WI - 2	2.10E+08	4.31E+10	NF	2546549684	3.78E+08
6WI - 3	1.83E+08	5.04E+10	NF	2251777783	3.83E+08
6WI - 4	2.53E+08	5.59E+10	NF	2026431128	3.56E+08
6WI - 5	2.54E+08	5.44E+10	1.33E+04	2325265627	2.98E+08
12WI - 1	2.41E+08	5.26E+10	NF	2110055063	1.98E+08
12WI - 2	2.43E+08	5.30E+10	NF	2338708283	2.07E+08
12WI - 3	2.37E+08	6.18E+10	NF	2619639818	2.75E+08
12WI - 4	2.57E+08	5.07E+10	NF	2622011539	2.61E+08
12WI - 5	2.58E+08	5.13E+10	NF	2989096063	3.16E+08
30WI - 1	2.46E+08	6.24E+10	NF	4736618364	4.47E+08
30WI - 2	2.65E+08	6.57E+10	1.22E+04	2541102364	1.45E+08
30WI - 3	2.47E+08	7.25E+10	NF	4241220580	1.09E+08
30WI - 4	2.70E+08	6.54E+10	NF	2823906161	2.14E+08
30WI - 5	2.57E+08	6.69E+10	NF	4620531721	2.19E+08
6CI - 1	2.58E+08	6.09E+10	NF	2033054224	9.27E+08
6CI - 2	1.83E+08	6.30E+10	1.61E+05	1676862156	9.58E+08
6CI - 3	2.91E+08	6.74E+10	2.64E+05	2251711762	9.36E+08
6CI - 4	2.89E+08	6.67E+10	8.19E+04	1761828349	9.59E+08
6CI - 5	2.61E+08	7.13E+10	1.98E+06	3049046268	1.48E+09
12CI - 1	3.07E+08	6.56E+10	7.10E+05	2205501600	1.13E+09
12CI - 2	2.74E+08	6.53E+10	6.30E+04	2967224556	1.07E+09
12CI - 3	2.93E+08	6.07E+10	6.40E+05	2316860544	9.02E+08
12CI - 4	2.85E+08	6.88E+10	1.61E+05	2143187037	9.60E+08
12CI - 5	3.00E+08	5.32E+10	1.52E+06	2362565166	1.38E+09
30CI - 1	3.12E+08	6.04E+10	5.21E+05	2197218931	1.15E+09
30CI - 2	2.88E+08	6.40E+10	2.58E+05	2998831898	9.22E+08
30CI - 3	2.94E+08	6.59E+10	1.71E+05	2916795127	9.21E+08
30CI - 4	3.02E+08	5.83E+10	5.85E+05	2390075219	8.10E+08
30CI - 5	3.00E+08	5.98E+10	2.68E+06	2129212252	1.39E+09
240CI - 1	3.41E+08	4.64E+10	5.21E+04	2372568949	5.10E+08
240CI - 2	3.27E+08	6.09E+10	4.42E+04	2671345830	4.92E+08
240CI - 3	3.23E+08	4.57E+10	4.27E+04	2375153239	5.05E+08
240CI - 4	3.28E+08	4.41E+10	7.53E+04	2702741371	5.47E+08
240CI - 5	3.14E+08	4.61E+10	5.68E+04	2474095277	3.49E+08
480CI - 1	3.47E+08	4.14E+10	NF	2427041544	7.71E+08
480CI - 2	3.56E+08	6.07E+10	NF	3914864683	4.77E+08
480CI - 3	3.48E+08	5.78E+10	NF	3170157291	4.49E+08
Control	239598634	44567841091	0	2406487636	458971349
Control	239225815	39021973204	0	1711562381	570522555
Control	239114169	52735458956	0	2089418239	527643320
Control	186902413	33809665914	0	1821644463	356363034
Control	231888151	49268916234	0	2201550616	543936989
240WI	228985974	53389513726	0	8145498738	17499343
240WI	200467355	44600391071	0	4997399917	18340405
240WI	250777573	58278993561	0	4726276168	14696069
240WI	209569547	53243421104	0	5070358921	11481023

Appendix 1: Mouse LC-MS data

condition	citrulline	creatine	cytidine	dihydro-thymine	ethanolamine
Control - 1	843487411.5	8.41E+10	2.12E+07	64923748.38	6.19E+07
Control - 2	898978502.9	9.03E+10	1.82E+07	77083211.17	7.41E+07
Control - 3	1068611767	1.08E+11	1.70E+07	93963472.66	8.74E+07
Control - 4	1182708727	1.10E+11	9.53E+06	96061310.48	7.57E+07
Control - 5	903623934	9.72E+10	1.98E+07	80289163.15	6.36E+07
Control - 6	1193915258	1.00E+11	4.28E+07	96349174.93	2.22E+08
6WI - 1	1059928746	1.03E+11	2.53E+08	101053246.5	1.68E+08
6WI - 2	735531373.7	9.09E+10	2.07E+08	65017560.39	1.25E+08
6WI - 3	1081709300	1.05E+11	2.56E+08	67597743.64	8.02E+07
6WI - 4	1418826094	1.13E+11	3.67E+08	100144452	9.84E+07
6WI - 5	993290098.5	1.12E+11	2.63E+08	90604019.23	1.12E+08
12WI - 1	1145064128	1.04E+11	1.73E+08	80685177.68	1.03E+08
12WI - 2	1017027171	1.08E+11	2.43E+08	73099508.06	1.08E+08
12WI - 3	1078278833	1.10E+11	3.73E+08	96908406.36	1.07E+08
12WI - 4	1322333378	1.08E+11	2.42E+08	106052234.9	9.72E+07
12WI - 5	1544529386	1.08E+11	2.71E+08	110027650.3	1.09E+08
30WI - 1	1102966357	1.01E+11	3.11E+08	77618655.15	2.47E+08
30WI - 2	1132642767	1.04E+11	2.52E+08	73224817	1.75E+08
30WI - 3	1375516221	1.10E+11	2.63E+08	107225796.4	1.98E+08
30WI - 4	1207674484	1.13E+11	2.27E+08	96209572.69	1.26E+08
30WI - 5	1659249885	1.05E+11	2.75E+08	131447560.7	2.65E+08
6CI - 1	1019108459	1.02E+11	1.12E+07	58170973.72	7.99E+07
6CI - 2	1052959682	9.53E+10	1.02E+07	62190449.98	6.50E+07
6CI - 3	1117102148	1.07E+11	7.00E+06	70430641.5	8.53E+07
6CI - 4	1238035296	1.18E+11	1.30E+07	82797724.42	7.16E+07
6CI - 5	1657700912	1.08E+11	2.63E+07	79865688.13	1.46E+08
12CI - 1	1007492983	1.16E+11	1.53E+07	50567336.3	9.08E+07
12CI - 2	1499274879	1.09E+11	1.05E+07	85164202.58	1.28E+08
12CI - 3	954471045.9	1.13E+11	1.39E+07	71930092.66	7.06E+07
12CI - 4	1068185092	1.09E+11	1.02E+07	68754629.98	8.04E+07
12CI - 5	1203456390	1.07E+11	1.55E+07	55401346.38	9.15E+07
30CI - 1	1152500571	1.17E+11	8.45E+06	64799172.45	5.18E+07
30CI - 2	1161206138	1.11E+11	4.75E+06	67491970.09	7.48E+07
30CI - 3	1529770032	1.08E+11	1.56E+07	76885163.51	1.35E+08
30CI - 4	1278173849	1.05E+11	3.13E+07	66884639.16	5.42E+07
30CI - 5	1122856185	1.12E+11	2.07E+07	58016467.94	7.33E+07
240CI - 1	923716312.8	1.04E+11	5.97E+06	23853956.71	5.00E+07
240CI - 2	1366206638	1.11E+11	7.36E+06	56597832.49	7.77E+07
240CI - 3	851831960.6	9.70E+10	2.00E+07	24291814.7	5.53E+07
240CI - 4	781266733.1	8.77E+10	2.26E+07	18157609.51	5.41E+07
240CI - 5	1025782947	1.02E+11	1.29E+07	32424219.7	5.36E+07
480CI - 1	654033244.8	7.80E+10	6.45E+07	11830439.05	5.88E+07
480CI - 2	1477164340	1.02E+11	9.36E+07	74180517.26	1.33E+08
480CI - 3	1458794792	1.07E+11	7.36E+07	42266448.75	1.02E+08
Control	769544269	52283444176	5113277	37092104	50901651
Control	891733412	57786467646	4409194	33503980	39434340
Control	834714579	56004605038	4343821	34516903	46463797
Control	823078413	52614718389	3228456	33063551	30094125
Control	815264852	55521084788	6698623	35778056	47540303
240WI	802108585	59062408034	231205792	40755966	519584713
240WI	860063843	51944447912	151083770	26219688	303070108
240WI	1066620151	65853152899	126088154	38623237	256515470
240WI	799534730	58793311988	154326940	25151347	374445273

Appendix 1: Mouse LC-MS data

condition	fructose 6-phosphate	fructose-1,6-Biphosphate	fumarate	GDP	GABA
Control - 1	2.94E+07	NF	659389579.1	7.83E+04	11722515.25
Control - 2	2.18E+07	NF	293183228.6	NF	4719989.892
Control - 3	2.53E+07	NF	552107934.6	NF	9763754.894
Control - 4	2.27E+07	NF	501565627.8	NF	17421767.95
Control - 5	3.64E+07	NF	543416216.9	NF	16378011.07
Control - 6	3.96E+07	1.02E+06	593147756.8	1.06E+05	13933928.45
6WI - 1	1.85E+07	NF	197811031.5	NF	13096051.27
6WI - 2	8.12E+06	NF	154886890	NF	5963305.996
6WI - 3	8.77E+06	NF	111084713.1	2.25E+05	5999463.264
6WI - 4	1.51E+07	NF	131844320.6	NF	9598563.569
6WI - 5	1.97E+07	NF	201314746.1	NF	9321617.758
12WI - 1	1.67E+07	NF	70574274.7	NF	5959788.414
12WI - 2	9.34E+06	NF	63545324.36	NF	4516782.466
12WI - 3	1.45E+06	NF	71191824.08	NF	9232522.86
12WI - 4	1.24E+07	NF	79823648.64	NF	13626852.07
12WI - 5	7.28E+06	NF	221330565.3	7.95E+04	14537321.17
30WI - 1	4.09E+06	NF	54287692.06	NF	14667898.89
30WI - 2	4.72E+06	NF	18300750.17	NF	4747487.666
30WI - 3	3.31E+06	NF	46666503.47	NF	13194638.13
30WI - 4	4.44E+06	NF	15593025.82	NF	11506371.1
30WI - 5	2.67E+06	NF	179638848.7	1.84E+04	13088979.79
6CI - 1	2.04E+07	NF	644935930.6	NF	7501325.781
6CI - 2	5.62E+06	NF	217412226.6	3.00E+05	6768937.325
6CI - 3	9.50E+06	NF	797158598.1	NF	10245000.14
6CI - 4	1.47E+07	NF	485507879.3	NF	16332860.34
6CI - 5	5.76E+06	NF	728890444.4	1.74E+06	8655826.103
12CI - 1	1.05E+07	NF	361057599	6.88E+05	6624075.129
12CI - 2	1.41E+07	NF	501057524.4	3.11E+04	6579234.254
12CI - 3	1.28E+07	NF	338621654.8	3.19E+05	9649742.31
12CI - 4	1.03E+07	NF	500193518.8	3.32E+04	6800007.878
12CI - 5	8.57E+06	1.41E+06	592159896.6	2.34E+06	10262664.11
30CI - 1	1.91E+07	NF	377449697.8	6.50E+05	8695314.322
30CI - 2	1.65E+07	NF	417927902.7	2.42E+05	9275186.25
30CI - 3	1.74E+07	NF	188710860.2	NF	5054561.22
30CI - 4	1.84E+07	NF	397825538.1	4.51E+05	12386164.99
30CI - 5	8.23E+06	4.93E+06	570993543.9	3.47E+06	9651891.089
240CI - 1	3.65E+07	NF	161786403.2	4.45E+05	2665280.199
240CI - 2	2.89E+07	NF	208723526.5	NF	9099564.84
240CI - 3	1.11E+07	NF	190551312.8	6.92E+04	2298024.142
240CI - 4	8.38E+06	NF	166543554	2.40E+05	1320233.208
240CI - 5	8.11E+06	NF	146988678	8.25E+04	3585527.048
480CI - 1	7.17E+06	NF	119356450.1	1.96E+05	201739.7181
480CI - 2	3.96E+06	NF	103857836.2	NF	9914549.427
480CI - 3	3.42E+06	NF	95267119.78	NF	6704780.747
Control	22039710	0	3.29E+08	25063	13721296
Control	24230457	0	3.14E+08	16707	14523350
Control	24992046	0	2.49E+08	0	13443772
Control	20724612	0	3.53E+08	0	14496347
Control	29518677	0	3.20E+08	12279	15707634
240WI	3295968	0	5.65E+07	0	18453075
240WI	1614542	0	4.17E+07	0	13370612
240WI	3610457	0	6.29E+07	0	14374506
240WI	3847017	0	2.76E+07	0	11940765

Appendix 1: Mouse LC-MS data

condition	glucose	glucose 6-phosphate	glutamate	glutamine	glyceraldehyde-3-phosphate
Control - 1	7436035541	3.00E+07	23483977571	23623370956	8.32E+06
Control - 2	6341026079	2.62E+07	14452395811	26396680797	6.26E+06
Control - 3	3219522130	3.17E+07	22901065008	36325263267	3.46E+06
Control - 4	4746523371	2.46E+07	24907048675	35977403639	1.37E+07
Control - 5	6668157935	4.59E+07	25345596674	29246597042	5.66E+06
Control - 6	4286429034	3.96E+07	23563643890	37255247789	5.61E+06
6WI - 1	971629320.7	2.17E+07	18596679256	37900813486	8.34E+06
6WI - 2	1563068182	1.01E+07	15143446934	27382649086	8.81E+06
6WI - 3	1383536262	1.13E+07	15033614021	27912490448	1.22E+07
6WI - 4	682663180.4	1.69E+07	18708536961	35989650996	1.02E+07
6WI - 5	672128231.7	2.37E+07	17147926304	33333785228	2.01E+07
12WI - 1	523397124.7	1.72E+07	15334255953	33044488581	2.04E+07
12WI - 2	323753789.5	1.07E+07	12532333723	32318544770	9.45E+06
12WI - 3	312283878.7	1.73E+06	16346800284	35036274507	6.24E+06
12WI - 4	239698027.7	1.50E+07	18943399694	39997093154	1.26E+07
12WI - 5	228848863.9	8.42E+06	21035008946	44576487765	8.30E+06
30WI - 1	1444103969	3.78E+06	22205770113	29195621961	9.07E+06
30WI - 2	257066941.7	4.32E+06	12892605770	32250334364	3.67E+06
30WI - 3	268439566.1	3.02E+06	17249373731	38679932724	8.34E+06
30WI - 4	200784415.1	5.05E+06	17170546973	36751926445	4.03E+06
30WI - 5	369781065.4	2.43E+06	16073754882	54168113559	3.06E+06
6CI - 1	4863960398	2.28E+07	18508659372	28767690469	7.05E+06
6CI - 2	1975458152	6.92E+06	17282331828	27886822518	7.09E+06
6CI - 3	4377588951	1.06E+07	18696955962	37238719242	1.05E+07
6CI - 4	3678845646	1.74E+07	26002291104	35718785049	8.47E+06
6CI - 5	4333641475	5.30E+06	20095668296	40111201684	6.34E+06
12CI - 1	3877895261	1.27E+07	19639077331	28992429864	8.05E+06
12CI - 2	4598137291	1.56E+07	16152607309	37958266251	6.65E+06
12CI - 3	2804926922	1.61E+07	20779868172	33198320568	1.28E+07
12CI - 4	3160774269	1.18E+07	18005010062	30659132751	4.93E+06
12CI - 5	3448018513	8.89E+06	20979659681	30603723201	6.91E+06
30CI - 1	1681111583	2.48E+07	20758047174	30777930819	1.05E+07
30CI - 2	2891225397	2.05E+07	15665447350	37911478391	7.84E+06
30CI - 3	971287453.5	2.19E+07	17243989491	36482764307	6.54E+06
30CI - 4	3367988559	2.16E+07	20624962703	37481967783	9.05E+06
30CI - 5	1606196787	7.96E+06	23093687469	29163081052	1.04E+07
240CI - 1	965287718.5	3.90E+07	12332753558	20425211724	1.80E+06
240CI - 2	591607120.2	3.53E+07	16695832404	33132474780	1.17E+06
240CI - 3	625462009.6	1.20E+07	12795353513	20909383870	NF
240CI - 4	805875850.7	1.00E+07	10819917339	18119654533	6.54E+05
240CI - 5	699312615.1	9.39E+06	15151469323	24853002393	NF
480CI - 1	585377559.1	6.37E+06	8548783965	13834658806	7.61E+05
480CI - 2	360370638.5	4.60E+06	20484061304	49117943369	NF
480CI - 3	731633099.4	3.09E+06	16641533665	31301221245	1.84E+05
Control	1923826093	20836537	14237424523	15969187876	827826
Control	1300152503	24016827	22565391819	18120048135	3846668
Control	1421020793	20900337	19703380979	18395517087	3535606
Control	1944366837	13963308	21509925100	16896452767	4003452
Control	2077647613	24706940	16966494163	12991379638	361543
240WI	1465296699	4542863	20280688904	15824141071	2468979
240WI	257126385	2641481	15557995601	12250242936	423426
240WI	1101887282	3323872	22762901863	20495056824	3643942
240WI	111349487	3690563	16391018367	12991988362	1019388

Appendix 1: Mouse LC-MS data

condition	glycerate	glycerol	glycerylphosphoryl-choline	glycerylphosphoryl-ethanolamine	glycine
Control - 1	NF	9.38E+06	86310403.95	1.66E+07	972617286.8
Control - 2	NF	6.63E+06	211645568.7	1.61E+07	671444241.9
Control - 3	NF	7.07E+06	57202353.24	1.53E+07	826630486.7
Control - 4	NF	4.62E+06	203737319.1	1.56E+07	1127342821
Control - 5	NF	8.77E+06	177279198	1.55E+07	977416437.2
Control - 6	NF	6.38E+06	76614902.23	1.58E+07	1053369149
6WI - 1	NF	2.79E+07	162135390.1	1.30E+07	1053143496
6WI - 2	NF	3.12E+07	398922204.4	2.68E+07	851998927.8
6WI - 3	NF	2.15E+07	411975996.4	1.41E+07	910804654.4
6WI - 4	NF	2.11E+07	55587580.84	1.80E+07	850628454.6
6WI - 5	NF	2.07E+07	50887065.8	1.22E+07	814693050.7
12WI - 1	NF	4.34E+07	364004800.8	1.33E+07	998682601
12WI - 2	NF	4.13E+07	323701928.9	1.16E+07	830748638.2
12WI - 3	NF	4.06E+07	69487025.26	1.48E+07	910096101
12WI - 4	NF	4.35E+07	175897541.3	1.36E+07	1072438969
12WI - 5	NF	4.43E+07	139713676.1	1.71E+07	1609842890
30WI - 1	NF	1.19E+08	134162853.5	1.40E+07	1590884349
30WI - 2	NF	9.98E+07	394184704.8	1.32E+07	826674835.2
30WI - 3	NF	1.23E+08	125582490.6	1.01E+07	1144985891
30WI - 4	NF	9.54E+07	95611970.6	1.53E+07	1048692785
30WI - 5	NF	1.10E+08	90665640.92	8.64E+06	1527050164
6CI - 1	NF	6.65E+06	136050748.9	1.45E+07	1003306880
6CI - 2	NF	2.81E+06	199879264	1.86E+07	774833191.5
6CI - 3	NF	2.59E+06	187719488.2	9.98E+06	1093426528
6CI - 4	NF	3.68E+06	312506758.9	1.64E+07	1150889217
6CI - 5	NF	3.65E+06	353642088.4	1.27E+07	979663839.8
12CI - 1	NF	6.18E+06	630549552.9	1.32E+07	754491870
12CI - 2	NF	4.13E+06	342062986.8	9.75E+06	769800495.1
12CI - 3	NF	3.04E+06	61484262.22	1.67E+07	825869426.3
12CI - 4	NF	5.88E+06	61220952.67	1.23E+07	753882068
12CI - 5	NF	7.25E+06	127707070.1	1.63E+07	1233435661
30CI - 1	NF	4.01E+06	81226396.3	1.35E+07	829356207.7
30CI - 2	NF	5.00E+06	213888685.6	1.29E+07	1054317925
30CI - 3	NF	4.29E+06	496777773.2	1.33E+07	818158957
30CI - 4	NF	2.95E+06	254206286.8	1.25E+07	940834207.7
30CI - 5	NF	5.53E+06	452189094.6	1.55E+07	963285493.9
240CI - 1	NF	7.28E+06	419543775.2	1.10E+07	644549595
240CI - 2	NF	1.04E+07	212866788.8	1.32E+07	991718418.5
240CI - 3	NF	6.91E+06	443780766.9	8.69E+06	593788707.8
240CI - 4	NF	6.21E+06	456419909.4	8.67E+06	583019848.7
240CI - 5	NF	5.34E+06	93177318.18	1.08E+07	732655159.6
480CI - 1	NF	2.00E+07	45942571.51	5.58E+06	611018914.3
480CI - 2	NF	3.61E+07	66450063.8	2.87E+06	1045878015
480CI - 3	NF	2.01E+07	50916327.56	5.18E+06	915282431.1
Control	0	7691981	157910723	16946975	644919850
Control	0	7480448	209201629	15773976	708960408
Control	0	7869356	172250283	13006787	651107255
Control	304892	0	196607201	7041923	601224320
Control	0	11535263	206913007	15604236	558280791
240WI	5818743	5.76E+08	160234886	29694796	1927288134
240WI	4596650	4.54E+08	120393309	15753343	1265752063
240WI	532385	5.01E+08	137715325	22891983	1462926863
240WI	1546991	4.4E+08	129555572	24990077	1487736172

Appendix 1: Mouse LC-MS data

condition	GMP	GSH	GSH	GSSG	GSSG	guanine
Control - 1	NF	9.48E+08	2461276420	2.88E+07	14918523.95	1.61E+06
Control - 2	NF	8.55E+08	2621352339	1.81E+07	3151964.595	2.28E+05
Control - 3	NF	1.15E+09	3998048932	1.34E+07	5521309.982	6.46E+05
Control - 4	NF	1.14E+09	3098007585	1.25E+07	9437712.332	5.81E+05
Control - 5	NF	1.21E+09	3178158640	9.86E+06	6858274.586	1.18E+06
Control - 6	NF	9.85E+08	3633031576	2.58E+07	8655822.118	1.48E+06
6WI - 1	1420106.293	9.52E+08	2579494973	7.03E+06	7978153.419	6.09E+06
6WI - 2	25941080.31	8.65E+08	2815930124	5.59E+06	3082335.145	9.04E+06
6WI - 3	15225968.65	9.91E+08	3068721807	4.24E+06	3588321.771	6.93E+06
6WI - 4	8646800.416	1.07E+09	3469187100	1.01E+07	9054362.37	5.45E+06
6WI - 5	8097129.675	1.19E+09	3720288148	4.94E+06	7698623.369	6.49E+06
12WI - 1	27134059.28	1.16E+09	3925172229	4.55E+06	6844221.912	1.30E+07
12WI - 2	29455717.17	1.01E+09	3469327866	6.27E+06	5813166.592	9.26E+06
12WI - 3	9473007.139	1.00E+09	3279094517	5.34E+06	6333530.946	1.29E+07
12WI - 4	1279150.631	1.10E+09	3272307244	5.24E+06	7189457.006	1.25E+07
12WI - 5	754516.1423	1.16E+09	3095398120	9.86E+06	23640877.27	1.63E+07
30WI - 1	696799.997	8.53E+08	2287607140	2.19E+07	7990515.487	2.24E+07
30WI - 2	35589069.63	9.97E+08	3590026082	4.59E+06	6813166.599	1.26E+07
30WI - 3	3432640.236	1.02E+09	2286988764	2.56E+06	10395586.06	2.07E+07
30WI - 4	831840.2946	1.12E+09	2927801872	7.54E+06	12097245.88	2.46E+07
30WI - 5	2994773.276	9.26E+08	2962191895	1.06E+07	11527666.02	2.32E+07
6CI - 1	NF	1.14E+09	2725608430	1.29E+07	10244550.49	4.46E+05
6CI - 2	3306976.265	9.95E+08	3406185270	7.38E+06	7627581.162	8.04E+05
6CI - 3	NF	1.19E+09	1624720753	1.27E+07	37570655.05	3.08E+05
6CI - 4	NF	1.25E+09	3042531052	1.03E+07	13476294.48	4.23E+05
6CI - 5	16950221.5	1.13E+09	4439835920	1.45E+07	6246479.871	7.46E+05
12CI - 1	10141069.68	9.09E+08	3530973323	4.22E+07	23342137.48	9.50E+05
12CI - 2	6202826.085	1.06E+09	3815408868	7.97E+06	8356012.581	2.85E+05
12CI - 3	4257077.913	1.33E+09	3924979277	9.84E+06	18734949.55	4.83E+05
12CI - 4	2154111.892	1.21E+09	3706608433	9.16E+06	11400822.24	8.50E+04
12CI - 5	NF	1.07E+09	4134425024	2.88E+07	12691367.73	5.49E+05
30CI - 1	2294863.786	1.05E+09	3494874096	2.93E+07	13387688.23	1.98E+05
30CI - 2	NF	1.24E+09	2409978915	1.09E+07	19697068.72	2.53E+05
30CI - 3	9478182.293	1.09E+09	3966052922	1.12E+07	8560349.927	3.80E+05
30CI - 4	NF	1.35E+09	2780798095	9.29E+06	23607380.77	1.34E+06
30CI - 5	27432302.84	1.09E+09	4248795098	2.80E+07	12153465.85	5.33E+05
240CI - 1	7263710.707	9.29E+08	3452656745	4.45E+07	29454181.54	7.01E+05
240CI - 2	305276.4762	1.22E+09	2917590679	1.94E+07	26161848.41	9.58E+05
240CI - 3	25444707.08	1.11E+09	3633296457	2.71E+07	21509884.03	1.10E+06
240CI - 4	31278214.99	1.07E+09	3405690292	3.72E+07	35759181.21	4.36E+05
240CI - 5	NF	1.12E+09	3175084541	1.80E+07	17347946.03	8.38E+05
480CI - 1	5278378.302	9.38E+08	3063846052	4.84E+07	14213117.92	4.70E+06
480CI - 2	37883217.35	1.23E+09	3290207735	1.21E+07	25158319.74	3.72E+06
480CI - 3	23405474.72	1.27E+09	3015305845	1.75E+07	24508839.37	4.35E+06
Control	0	2.481E+09			1943275	109262
Control	0	1.842E+09			11089520	0
Control	0	2.454E+09			3637616	526491
Control	0	2.647E+09			1338654	0
Control	0	2.169E+09			3382792	0
240WI	0	1.091E+09			3954217	15772113
240WI	0	1.26E+09			852095	29119747
240WI	0	1.057E+09			17898527	1879470
240WI	0	1.037E+09			2249902	4940104

Appendix 1: Mouse LC-MS data

condition	guanosine	histamine	histidine	hypotaurine	hypoxanthine	inosine
Control - 1	NF	48235271.89	277922377	36433482.39	2092995.803	289235.264
Control - 2	NF	19012021.17	318572242.9	44085326.3	1208274.325	NF
Control - 3	NF	7063231.966	214477385.5	46298786.47	NF	NF
Control - 4	NF	21496648.96	399184379.6	31361452.9	1957043.595	NF
Control - 5	NF	39581860.72	314581772.2	30201744.82	3568594.281	218238.323
Control - 6	NF	8665005.007	377634657	94382017.42	NF	NF
6WI - 1	41208081.1	38395408.94	480369426.4	92540544.9	1689709891	990440065
6WI - 2	42241702	69133642.14	332138895.7	84395240.97	1620292345	785113775
6WI - 3	49660441.9	23273555.45	359901489	38704503.52	1606267714	764030211
6WI - 4	44799005.1	13715092.1	326375702.2	43429957.17	1693896146	794424955
6WI - 5	48055720.5	17311384.48	227873330.7	37049458.16	1670148369	743769045
12WI - 1	116729570	59127200.37	477883675.3	37165376.65	2487837860	2149634762
12WI - 2	107806802	42519234.12	387130729.5	36914680.87	2263918350	1663832481
12WI - 3	176839550	37141290.41	157177845.1	33637808.03	2536315573	1743321914
12WI - 4	136982295	13914409.81	474531233.1	31117076.85	3130763126	2080184192
12WI - 5	148920198	6011323.313	481480215.9	37810624.53	4487863900	2174964530
30WI - 1	198845340	113348537.8	307629410.6	38620675.12	9334178612	5699905080
30WI - 2	188466478	6548968.37	434331831	40352072.62	5807521859	5386369510
30WI - 3	241399194	38203597.8	421029408	40375322.56	8405051415	6814413668
30WI - 4	206212753	3872607.537	187100385.1	32120621.65	5898352261	5472220384
30WI - 5	267734353	18670758.14	634529988.9	79885962.79	9108503732	6799883218
6CI - 1	NF	85850056.39	282885739.7	35853779.56	53296934.74	24455053
6CI - 2	NF	104695450.9	299592712.4	38730475.17	67030092.34	41141291.1
6CI - 3	NF	74885846.92	381963674.1	27911341.87	90844997.62	28923468.4
6CI - 4	NF	13180240.61	420944846.8	31530031.62	49222555.06	22650691.1
6CI - 5	NF	24577853.94	507650450.3	102818157.7	127081155.7	67685599.7
12CI - 1	NF	43573015.96	430594641.3	26945261.16	64603014.55	35076480.9
12CI - 2	198056.086	47868812.93	478862089.5	64179858.92	48825704.81	46530044.2
12CI - 3	NF	51994416.39	287457342.4	29383224.4	104060066.6	65763666
12CI - 4	NF	23615776.05	324048887.8	32739858	56091006.4	44082797.7
12CI - 5	216576.752	27662740.43	373429551.3	23160592.3	283096142.2	133494453
30CI - 1	202007.844	17338201.29	202526051.6	26914890.15	210206932.4	179879030
30CI - 2	NF	31951027.33	349114069.4	31133260.71	190289689.7	181317362
30CI - 3	642725.665	42781909.18	545453278.2	98028618.9	176863507.9	273529031
30CI - 4	3951146.97	43138362.85	397091116.4	27184283.12	325101659.4	283355102
30CI - 5	NF	17707083.25	398903218	30378036.31	364403923.5	278635385
240CI - 1	3578039.88	77810864.06	339213134.2	17617959.02	1116934334	1466029540
240CI - 2	4315952.51	45113244.99	420142766.6	32792893.06	861669374.9	1410647155
240CI - 3	2914136.31	69523236.81	317501794.8	15592869.42	667093342.2	1255633648
240CI - 4	764555.945	59009401.09	274456548.1	13815537.24	670077968.5	1255363766
240CI - 5	4698222.75	20607357.6	258099130	20691027.58	820391794.6	1378610308
480CI - 1	28727460.2	53295179.44	157250288.2	7776965.672	2442468422	2778787553
480CI - 2	28165273.9	19631368.97	707975351.4	68852025.66	1983028931	2593929086
480CI - 3	22802954.9	44658043.64	391508029	27314597.3	1984859875	2527922327
Control	0	25773761	81405034	51394621	0.00E+00	0
Control	0	5143927	109429059	48115215	0.00E+00	0
Control	0	23005019	95999125	44816041	0.00E+00	0
Control	0	0	84347524	42556248	0.00E+00	0
Control	0	11004578	116229353	54306759	0.00E+00	0
240WI	61323961	25609223	310455585	52035999	1.14E+10	4306104693
240WI	45712405	20079997	189663606	40589598	9.42E+09	4349612706
240WI	22926984	1193424	145191819	54628081	1.28E+10	6242586442
240WI	20033776	26082365	112754576	32584975	1.02E+10	4334062548

Appendix 1: Mouse LC-MS data

condition	Isovalerylcarnitine	lactate	leucine / isoleucine	linoleic acid	lysine
Control - 1	2.02E+07	2273803741	8576259358	6.81E+07	1363039325
Control - 2	3.49E+07	1794776936	9077869773	7.95E+07	1791712299
Control - 3	3.03E+07	1753599326	4297163343	3.83E+07	1829698157
Control - 4	9.99E+06	2250792304	5974523828	9.16E+07	2023160231
Control - 5	2.59E+07	2602148558	9217477467	7.17E+07	1818863367
Control - 6	2.00E+07	1306140377	4948383227	1.39E+07	1104479497
6WI - 1	1.01E+08	8686868487	6484167514	4.36E+07	1664156733
6WI - 2	1.07E+08	6530130328	5661580040	5.82E+07	947360819.1
6WI - 3	1.15E+08	7547794555	7311490051	3.86E+07	1227819701
6WI - 4	1.15E+08	7301704394	5934092416	1.14E+07	2106580761
6WI - 5	1.28E+08	8623959972	7319179864	9.66E+06	1793999293
12WI - 1	3.37E+08	12542441154	7765929157	8.13E+06	2530155242
12WI - 2	3.73E+08	11792324851	6262967962	8.58E+06	2371545745
12WI - 3	2.51E+08	8809490001	7116195159	1.11E+07	1995434529
12WI - 4	4.19E+08	13395052574	8275080757	1.46E+06	3016699805
12WI - 5	3.40E+08	14213876375	8008510409	1.80E+07	2430486761
30WI - 1	2.87E+08	11066746903	12843911132	1.04E+08	2078592758
30WI - 2	8.44E+08	13312023799	10725663863	3.11E+07	1871930008
30WI - 3	3.23E+08	11998523083	8488867041	6.35E+07	2391019044
30WI - 4	5.95E+08	12677656037	8540216409	2.64E+07	2758846050
30WI - 5	4.00E+08	14067563647	10396631208	7.44E+07	1887528101
6CI - 1	1.74E+07	2945100317	4841454549	4.58E+07	1761453188
6CI - 2	1.43E+07	2831452337	4460057964	5.10E+07	1274066340
6CI - 3	1.77E+07	4203374006	4790379895	1.89E+07	2800223894
6CI - 4	1.99E+07	3646127439	5509856944	5.48E+07	1811023208
6CI - 5	2.60E+07	2965952444	4940010076	9.77E+06	986419830.6
12CI - 1	1.84E+07	3525364519	9069470219	3.31E+07	1803349960
12CI - 2	2.68E+07	3055274375	5164694037	1.94E+07	1384427775
12CI - 3	1.65E+07	4495229578	5801615172	1.36E+07	2213324979
12CI - 4	2.01E+07	3310658480	6165697692	1.59E+07	1654985818
12CI - 5	1.61E+07	6205958551	6590344700	3.58E+07	1675357759
30CI - 1	1.92E+07	6198188637	5837891668	2.11E+07	1742812416
30CI - 2	1.02E+07	6586495546	5116632889	9.11E+06	1654505280
30CI - 3	1.31E+07	4974024566	3176078113	1.12E+07	1165531232
30CI - 4	1.58E+07	7674629098	5809542155	1.29E+07	2144581920
30CI - 5	1.48E+07	6376111861	5841063523	1.71E+07	1344526324
240CI - 1	7.02E+07	10009273663	5946934022	3.19E+08	1171824735
240CI - 2	7.45E+07	11602256043	6063568695	5.87E+06	1945535605
240CI - 3	6.34E+07	8025438141	4863796612	1.34E+07	1348849818
240CI - 4	5.01E+07	7103443918	4753374890	5.00E+07	1197145844
240CI - 5	6.52E+07	10375489599	5500336465	2.26E+06	1592837422
480CI - 1	8.35E+07	6558610702	5020628617	7.88E+07	1038881623
480CI - 2	1.19E+08	9318910993	4825811100	4.78E+07	1716074554
480CI - 3	7.77E+07	7538409475	5592539358	3.49E+07	2209710706
Control	9879908	1557169687	1953620445	49737418	1379481518
Control	13408532	1529521430	2964326400	113915737	1139481880
Control	12681762	1115095901	1890983128	88718274	1190448489
Control	9810203	1013777467	2115918408	43684391	956264556
Control	20384607	1012494181	1964283893	63886979	1031827872
240WI	16942314	9589859763	32701995619	1.267E+09	5241154577
240WI	16044986	7211457593	29273259006	1.628E+09	4113344243
240WI	11501354	8776805099	8434382967	728976803	2082313542
240WI	10802533	6780895387	11943511525	1.184E+09	2114822835

Appendix 1: Mouse LC-MS data

condition	malate	malonate	mannitol / sorbitol	methionine	myristic acid	myristoylcarnitine
Control - 1	1.59E+09	112159925.6	NF	1268521050	1.30E+07	1.69E+07
Control - 2	1.31E+09	73706695.02	NF	1751318986	9.25E+06	4.28E+06
Control - 3	1.81E+09	70527405.72	NF	1047749880	8.80E+06	1.31E+07
Control - 4	1.32E+09	197591015.4	NF	702849575.6	7.87E+06	4.31E+06
Control - 5	1.72E+09	140547464.6	NF	888867114.2	5.65E+06	4.72E+06
Control - 6	1.56E+09	101071636.4	NF	927003230.4	6.31E+06	2.95E+07
6WI - 1	8.34E+08	111966543.7	NF	697600575.7	7.97E+06	1.48E+07
6WI - 2	8.14E+08	71698951.37	NF	1405393366	1.16E+07	3.84E+07
6WI - 3	5.80E+08	74065471.3	NF	1167315927	1.19E+07	2.62E+07
6WI - 4	5.69E+08	82070035.45	NF	1324698448	8.23E+06	3.33E+07
6WI - 5	9.66E+08	72538975.29	NF	1103095440	6.51E+06	2.56E+07
12WI - 1	4.62E+08	56656274.51	NF	2059810926	8.89E+06	9.73E+06
12WI - 2	4.31E+08	55600865.78	NF	1717663360	7.99E+06	5.50E+06
12WI - 3	3.45E+08	50487484.21	NF	1086724632	9.56E+06	2.74E+07
12WI - 4	4.20E+08	117627268.4	NF	1055774928	4.83E+06	3.87E+06
12WI - 5	6.22E+08	166307290	NF	1154457594	4.80E+06	1.43E+07
30WI - 1	2.97E+08	173923109.9	NF	846613127.2	1.74E+07	1.37E+07
30WI - 2	1.06E+08	53644259.4	NF	1581746304	7.87E+06	3.71E+06
30WI - 3	2.32E+08	119795770.9	NF	636979815.1	8.97E+06	1.23E+07
30WI - 4	1.02E+08	82073918.65	NF	1626802275	9.48E+06	1.82E+06
30WI - 5	3.27E+08	135648289.2	NF	674821110.2	1.06E+07	8.44E+06
6CI - 1	1.97E+09	118856416.4	NF	946472907.4	1.40E+07	4.34E+07
6CI - 2	9.39E+08	75792602.51	NF	1312996519	1.12E+07	1.02E+07
6CI - 3	1.90E+09	221363224.8	NF	869083728.4	9.68E+06	9.92E+06
6CI - 4	1.53E+09	163927605.6	NF	684381961.3	9.61E+06	1.26E+07
6CI - 5	1.88E+09	85415092.79	NF	1599510519	3.21E+06	5.38E+07
12CI - 1	1.29E+09	67588186.94	NF	1557134592	1.04E+07	6.78E+06
12CI - 2	1.74E+09	76620771.92	NF	1241631981	9.42E+06	2.05E+07
12CI - 3	1.16E+09	73964678.81	NF	1908543219	1.03E+07	7.27E+06
12CI - 4	1.97E+09	74208607.3	NF	1421480176	1.06E+07	1.46E+07
12CI - 5	1.91E+09	127374494.2	NF	1084041656	7.20E+06	4.54E+07
30CI - 1	1.43E+09	79753605.51	NF	1269393988	6.94E+06	1.99E+07
30CI - 2	1.21E+09	187184967.9	NF	532806439.1	6.29E+06	5.23E+06
30CI - 3	7.89E+08	47156106.34	NF	1127402492	1.19E+07	1.55E+07
30CI - 4	1.28E+09	189810579.3	NF	793902569.9	6.91E+06	1.15E+07
30CI - 5	1.56E+09	100350442.3	NF	1321792393	7.07E+06	5.70E+07
240CI - 1	7.40E+08	63112044.53	NF	1475353362	3.08E+07	5.11E+07
240CI - 2	9.03E+08	165728220.6	NF	744137909.7	8.69E+06	4.85E+07
240CI - 3	8.48E+08	51094231.98	NF	1470807956	1.14E+07	5.07E+07
240CI - 4	8.19E+08	48506590.71	NF	1280398601	1.11E+07	7.85E+07
240CI - 5	7.75E+08	75464505.7	NF	1277294604	7.97E+06	4.79E+07
480CI - 1	6.96E+08	62564947.05	NF	906452462.2	1.24E+07	2.96E+07
480CI - 2	5.39E+08	120220341.5	NF	980975625.7	1.14E+07	3.26E+07
480CI - 3	5.88E+08	124806331.8	NF	876899123.9	1.10E+07	2.58E+07
Control	1.41E+09	0.00E+00	612869	688351125	7119454	4324109
Control	1.33E+09	7.95E+05	632685	773273321	8917159	1552742
Control	1.31E+09	0.00E+00	3107433	531200990	11640953	3535927
Control	1.16E+09	0.00E+00	1171927	520260093	4965874	3537578
Control	1.57E+09	0.00E+00	2240267	528529056	9708799	7024659
240WI	68995212	1.13E+07	21686674	4872978102	28249638	0
240WI	24953516	4.10E+06	4421469	4109035248	56587823	723338
240WI	14751717	2.90E+06	13619569	1364932667	20350816	0
240WI	49309283	3.31E+06	14076736	1742319981	31065328	0

Appendix 1: Mouse LC-MS data

condition	n-acetyl aspartate	NAD	NADH	nicotinamide	octanoylcarnitine
Control - 1	359705037.9	2.13E+07	NF	2828477605	5.06E+06
Control - 2	73528051.42	2.24E+07	NF	1986877679	1.38E+06
Control - 3	94996110.16	3.25E+07	1.33E+06	1435256181	2.35E+06
Control - 4	144152733	3.20E+07	7.06E+05	2747655471	7.95E+05
Control - 5	285003344.9	2.54E+07	1.56E+06	1264741013	5.99E+05
Control - 6	166009172	3.12E+07	5.78E+06	1926342068	7.49E+06
6WI - 1	134267352.3	2.33E+07	9.58E+06	2880646777	1.20E+07
6WI - 2	285593193.8	1.59E+07	5.44E+06	1627562860	1.76E+07
6WI - 3	92077642.28	2.33E+07	1.19E+07	1426351156	1.79E+07
6WI - 4	69987959.71	2.29E+07	1.46E+07	1049508819	1.44E+07
6WI - 5	79544736.31	2.46E+07	1.33E+07	1543230914	1.75E+07
12WI - 1	96541586.32	1.66E+07	1.06E+07	1499226344	2.01E+07
12WI - 2	82691632.2	1.89E+07	1.14E+07	1612697037	2.54E+07
12WI - 3	98017286.79	1.96E+07	1.80E+07	1157186565	2.67E+07
12WI - 4	115268181.5	1.91E+07	1.68E+07	1272338157	1.44E+07
12WI - 5	176461289.2	2.99E+07	8.64E+06	3507236697	2.65E+07
30WI - 1	602827373.3	9.95E+06	1.72E+07	1348957098	2.28E+07
30WI - 2	88442885.31	1.45E+07	1.92E+07	1611846320	1.74E+07
30WI - 3	133736714.5	1.10E+07	2.72E+07	1231563528	9.75E+06
30WI - 4	106011445.5	1.08E+07	2.20E+07	943680474.4	8.13E+06
30WI - 5	235780395.8	1.96E+07	1.89E+07	3175587423	3.14E+07
6CI - 1	349930538.4	2.21E+07	3.17E+06	1868743477	9.16E+06
6CI - 2	163915386.3	2.28E+07	7.09E+06	2112047964	1.68E+06
6CI - 3	168488804.9	2.61E+07	2.07E+06	3530994694	7.38E+06
6CI - 4	125081681	2.47E+07	1.01E+07	1841798145	2.48E+06
6CI - 5	172764494.8	2.53E+07	2.69E+06	4672977925	1.37E+07
12CI - 1	99783841.71	2.59E+07	7.33E+06	3109860437	1.46E+06
12CI - 2	124952034.4	2.85E+07	1.10E+07	1253168828	2.92E+06
12CI - 3	95103271.55	2.64E+07	7.03E+06	2885359445	2.38E+06
12CI - 4	93868656.17	2.56E+07	1.19E+07	775107205	2.42E+06
12CI - 5	273749724	2.42E+07	4.42E+06	4053282554	7.96E+06
30CI - 1	102899872.3	2.51E+07	1.33E+07	2346152366	2.22E+06
30CI - 2	158131699.2	2.54E+07	9.25E+06	1789433706	5.92E+05
30CI - 3	107015472.7	2.50E+07	1.51E+07	1771764829	1.65E+06
30CI - 4	162570497.9	2.72E+07	1.39E+07	2369389340	3.25E+06
30CI - 5	130486619.5	2.41E+07	6.85E+06	4848853632	8.15E+06
240CI - 1	106449946.1	2.38E+07	5.30E+06	1288438985	4.37E+06
240CI - 2	180097419	2.74E+07	1.38E+07	1062472005	4.48E+06
240CI - 3	180702793.4	2.15E+07	1.04E+07	915499038.6	4.78E+06
240CI - 4	477199052.7	1.95E+07	9.00E+06	741244489.9	5.68E+06
240CI - 5	122223318.7	2.13E+07	1.17E+07	667029724.6	4.87E+06
480CI - 1	619952190.2	1.41E+07	1.25E+07	464553328.4	6.21E+06
480CI - 2	190904510.3	1.74E+07	3.01E+07	499982173.1	8.00E+06
480CI - 3	225880727.2	1.66E+07	2.91E+07	623870290.9	3.46E+06
Control	128903242	2.3E+07	3954239	76821054	724651
Control	101848275	2.3E+07	8364852	117211363	203776
Control	123844736	3.1E+07	9396270	141714897	261045
Control	87416805	1.5E+07	3468843	98118210	345896
Control	106163706	2.6E+07	6748266	129413050	1197708
240WI	131342218	209315	3215798	1317258319	0
240WI	174609347	349530	4065605	1037900565	0
240WI	124119376	657710	2626142	2003503411	92931
240WI	94381170	652791	3795573	1463774643	0

Appendix 1: Mouse LC-MS data

condition	oleic acid	oleyl carnitine	ornithine	orotate	palmitic acid	palmitoleic acid
Control - 1	5.96E+07	7.81E+07	170335182.1	1325659.108	1.62E+08	1.22E+07
Control - 2	5.95E+07	3.97E+07	284923987.9	590154.0182	1.38E+08	7.70E+06
Control - 3	3.02E+07	4.70E+07	133515878.2	570728.2054	1.17E+08	3.43E+06
Control - 4	4.25E+07	6.95E+07	166517522.3	566416.9508	1.31E+08	3.84E+06
Control - 5	4.65E+07	2.72E+07	179251676.2	426089.8324	1.16E+08	5.60E+06
Control - 6	1.74E+07	5.95E+07	77688340.88	335580.0529	9.01E+07	1.83E+06
6WI - 1	2.86E+07	3.19E+07	159887756.6	1541291.293	1.06E+08	2.22E+06
6WI - 2	6.52E+07	7.31E+07	183967441.6	698534.6603	1.39E+08	1.19E+07
6WI - 3	4.77E+07	7.69E+07	126320932.6	681118.1906	1.23E+08	5.92E+06
6WI - 4	1.40E+07	8.34E+07	89019731.54	648094.5553	1.19E+08	9.90E+05
6WI - 5	1.10E+07	4.16E+07	99142968.67	552372.8879	9.30E+07	NF
12WI - 1	1.10E+07	3.10E+07	207162357	1259685.801	9.38E+07	1.49E+06
12WI - 2	1.11E+07	2.38E+07	154249061.5	873002.0692	9.75E+07	1.91E+06
12WI - 3	1.50E+07	8.06E+07	94133694.68	413029.0435	1.22E+08	2.33E+06
12WI - 4	4.76E+06	1.43E+07	178793939.3	1015102.728	6.95E+07	NF
12WI - 5	1.23E+07	3.95E+07	170103530.7	1406107.872	7.06E+07	NF
30WI - 1	9.44E+07	1.13E+08	248878096.9	1910046.074	2.18E+08	1.75E+07
30WI - 2	2.56E+07	2.69E+07	161663401	853568.1569	1.13E+08	3.79E+05
30WI - 3	5.70E+07	6.63E+07	94697614.65	719728.1226	1.39E+08	3.65E+06
30WI - 4	2.09E+07	2.22E+07	212949077.3	2136693.198	1.30E+08	9.15E+05
30WI - 5	4.72E+07	6.41E+07	141939250.7	2209915.361	1.56E+08	6.42E+06
6CI - 1	4.84E+07	1.27E+08	81349228.51	629987.4299	1.76E+08	6.92E+06
6CI - 2	5.07E+07	5.64E+07	101989666.7	137894.0992	1.38E+08	6.73E+06
6CI - 3	1.11E+07	4.07E+07	101758648.3	951752.7111	1.22E+08	NF
6CI - 4	3.03E+07	5.37E+07	85136980.07	535844.385	1.34E+08	5.55E+06
6CI - 5	7.96E+06	1.06E+08	101278103.6	244291.7225	7.14E+07	4.09E+05
12CI - 1	2.03E+07	8.23E+07	145965221.4	400398.2844	1.33E+08	9.23E+05
12CI - 2	1.29E+07	7.02E+07	108835651.9	649897.2068	1.25E+08	2.28E+06
12CI - 3	1.42E+07	4.03E+07	128173284.9	481637.109	1.04E+08	NF
12CI - 4	7.47E+06	4.12E+07	96021398.67	382216.6968	1.13E+08	NF
12CI - 5	2.27E+07	2.18E+08	109841289.7	285814.9695	1.00E+08	2.20E+06
30CI - 1	1.39E+07	2.09E+08	99559567.53	772860.7976	1.14E+08	1.15E+06
30CI - 2	8.58E+06	3.56E+07	90722624.61	398226.1584	1.15E+08	NF
30CI - 3	8.09E+06	8.42E+07	100390501.3	293573.6246	1.17E+08	1.62E+05
30CI - 4	1.18E+07	6.85E+07	113606556.6	645621.1261	1.03E+08	NF
30CI - 5	1.41E+07	1.44E+08	76481547.34	891770.5518	1.04E+08	1.99E+05
240CI - 1	3.42E+08	3.37E+08	103413424.9	979755.5172	3.37E+08	6.47E+07
240CI - 2	8.31E+06	2.70E+08	86358896	1415064.981	1.19E+08	NF
240CI - 3	1.81E+07	2.57E+08	84350449.92	834212.1824	1.18E+08	1.71E+06
240CI - 4	6.94E+07	4.76E+08	82414383.94	1257486.077	1.22E+08	1.37E+07
240CI - 5	2.89E+06	2.41E+08	78750289.54	1342850.659	9.11E+07	NF
480CI - 1	8.78E+07	1.89E+08	109575671.2	1549721.509	1.68E+08	1.80E+07
480CI - 2	2.99E+07	1.70E+08	133619756.1	5610666.593	1.14E+08	1.99E+06
480CI - 3	2.59E+07	1.24E+08	78245101.17	2288882.787	1.42E+08	1.19E+06
Control	37118126	16747882	48973348	51064	1.22E+08	4808499
Control	78339085	7900238	57099994	260090	1.5E+08	10053364
Control	53484333	12004873	34749159	87653	1.46E+08	12523579
Control	26390807	12755628	26165663	267105	79932651	5662729
Control	40323554	24605915	29804950	112648	1.31E+08	8609245
240WI	600980789	5043125	757025535	588007	7.92E+08	52302883
240WI	798813453	4932195	1011011215	2738730	1.01E+09	111593978
240WI	412630602	11312485	143358468	150453	6.31E+08	38453180
240WI	577109247	5353573	288086825	2230496	7.58E+08	55397702

Appendix 1: Mouse LC-MS data

condition	palmitoyl carnitine	pantothenic acid	phenyl-alanine	phosphoenol-pyruvate	proline
Control - 1	77864802.59	457283932.2	1507503785	8.62E+05	1746308401
Control - 2	44450143.49	460268488.8	1880858657	NF	1977990791
Control - 3	56788629.93	536834111.6	1123636102	NF	1956123653
Control - 4	52479203.47	1068821847	1326362917	NF	2339464018
Control - 5	32323088.08	570879971.4	1435422280	NF	2253553696
Control - 6	78584219.86	611802233.8	1272531771	6.76E+05	1590679935
6WI - 1	47444034.4	969307299.3	2104241013	NF	2535781845
6WI - 2	83910764.29	644878669.6	1664695167	NF	1977364378
6WI - 3	64288726.03	777516309.5	1482477279	NF	1782433452
6WI - 4	66986953.65	870506514.3	1159475117	NF	1845390646
6WI - 5	49275960.43	892757883.8	1313409205	1.27E+05	1697917343
12WI - 1	38466450.1	846687411.9	1673609839	NF	2905856549
12WI - 2	29594948.79	781078411.3	1542645287	NF	2581969033
12WI - 3	74343412.54	1016600817	1500867996	NF	1761124099
12WI - 4	25568043.52	1161207627	1960093446	NF	3270601050
12WI - 5	49582143.75	1629396663	2043455591	NF	3724847614
30WI - 1	94500397.62	1077902736	2570607558	NF	3411318962
30WI - 2	25281192.6	870110323.9	2158648633	NF	2846931270
30WI - 3	58726557.94	1322086476	1975132212	NF	2755815102
30WI - 4	17907152.5	1044670375	1904823310	NF	3844425721
30WI - 5	57278874.45	2285805847	3634919176	NF	3560848629
6CI - 1	156921004.4	663564424.1	996375281.2	NF	1450330712
6CI - 2	53234773.27	513055344.2	991984783.7	4.44E+05	2006136809
6CI - 3	52622452.19	959842922.1	1399454946	4.05E+05	1914213512
6CI - 4	72472951.78	838013548.7	1208547026	1.95E+05	1890854542
6CI - 5	137703442.5	660058740.7	1547065766	4.71E+06	1875383553
12CI - 1	71286362.96	687373041.4	1404966617	2.19E+05	2075826578
12CI - 2	94385672.02	678678794	1471817075	NF	1435856083
12CI - 3	48182177.03	632878594.3	1361121743	3.14E+05	2214056252
12CI - 4	72189735.72	652548487.1	1262148260	NF	1457074509
12CI - 5	157971516.8	829818526.2	1174224078	1.49E+06	3053105731
30CI - 1	201094443	772581299	1074749205	NF	1570945598
30CI - 2	59715100.94	771023548	1167831992	NF	1693885643
30CI - 3	110821689	720229992.4	1391078385	NF	1423369116
30CI - 4	100507410.7	905077551.5	1532026407	NF	1914459571
30CI - 5	130522680.8	636414439.5	1089974335	3.72E+06	1911661111
240CI - 1	295166699.1	713503215.7	1093841022	1.66E+05	2526889998
240CI - 2	283495792.3	1470427821	1357442915	NF	1634405024
240CI - 3	242311413.6	555695372.8	931048969.4	NF	1579354869
240CI - 4	393100564.3	548209933.8	873976527.4	NF	1709611321
240CI - 5	246731158.8	765989997.7	1079437273	NF	1732908272
480CI - 1	173680762.3	493232544.7	791734793.9	NF	2501547789
480CI - 2	210019636	1306661922	2118111645	NF	2923504223
480CI - 3	179781731.9	1128674613	999462334.2	NF	1815096813
Control	36510680	321895420	444755002	0	798204529
Control	14640784	484504059	694963852	0	1090095428
Control	19614028	416248744	525163365	0	746963009
Control	23837390	372210436	593160931	0	632674636
Control	44275319	342759657	539098465	0	549678407
240WI	10936209	1178314666	11635046168	0	8878266669
240WI	6325104	754178126	10771710731	0	4516293297
240WI	11772007	1338636880	2565708504	0	2742885314
240WI	4309641	970269852	4037612430	0	3148351420

Appendix 1: Mouse LC-MS data

condition	propionyl-carnitine	pyro-glutamate	pyruvate	ribulose 5-phosphate	S-(2-Succinyl) cysteine
Control - 1	139604361	170765315	3.78E+07	NF	6.91E+04
Control - 2	67716882.62	109388045.7	2.86E+07	NF	6.49E+04
Control - 3	92858286.62	186334169.7	9.74E+06	NF	1.29E+05
Control - 4	94050646.51	312928549.8	8.47E+06	NF	1.90E+05
Control - 5	127871710.6	201619759.8	9.12E+06	NF	1.59E+05
Control - 6	149474157.5	226383842.3	7.45E+06	NF	2.17E+05
6WI - 1	1074548459	360177359.8	4.33E+06	1.68E+07	1.05E+05
6WI - 2	883321555.1	160357160.1	2.19E+06	1.26E+07	3.46E+04
6WI - 3	914044266.5	171053178.3	4.33E+06	1.91E+07	4.22E+04
6WI - 4	1012314592	225303414.1	2.51E+06	2.03E+07	7.96E+04
6WI - 5	1263414158	253709350.7	NF	1.95E+07	8.18E+04
12WI - 1	2008233435	172756169.7	NF	3.29E+07	4.75E+04
12WI - 2	1883679036	153527166.6	NF	2.35E+07	7.42E+04
12WI - 3	1400995657	290142193.4	NF	3.10E+07	2.50E+04
12WI - 4	2350547704	341125319	NF	3.33E+07	9.46E+04
12WI - 5	1940277347	457603215.6	3.13E+06	3.58E+07	1.29E+05
30WI - 1	978954563.1	393385954.6	NF	6.32E+07	4.28E+04
30WI - 2	2406494637	205647856	NF	6.77E+07	2.11E+04
30WI - 3	943951804.5	501688830.6	NF	7.78E+07	3.74E+04
30WI - 4	1660135642	408654628.9	4.46E+06	7.29E+07	6.80E+04
30WI - 5	1101133066	720837078.3	6.57E+06	8.61E+07	5.15E+05
6CI - 1	152112041.8	275293029.8	2.74E+06	4.23E+05	4.82E+04
6CI - 2	94277234.53	228553797.2	4.36E+06	1.57E+05	3.73E+04
6CI - 3	130274409.1	448502269.2	4.60E+06	NF	1.87E+05
6CI - 4	125322346	372711654.9	3.81E+06	1.48E+05	9.33E+04
6CI - 5	245521972.4	215528146	9.74E+06	2.88E+06	3.97E+05
12CI - 1	143606298.1	188404376.8	3.66E+06	NF	1.15E+05
12CI - 2	323732168.1	180487167.4	2.60E+06	3.53E+05	1.62E+05
12CI - 3	137718153.7	268731783.8	2.80E+06	3.36E+05	1.53E+05
12CI - 4	132890277.5	193127995.6	NF	NF	1.67E+05
12CI - 5	198844282.5	319929867.5	4.57E+06	1.77E+06	1.46E+05
30CI - 1	230084708.1	298039033.9	NF	NF	1.10E+05
30CI - 2	166236021.5	481728686.1	1.78E+06	7.39E+05	1.16E+05
30CI - 3	224593570.3	223194707.2	1.72E+06	NF	1.42E+05
30CI - 4	222132260.6	580984772.3	NF	1.05E+06	1.94E+05
30CI - 5	173049936.2	216112564.6	7.75E+06	3.56E+06	1.93E+05
240CI - 1	810415752.6	325008128	2.32E+06	2.82E+06	5.27E+04
240CI - 2	883583609.9	783037131.1	NF	5.34E+06	8.39E+04
240CI - 3	716766365	338141115.8	NF	2.50E+06	9.27E+04
240CI - 4	604393397.9	410376362.3	NF	1.86E+06	5.31E+04
240CI - 5	741879393.8	506171223.7	NF	3.15E+06	5.08E+04
480CI - 1	471716409.9	478767116.8	2.18E+06	1.76E+07	6.83E+04
480CI - 2	558664666.2	920565739.3	NF	2.09E+07	1.10E+05
480CI - 3	373403250.2	671144065.4	NF	2.16E+07	7.67E+04
Control	51640569	51337973	31136587	344511	31507
Control	56173280	105202849	10119083	174376	0
Control	51795355	110440259	5850605	0	0
Control	73076155	99404961	3778805	0	0
Control	75117739	42429022	8139521	0	34398
240WI	38368818	548330618	9650758	64682971	36746
240WI	45264917	270620073	0	56750955	11841
240WI	45171471	514631751	0	69919172	19757
240WI	52029090	365182221	0	63786186	0

Appendix 1: Mouse LC-MS data

condition	S-adenosyl-homocysteine	S-adenosyl-methionine	sedoheptulose-7-phosphate	serine	serotonin	stearic acid
Control - 1	7.66E+05	4.30E+07	NF	763786372.4	2.13E+07	1.23E+08
Control - 2	1.45E+05	5.46E+07	NF	889536887.6	2.20E+07	1.05E+08
Control - 3	NF	6.06E+07	NF	776503964	1.24E+07	9.65E+07
Control - 4	NF	4.52E+07	NF	1297847349	1.14E+07	1.14E+08
Control - 5	2.82E+05	4.84E+07	NF	906569978.1	1.04E+07	8.40E+07
Control - 6	2.05E+05	3.04E+07	NF	939954049.1	8.28E+06	5.55E+07
6WI - 1	5.54E+06	2.63E+07	NF	940182621.4	5.81E+06	7.65E+07
6WI - 2	1.52E+07	2.62E+07	NF	683992781.8	1.48E+07	1.13E+08
6WI - 3	5.59E+06	2.27E+07	NF	913780017.1	9.01E+06	1.18E+08
6WI - 4	7.19E+06	2.69E+07	NF	865608711.9	7.01E+06	1.19E+08
6WI - 5	1.12E+07	2.49E+07	NF	806021019.8	4.86E+06	9.77E+07
12WI - 1	8.38E+06	2.78E+07	NF	1090267288	5.42E+06	9.31E+07
12WI - 2	1.31E+07	2.96E+07	NF	1220302565	5.28E+06	1.27E+08
12WI - 3	1.07E+07	2.35E+07	NF	1024114347	6.40E+06	1.26E+08
12WI - 4	8.49E+06	2.68E+07	NF	1659003952	5.19E+06	8.07E+07
12WI - 5	1.16E+07	2.31E+07	NF	1694830835	5.40E+06	6.06E+07
30WI - 1	6.95E+07	2.30E+07	NF	1093128421	2.00E+07	1.82E+08
30WI - 2	2.63E+07	2.76E+07	NF	852846951.2	4.22E+06	1.05E+08
30WI - 3	3.55E+07	2.52E+07	NF	994765889	4.29E+06	1.14E+08
30WI - 4	5.65E+07	3.14E+07	NF	1739221779	3.55E+06	1.29E+08
30WI - 5	3.72E+07	2.00E+07	NF	1560531440	3.91E+06	8.89E+07
6CI - 1	1.66E+06	2.80E+07	NF	922040912.2	8.70E+06	1.33E+08
6CI - 2	8.44E+05	1.88E+07	NF	613587989.7	7.34E+06	1.25E+08
6CI - 3	3.41E+06	2.50E+07	NF	1316048878	4.91E+06	1.07E+08
6CI - 4	2.36E+06	3.42E+07	NF	1473890106	4.39E+06	1.44E+08
6CI - 5	1.30E+06	1.64E+07	NF	782353994.1	2.94E+06	4.48E+07
12CI - 1	2.28E+06	1.53E+07	NF	724884877.1	5.13E+06	1.42E+08
12CI - 2	7.44E+05	2.51E+07	NF	662827930.1	4.64E+06	1.01E+08
12CI - 3	4.42E+06	2.27E+07	NF	1227492596	6.25E+06	1.04E+08
12CI - 4	1.52E+06	2.67E+07	NF	871473281	4.07E+06	9.86E+07
12CI - 5	5.51E+06	1.24E+07	NF	1173992621	6.36E+06	4.92E+07
30CI - 1	4.00E+06	2.27E+07	NF	1077741400	5.92E+06	1.15E+08
30CI - 2	3.21E+06	2.05E+07	NF	1029425207	5.94E+06	9.90E+07
30CI - 3	9.75E+05	2.51E+07	NF	767992752	4.36E+06	1.08E+08
30CI - 4	7.38E+06	2.25E+07	NF	1402419231	8.42E+06	1.09E+08
30CI - 5	3.39E+06	1.41E+07	NF	1030478889	4.36E+06	7.02E+07
240CI - 1	5.51E+06	1.29E+07	NF	909450230.2	1.36E+07	1.55E+08
240CI - 2	8.14E+06	2.04E+07	NF	1094568600	6.11E+06	1.30E+08
240CI - 3	6.60E+06	1.78E+07	NF	873645827.3	8.89E+06	1.17E+08
240CI - 4	6.49E+06	1.42E+07	NF	544348116.9	1.13E+07	9.43E+07
240CI - 5	6.41E+06	1.90E+07	NF	1184470104	6.68E+06	9.87E+07
480CI - 1	1.63E+07	1.17E+07	NF	617534738.3	1.84E+07	9.55E+07
480CI - 2	8.39E+06	2.13E+07	NF	1207855896	3.47E+06	8.48E+07
480CI - 3	9.71E+06	2.32E+07	NF	1215828540	6.64E+06	1.08E+08
Control	19622	71695526	0	649442734	12352236	83576114
Control	103916	65989237	0	946871631	7982069	87739549
Control	21864	59519452	0	555456969	4318761	88421766
Control	18273	51270906	0	786069731	3499146	59717151
Control	75001	64356221	0	721805699	7309712	92047333
240WI	91268701	15914816	5307393	1878799460	11945023	4.17E+08
240WI	67732595	12406727	3748479	1402388967	7851626	4.52E+08
240WI	91487640	22222239	5595237	1063748051	3386210	3.33E+08
240WI	85172226	13536996	5582509	1176934307	7666215	3.61E+08

Appendix 1: Mouse LC-MS data

condition	stearoyl carnitine	succinate	succinic acid semialdehyde	succinyl-adenosine	taurine
Control - 1	1.85E+07	410970884.1	4.06E+07	NF	11751224674
Control - 2	8.00E+06	453836246.6	4.59E+07	NF	11654139567
Control - 3	1.33E+07	991867872.8	2.14E+07	NF	11850115686
Control - 4	8.62E+06	654649481	2.52E+07	NF	12786911579
Control - 5	6.68E+06	819340334.5	4.10E+07	NF	12060076506
Control - 6	2.79E+07	808025866.7	2.56E+07	NF	11801600582
6WI - 1	1.84E+07	7035155042	3.08E+06	1.09E+06	12427683909
6WI - 2	3.17E+07	5082346889	NF	1.79E+06	11093423090
6WI - 3	3.87E+07	5346196474	NF	3.28E+05	11889921639
6WI - 4	3.72E+07	6437135668	NF	4.06E+05	11747089979
6WI - 5	2.15E+07	7513795713	NF	1.88E+06	11959361843
12WI - 1	1.68E+07	7193485969	NF	2.81E+06	12041594301
12WI - 2	1.45E+07	6554397401	NF	1.53E+06	11847556637
12WI - 3	6.21E+07	6813385311	NF	1.31E+06	11719461090
12WI - 4	1.18E+07	10158118460	NF	3.20E+06	12673864148
12WI - 5	2.35E+07	9787014635	NF	4.16E+06	12623714372
30WI - 1	1.44E+08	8408268472	NF	6.32E+06	12655088865
30WI - 2	5.87E+07	8504302623	NF	7.25E+06	11890362104
30WI - 3	1.20E+08	7855248346	NF	2.04E+06	13242753228
30WI - 4	6.90E+07	9338957473	NF	8.62E+06	11760153023
30WI - 5	1.44E+08	9117132897	NF	3.49E+06	13476008252
6CI - 1	3.54E+07	1586665848	3.03E+07	1.31E+05	12204258091
6CI - 2	1.64E+07	1119460197	NF	NF	11464915406
6CI - 3	1.68E+07	1668083430	2.05E+07	7.88E+04	12903551121
6CI - 4	9.12E+06	1895801115	1.98E+07	NF	12937547035
6CI - 5	4.47E+07	1299001720	2.93E+07	1.64E+05	11977857609
12CI - 1	2.37E+07	1402616867	2.67E+07	NF	11459780612
12CI - 2	2.13E+07	1553286559	2.86E+07	3.08E+04	11917632535
12CI - 3	1.90E+07	1646323704	1.70E+07	NF	11647263793
12CI - 4	2.07E+07	1705169290	2.07E+07	NF	11754360214
12CI - 5	4.10E+07	2106063995	1.86E+07	3.09E+05	11792761217
30CI - 1	3.83E+07	2656934572	8.71E+06	5.42E+04	11296735280
30CI - 2	1.84E+07	2281210043	1.41E+07	6.19E+04	12726909577
30CI - 3	3.26E+07	1938720377	NF	NF	11911183195
30CI - 4	3.22E+07	3052857864	1.98E+07	NF	12918365545
30CI - 5	5.13E+07	2063943075	NF	8.28E+04	11616919512
240CI - 1	1.50E+08	3840365375	4.11E+06	9.98E+04	10756776560
240CI - 2	1.51E+08	5775581653	NF	8.03E+04	12855923983
240CI - 3	1.64E+08	3711134205	NF	1.75E+05	10488074019
240CI - 4	1.73E+08	3576547147	2.16E+06	1.36E+05	10507462154
240CI - 5	1.63E+08	4891583976	NF	1.32E+05	11383007366
480CI - 1	1.32E+08	4259730053	NF	3.61E+06	10094755731
480CI - 2	2.04E+08	6796970173	NF	1.31E+06	12628748437
480CI - 3	1.54E+08	6070019696	NF	1.26E+06	12389559846
Control	6596751	6.95E+08	92229251	21162	6668389858
Control	2426032	8.12E+08	75690946	0	6676378196
Control	2743035	6.65E+08	111800020	0	7090772563
Control	2981503	7.63E+08	73594407	0	6909448031
Control	5338695	7.08E+08	106711239	0	7052123875
240WI	22472552	8.21E+09	113692829	3975374	7073029469
240WI	16723584	6.79E+09	89440671	2288357	6703981795
240WI	27743185	8.02E+09	144583151	921859	7169503745
240WI	18224081	6.65E+09	118662136	762865	6644555355

Appendix 1: Mouse LC-MS data

condition	threonine	thymine	tryptophan	tyrosine	uracil	uric acid
Control - 1	2213628318	5071165.228	650813215.3	329733982	NF	6339944.8
Control - 2	2393257094	6214353.301	566794966	522786306	NF	3277654.5
Control - 3	2006930993	7783316.033	352378898.6	345723521	NF	1512396.5
Control - 4	2400832469	8935030.073	374945424.1	539388746	185292.847	1083020.5
Control - 5	2191684320	7653387.05	511902849	786676672	NF	1972227.9
Control - 6	1600643231	7242438.109	428478196.9	475813537	NF	3658427.7
6WI - 1	1696506757	10451869.62	547848026.6	1093086987	62083772.9	35247633
6WI - 2	1749298091	5738522.317	458053168.8	390062831	25196377.7	42314820
6WI - 3	1874294774	4890617.377	342982455.3	302506376	46741021.1	27827099
6WI - 4	2266368307	8584063.519	388646651.6	315871652	50138764.7	22516230
6WI - 5	2237192350	7631597.664	443677353.1	380557542	39648137.3	20234475
12WI - 1	2566082085	5808080.199	362543717.9	401565153	61812621.3	15678803
12WI - 2	2654219016	5180849.199	339315644.3	368066501	59503761.8	23178883
12WI - 3	2183661056	9066374.273	337673815.7	385032058	66916799.7	23003526
12WI - 4	2858589924	9727231.836	443807487.2	940237200	88599897.3	12799793
12WI - 5	2509140311	10029118.04	489582739.3	798460838	129600277	33515684
30WI - 1	2722468542	7307243.027	584543965.5	984134842	241799448	55724856
30WI - 2	1787506219	5504224.969	517938167.5	520424723	139930653	4712516.3
30WI - 3	2035966001	10323182.35	447845241	767465947	246876525	24625560
30WI - 4	2602280788	8376584.292	504875848.3	883084272	158244298	3485794.7
30WI - 5	1923188107	13805825.22	550762302.9	1139045542	313710464	21978873
6CI - 1	1819145561	3775192.734	378750345.1	483182656	NF	5764927.2
6CI - 2	1540056044	4486948.117	243374625.6	269100520	NF	1569431
6CI - 3	2553440034	5445671.348	442990104.2	839643369	1053284.97	3058447
6CI - 4	2096198641	6476086.411	351924626.5	782292157	936651.063	1903768
6CI - 5	1663108586	6242422.799	483298521.3	591414913	NF	8023867.5
12CI - 1	1796690117	2877489.722	399028279.7	557452929	NF	3149335.9
12CI - 2	1732493197	7721732.267	406320422.5	517014442	NF	5903857.8
12CI - 3	2453459615	5574050.088	402158732	455504423	NF	1742323
12CI - 4	2150022114	4580578.274	359793847.1	336996563	NF	596142.16
12CI - 5	2268904509	4695756.639	354637244.2	709216780	NF	5926889.8
30CI - 1	1841790054	4792257.628	335713070.5	499209608	353084.018	2136492.3
30CI - 2	1614146486	4696403.809	283930196.4	795632802	424977.445	1985799.4
30CI - 3	1475729233	6284809.041	372459978.9	493503702	NF	2478549.4
30CI - 4	2074124153	4765883.077	440188891.8	1063676241	457429.508	5337272.1
30CI - 5	2199869398	4021461.711	325965856.6	386226313	NF	4489742.8
240CI - 1	1266819068	606314.9574	262485409.4	407178224	NF	732318.41
240CI - 2	1671573087	4010456.053	288095835.9	807790884	NF	442524.91
240CI - 3	1383938014	NF	218770543	293481101	NF	210327.29
240CI - 4	1178601621	NF	207788041.3	242844869	NF	299614.78
240CI - 5	1647560808	1086492.108	266514184.1	482309467	NF	NF
480CI - 1	997911103	162431.8818	189658999.6	510127074	9877296.32	698074.66
480CI - 2	1533700891	4856175.706	373504091.5	908556412	34090684.5	957654.65
480CI - 3	1884758018	2088874.027	247884001.8	478761690	38713382.8	163039.46
Control	1235476691	3426497	149198236	262087112	540422	1713747
Control	1544525221	2978677	262330985	418627085	734782	140860
Control	1281211910	2431144	191401717	318388636	434075	180122
Control	1381764786	2661700	175713484	286502712	0	1465709
Control	1098835498	3176817	193681019	245802022	215937	1283741
240WI	4495181484	4122365	1785478901	2936928880	374445418	4257577
240WI	3446839077	2410344	1526553111	3115596276	380133418	2057382
240WI	2254360561	3536323	444413290	1047615872	293428756	5863161
240WI	2345010121	1696915	606635962	1307346403	315211745	12433954

Appendix 1: Mouse LC-MS data

condition	uridine	valine	xanthine
Control - 1	3069343.265	2208768577	223484.8142
Control - 2	2565130.313	2697964226	200027.6451
Control - 3	2098846.009	1837209331	NF
Control - 4	3223497.793	2357676098	NF
Control - 5	919441.8517	1815754042	349183.9913
Control - 6	2193351.537	3331026862	NF
6WI - 1	1398091.592	2862983018	330511904
6WI - 2	NF	2847742382	346250206.9
6WI - 3	2137532.142	1995222469	330827734.2
6WI - 4	2528084.968	1882731907	320497376.2
6WI - 5	1744044.601	1998770691	276433603.9
12WI - 1	2219313.003	1682429477	630760630
12WI - 2	1423536.504	1887271473	635160338
12WI - 3	2187222.342	1778116732	621582523.4
12WI - 4	2727654.95	2278382806	806477880.1
12WI - 5	5074014.278	2100330276	824440487.1
30WI - 1	3391964.755	2502297440	1622034511
30WI - 2	2523536.087	1833078233	1382669660
30WI - 3	2670241.02	1970523988	1671209727
30WI - 4	541009.4691	2663718734	1124240765
30WI - 5	3972539.382	3631715484	1668334744
6CI - 1	2255679.319	1779321191	605286.7038
6CI - 2	404194.0351	3340555657	1105917.298
6CI - 3	946835.2377	1847517749	327493.3775
6CI - 4	4154192.008	2110893799	202828.4281
6CI - 5	1554188.462	3197219906	1944252.118
12CI - 1	2331331.767	2045556880	1726138.122
12CI - 2	1744161.218	2523935483	778272.7422
12CI - 3	544876.2587	1720643717	1579232.874
12CI - 4	1809291.356	1665789127	372479.4913
12CI - 5	981955.9122	1778996350	1709834.837
30CI - 1	915720.5198	2067594254	926226.0918
30CI - 2	1743786.83	2259441739	6833377.692
30CI - 3	NF	3004613663	9851042.442
30CI - 4	1336844.741	2144050500	16376797.39
30CI - 5	3015148.249	1906397842	15934833.01
240CI - 1	NF	3612150843	27882924.96
240CI - 2	497645.7606	2296374690	16883856.14
240CI - 3	NF	2060173662	16952657.16
240CI - 4	NF	1922641204	9874521.383
240CI - 5	412845.7745	2287681944	16476359.32
480CI - 1	206542.5218	1749918942	28403881.85
480CI - 2	196447.3435	2999934950	22912110.9
480CI - 3	NF	1922758373	18200149.6
Control	0	1750843745	0.00E+00
Control	738132	2156582264	0.00E+00
Control	0	1785438989	0.00E+00
Control	658759	2118360817	0.00E+00
Control	0	1887341410	0.00E+00
240WI	56604906	12406756055	3.93E+09
240WI	63955508	10121225874	3.21E+09
240WI	31535408	5970244752	4.79E+09
240WI	32458618	7269116967	4.07E+09

Appendix 2: Pig LC-MS data

Appendix 2: Pig LC-MS data

		peak area (a.u.)					
		HEPES	succinyl-acetone	fumarate	succinate	3-hydroxy-butyrate	lactate
Heart 1	Control	17024381	0	51978896	853649949	20402397	4222260
	6WI	11031072	0	94777230	2107847153	22985089	11087629
	12WI	7530629	0	99020675	2213128974	22206310	12119207
	30WI	15021385	0	36606086	1238096859	17800731	6189381
	60WI	14746700	0	117401818	8524662632	78989478	29707457
	240WI	18904728	0	88938531	5878564521	54538810	33408326
	6CI	15670751	0	39119989	1022674566	20781822	4657149
	12CI	13341629	0	30816206	959101798	19282361	3246651
	30CI	12943227	0	101823767	5014465295	44283696	22301730
	60 CI	15726817	0	34234860	1285921019	18140657	7599598
	240CI	15500735	0	40825427	906497812	14491491	8696817
	480CI	14862883	0	33028965	1024807137	15218861	10879267
Heart 2	Control	28195319	14949705	61460273	1169318830	43197588	6749835
	6WI	25763237	12544606	150574580	3362413936	37695386	24974264
	12WI	21082135	10315738	147631258	3961265313	43324446	25737152
	30WI	21799613	12395341	163222779	4719613998	56390682	26920209
	60WI	20061743	9892238	189050043	5269662105	53683283	30218835
	240WI	20399389	13284747	90879982	3247150913	60927074	26671329
	6CI	22889294	10541737	49228681	1279206489	26109175	5822367
	12CI	23730417	12836153	40958160	976588123	20377036	5464117
	30CI	22773729	11900224	49786688	1536363885	26635727	11202378
	60 CI	15873261	12174396	48048783	1116775452	18915093	6734127
	240CI	21565238	9442834	68110672	1812311708	26394220	17341682
	480CI	18619856	12769268	28769599	452702744	10022063	6238845
Heart 3	Control	18120936	12688939	54465098	514198600	25931438	2320761
	6WI	2309744	1675939	37105556	992085193	12194373	5575413
	12WI	20777765	12557964	103856235	3401814445	34082571	20886509
	30WI	18631192	9886638	139176769	7985253979	72445403	31993636
	60WI	17979821	14552763	93477444	7991588898	78133820	29090762
	240WI	19890872	9616728	35877890	7077280739	58782538	23135217
	6CI	21418111	10407938	40050223	785403612	19660273	3066171
	12CI	25595507	11185611	57719026	1417193558	29008766	5607263
	30CI	23484705	9189748	47570319	1347652165	19490223	6028942
	60 CI	20774473	13574268	39647408	882293771	13388462	5438846
	240CI	29355460	11340065	71619766	2048096407	23880616	15634768
	480CI	19014582	5974279	30741923	1082444264	23666387	11507294
Heart 4	Control	16897147	7270420	57361409	824124858	24901185	2817590
	6WI	21016048	6424131	170991165	4254252751	36199750	20570496
	12WI	22675729	7784716	209193991	5179605197	32980050	26998184
	30WI	21571864	8438180	218940207	7496668437	57656248	28966012
	60WI	19910818	6902031	194222678	6305731745	51485012	30013347
	240WI	27869323	7041527	53974397	6900673516	50882074	25435531
	6CI	27402128	6645910	61710572	1625068778	26281810	6243941
	12CI	24039779	7845752	38307294	789843003	19343050	3240345
	30CI	16628783	6796844	54178122	1602847532	22656714	6363560
	60 CI	20858262	6645530	63837940	2033539115	22630085	9596526
	240CI	20656793	8680061	67777003	1656331689	16585610	12243442
	480CI	24956054	9366126	57672214	2014698223	22913179	21787355
Heart 5	Control	25587254	6015529	56796842	676047298	29419214	3995704
	6WI	18489884	5942846	138242937	3984239685	31856210	19834735
	12WI	20622569	8718781	216242880	4847811725	43839829	26391511
	30WI	21975775	6927421	174867972	6005062059	64151074	30385682
	60WI	22051213	15811173	167256908	8031018735	89064684	32289555
	240WI	19655465	9670544	154652996	5752662355	60524588	32890011
	6CI	23745240	9996600	48421288	883588527	19583732	5600927
	12CI	22080994	9730034	60484853	1293106355	25863508	8612600
	30CI	22714476	7603654	41421018	1234138874	18828130	6640042
	60 CI	21599434	8553719	43009315	1100778045	16337967	6634020
	240CI	25040598	13653741	52284985	635193690	16829593	6897118
	480CI	23103820	8675143	41338483	1040120274	20369813	12722814

Appendix 2: Pig LC-MS data

		N-acetyl aspartate	aconitate	aKG	pyroglutamic acid	pyruvate	malon
Heart 1	Control	282297632	187724774	65756485	231083172	14373791	6757
	6WI	276862621	241470410	25063093	180879473	15805127	12777
	12WI	157003214	96800718	0	130677415	10603046	14707
	30WI	198000312	126965550	0	318598488	10250258	7717
	60WI	251288519	44362461	0	325356847	27444906	16428
	240WI	249643275	13389607	4646877	898933767	38172946	14296
	6CI	245390900	158078326	17532392	366384500	20907694	4673
	12CI	272750488	126469866	20478698	322282930	14347263	8366
	30CI	202457200	56525365	0	245940221	22391195	17564
	60 CI	280169999	128479761	5360749	324249568	18551778	6770
	240CI	163122655	37035539	0	659645768	22972357	6024
	480CI	142134118	14134932	0	475794900	18538272	6170
Heart 2	Control	980362086	226783044	24798501	199551670	15405786	22068
	6WI	623518983	109428503	3033999	271968125	21737190	25300
	12WI	598162325	37518822	0	240646977	25013598	27348
	30WI	559047817	73649884	0	299028764	31879175	25822
	60WI	551650978	58876569	3324945	314390291	32955340	21952
	240WI	612786248	13877935	0	612922735	27466193	25406
	6CI	593110466	160117692	13077537	406861224	9179441	18358
	12CI	562047061	131659674	7630363	610879227	10649316	6162
	30CI	793950293	157377958	7816219	473259270	20682117	18549
	60 CI	485628340	121143966	0	413687441	10400471	7901
	240CI	585214836	67336150	5178243	468951820	18272952	22343
	480CI	134295370	9718712	0	805645483	17216636	9256
Heart 3	Control	370888139	185718742	83421971	115995352	10787891	14761
	6WI	69868603	48603722	0	29074899	4990790	4224
	12WI	258349026	54627223	0	111644505	35334475	18998
	30WI	516606353	100736593	0	117190118	36296176	24114
	60WI	323494855	60970448	0	157349076	40668919	18240
	240WI	249200494	7232897	0	203109726	25367322	16190
	6CI	381394870	122469341	14663662	268184237	20605114	9581
	12CI	504804053	219555362	28315651	336091656	38373117	12488
	30CI	384006186	159049885	16328363	277907266	24803315	18426
	60 CI	229779542	115794669	6026674	573097484	20259634	11972
	240CI	271846912	102575102	0	790728575	33498346	16744
	480CI	142564998	16395132	0	502671115	24647708	11261
Heart 4	Control	380598054	169760211	35950703	65345701	14858694	11061
	6WI	458232256	327200976	30890712	159048701	17066647	15755
	12WI	393515458	125731638	21492193	267558012	22273212	20904
	30WI	454617125	88987324	7177536	242649503	30525102	18687
	60WI	395574292	39190097	29053307	186565263	36519764	11560
	240WI	279855042	3711143	0	379230967	24121560	18736
	6CI	427010388	203511329	18495036	253004076	10731506	16550
	12CI	300580635	140230706	10230192	433600157	7982387	11555
	30CI	408074073	190509936	9693541	241190750	12803476	8882
	60 CI	388195401	234300686	7187092	485194782	15832636	8039
	240CI	258334015	77081438	4091525	607567879	22078061	11075
	480CI	400075819	21371307	3806902	553234534	27309600	14004
Heart 5	Control	533762555	150869621	55374549	169324680	16976628	22199
	6WI	506464064	283296763	20285149	121309384	19339149	24230
	12WI	561708043	102964241	9771562	156897510	30195623	27852
	30WI	516170766	73817321	6475444	144762381	32651404	29186
	60WI	539088427	48101350	9184060	188965891	34197478	30861
	240WI	463292223	18423811	0	494688823	43415582	29307
	6CI	396328336	105842424	10956675	284326703	13506812	12334
	12CI	504164259	158758829	14048336	363116424	29576531	12095
	30CI	447724915	139289082	10351749	516302061	18908429	4709
	60 CI	317713096	118366984	0	574317312	16155958	14032
	240CI	118899312	49122067	0	709242224	20095265	16065
	480CI	207475192	27728208	0	720667428	23141737	11557

Appendix 2: Pig LC-MS data

		uracil	malate	2-HG	xanthine	nicotinamide	hypoxant
Heart 1	Control	0	616993692	747384061	9121054	192792358	494375
	6WI	4881205	1011330502	491164019	10184457	812838455	1139781
	12WI	6330613	1050608592	490330348	3992677	980217350	1422670
	30WI	0	488006273	495452387	7561755	618886611	7429013
	60WI	97907040	1350171588	736235593	28964091	2916170471	8807578
	240WI	245211731	1684390636	657347358	52823188	7933008485	2034962
	6CI	0	473758340	556912262	11590449	302764341	493563
	12CI	0	356002584	536098428	12185933	303607962	421964
	30CI	30635393	1066604745	582293321	5182856	1667246544	461458
	60 CI	0	452901459	510646191	11281927	913030351	820987
	240CI	0	673137697	336826152	4434460	807648056	130022
	480CI	2836395	358878374	361762138	5882576	984353474	239648
Heart 2	Control	5115575	672758502	353967562	11863483	444626839	668184
	6WI	20066114	0	284508958	8333894	4791215277	267178
	12WI	44711879	1654192615	263291062	6729388	6196782338	581287
	30WI	64567675	2108111585	359706813	13922287	3434869172	858517
	60WI	95874719	2429662826	353610933	5285041	5619743664	1170888
	240WI	216681384	1403370336	262721667	9368047	9550531055	2180833
	6CI	1816081	401798420	257807271	4828523	400974578	480651
	12CI	2354365	299515814	221857265	2800887	767062966	534009
	30CI	4888035	480329221	222426408	7212443	1748763289	995253
	60 CI	0	329369114	193023488	1487521	782507425	640434
	240CI	5226127	813750158	243088454	9103399	852475763	136612
	480CI	0	175655877	76039830	0	399362806	110265
Heart 3	Control	0	527561798	739305296	13009765	132738685	655078
	6WI	571283	278248965	135811497	419552	537532531	529293
	12WI	15865838	1277882699	467218566	7460204	2157193135	341282
	30WI	51525586	1974255109	711350773	23577669	2938843132	709811
	60WI	76040913	1173418356	644030022	16976441	2632351356	890511
	240WI	80721955	214760010	564493078	7673118	3223691020	1195816
	6CI	0	306253292	653666311	13043781	367185223	967562
	12CI	0	560255548	915197916	11246865	802212548	143179
	30CI	0	557385821	900454859	18150699	800727052	132844
	60 CI	0	371963240	393318171	9193361	872859025	228146
	240CI	890704	960912653	672207249	11830614	1895544158	420056
	480CI	0	201423555	347623175	5719666	969330413	370830
Heart 4	Control	0	595844961	669280413	5143042	153738279	591868
	6WI	8971232	2061919949	803545271	8144362	2211627640	250916
	12WI	23968440	2381161387	761986216	5009791	3259194750	453636
	30WI	63991504	2830774998	738450640	8051452	2785574254	866152
	60WI	67680425	2488070279	719210579	4030662	4065486091	976887
	240WI	110179987	587526998	749689060	5258248	5205398594	136582
	6CI	0	607495669	834807275	7004218	343158888	739856
	12CI	162004	342990032	495666427	1481410	334456840	515149
	30CI	0	538868978	745004863	3208455	550747512	851075
	60 CI	537308	749048218	581506909	4526232	990187648	992146
	240CI	0	996822918	525024419	405381	896547887	161064
	480CI	3184870	617399220	466463533	3791965	1209870212	3119616
Heart 5	Control	0	532034596	801483784	4613394	344747898	680808
	6WI	8898085	1694461392	728215354	3661858	1802645129	2385258
	12WI	33387804	2878088169	638749665	7790044	4078118970	519064
	30WI	58351776	2116685347	750307590	6607334	3606720893	762355
	60WI	98498216	2148661730	714008363	5273299	4649438078	121907
	240WI	202791040	2501850149	800333680	4977356	7450117718	203891
	6CI	0	456290463	539447398	4256868	587069181	796577
	12CI	0	688456605	739974526	6110772	1127871220	117762
	30CI	0	374887940	503644311	5224988	914945312	1254381
	60 CI	593333	435327257	367366558	4633528	1067641493	166912
	240CI	827079	508269282	198285992	4672321	776153585	265849
	480CI	0	450320377	308835480	2877383	1018604722	342316

Appendix 2: Pig LC-MS data

		orotate	succinyl-adenosine	urea	allopurinol / inosine	ascorbic acid	uridi
Heart 1	Control	0	0	2834632873	100802485	134947491	5054
	6WI	0	0	2313438921	814385239	336479169	4345
	12WI	0	948115	1671834405	1499407193	272087616	2535
	30WI	0	0	1529756897	671092692	61351729	3675
	60WI	0	9874384	2610845772	5468394944	509112115	7269
	240WI	0	11931066	2609651505	6729528770	357604939	12293
	6CI	0	0	2236037980	229429209	232543032	3409
	12CI	0	0	1766278604	375644656	475972540	4147
	30CI	0	2170161	2055401491	3859607603	318269058	5178
	60 CI	0	0	1859880102	894644713	213198987	4833
	240CI	0	0	417381661	2253154072	520985	1667
	480CI	0	535885	376925162	4230625408	51413724	5110
Heart 2	Control	1012726	0	5516672280	119820208	151892	27073
	6WI	0	1202060	3909874057	2625603193	0	20324
	12WI	0	2778763	3351036846	5357627949	3338630	17771
	30WI	0	2352808	4065611042	4798569305	326977508	21656
	60WI	0	8751213	3257497054	6524088223	48856036	19112
	240WI	0	2745647	2748974303	5161041897	186723479	19524
	6CI	671422	0	3196933564	231163865	25441266	14678
	12CI	264663	0	2794837042	602235816	2770039	12603
	30CI	529799	0	2967868056	1359993493	17454683	15754
	60 CI	88414	0	1164603555	1216708798	170856411	7202
	240CI	378525	265255	2266215886	1822833348	33081565	11116
	480CI	0	0	262470940	2273048854	4563363	9130
Heart 3	Control	0	0	4195881191	80028099	0	11844
	6WI	0	0	792463052	476930985	19526899	9137
	12WI	0	1463406	2165614944	2776895500	9010850	7143
	30WI	0	10107307	3633757359	5450303593	449338895	12630
	60WI	0	6246009	2573740691	5304990805	274534014	9467
	240WI	0	2272471	1424942652	4135512281	30447349	5359
	6CI	352148	0	3744553405	293202077	130478404	11918
	12CI	994621	0	4038553755	482828554	305512815	12159
	30CI	740780	0	3483870937	914816321	262458483	12021
	60 CI	3897792	0	576260553	2014499276	106070265	2823
	240CI	4302190	0	834732801	4602464016	0	5712
	480CI	5103966	0	237264056	4648248586	2183382	1507
Heart 4	Control	0	0	2356512528	86498218	0	9268
	6WI	0	1749040	2618621475	1948098482	259399906	10396
	12WI	0	6837240	2337380200	3915444022	143724927	10074
	30WI	0	9182741	2297568227	5669124541	356453914	10260
	60WI	0	9913782	1668159949	5724950813	501896405	7498
	240WI	0	5222045	1163657013	5606034227	71416258	6665
	6CI	0	0	2454479686	306019034	255580493	10168
	12CI	0	0	1245356952	342008871	4817510	6203
	30CI	0	0	1767941722	643862187	152822178	7800
	60 CI	0	0	1551663431	1106191292	338077884	6280
	240CI	0	0	776750102	2290495520	758377	3589
	480CI	0	841744	887717629	4755132110	166146116	4659
Heart 5	Control	129581	0	4943616650	164961199	3625947	12024
	6WI	0	779529	3948485210	1807648886	480784007	11057
	12WI	0	6798628	4034809827	4065819860	399435156	9555
	30WI	0	9173410	3697199155	5859857857	675917556	9977
	60WI	0	11247104	3384033042	6773199782	355737311	9693
	240WI	126142	14646429	3201121974	6138419989	605777551	12528
	6CI	183794	0	3113003378	517075561	157935629	7677
	12CI	200612	0	3425056438	894698866	249321151	8936
	30CI	279533	0	2803140904	1093278089	21939575	7277
	60 CI	468090	0	1309069345	1892662707	11527000	4607
	240CI	1725184	0	376379563	4334097622	0	6157
	480CI	2609530	0	283252300	5285090873	2829636	9755

Appendix 2: Pig LC-MS data

		uric acid	guanosine	tryptophan	adenosine	methionine	allantoi
Heart 1	Control	5236944	13498055	111897387	531572546	336226032	2203011
	6WI	4977515	43325280	94878657	2305364574	352540050	1892203
	12WI	2571769	74477037	72772871	3001303656	242631177	1180319
	30WI	2592041	19860075	81906700	6560674913	282782381	1391316
	60WI	6738503	278474284	163265674	1699289325	353782949	1846201
	240WI	8631321	622740537	262705597	210095470	410575013	2320726
	6CI	2302940	10826672	73917312	9517662204	349023134	1259357
	12CI	3629967	7249578	74866259	7411652360	295993987	1147185
	30CI	3896362	186159949	111731414	1484992544	248373361	1738661
	60 CI	5640453	13924886	84848055	5965311240	348832449	1383977
	240CI	1255492	15695406	54768381	16898926196	172396385	159413
	480CI	2874518	36905241	56392688	7792427133	201076939	564246
Heart 2	Control	5529480	27051542	253694281	644355958	672792859	3122354
	6WI	5888509	177428815	185746739	7335829986	453738577	2138917
	12WI	5606804	307940248	179021632	6072746479	400483594	1959419
	30WI	10669299	359868560	249228225	2222163492	393237643	2615526
	60WI	3369658	387572886	219535074	748813474	372072092	1753370
	240WI	3670845	685980983	306925757	156974917	466630771	1660934
	6CI	3203483	15910430	139342239	8857999564	383843548	1364444
	12CI	1900131	12406679	114165461	16178535527	335316924	1220564
	30CI	3729324	23619062	149677257	9557732341	377153131	1532077
	60 CI	784817	8785032	101283771	10515376558	378380605	557687
	240CI	2773983	22746947	132911863	8427403441	447623315	1232746
	480CI	0	7540111	28686433	23188371892	92467567	0
Heart 3	Control	1914714	12908996	144026971	156523671	196492977	4735197
	6WI	244168	20538528	23724815	1865332169	65750975	631286
	12WI	761676	154550552	98359818	4733544615	135776142	2774997
	30WI	3731251	307026963	146127724	3274202473	162619968	3302704
	60WI	1299029	288517151	144146633	1363805426	149199098	2665897
	240WI	436975	320956063	168308743	388202742	270537718	1916949
	6CI	1677118	15543188	119092094	5811485813	224085438	3720602
	12CI	1550499	18965343	132730601	8459249783	257804239	3635278
	30CI	2114129	15354535	125707176	5729495566	222260711	3654935
	60 CI	218723	6184435	64352148	15777824392	117548467	915105
	240CI	1276085	18766955	105351312	16008772147	192541574	1506579
	480CI	629538	23695942	54677770	13307673388	91128254	525454
Heart 4	Control	1385878	14791727	136084959	397367116	260200565	3181339
	6WI	1520077	116954133	129048532	6568944001	359794408	3123925
	12WI	522901	225146349	134554281	7807915862	291788286	3401084
	30WI	1097104	289737988	154204250	1996128277	297854084	3383917
	60WI	641785	300488771	157075240	651732872	302108673	2260207
	240WI	712753	411368486	210331232	371895127	347949652	1998881
	6CI	1031891	19458244	112123191	4456224302	335667323	3323817
	12CI	144291	11459601	68321976	12677922980	253757441	1392160
	30CI	446112	16591012	91243155	6060905589	349007301	2057406
	60 CI	875045	18107483	96408238	12210464841	349899322	2007045
	240CI	0	15711902	70222371	13813322180	228251787	1169716
	480CI	619144	47739482	102565166	7461965292	301416023	1742611
Heart 5	Control	750966	19102148	236520251	1119328120	328693182	3786188
	6WI	228014	128015611	174626311	6231933724	363126832	2062914
	12WI	812500	272800664	186405775	6567816853	309293345	2575791
	30WI	476952	327992930	204687568	2495082895	327047768	2410484
	60WI	489778	463030093	246216538	763184248	326526937	2561327
	240WI	264779	614112551	326135412	624300714	420223025	2146128
	6CI	268807	24311113	136463731	7169402045	202221025	2143729
	12CI	617277	29837770	165696788	9813413160	262673742	2169833
	30CI	289020	12387958	144451287	11133437386	289726057	1958268
	60 CI	0	9491142	100473288	15975755499	210284834	879972
	240CI	0	10530276	43255397	20530386118	111201907	526969
	480CI	0	18515835	80344053	12564101341	158080726	247193

Appendix 2: Pig LC-MS data

		glucose	leucine and isoleucine	propionyl carnitine	GABA	guanine	homocyst
Heart 1	Control	2291881741	3366808653	99310594	117830186	13684056	378341
	6WI	1872730805	3201781846	148419521	96696946	14988199	323169
	12WI	1506767676	2050098556	160811330	52668211	11662575	212543
	30WI	1417105917	2480330871	72844715	39594368	8901963	251926
	60WI	524698928	5297013765	818568773	48918479	45622259	370114
	240WI	1252167179	7326634165	176160416	33001096	185319066	278639
	6CI	1306657636	2724309004	79247662	39947306	7490317	313263
	12CI	1142241320	2391431085	54046306	38767590	6686790	254581
	30CI	1093020844	3243355622	432890839	52617058	32186769	266748
	60 CI	668982847	2872977289	62200010	52161812	9223422	249572
	240CI	458685715	1488866638	64025515	8741707	1622763	870564
	480CI	887292281	1433762453	41886590	10527616	3950242	902975
Heart 2	Control	3712148960	7923287912	231303962	214406833	36536030	499833
	6WI	3197295977	6290311210	537423326	144709782	30890527	287877
	12WI	3871473665	5826747586	481459589	113335824	44781181	181769
	30WI	3745144695	7178002699	522481465	101860900	65392440	218113
	60WI	1153238249	6875939714	951673099	75039658	73030675	197088
	240WI	1215515168	8351710247	211045234	48904814	318156169	257374
	6CI	2127267840	4658573803	141422806	63916746	13619329	279855
	12CI	1383164969	4295563290	114280472	38625800	7171541	236649
	30CI	2382480005	4768883159	186246741	53195801	13880183	316749
	60 CI	410254646	3121794635	104326222	42407691	6105317	137816
	240CI	936266350	4538184034	165303190	45303117	13299417	185136
	480CI	223377305	865753154	57322463	3152704	0	223437
Heart 3	Control	3552588377	4504249244	62679809	180923207	14721043	432728
	6WI	700472612	937716338	79090091	39788832	4202368	725731
	12WI	1930219891	3204008100	352607394	67813800	25571390	979922
	30WI	1330928744	5248977429	1062397280	94239697	44791540	292378
	60WI	509177799	4731186668	1060298322	63198471	48848944	162044
	240WI	2540235462	4741141145	79093461	43222453	88960839	102689
	6CI	1964965951	4313057508	59321158	88817681	12807529	353579
	12CI	1852294289	4761498531	107007354	82902396	12585005	486507
	30CI	1467636180	4350933045	74140661	75356124	14497486	377267
	60 CI	127382530	1754778227	56673241	17133598	1269293	121669
	240CI	443256132	2741200016	80310200	16681820	3763797	174239
	480CI	611863569	1402176090	38442648	5948600	1631361	692868
Heart 4	Control	3636676842	3743879825	77416246	155223435	13183809	390906
	6WI	2584245331	4513581553	355835979	132582106	20874514	430464
	12WI	2408033415	4772583207	445821462	110964744	32705616	354936
	30WI	1190591445	5245229812	775609096	85424983	43422181	313879
	60WI	2192728110	4423483489	616021204	60938357	45933782	236632
	240WI	2690906194	5816193244	89430974	50088791	92137087	139085
	6CI	2118490505	3943486421	97884961	110533442	13501141	398588
	12CI	891698631	2216008950	60964443	38582060	4869853	215901
	30CI	1490246313	3096968944	79914602	72123097	9287647	309965
	60 CI	633060383	3347484713	103773885	43199980	6351104	321591
	240CI	372432824	2060708752	72195112	18287538	4792324	177373
	480CI	1194329883	2795091726	54633932	22967199	7287725	259798
Heart 5	Control	3711645125	5342609852	124215465	180443655	15997288	389605
	6WI	1914666975	4936072224	403262342	158275839	24262067	473442
	12WI	2358492410	5257575572	565669448	127625933	34049194	437537
	30WI	1064682800	5633808845	760749252	117561804	42693245	417014
	60WI	1253751964	6917779889	787596089	112861657	84254731	289201
	240WI	1270768935	8187266705	209313927	62887519	199916042	329387
	6CI	2283085082	3318337468	107125084	62654678	9566764	354400
	12CI	2998196459	4056751386	155429705	60444836	11897831	417243
	30CI	743245686	3818225241	76087957	44596465	7079923	372310
	60 CI	228771049	2190993266	54187283	18859682	3625776	188862
	240CI	324094776	1054011745	49707625	4540787	373337	627749
	480CI	369880387	1584299514	79329693	14837921	0	100918

Appendix 2: Pig LC-MS data

		GSH	acetylcarnitine	tyrosine	AMP	GMP	palmitoyl carnitin
Heart 1	Control	4142746120	3530212134	231282644	188710826	349993	26761556
	6WI	3484776325	5262614553	210216797	314240323	2998285	35693179
	12WI	2114665336	4018282681	153688933	177385291	1900379	13985404
	30WI	2540843866	4490153082	146330551	302536443	3137786	42422162
	60WI	4383887144	5449474158	381727359	761693381	12392115	46636896
	240WI	3311453854	4011841165	521401195	506845144	8358656	50091407
	6CI	2710861949	4598133941	134238115	65105767	0	33637246
	12CI	2565100032	4076887692	132469613	175552605	0	60769582
	30CI	3033246720	4657668548	257442062	287836740	7110375	22901339
	60 CI	3050211127	4769767298	168138665	492280019	2617187	67658817
	240CI	1648256006	2988165413	60630428	252587555	0	28820386
	480CI	1607723970	2683300781	69424163	670227909	3310246	15121636
Heart 2	Control	7965388293	8224879144	670282084	520171279	1118830	79162548
	6WI	5621873026	7658088815	527846826	982035273	10981690	37575736
	12WI	4508304735	5297152397	464326231	870259778	20218476	36243534
	30WI	4276575751	5020755368	520979664	298399707	3221367	39524068
	60WI	4275071346	4698596339	552186859	740701371	14477447	41900027
	240WI	1772477154	3566602121	488860416	210520667	6671397	45274758
	6CI	4094834094	7173214165	320457086	191884028	882470	78290875
	12CI	2912007551	5331047434	225453265	197893629	421926	65131973
	30CI	3739375067	7463356694	320978282	624430097	3671221	52323180
	60 CI	2504221369	5569457915	151229339	289790677	1210833	22295660
	240CI	3568889515	7765642662	274675695	450193007	582788	15041367
	480CI	881607841	1418071652	41568503	210935901	0	5554801
Heart 3	Control	4875784946	3092620287	277048278	64065876	0	19381780
	6WI	977694124	2091693715	53296414	174940854	1169084	881827
	12WI	2774648897	3178965113	116489562	821047648	9649438	11685661
	30WI	4976360724	6397007419	313532273	749921082	9148314	17747290
	60WI	4153572500	3615717401	293671235	792280698	10518746	31314938
	240WI	2647084330	1894896797	204163118	657167979	8570248	25779854
	6CI	4480619161	3885808415	215495582	130263165	0	12472414
	12CI	4692658126	5467630398	221675383	157651350	0	28749584
	30CI	4821700322	5055647706	223148836	298979270	1233570	45677034
	60 CI	2020807608	3504355217	59494032	317988620	0	5496863
	240CI	3204904102	5873071205	109307542	531810995	409112	19926722
	480CI	1891001439	2675918155	56960968	461758495	866457	9121114
Heart 4	Control	4745695430	4537987073	270188605	66031869	0	124994623
	6WI	5979018945	9061764223	336184014	591207138	4797372	109708193
	12WI	5076064854	7545376052	329509169	530437726	8700881	96027858
	30WI	5249354634	6624746819	370573683	433564696	5114745	52154890
	60WI	3847594996	5429076705	292858116	846100860	14717276	52224084
	240WI	3357698689	2801989737	307579442	674446663	11717058	44759328
	6CI	5353836579	6595652938	261452920	114988815	421673	214247153
	12CI	2879056333	5022161902	110023596	82575263	0	90479066
	30CI	3867707039	6366186175	187053071	217435187	938839	175056661
	60 CI	3809293488	7200085241	160441065	278713896	0	198262090
	240CI	2704386630	5375235597	106143874	256665897	305238	110705847
	480CI	3456164736	6222907359	149401328	711561255	2608607	83874043
Heart 5	Control	4741431731	3288287104	361345088	294827276	352989	10791416
	6WI	4725969588	7782920381	337423020	493868577	6738357	7882509
	12WI	4659645145	6886131465	401643186	704797763	14019668	6901235
	30WI	4366451597	6567237211	397071406	493302820	9529399	10950347
	60WI	4150847441	4302128033	462557620	777997069	18259502	22729399
	240WI	3191344939	3868995510	564629448	462599045	6504062	28575581
	6CI	3069759146	3626452491	216231788	260425334	782472	1394082
	12CI	3193516287	4903053064	239216146	339504312	1115130	1874759
	30CI	3662387150	5737351911	208419922	390891067	1551562	10493406
	60 CI	2702136644	4490895570	117819985	353590905	1089935	2397600
	240CI	1756982183	2184629437	46858851	467678039	0	3346370
	480CI	2101999223	2928522838	69032842	525844464	0	4768456

Appendix 2: Pig LC-MS data

		proline	taurine	2-succinyl cysteine	cysteine	alanine and sarcosine	glutan
Heart 1	Control	2112435387	4529228859	472703	9920507	1797572315	138405
	6WI	2255794954	3017373708	0	13604669	2499253051	108880
	12WI	1282060963	3508220232	307952	4446306	2290551525	561415
	30WI	1519455487	2195797077	0	23487584	1601483578	820665
	60WI	2722232517	3747555584	304949	87152753	6634048135	586807
	240WI	3402056507	3283399065	0	474618097	7533140183	434788
	6CI	2010365096	1425984483	0	29757420	1624588123	985184
	12CI	1576119054	1587445147	0	11484446	1439143562	879267
	30CI	1900892835	3539566886	0	36658711	4006086199	583724
	60 CI	1800886582	2035556157	0	40693740	1760842505	103220
	240CI	750806149	262417462	0	19460532	1057561767	382357
	480CI	755717280	358786571	0	30240629	1130766122	368578
Heart 2	Control	4662108391	5909638734	2032394	58007696	2077853229	315554
	6WI	3608358757	4769883082	2387963	54724858	3446641486	215402
	12WI	3307059175	4072142699	2783227	54414097	3581277692	167676
	30WI	3520141067	5471820222	1130194	171811823	4359054097	156500
	60WI	3495452633	4529345248	1402728	179139410	5586299794	105456
	240WI	3635169184	3446416381	1010954	1067664700	5722957201	706311
	6CI	2679690646	2942275290	735746	29249383	1782184407	175835
	12CI	2201099733	1233121981	371295	19765218	1509567069	146579
	30CI	2607670393	1936383993	0	37601527	2050493796	163937
	60 CI	1442528278	1119900396	347835	24174188	1294390261	109998
	240CI	2213179719	2841615497	1694963	11958416	2307821206	152247
	480CI	572994816	130311182	0	5363619	642703815	236085
Heart 3	Control	3198779835	6887239923	494799	4239649	2350251149	228588
	6WI	821528120	2175132774	0	2722249	1113903659	405810
	12WI	2525407484	3583419028	489347	19625018	3562103099	983398
	30WI	3403605146	5288717687	781217	199296124	6822683819	129052
	60WI	3208499108	4425365682	0	91597027	6852153870	850381
	240WI	2622172424	3831680797	0	295082687	5890118152	524189
	6CI	3234151359	4779129395	1379268	1714090	2428805459	197516
	12CI	3535138267	3079397611	245916	50009901	3023420634	202147
	30CI	3279935256	4355618022	0	18887169	2949531888	186146
	60 CI	993800041	449158572	311086	38334688	1218471053	667925
	240CI	1582735591	674517074	0	52815483	2723466252	912241
	480CI	786525452	433898128	0	51325371	1421675980	438513
Heart 4	Control	1913328371	6284042377	0	4073713	2020101688	184339
	6WI	2818246695	4751704273	0	42422028	4614278335	187836
	12WI	2719637370	5101737773	0	6611795	5317479267	167260
	30WI	2772599097	4689004556	677684	113418828	7172864757	122210
	60WI	2317240388	3478770886	0	253915404	5938269753	850797
	240WI	2427399002	3392402604	0	166395252	6551417980	688913
	6CI	2466953680	4578729502	582199	7954022	2786978546	202181
	12CI	1505224614	1226077063	0	4186901	1386054488	111717
	30CI	1836019890	2925454749	0	29664814	2321083126	150551
	60 CI	1880049786	1694778359	445534	31396795	2650757754	137304
	240CI	1153005629	1080943751	0	10736002	2101843351	775418
	480CI	1517321013	1385694877	0	30969303	2661262899	103604
Heart 5	Control	2997378224	6338055203	676504	11134932	2614202952	255231
	6WI	2964547727	5258210985	0	45012385	4482745790	222900
	12WI	3052717641	5268567745	393314	118288351	5388491261	186409
	30WI	2921887311	5091404689	606701	107633793	5927415648	168821
	60WI	3084493387	5262276269	391408	238232976	7476665565	149185
	240WI	3339782809	5348673821	0	470022889	7793963180	862580
	6CI	1991680702	3517953290	0	19748359	2089425116	150384
	12CI	2093997588	2999265530	0	86179275	2534268021	161855
	30CI	2191948350	2317262754	352062	17982660	2215793175	168763
	60 CI	1244774805	1253193585	0	20270310	1548112271	978870
	240CI	620722949	195661502	0	12788229	958642417	463480
	480CI	799045440	348775796	0	90835832	1585950494	622239

Appendix 2: Pig LC-MS data

		glutamine	phenylalanine	aspartate	threonine	acetylcholine	butyryl carnitine
Heart 1	Control	39902486863	671200814	171346639	325789792	2960442893	44431739
	6WI	31257433426	595049328	206652353	365912581	2525152795	374272742
	12WI	27038065396	434667646	198467633	240336252	2021424070	380683590
	30WI	27299208734	490688269	158461874	244941072	2170995253	148206966
	60WI	40205657509	1233860409	263744816	504802132	2969289049	1447376072
	240WI	38123119247	1939491291	885678331	584984462	2995951524	1093977734
	6CI	31945626510	545363367	177572347	255159183	2694836283	68721352
	12CI	27351216899	477709858	198351583	231752101	2285427418	101123719
	30CI	34198748449	696216075	207153532	338892471	2563900343	894176963
	60 CI	30584716639	584587229	199248975	301541731	2397559291	151735143
	240CI	13609529217	251053620	230032874	115752506	1100399897	246455022
	480CI	14670027332	247725510	245355485	117245898	1156988659	377941390
Heart 2	Control	42098941953	2246140349	217795474	1147493261	5297027155	404200834
	6WI	34572134846	1749059432	486524081	896724062	4173660671	813847663
	12WI	32085198068	1613171229	549273772	842049001	3728043714	973170583
	30WI	29254529287	2008056615	674005458	809432933	4081955371	1230144921
	60WI	30735993994	1936026077	1567113633	892433251	3649920063	1016496945
	240WI	24209240202	2267391212	2294980320	865983172	3056783897	1082168866
	6CI	29760809103	1265356268	246058207	668474171	3657361737	290904485
	12CI	25077839476	1110345885	188338849	539486529	3342807941	112528988
	30CI	28135878024	1345241090	266818431	667010759	3570360943	250676467
	60 CI	19144335510	721352830	192892096	395284610	2473101575	134613466
	240CI	24070640363	1113532745	394069237	585198771	3206131542	480199522
	480CI	5391974197	173671684	203817000	101531039	673783532	220831539
Heart 3	Control	25654550943	873503517	401464353	471515390	3760215346	25158778
	6WI	6495108833	153401504	103863260	127514798	1066228811	126046075
	12WI	15875797275	664416326	386058560	343726850	2404841877	693127889
	30WI	24597279493	1041765305	301424198	482953642	3948358725	1563959221
	60WI	20286696608	1049960624	452421050	467441068	3279113861	1339258822
	240WI	15801880181	1160358809	101924509	423167471	2770189467	548070712
	6CI	24721185603	796944233	354976853	473219539	3922015045	24062816
	12CI	26659361190	910057062	350476145	484652417	4408406534	46399999
	30CI	23301363877	848938593	387758077	474194610	3843121121	76193557
	60 CI	8975861727	288420209	179203731	145399302	1530715462	60598094
	240CI	13338078115	508024794	264333333	232968390	2260030283	635164452
	480CI	6782946912	240723844	137533988	113695183	995982071	578560333
Heart 4	Control	31469074746	824926413	406340934	381369851	3814135856	115338269
	6WI	33668929113	1075610508	173966373	480250443	3974980592	1145480035
	12WI	32720280380	1084642878	225620899	464672374	3734594425	1337862192
	30WI	29285012153	1210677901	415294795	474157008	3798934362	1531636211
	60WI	24230063158	1022405617	423158037	410167737	3551419443	1275000268
	240WI	22684457239	1604761101	249002608	470363966	2750478346	816017949
	6CI	31791986516	872474721	315327079	414547460	3976476933	313194543
	12CI	21480003395	506543517	266515332	231720728	2812260471	127434453
	30CI	26575403402	689585227	274376181	322915001	3542328916	392672215
	60 CI	26095961002	712635720	308102063	295825979	3426727576	372767301
	240CI	16708997423	439830541	291279455	165977362	2211980595	495631641
	480CI	19102335626	615261766	353198116	220535881	2544771453	1001288871
Heart 5	Control	30031595801	1345744839	364766768	839543420	4505310145	31443560
	6WI	27977011880	1158175712	275446680	807484944	4379317809	621960732
	12WI	27112836821	1342332330	546839360	847715251	4114833693	847422874
	30WI	26104771857	1391093364	533589103	816432147	4032537347	1092979107
	60WI	24627944597	1591736642	487593722	843295158	4055371256	1003593502
	240WI	22876780832	2186611340	1260059104	846472133	3563410031	792740160
	6CI	18940082519	797030259	382715307	512814425	3317313262	26420977
	12CI	20998322328	961885186	379966844	569550230	4068579300	48208673
	30CI	21041948236	866312458	257158176	532244041	3366574970	80429717
	60 CI	14328079681	532104583	176884423	284359959	2164278124	69685593
	240CI	6255748083	176211927	139765325	131102337	895421097	218272624
	480CI	9049754876	300246383	240569416	188475914	1437928118	880437840

Appendix 2: Pig LC-MS data

		dihydrothymine	glyceryl phosphorylcholine	CMP	asparagine	serine
Heart 1	Control	117682557	907919697	529970	76653036	375123446
	6WI	105473594	837579250	0	96007984	490817668
	12WI	96345467	435586320	391880	50442606	267982139
	30WI	60352677	625316037	0	41160321	267426032
	60WI	127582782	990189565	1076424	109647637	581223470
	240WI	119126095	1197853956	1077494	127980889	718771103
	6CI	60497308	761742996	0	58853248	408311502
	12CI	55738068	733115053	0	43551289	295041042
	30CI	114902388	642417178	717675	71673452	343413357
	60 CI	62108906	822214379	0	55478700	366440641
	240CI	20234052	434577959	337906	18677705	148483516
	480CI	23168650	430264433	0	17992640	147924771
Heart 2	Control	99372880	3869845902	622811	266169735	732299001
	6WI	91760711	2862101235	236506	223170899	637817031
	12WI	91067607	2858701203	411268	206067488	589607965
	30WI	82282660	2431342160	697343	174812568	582812975
	60WI	90819955	2802202790	284631	207381774	663045223
	240WI	71783132	2307956369	658343	201789162	740357377
	6CI	51501568	2768373186	897502	118414374	475757315
	12CI	35712545	2167002565	0	85218269	358608226
	30CI	47128467	2620633241	1349645	107165006	414209772
	60 CI	35069538	2093507467	0	78811632	272747342
	240CI	35468258	2550239959	254997	85099503	377034175
	480CI	5033749	705709258	0	16489205	85048897
Heart 3	Control	74372120	1201132426	0	76111811	498309423
	6WI	28432243	298813021	0	24421365	128629680
	12WI	52002568	920577995	4940054	63161197	405782219
	30WI	77188451	1328879478	1510050	79489328	475861625
	60WI	67803226	1190085000	1436861	79762500	510537643
	240WI	60147015	1252482469	1693044	81254481	512606538
	6CI	44655544	1546747333	272662	52340183	445772825
	12CI	47464497	1483805876	0	57468448	464770597
	30CI	42352059	1224537900	646846	49495384	412250413
	60 CI	12295771	702551253	190277	13560991	137007633
	240CI	13642985	874105922	1079528	16868271	223889133
	480CI	6382531	471069956	346972	6344248	96317469
Heart 4	Control	93038826	876690949	610844	94971642	323090106
	6WI	89560350	1571654356	0	102152676	424507830
	12WI	91403919	1350591498	576564	92067787	401646161
	30WI	85199572	1553306936	722683	91110755	431914198
	60WI	75351209	1148278866	0	89646647	369814788
	240WI	76121926	1356800387	1541029	96371318	471553537
	6CI	69014934	1398778216	514825	71649041	350098327
	12CI	36401369	913955562	0	39320106	230606836
	30CI	56402433	1226468977	0	60631476	294325926
	60 CI	42043325	1220902117	600436	45970241	269725251
	240CI	24341282	735114305	542420	22520307	157459601
	480CI	24399550	1059917097	1183219	27787683	201404572
Heart 5	Control	78340572	1527059645	302366	123163849	524573374
	6WI	72973898	1200504657	257987	128469518	562059491
	12WI	72749174	1283590092	746208	131170808	584964055
	30WI	73574369	1197292876	536631	127735319	583189885
	60WI	75567851	1144252316	1496576	148394879	634012251
	240WI	74969490	1142646239	408963	136395675	627859297
	6CI	36794282	929240554	0	52980031	289544768
	12CI	41902147	1112952357	407785	62547079	316154538
	30CI	27703454	1085502151	0	50026984	370945288
	60 CI	17525232	564688893	396786	25347626	202380536
	240CI	4516040	347416437	462476	9489013	104282352
	480CI	11389009	605368844	1802895	22283524	158815482

Appendix 2: Pig LC-MS data

		sarcosine	adenine	glycine	GSSG	carnitine	citrulline
Heart 1	Control	38650421	1.42E+07	1171805047	749520	6828471704	426250164
	6WI	38994617	1.76E+07	640795274	1262438	4519266680	527516135
	12WI	27547921	2.16E+07	450744871	3550648	3500044317	206080374
	30WI	30555657	1.58E+07	432887375	6674293	5313964230	321099071
	60WI	78956532	4.32E+07	817639247	2013171	5506387283	545145022
	240WI	88470532	1.76E+07	1149672168	670188	7014075371	704707249
	6CI	31876861	5.99E+06	512810304	18382449	7408991059	490279456
	12CI	29859271	1.33E+07	451844441	22073443	6198336197	361679976
	30CI	34298058	2.97E+07	653120741	1159946	4249336433	308996911
	60 CI	33123015	1.49E+07	538295560	7113469	6158731717	438570054
	240CI	18958513	3.85E+07	226571259	30622522	3482715030	202772159
	480CI	20741245	2.97E+07	218552192	9690662	3960421943	235730622
Heart 2	Control	124383686	2.06E+07	1154572075	2897526	9713972394	2262569134
	6WI	90533183	5.94E+07	971122653	1909164	6817636978	1632818522
	12WI	99139159	7.81E+07	950093019	754735	6731907198	1539319848
	30WI	133089314	1.76E+07	1187803757	2801031	6410829314	1044367515
	60WI	101288217	3.92E+07	1026333245	527594	7030438140	1384817270
	240WI	80714153	4.02E+06	1590772139	0	7086849695	1257530566
	6CI	77604904	1.32E+07	661631422	22962037	7676444605	1163358266
	12CI	72537038	2.35E+07	569667330	49637072	8170002684	914701480
	30CI	81705001	3.23E+07	717013107	24508977	7121240348	1191458350
	60 CI	57912881	1.70E+07	373780761	28953376	6587615509	797318454
	240CI	93300956	3.37E+07	548370513	27839626	7016108673	1086173875
	480CI	24440602	5.86E+07	144369498	119225216	2317301733	243925887
Heart 3	Control	91718351	9.30E+06	969066256	2236416	8499234161	1164844786
	6WI	16946708	2.12E+07	198950381	119131	1609541172	234046914
	12WI	65431517	8.41E+07	713186385	2973133	4415022945	833827828
	30WI	99980129	7.00E+07	1048227466	684527	6398236138	1306997052
	60WI	113300159	4.19E+07	873851718	697753	5879563369	1130811026
	240WI	86671667	1.99E+07	696602538	126929	7279417225	864128541
	6CI	76821672	2.28E+08	802184983	18403004	8753221984	1159579830
	12CI	92125497	4.25E+08	909990486	22668776	10286823920	1308926492
	30CI	81340265	3.65E+08	823221811	12838969	8295633435	1152077978
	60 CI	40547020	1.45E+09	322557515	34482345	3959851101	414315724
	240CI	73392231	1.54E+09	486738399	34867408	4181254057	674893071
	480CI	44979259	1.75E+09	314158223	28448121	2209604340	267319700
Heart 4	Control	67728594	1.64E+06	912434450	5165422	8238983470	648423639
	6WI	60860264	4.24E+07	996005199	7899031	6102086663	1082486953
	12WI	60199892	7.05E+07	983360982	32021986	5706946180	807551668
	30WI	74022666	3.11E+07	1127772419	3199758	6173418794	978043080
	60WI	54640687	3.37E+07	896424744	369022	7577336431	826152852
	240WI	51565601	2.31E+07	854732974	199821	6678475103	795544412
	6CI	57787071	9.40E+06	855066305	18809466	7907493160	945604335
	12CI	38398218	1.17E+07	491391181	56171484	7020529772	498527710
	30CI	41040828	7.89E+06	658882726	17971769	7717028697	783155707
	60 CI	51986212	1.45E+07	642987973	34422845	7598858094	781141585
	240CI	38337859	3.24E+07	387057910	41676047	4933400444	410594206
	480CI	51804304	2.94E+07	588897695	28800912	5549214978	648093385
Heart 5	Control	74990061	2.01E+07	1251639456	3878057	8832854626	1022049372
	6WI	68634793	4.65E+07	1038529436	827928	7235270428	1032096430
	12WI	74366603	8.27E+07	1183003985	1741581	6907415527	1001181029
	30WI	66623942	4.22E+07	1139785463	1257353	7094472461	979513208
	60WI	101043054	4.19E+07	1189511173	183739	8272103275	987721892
	240WI	79851720	1.06E+07	1349876088	241698	8414427304	807327515
	6CI	54985630	2.17E+08	792267684	17404653	6987970536	526333322
	12CI	84157195	2.94E+08	887856268	23862045	8646670746	573999808
	30CI	54520772	3.75E+08	702907974	32860876	7813789586	826703563
	60 CI	46200954	6.52E+08	433232120	52284975	5353141108	409161911
	240CI	18061941	1.24E+09	274518072	62490832	2539528030	232549074
	480CI	37372595	1.08E+09	368502253	24957085	3603146591	367694594

Appendix 2: Pig LC-MS data

		creatinine	choline	aminolevulinic acid	phosphorylcholine	argininosucci
Heart 1	Control	2861170379	2819204961	606381168	13938070	0
	6WI	1362854281	4364154209	675419370	14028941	0
	12WI	824973574	4157165140	356319247	8792728	0
	30WI	1301943649	2581215668	409445167	10197956	0
	60WI	1252512327	6199825793	680094174	17752749	819470
	240WI	2035662115	8287184271	780278409	17781681	560543
	6CI	2430840926	2747326434	512100721	13746753	0
	12CI	2164760436	2411172618	411376777	12917248	0
	30CI	1010997204	5424570364	487985292	11786279	0
	60 CI	1244532886	2886034481	506681784	11883518	0
	240CI	487649273	1612709163	175230758	5251895	0
	480CI	409264468	1425346975	189252671	5370627	0
Heart 2	Control	3053578028	6165411254	889006997	21765488	0
	6WI	1832310375	8292307994	665972798	13754051	0
	12WI	1598903147	8018196530	589581221	11381978	426161
	30WI	1836749001	9971595897	629697236	10300985	0
	60WI	1606364229	8860370823	571686569	12131915	866943
	240WI	1678073659	11186728739	516405713	17875798	0
	6CI	2343376436	3707460891	459806411	13900600	0
	12CI	1686918569	3636906645	346053910	11459375	0
	30CI	1536449293	4933815858	455472985	13724957	0
	60 CI	962047964	2918097379	237828954	10235083	0
	240CI	1288433264	5071438080	378727012	11586168	0
	480CI	273742412	1580616131	75229989	2177124	0
Heart 3	Control	5859098700	3054132622	860465516	18913338	0
	6WI	372601540	875266668	209743485	3160374	0
	12WI	1273165107	3788308250	650747208	8276179	0
	30WI	2133941797	5447135525	893723469	20411980	0
	60WI	1630618626	4108542157	750631495	13762293	0
	240WI	1314256745	4566160774	591587035	11234841	0
	6CI	6010254880	2728685857	854683000	16341982	0
	12CI	4199849063	3160733827	922883634	22039261	0
	30CI	3376743921	2912940881	847369720	17057853	0
	60 CI	760971739	1407295906	224182894	7692930	0
	240CI	920777531	2691339315	363036960	10421098	0
	480CI	421049311	1784874039	167351177	5156950	0
Heart 4	Control	3688240696	3205631368	742885914	13484606	0
	6WI	1768923461	7338536304	1048738453	18053934	0
	12WI	1681191943	7555017032	973429032	15658659	382593
	30WI	1700385363	7095541686	976362723	16480836	1435692
	60WI	1570816765	7251864389	781403319	13860015	758997
	240WI	1450571847	5894694651	672524783	10305135	0
	6CI	3123790529	3655185882	928195099	17015754	0
	12CI	2072578191	2390651570	469492191	11736413	0
	30CI	1787469941	3259209153	692033907	14027048	0
	60 CI	1397027639	2997325183	612494297	15927631	0
	240CI	814614110	2758761226	343332680	8855399	0
	480CI	901453692	3113043425	512945286	11148102	0
Heart 5	Control	4372341781	4380818087	727665020	17809626	0
	6WI	1673344598	5882202146	673761252	22325611	0
	12WI	1761920966	6616602279	719433471	22452652	658105
	30WI	1743021277	5749714623	665078282	18723564	511441
	60WI	1680965385	6875495136	635728805	19225178	710232
	240WI	1988267635	7848453434	577106093	18042561	833355
	6CI	1973077775	3201980697	452857950	11577523	0
	12CI	1887567394	4507922677	462191460	13606691	0
	30CI	2271713992	3116093997	486211481	13230948	0
	60 CI	1210697101	2126487888	250298140	8858079	0
	240CI	330747475	1447569590	116144838	3466762	0
	480CI	418659237	2471319363	171168599	8989590	0

Appendix 2: Pig LC-MS data

		histidine	hypotaurine	lysine	ornithine	arginine	histar
Heart 1	Control	84514856	78484713	259337513	106297495	445871135	17952
	6WI	68402519	63056177	243647291	84728499	381985753	23128
	12WI	61165079	84599239	175009207	54550995	304963178	3420
	30WI	65374912	45822878	217932345	67012938	392454113	8388
	60WI	124872621	57918773	474917865	108089353	679753288	9922
	240WI	144397656	50083892	660160691	172976155	953149064	26753
	6CI	73704246	31541886	218212075	82303032	382899880	10359
	12CI	58789798	24903759	191806196	61503378	332094940	14024
	30CI	92021368	71050009	297923123	81779705	520759258	8142
	60 CI	77789351	39108790	249215799	76471611	447687936	75291
	240CI	30901039	6221287	120148063	42607330	228757994	7520
	480CI	31820225	5703150	117354208	36091240	206635212	31705
Heart 2	Control	286340823	27055923	928579520	97180002	995542173	69189
	6WI	199719132	20062031	732405856	73411808	786183314	15821
	12WI	178483547	17552209	670203402	63204959	732620206	38664
	30WI	177808625	32507158	723459849	66184220	776506407	49301
	60WI	191451892	20568025	764433014	71870865	829806551	20035
	240WI	197663131	15037571	887440343	99234379	1087420599	14168
	6CI	158774842	16562181	529451320	74923453	566203265	10996
	12CI	144379534	4488866	456072867	40171132	527438793	75789
	30CI	145910281	8779992	513709965	53714345	589281720	22536
	60 CI	93448264	4708018	306458323	25208466	354614190	47000
	240CI	134737695	9619461	474265970	39354296	549404639	65215
	480CI	20536107	0	89086578	9462784	102235091	13636
Heart 3	Control	64016982	59721598	241994811	70659171	480143649	25181
	6WI	9353822	21384464	46864985	10805707	83977331	4978
	12WI	39787028	24546132	193279493	52087637	360182351	63758
	30WI	63467362	29041670	301824355	76318407	583514928	50411
	60WI	58251822	30338678	297579184	56396085	530916873	18801
	240WI	53478879	28192756	324690755	55356973	469990500	15498
	6CI	48696635	30684253	210133236	62561544	445412239	19368
	12CI	70506813	22374083	241303636	67915492	533822479	50698
	30CI	49507349	29364945	216670657	57645943	440120300	12973
	60 CI	15453720	1861207	87372153	24647304	194256938	15547
	240CI	29879227	4590685	141732444	44993504	306144150	15703
	480CI	17387032	3308228	80139998	19616064	154888979	10387
Heart 4	Control	124341361	72139153	377867211	69159321	711869696	22269
	6WI	136002299	35931031	463257482	95312378	853800884	42253
	12WI	129596666	39131237	462244946	85600863	888021194	29827
	30WI	117809120	30810521	509103030	86794459	962746852	69394
	60WI	114816680	23033613	411946050	75689763	768880099	46265
	240WI	93899882	27355341	505040163	86848933	779791417	81275
	6CI	113834283	36985489	387159013	78046691	738972588	30940
	12CI	70694466	11553333	219600861	51703054	436576678	32265
	30CI	105464138	23786075	308194535	59053673	637279778	12640
	60 CI	89772320	16692665	312494471	69406368	634857938	28715
	240CI	57313840	8865110	207980807	45051490	417173920	31894
	480CI	67523463	13188845	252071327	58076548	552252024	38985
Heart 5	Control	155303791	60564606	451399852	91399541	903110277	79770
	6WI	156722501	47742674	407979987	64370242	803678896	30097
	12WI	139206384	44780442	450634799	84710171	831311892	63353
	30WI	142462521	49260964	446952067	69187314	797352238	28653
	60WI	161358288	50130325	544532888	75430501	945855147	26390
	240WI	181587476	55172619	691554549	99601082	1072972503	40689
	6CI	92393356	33518305	266076783	53247011	570001164	75396
	12CI	120775564	33819603	339180207	64626543	725751867	85971
	30CI	93944855	17955672	288698016	55821357	602600464	33330
	60 CI	60829439	11904969	173044379	34180692	359027586	26121
	240CI	21664624	636969	86357284	20886118	160311936	19003
	480CI	36147668	3896129	117968457	24719998	247700848	41543

Appendix 2: Pig LC-MS data

		cytosine	putrescine	ammonium and isovalerate	spermidine	cytidine
Heart 1	Control	1547296	44184261	9475531	50122937	13520694.47
	6WI	0	29369193	9032391	1918113	38199575.1
	12WI	0	19986176	4206573	3085916	35419529.89
	30WI	563718	30704087	7316019	31241468	18722814.43
	60WI	2509887	49559518	3324163	20157335	66223544.15
	240WI	2855681	59218189	2798149	53975916	136984054.3
	6CI	0	41567430	8993644	4131921	12641391.19
	12CI	1220925	23835960	8813143	0	8212604.456
	30CI	957686	34227605	8070217	26267562	50433732.33
	60 CI	976711	33726544	9691760	0	17642849.63
	240CI	0	18147266	9188821	0	12988715.13
	480CI	0	15196201	11429771	0	17836864.39
Heart 2	Control	5707703	74916169	17691352	21695549	37697064.16
	6WI	4469364	57195180	11924196	53209693	125196597
	12WI	5592859	48946139	8680038	6385733	118926675.3
	30WI	6261514	55865205	4455274	114064378	130269872.8
	60WI	5693677	58584995	7783496	11094848	98021057.14
	240WI	5351345	47381175	6281131	4140763	218379494.2
	6CI	3916647	46097025	9553263	2727397	19693974.95
	12CI	1787178	42884117	13235268	28320550	18488421.92
	30CI	3599575	46599410	13877242	16671542	51165298.43
	60 CI	945779	26739033	19525433	0	13350706.57
	240CI	2304452	34777787	12980140	1037790	40519341.92
	480CI	0	7673886	10368066	0	8295967.831
Heart 3	Control	3685747	55472935	10009106	20479406	10740131.03
	6WI	0	5829437	1276629	0	14581998.2
	12WI	1759296	27581666	6499958	0	58602266.66
	30WI	5405699	70905961	24298622	3596545	101996490.8
	60WI	3514457	39855991	6200988	0	57633873.73
	240WI	2394655	45959374	7064671	2194115	55620178.78
	6CI	3478638	35673085	6948697	1332309	9988298.853
	12CI	3566653	44534557	12520944	0	13449156.3
	30CI	3686961	41810352	7352442	538370	11282338.37
	60 CI	446046	22277617	7097406	1529477	5371108.312
	240CI	924328	40799383	14859887	24442007	16352740.36
	480CI	911493	19718448	13030175	599043	16370070.5
Heart 4	Control	2413346	27741351	10009955	0	11894839.88
	6WI	3645915	38119623	9841896	0	95465184.76
	12WI	4242401	35476272	5950426	2227066	91767332.58
	30WI	5104904	37679755	6039984	8324757	84015020.14
	60WI	2635549	37197699	8220217	0	63454922.21
	240WI	3597421	27879257	4845242	79787844	74819888.82
	6CI	3290493	26393278	11909693	15171155	15129948.63
	12CI	1216529	24084601	12714548	0	6509233.113
	30CI	1369661	24665953	14242564	0	14038828.47
	60 CI	2033256	36818724	12835998	0	13485558.47
	240CI	1160948	21802775	15769625	15852032	11509051.35
	480CI	1829601	23274901	15728982	24750750	32345824.52
Heart 5	Control	2922634	30401186	8768067	19836652	22262712.58
	6WI	2053070	37878926	10622574	3503833	95501185.97
	12WI	1330423	37560106	15367971	0	105682591.3
	30WI	2180319	37027792	4913788	3849817	89590561.26
	60WI	3701897	41490746	5487996	0	90785660.52
	240WI	3119924	40249966	2860870	0	144471330
	6CI	2105912	26939398	4497103	15552792	22482152.94
	12CI	1888494	34450284	8149774	0	35300224.93
	30CI	1881960	24979666	12528978	24230136	12378041.84
	60 CI	980244	18424950	11705236	626413	8302635.734
	240CI	0	9951978	13888863	5394113	13903090.1
	480CI	0	14101171	22821890	0	15227340.45

Appendix 3: Human LC-MS data

Appendix 3: Human LC-MS data

		peak area (a.u.)					
	sample	HEPES	succinyl-acetone	fumarate	succinate	itaconic acid	3-hydroxybut
Heart 1	Control	1.73E+07		155015235	578505528	51730945	1867598
	6WI	1.84E+07		332693387	5338385773	52726737	1322194
	12WI	1.44E+07		222707768	6278955683	31238932	1228054
	30WI	1.93E+07		100220942	6047224501	0	1011156
	60WI	1.97E+07		129179374	7458784535	15473002	1368972
	240WI	1.30E+07		152094152	3311469243	0	9831349
	6CI	1.58E+07		151275941	807778019	25858547	8094752
	12CI	2.21E+07		165609426	3296900454	31228466	1169025
	30CI	1.85E+07		149073572	2070397842	32446962	1018073
	60 CI	1.60E+07		198507900	4084705609	38159897	9313048
	240CI	2.28E+07		261337200	3479570187	22218726	9191436
	480CI	2.00E+07		130396114	4203880803	10765369	7763579
Heart 2	Control	1.65E+07		1.31E+08	9.18E+08	9.65E+06	1.51E+0
	6WI	1.33E+07		4.05E+08	6.83E+09	6.34E+06	1.01E+0
	12WI	1.51E+07		4.47E+08	8.84E+09	8.45E+06	1.30E+0
	30WI	1.37E+07		3.14E+08	1.19E+10	8.55E+06	1.60E+0
	60WI	1.67E+07		3.42E+08	1.72E+10	1.17E+07	2.48E+0
	240WI	1.11E+07		8.71E+08	7.86E+09	9.61E+06	2.13E+0
	6CI	1.90E+07		1.10E+08	1.32E+09	9.69E+06	1.02E+0
	12CI	1.21E+07		9.26E+07	1.30E+09	1.00E+07	8.48E+0
	30CI	1.69E+07		7.14E+07	1.06E+09	1.04E+07	5.04E+0
	60 CI	1.79E+07		1.21E+08	1.53E+09	1.32E+07	4.97E+0
	240CI	1.34E+07		1.02E+08	2.34E+09	7.41E+06	5.35E+0
	480CI	1.10E+07		5.27E+07	2.20E+09	8.33E+06	3.17E+0
	1440CI	1.43E+07		3.71E+07	3.79E+09	8.89E+06	4.00E+0
Heart 3	Control	22448769	26260651	171153411	1129318816.29	23771193	8449870
	6WI	39910347	46979229	279946230	5663938666	63516221	1344083
	12WI	26933665	33560337	357240409	7265330979	35829041	1351291
	30WI	29421041	27949554	302721184	4930891909	25058376	1317697
	60WI	27548100	18807833	165624526	9743020952	24991670	1880852
	240WI	26473177	31972371	287037618	7222249222	35906790	1522565
	6CI	25224272	24640736	156530288	2258807319	29202430	8530671
	12CI	28677878	37391442	144782706	2670836762	35693813	9373745
	30CI	26169780	40984145	122472628	2317381880	34678945	7514033
	60 CI	24121420	29002105	91674148	2864732513	30582323	7711256
	240CI	22860044	30268034	95761696	2501792307	31027020	6090503
	480CI	24054976	36715536	101200772	3155632003	37608867	6395189
	1440CI	23819160	23935437	36307800	4222482193	29824415	4270291
Heart 4	Control	1.98E+07	1.62E+07	4.72E+08	2.01E+09	3.53E+07	1.08E+0
	6WI	1.89E+07	2.18E+07	8.45E+08	7.74E+09	4.96E+07	8.69E+0
	12WI	2.38E+07	5.45E+07	8.01E+08	1.00E+10	6.00E+07	1.34E+0
	30WI	1.71E+07	2.30E+07	7.55E+08	9.67E+09	4.21E+07	1.50E+0
	60WI	1.43E+07	2.87E+07	3.90E+08	8.28E+09	4.60E+07	1.64E+0
	240WI	1.52E+07	2.09E+07	4.64E+08	8.47E+09	4.30E+07	2.05E+0
	6CI	1.64E+07	2.92E+07	4.08E+08	3.98E+09	5.00E+07	1.01E+0
	12CI	1.71E+07	3.34E+07	3.50E+08	4.02E+09	4.90E+07	8.00E+0
	30CI	1.56E+07	2.03E+07	1.95E+08	2.77E+09	4.16E+07	5.38E+0
	60 CI	1.53E+07	3.68E+07	2.75E+08	3.73E+09	4.17E+07	6.60E+0
	240CI	1.62E+07	4.62E+07	3.47E+08	4.13E+09	6.22E+07	9.30E+0
	480CI	1.30E+07	3.15E+07	1.61E+08	2.45E+09	5.43E+07	2.82E+0
	1440CI	1.14E+07	2.54E+07	6.17E+07	4.09E+09	5.61E+07	9.53E+0

Appendix 3: Human LC-MS data

	sample	lactate	N-acetyl aspartate	aconitate	pyro-glutamate	pyruvate	malonate
Heart 1	Control	2795236299	73240796	332718987	57326409	56354953	1.28E+07
	6WI	15397837660	64738999	388540927	107528621	27914145	1.77E+07
	12WI	14469865183	52219829	209397540	123934965	26111088	1.65E+07
	30WI	13538968979	44917615	23360441	104621890	24882340	2.23E+07
	60WI	20267157520	63884505	105736779	268602088	36237867	1.79E+07
	240WI	18912461383	48240767	19622674	355887684	24637925	1.59E+07
	6CI	3536536278	41947568	165905278	315458757	11021612	1.46E+07
	12CI	10724276318	69310303	236271507	486791215	37350834	2.34E+07
	30CI	7958152283	59899180	226484492	349872149	26938919	1.75E+07
	60 CI	16462106866	57383408	266361920	398191080	29622729	2.29E+07
	240CI	18899098733	79858809	180432438	630469483	36061482	2.08E+07
	480CI	15342250779	63938584	101095113	589174787	27781942	1.75E+07
Heart 2	Control	3.69E+09	1.27E+08	1.53E+08	8.38E+07	0.00E+00	
	6WI	2.30E+10	7.05E+07	2.55E+08	5.82E+07	0.00E+00	
	12WI	3.12E+10	9.55E+07	1.78E+08	9.42E+07	0.00E+00	
	30WI	3.46E+10	1.20E+08	2.67E+08	7.46E+07	0.00E+00	
	60WI	5.70E+10	1.16E+08	8.39E+07	1.57E+08	2.36E+07	
	240WI	5.67E+10	8.50E+07	7.23E+07	2.50E+08	6.16E+07	
	6CI	4.52E+09	1.06E+08	1.60E+08	1.70E+08	0.00E+00	
	12CI	4.30E+09	9.21E+07	1.52E+08	8.78E+07	0.00E+00	
	30CI	3.33E+09	7.29E+07	1.22E+08	2.74E+08	0.00E+00	
	60 CI	7.68E+09	1.02E+08	1.20E+08	4.68E+08	0.00E+00	
	240CI	1.92E+10	8.25E+07	3.88E+07	1.94E+08	0.00E+00	
	480CI	1.12E+10	6.72E+07	1.47E+07	3.05E+08	0.00E+00	
	1440CI	1.71E+10	7.48E+07	6.71E+06	5.30E+08	0.00E+00	
Heart 3	Control	4190603106	149162783	175889021	184438459		
	6WI	26949157173	176240612	222052651	552175545		
	12WI	32781661379	140721338	104925355	244250374		
	30WI	33301102965	137547416	26196201	244098877		
	60WI	43472817780	111793664	24752477	390193517		
	240WI	46655755841	140467314	5001659	736557402		
	6CI	7603626112	147985638	306162739	268979256		
	12CI	9351770945	147093401	250092893	275432189		
	30CI	9685143896	185327503	299532785	265529750		
	60 CI	11719407955	139702731	252525413	277604062		
	240CI	16843936939	114944491	72405121	266219489		
	480CI	14955068100	191293615	43740677	391285731		
	1440CI	17928422168	115048026	26916017	469079098		
Heart 4	Control	6.17E+09	7.32E+07	1.76E+08	2.24E+08		
	6WI	2.29E+10	7.32E+07	1.34E+08	1.62E+08		
	12WI	2.62E+10	7.95E+07	9.67E+07	2.80E+08		
	30WI	2.99E+10	8.60E+07	1.02E+08	2.31E+08		
	60WI	1.85E+10	9.19E+07	6.51E+07	3.23E+08		
	240WI	2.30E+10	1.76E+08	1.13E+08	1.90E+09		
	6CI	1.09E+10	6.70E+07	2.06E+08	2.32E+08		
	12CI	1.00E+10	8.31E+07	1.53E+08	2.45E+08		
	30CI	1.24E+10	6.37E+07	1.19E+08	2.47E+08		
	60 CI	9.70E+09	7.45E+07	1.76E+08	2.64E+08		
	240CI	1.47E+10	7.00E+07	6.84E+07	3.21E+08		
	480CI	7.74E+09	5.78E+07	2.90E+07	4.31E+08		
	1440CI	2.56E+09	5.59E+07	1.38E+07	4.55E+08		

Appendix 3: Human LC-MS data

	sample	uracil	xanthine	nicotinaminde	hypoxanthine	orotate	succinyl-adenosine
Heart 1	Control	0	370176	94645688	25984379		0
	6WI	228378	3708296	1513257111	1561784513		0
	12WI	21102202	10118062	2055069160	4310013090		6055297
	30WI	43811208	22228406	1598964510	6418562259		7982359
	60WI	61629399	58664415	2376941974	9296441461		12913501
	240WI	201402012	216981377	6356232855	22862090385		15517997
	6CI	0	782321	179525099	87782962		0
	12CI	11257537	14417373	912981223	2781728373		2795615
	30CI	223448	1110739	668636995	282167586		0
	60 CI	51648948	64016957	2388944477	8055616065		3431044
	240CI	10977251	21787247	1638528842	3208332491		1373064
	480CI	6329435	9367145	1127047580	2913432333		1571776
Heart 2	Control	0.00E+00	5.31E+05	2.05E+08	1.25E+08	1.62E+06	0.00E+00
	6WI	0.00E+00	6.36E+05	1.58E+09	9.40E+08	1.09E+06	1.40E+05
	12WI	0.00E+00	3.93E+06	2.56E+09	1.96E+09	1.10E+06	1.19E+06
	30WI	0.00E+00	1.49E+07	1.91E+09	2.58E+09	1.21E+06	3.52E+06
	60WI	3.23E+06	2.17E+07	3.36E+09	4.87E+09	7.77E+05	1.65E+07
	240WI	2.50E+07	1.07E+08	6.44E+09	9.24E+09	4.27E+05	3.98E+07
	6CI	0.00E+00	6.20E+05	2.49E+08	1.17E+08	1.27E+06	0.00E+00
	12CI	0.00E+00	5.62E+05	2.28E+08	2.33E+08	1.91E+06	0.00E+00
	30CI	0.00E+00	0.00E+00	2.15E+08	1.05E+08	6.81E+05	0.00E+00
	60 CI	0.00E+00	0.00E+00	4.83E+08	2.82E+08	7.63E+05	0.00E+00
	240CI	0.00E+00	0.00E+00	1.13E+09	4.74E+08	9.55E+05	0.00E+00
	480CI	0.00E+00	1.67E+05	3.01E+08	3.05E+08	3.17E+05	0.00E+00
	1440CI	0.00E+00	1.47E+06	3.08E+08	1.20E+09	1.51E+05	0.00E+00
Heart 3	Control	2379816	1282553	209838881	75683031	3705582	NF
	6WI	51698458	12650141	2171878838	1553465575	3015194	1068169
	12WI	105196999	16863466	3806522083	2695714733	1537240	4414912
	30WI	94936518	59815196	4786952123	5054869994	1721497	11072043
	60WI	117765573	72603235	3526323701	6191922407	1073781	19915958
	240WI	130215210	491343204	6893066975	10787803015	2051185	30999863
	6CI	4448024	2127861	190300131	90816700	2456435	NF
	12CI	5021484	6458622	264991800	263528167	2336416	NF
	30CI	6509824	1903715	299189552	151214443	2716997	NF
	60 CI	6254316	2157721	343457540	201974893	2022555	NF
	240CI	11750727	2470312	815838214	436128419	976309	NF
	480CI	2628748	1254657	339985925	443019043	399250	NF
	1440CI	639192	1259917	320754076	1163204523	162534	NF
Heart 4	Control	7.75E+05	4.50E+06	4.92E+08	7.57E+08	3.60E+05	NF
	6WI	1.97E+05	3.63E+06	3.12E+09	3.24E+09	2.15E+05	1.33E+06
	12WI	8.72E+06	1.97E+07	5.15E+09	5.81E+09	2.20E+05	1.29E+07
	30WI	1.21E+07	3.64E+07	5.69E+09	8.62E+09	NF	2.46E+07
	60WI	6.42E+07	1.16E+08	4.55E+09	1.47E+10	1.02E+05	2.14E+07
	240WI	3.18E+08	5.15E+08	9.96E+09	4.47E+10	2.99E+05	5.03E+07
	6CI	NF	1.84E+05	4.61E+08	2.58E+08	8.64E+04	NF
	12CI	NF	1.74E+06	6.74E+08	3.65E+08	2.96E+05	NF
	30CI	NF	1.56E+06	1.12E+09	5.41E+08	9.70E+04	NF
	60 CI	NF	6.57E+05	3.67E+08	3.46E+08	9.54E+04	NF
	240CI	2.07E+05	3.38E+06	1.60E+09	1.42E+09	1.06E+05	1.68E+05
	480CI	NF	7.38E+05	6.90E+08	1.36E+09	NF	1.91E+05
	1440CI	8.21E+05	7.76E+06	3.37E+08	5.30E+09	NF	2.99E+05

Appendix 3: Human LC-MS data

	sample	urea	allopurinol	inosine	ascorbic acid	uridine	uric acid
Heart 1	Control	3818975038	9486888		0	5121299	109547016
	6WI	3724911902	1003327323		0	3473853	118208422
	12WI	3251572215	1873083468		0	2941879	89122558
	30WI	1705245026	2765336859		31770483	575559	65163667
	60WI	2844312026	3960562673		0	2224789	94550380
	240WI	2447958878	3946415478		0	5213001	72221585
	6CI	1919804529	90816040		0	949326	55612611
	12CI	2773451510	1263099338		3049378	1238537	80359676
	30CI	2466642340	485414372		0	1395882	90428406
	60 CI	2254069335	2167075913		13243889	2135204	84638311
	240CI	2047970244	2303646273		0	2516961	86344160
	480CI	1623852775	2807815475		7365667	1304225	61741627
Heart 2	Control	5.84E+09	8.03E+07	1.34E+08	5.23E+06	3.08E+06	8.91E+07
	6WI	4.32E+09	6.73E+08	1.09E+09	5.21E+07	6.03E+07	5.37E+07
	12WI	4.68E+09	1.39E+09	2.20E+09	3.87E+07	1.17E+08	7.47E+07
	30WI	3.68E+09	1.92E+09	3.21E+09	4.05E+07	9.37E+07	3.83E+07
	60WI	5.04E+09	3.38E+09	5.40E+09	9.04E+07	1.69E+08	6.47E+07
	240WI	3.86E+09	4.21E+09	6.84E+09	1.05E+08	2.14E+08	4.51E+07
	6CI	4.43E+09	1.51E+08	2.17E+08	0.00E+00	4.54E+06	7.15E+07
	12CI	4.28E+09	1.75E+08	2.59E+08	9.93E+07	4.50E+06	4.13E+07
	30CI	2.45E+09	2.08E+08	3.26E+08	0.00E+00	1.52E+06	4.16E+07
	60 CI	1.67E+09	5.55E+08	9.12E+08	0.00E+00	3.38E+06	3.84E+07
	240CI	1.48E+09	1.10E+09	1.72E+09	0.00E+00	1.19E+07	2.61E+07
	480CI	2.37E+08	1.08E+09	1.67E+09	0.00E+00	2.56E+06	9.00E+06
	1440CI	1.43E+08	3.10E+09	5.01E+09	0.00E+00	2.99E+06	1.68E+07
Heart 3	Control	3598190893	232965746	211878839	7800502	1648321	73623132
	6WI	4681898850	2401412679	2152552094	292527879	3648300	114527114
	12WI	4490293925	3390863634	3064511574	276258425	2483197	110425730
	30WI	3659278805	6829125115	5679924873	61050209	3114761	88505924
	60WI	3634852539	6771240472	6096906815	506760607	3518550	97437424
	240WI	3715772844	8718282348	7504643010	167395723	5865319	77943872
	6CI	2978660133	282657362	244335240	186162469	1679700	61537526
	12CI	3381646317	353288750	306248988	328837873	1815676	77408998
	30CI	2836389979	666831764	575557999	242772518	1846718	68214125
	60 CI	2940562581	726216517	651418726	68376159	1782010	67864151
	240CI	1613677093	1804860397	1670757418	5952137	1299289	51445903
	480CI	488012367	2256803626	2110466433	122290993	NF	29553951
	1440CI	282687889	4512916157	4016585784	8702568	NF	24886315
Heart 4	Control	5.92E+09		3.45E+08		8.59E+06	1.63E+08
	6WI	4.09E+09		3.24E+09		3.70E+06	9.48E+07
	12WI	4.61E+09		5.74E+09		6.08E+06	1.17E+08
	30WI	3.76E+09		8.83E+09		4.27E+06	9.62E+07
	60WI	3.99E+09		7.85E+09		6.48E+06	1.31E+08
	240WI	5.15E+09		9.59E+09		1.80E+07	1.55E+08
	6CI	3.49E+09		5.93E+08		3.30E+06	9.35E+07
	12CI	3.85E+09		9.56E+08		4.50E+06	1.06E+08
	30CI	3.04E+09		1.75E+09		2.43E+06	8.17E+07
	60 CI	2.95E+09		9.32E+08		3.70E+06	8.56E+07
	240CI	1.55E+09		4.33E+09		2.22E+06	5.93E+07
	480CI	3.04E+08		6.34E+09		NF	2.72E+07
	1440CI	1.16E+08		1.09E+10		NF	2.36E+07

Appendix 3: Human LC-MS data

	sample	guanosine	tryptophan	adenosine	methionine	glucose	leucine and isoleucine
Heart 1	Control	642307	50460096	7.13E+07	320108833	4909373615	981866010
	6WI	76799985	47873636	2495198480	315387403	682049734	1211760821
	12WI	122371383	44757461	3923075315	275778240	142971190	1281152762
	30WI	178819028	78419536	1021968436	225205634	118535321	1879653360
	60WI	293766627	102935696	3028725176	363527638	328109294	2482725871
	240WI	373596122	261566742	207363873	500522315	138912570	5971450684
	6CI	675512	22034165	8623271968	219697632	1128255250	478318408
	12CI	66258269	50464961	12035354445	288922309	1017127711	1167679408
	30CI	14069473	39135731	9800845266	234393528	771507927	715879266
	60 CI	140070660	83221928	6218563600	308810391	801469654	2152740971
	240CI	88424324	54041681	11745842883	312133094	594814273	1204054056
	480CI	74751029	35727155	9700420675	220739991	308105358	862209936
Heart 2	Control	6.71E+06	5.72E+07	1.74E+09	3.64E+08	4.51E+09	2.06E+09
	6WI	5.91E+07	5.58E+07	1.95E+09	2.78E+08	1.45E+09	1.48E+09
	12WI	1.10E+08	7.04E+07	1.88E+09	3.10E+08	1.22E+09	2.02E+09
	30WI	1.84E+08	7.80E+07	2.10E+09	2.67E+08	1.68E+09	2.19E+09
	60WI	3.77E+08	1.68E+08	2.20E+09	4.10E+08	1.16E+09	4.19E+09
	240WI	4.99E+08	1.01E+09	1.03E+09	1.94E+09	6.33E+09	1.88E+10
	6CI	8.98E+06	5.99E+07	7.36E+09	2.46E+08	1.84E+09	1.38E+09
	12CI	1.15E+07	4.81E+07	3.64E+09	3.46E+08	1.76E+09	1.53E+09
	30CI	4.52E+06	2.99E+07	1.19E+10	2.30E+08	6.15E+08	9.39E+08
	60 CI	1.21E+07	3.34E+07	2.06E+10	2.11E+08	2.29E+08	9.64E+08
	240CI	2.15E+07	2.76E+07	8.16E+09	1.65E+08	2.27E+08	8.51E+08
	480CI	1.86E+07	1.33E+07	1.38E+10	6.30E+07	8.47E+07	4.00E+08
	1440CI	3.06E+07	2.05E+07	1.05E+10	4.48E+07	1.86E+08	5.32E+08
Heart 3	Control	6905743	215524572	1.59E+09	535453908	888433838	1518673816
	6WI	110397156	298135159	6411281237	844850210	924342071	4032448252
	12WI	184953279	298769854	3887089321	693223245	678347902	2779647803
	30WI	304112931	400023256	3458136991	920167736	675291047	5335266548
	60WI	457775544	425505280	2736212805	811288684	396726398	5720413208
	240WI	568330737	2006579585	696178584	4097528953	1505616896	32349999558
	6CI	8957350	168951940	9870170539	456976202	465397512	1349850608
	12CI	13575543	205211119	6783666246	612833990	898208903	2489678385
	30CI	19860661	176183496	13724662553	478545698	462962267	1313639825
	60 CI	19142041	169190189	10119017795	532023725	596563217	1401143921
	240CI	54613723	124866219	11559185217	302320781	349971086	954215717
	480CI	23424728	111143282	18797145722	212690869	257081340	1004243721
	1440CI	21885344	83065092	13574903442	109109351	194632733	819814760
Heart 4	Control	1.33E+07	6.39E+07	1.12E+09	4.37E+08	4.31E+09	2.14E+09
	6WI	1.17E+08	5.07E+07	2.99E+09	2.98E+08	1.15E+09	1.64E+09
	12WI	2.65E+08	8.55E+07	4.45E+09	3.44E+08	7.64E+08	2.61E+09
	30WI	4.15E+08	1.22E+08	2.29E+09	4.02E+08	4.86E+08	3.37E+09
	60WI	4.79E+08	1.58E+08	1.30E+09	3.51E+08	1.10E+08	3.71E+09
	240WI	7.84E+08	5.49E+08	8.91E+08	9.92E+08	1.81E+08	1.01E+10
	6CI	1.63E+07	3.56E+07	8.11E+09	2.66E+08	7.10E+08	1.45E+09
	12CI	2.55E+07	3.54E+07	8.44E+09	2.87E+08	7.16E+08	1.24E+09
	30CI	4.43E+07	2.60E+07	8.56E+09	3.01E+08	9.64E+08	8.59E+08
	60 CI	1.53E+07	4.32E+07	9.02E+09	3.22E+08	9.38E+08	1.36E+09
	240CI	9.37E+07	3.92E+07	1.42E+10	2.74E+08	3.31E+08	1.33E+09
	480CI	7.29E+07	2.08E+07	1.85E+10	1.28E+08	2.32E+08	5.56E+08
	1440CI	7.38E+07	4.68E+07	8.95E+09	1.78E+08	2.32E+08	9.96E+08

Appendix 3: Human LC-MS data

	sample	propionyl carnitine	GABA	succinic semialdehyde	guanine	homocysteine	GSH
Heart 1	Control		160051543		0	949421	5331505666
	6WI		124632665		10212390	2239068	5630484224
	12WI		92721491		28943818	3167353	6101380540
	30WI		78312373		38930862	0	3519110232
	60WI		69823664		59557514	3777090	3639339293
	240WI		46435307		222673619	5106325	3374388207
	6CI		46213551		0	3129109	2289786879
	12CI		53315979		7196524	3260188	2652377764
	30CI		62478198		0	3367982	3928351769
	60 CI		56871169		41014252	3505962	2961190231
	240CI		64103735		8934143	3628894	3211545717
	480CI		37395845		5122363	1775032	2063828869
Heart 2	Control	4.63E+08	2.45E+08	2.15E+07	0.00E+00	2.52E+06	3.81E+09
	6WI	1.47E+09	2.01E+08	1.45E+07	3.71E+06	9.96E+05	4.54E+09
	12WI	3.20E+09	2.03E+08	1.98E+07	0.00E+00	8.27E+05	4.22E+09
	30WI	4.09E+09	1.82E+08	1.57E+07	8.58E+06	9.67E+05	3.23E+09
	60WI	4.18E+09	1.60E+08	1.95E+07	2.62E+07	2.10E+06	4.54E+09
	240WI	7.73E+08	1.18E+08	3.30E+07	6.77E+07	2.01E+06	3.08E+09
	6CI	3.52E+08	2.15E+08	1.87E+07	0.00E+00	1.99E+06	4.43E+09
	12CI	3.12E+08	2.70E+08	1.96E+07	0.00E+00	2.11E+06	4.44E+09
	30CI	2.51E+08	1.76E+08	1.47E+07	0.00E+00	1.59E+06	3.04E+09
	60 CI	3.32E+08	1.10E+08	1.15E+07	0.00E+00	1.60E+06	2.85E+09
	240CI	2.46E+08	1.74E+08	1.02E+07	0.00E+00	8.78E+05	2.33E+09
	480CI	3.91E+08	5.86E+07	0.00E+00	0.00E+00	0.00E+00	1.37E+09
	1440CI	5.59E+08	5.79E+07	0.00E+00	5.53E+06	0.00E+00	1.62E+09
Heart 3	Control	912191251	219984494	57499175	164568	2113601	6053398495
	6WI	2387449795	244297310	71666462	11480390	3075783	6958986350
	12WI	3959910312	216791938	52350190	20981991	1415346	7691678678
	30WI	3459567841	161808274	41991813	26198485	1737960	5621281326
	60WI	5262117805	149020713	24473882	40218362	2392472	6305754418
	240WI	927686817	177560719	115555873	26240169	4373094	4927738424
	6CI	497559966	217595256	31862026	701156	1212623	6041034764
	12CI	561482896	241631416	59722320	235857	1134517	6281039071
	30CI	531487353	231580971	31695893	451231	1357340	6533946969
	60 CI	436596702	220650967	39459634	NF	700784	6121986684
	240CI	497435338	204055644	21481760	381480	1142762	5116121754
	480CI	919422586	127134540	16955055	NF	NF	4753082286
	1440CI	1677081962	122994119	13413116	179011	865121	4051508733
Heart 4	Control	4.97E+08	1.65E+08		1.68E+06	3.30E+06	7.29E+09
	6WI	1.08E+09	1.56E+08		1.50E+07	5.88E+06	6.11E+09
	12WI	1.63E+09	1.42E+08		3.28E+07	3.19E+06	6.73E+09
	30WI	2.03E+09	1.22E+08		4.02E+07	5.84E+06	6.21E+09
	60WI	6.09E+08	1.33E+08		1.28E+08	6.19E+06	4.90E+09
	240WI	3.14E+08	1.60E+08		5.61E+08	1.33E+07	5.62E+09
	6CI	3.40E+08	1.30E+08		NF	3.90E+06	4.75E+09
	12CI	2.66E+08	1.71E+08		NF	4.08E+06	5.59E+09
	30CI	1.66E+08	1.72E+08		2.58E+05	2.98E+06	4.59E+09
	60 CI	2.35E+08	1.57E+08		NF	3.94E+06	5.48E+09
	240CI	3.44E+08	9.69E+07		8.05E+05	2.13E+06	3.44E+09
	480CI	4.69E+08	4.80E+07		NF	NF	2.09E+09
	1440CI	2.92E+07	3.26E+07		5.84E+05	1.78E+05	2.02E+09

Appendix 3: Human LC-MS data

	sample	acetyl carnitine	tyrosine	AMP	GMP	palmitoyl carnitine	proline
Heart 1	Control	6192275081	237208854	68475839		119872646	1063431290
	6WI	8312815506	298839257	878461592		202759251	1490322081
	12WI	7562926471	273669930	1473800930		264422644	1868521681
	30WI	2944564515	144609089	1517338237		103724512	1682024857
	60WI	5485297736	397117834	1160864753		94755801	2436836574
	240WI	3299875719	702767342	324931758		93183016	2945107622
	6CI	6035898682	119785990	272922921		176732730	1148954655
	12CI	7178180968	208600993	567027941		207418257	1695096784
	30CI	7109839155	188754571	676148517		261014015	1115222828
	60 CI	8711100017	285730009	359855798		239138525	1638590962
	240CI	10970994282	194995115	251508733		454086835	1387798343
	480CI	8632393819	150045294	679987129		233816619	1283225430
Heart 2	Control	3.51E+09	2.15E+08	1.66E+08	0.00E+00	1.25E+07	2.21E+09
	6WI	1.23E+10	2.58E+08	1.07E+09	5.29E+06	7.79E+07	1.37E+09
	12WI	1.08E+10	1.86E+08	1.49E+09	1.89E+07	4.43E+07	1.85E+09
	30WI	1.46E+10	2.28E+08	9.94E+08	1.09E+07	3.99E+07	1.35E+09
	60WI	1.16E+10	3.55E+08	2.52E+09	9.72E+06	1.21E+08	2.34E+09
	240WI	5.61E+09	1.05E+09	5.55E+08	1.46E+06	8.39E+07	2.81E+09
	6CI	6.13E+09	2.85E+08	2.16E+08	2.90E+05	1.40E+07	1.33E+09
	12CI	7.83E+09	2.34E+08	1.71E+08	0.00E+00	2.87E+07	1.44E+09
	30CI	8.18E+09	1.50E+08	2.75E+08	4.66E+05	5.33E+07	1.11E+09
	60 CI	9.53E+09	1.31E+08	4.61E+08	2.89E+06	8.58E+07	9.85E+08
	240CI	8.45E+09	1.06E+08	1.10E+09	6.35E+06	1.55E+08	7.91E+08
	480CI	6.79E+09	4.41E+07	1.03E+08	4.64E+05	2.94E+08	4.48E+08
	1440CI	5.31E+09	6.15E+07	2.70E+08	2.44E+06	1.94E+08	5.02E+08
Heart 3	Control	12402239732	673563019	456851340	1.11E+06	46538958	450075032
	6WI	19376633722	1020214808	1174902882	14659105	117587284	871927729
	12WI	18262237382	880780160	1645039105	24383050	78109018	860903200
	30WI	12379098552	949533575	1338299928	28228409	61037013	1093908739
	60WI	12605812287	967673200	2290385138	17976586	83709855	1257818225
	240WI	8683857002	3184847996	1088290861	6792624	36591887	3948403990
	6CI	14775824032	589810362	498319407	2032084	77169630	479046717
	12CI	16875390114	673799287	413522168	1439503	77706097	585324639
	30CI	14194344395	628411064	455974031	2750704	88692953	500316726
	60 CI	15597318768	612513592	272670384	1043934	92569607	456127946
	240CI	12162768844	483571490	389155554	2912043	137436010	334625221
	480CI	12824676826	361341142	163123031	394952	199854644	452270638
	1440CI	9652842894	275835117	479738765	8181507	239708893	258044788
Heart 4	Control	1.19E+10	4.54E+08	1.34E+08	NF	1.22E+08	1.49E+09
	6WI	1.56E+10	4.22E+08	1.00E+09	1.90E+06	8.74E+07	1.36E+09
	12WI	1.43E+10	5.50E+08	1.85E+09	7.52E+06	1.03E+08	1.61E+09
	30WI	1.18E+10	5.76E+08	1.34E+09	1.63E+06	1.03E+08	1.71E+09
	60WI	7.03E+09	6.55E+08	1.31E+09	7.84E+06	1.40E+08	2.18E+09
	240WI	1.03E+10	1.47E+09	8.45E+08	NF	2.35E+08	5.53E+09
	6CI	1.65E+10	3.06E+08	5.07E+08	NF	8.48E+07	1.06E+09
	12CI	1.58E+10	3.41E+08	3.63E+08	NF	8.63E+07	1.09E+09
	30CI	1.00E+10	2.50E+08	3.34E+08	NF	1.57E+08	8.24E+08
	60 CI	1.36E+10	3.30E+08	5.13E+07	NF	1.29E+08	1.15E+09
	240CI	1.33E+10	1.91E+08	1.53E+09	7.46E+06	1.54E+08	6.87E+08
	480CI	5.45E+09	8.12E+07	6.46E+08	8.96E+05	1.59E+08	3.32E+08
	1440CI	9.80E+08	8.69E+07	1.76E+09	1.37E+07	1.07E+08	5.64E+08

Appendix 3: Human LC-MS data

	sample	taurine	cysteine	alanine and sarcosine	glutamate	glutamine
Heart 1	Control	5546554430	18984656	6072289809	22749509750	3535504887
	6WI	4849283935	79314937	9416443676	20385974455	3698546169
	12WI	4421409950	92561730	9730686748	14339099080	4379746850
	30WI	4561271343	177235264	7804397779	11138780471	3224794123
	60WI	3000506529	224058715	11006580817	13075009793	3362472743
	240WI	3945342538	679941112	10636111058	7733193982	2898893246
	6CI	1200154707	14092118	4399495681	10531015954	2152556209
	12CI	1540866109	2985132	7581203520	14664285455	2400887365
	30CI	2381410129	43353520	5986442621	15654402702	2377320295
	60 CI	2152197651	28880356	8190510281	12987202802	2543324158
	240CI	1589570012	31316491	7734558501	17041145380	2544809761
	480CI	1311573698	17777298	6633105496	10314410792	2245138327
Heart 2	Control	7.17E+09	1.16E+06	4.02E+09	2.44E+10	2.00E+10
	6WI	7.93E+09	2.56E+07	5.72E+09	1.93E+10	1.73E+10
	12WI	6.56E+09	1.53E+07	7.50E+09	2.21E+10	1.98E+10
	30WI	5.91E+09	3.22E+07	6.98E+09	1.30E+10	1.58E+10
	60WI	6.98E+09	8.98E+07	1.18E+10	1.35E+10	2.17E+10
	240WI	7.39E+09	2.02E+08	1.33E+10	8.31E+09	1.67E+10
	6CI	8.90E+09	1.62E+07	4.29E+09	2.37E+10	1.73E+10
	12CI	7.22E+09	1.05E+07	3.56E+09	2.38E+10	2.02E+10
	30CI	5.83E+09	4.73E+06	2.55E+09	2.14E+10	1.58E+10
	60 CI	4.85E+09	8.34E+06	2.26E+09	1.64E+10	1.24E+10
	240CI	4.49E+09	1.73E+07	2.42E+09	1.50E+10	1.24E+10
	480CI	2.26E+09	9.88E+06	1.06E+09	6.59E+09	5.07E+09
	1440CI	2.81E+09	1.25E+07	2.22E+09	7.44E+09	5.90E+09
Heart 3	Control	7806155160	257803	2724695117	14881162663	22910869648
	6WI	7086698526	3566612	5293606061	14174543433	30992550708
	12WI	7586067529	12563939	6344474899	13292976037	27091127823
	30WI	5928773580	13836985	5953818134	10043296882	23936525961
	60WI	6443931324	26375356	7883823506	9459735225	26501854071
	240WI	6421782173	121850723	10864212587	9585723343	23716264875
	6CI	8130903885	3250238	3042416675	15332914382	20738907909
	12CI	8046370871	2453545	3447198832	15362569632	21622690312
	30CI	7863726741	2028113	3035362584	18498494200	19126739844
	60 CI	7287037607	5037991	3062386653	15885342027	22455269615
	240CI	6379429392	1821369	2561804192	15382120952	16873555415
	480CI	4813449726	1541719	2421398793	12132118471	10803946269
	1440CI	3853411234	844402	2906753023	9919168894	12190073903
Heart 4	Control	1.07E+10	NF	7.61E+09	2.34E+10	3.66E+10
	6WI	9.96E+09	3.07E+07	9.97E+09	2.22E+10	2.85E+10
	12WI	1.01E+10	9.56E+07	1.17E+10	2.15E+10	3.23E+10
	30WI	9.54E+09	1.26E+08	1.27E+10	1.71E+10	2.92E+10
	60WI	9.55E+09	2.49E+08	1.09E+10	1.57E+10	2.63E+10
	240WI	1.15E+10	1.15E+09	1.87E+10	1.92E+10	3.55E+10
	6CI	7.96E+09	9.31E+06	7.58E+09	1.65E+10	2.83E+10
	12CI	9.06E+09	2.74E+07	7.22E+09	2.40E+10	3.28E+10
	30CI	7.35E+09	2.33E+07	4.47E+09	2.09E+10	2.92E+10
	60 CI	8.68E+09	7.77E+06	7.28E+09	2.13E+10	2.89E+10
	240CI	5.77E+09	1.37E+07	5.89E+09	1.28E+10	2.05E+10
	480CI	2.69E+09	1.48E+07	2.16E+09	7.69E+09	8.53E+09
	1440CI	1.92E+09	3.11E+07	1.98E+09	5.06E+09	7.19E+09

Appendix 3: Human LC-MS data

	sample	phenylalanine	aspartate	threonine	acetylcholine	butyryl carnitine	dihydro-thymine
Heart 1	Control	1548653913	2197358104	472717942	1140775668	557285324	54807720
	6WI	1849054064	1338218183	498962605	1079817756	1266162236	55058697
	12WI	1852918731	589043725	463595727	853192941	1532925657	67140687
	30WI	1611906441	384472676	466581208	666168639	1323506223	48466071
	60WI	2303414339	1184077173	573645340	955635888	2588019693	48501910
	240WI	3300071817	2248552781	903683498	798532469	290275209	42066085
	6CI	982257473	716995686	287610856	552232288	327706382	31104457
	12CI	1726379617	1027406308	504848079	898343807	1104178737	34978649
	30CI	1389501945	1146326231	537770441	876311496	443912820	34741674
	60 CI	1861490695	1223668145	545872378	914049035	994215057	35981646
	240CI	1667868066	830372356	500011761	906448184	1206462552	36500498
	480CI	1217375449	587826669	337841942	694383435	1446663462	31793187
Heart 2	Control	1.03E+09	1.10E+09	4.96E+08	2.23E+09	2.86E+08	6.13E+07
	6WI	8.82E+08	7.08E+08	4.51E+08	1.95E+09	1.01E+09	6.56E+07
	12WI	1.03E+09	6.65E+08	4.38E+08	2.22E+09	1.87E+09	5.38E+07
	30WI	9.60E+08	6.60E+08	3.44E+08	2.55E+09	4.05E+09	7.78E+07
	60WI	1.76E+09	1.65E+09	6.21E+08	2.74E+09	5.32E+09	7.25E+07
	240WI	6.47E+09	2.05E+08	9.74E+08	2.17E+09	1.10E+09	7.18E+07
	6CI	9.00E+08	1.53E+09	4.79E+08	1.99E+09	2.03E+08	4.19E+07
	12CI	9.18E+08	1.13E+09	4.33E+08	2.60E+09	3.06E+08	6.98E+07
	30CI	6.13E+08	8.52E+08	3.50E+08	1.70E+09	2.28E+08	2.38E+07
	60 CI	6.24E+08	5.52E+08	2.70E+08	1.38E+09	3.44E+08	7.55E+06
	240CI	5.13E+08	5.36E+08	2.36E+08	1.52E+09	4.48E+08	3.42E+07
	480CI	2.27E+08	1.37E+08	8.85E+07	6.78E+08	7.43E+08	9.19E+06
	1440CI	3.38E+08	1.30E+08	1.39E+08	6.82E+08	5.90E+08	4.71E+06
Heart 3	Control	1246069161	2000678483	468017070	1454763529	506537237	86612268
	6WI	2056710079	969502449	706539426	1438462582	2574682427	101849055
	12WI	1769051660	892677368	608320164	1536502197	3339920553	93470753
	30WI	2633334315	1211159546	620556519	1299247930	2053890469	83459139
	60WI	2715448105	1050348261	666196893	1510977544	4816654226	81441491
	240WI	12257057942	208429668	1360331061	1406249973	2158036010	72165881
	6CI	1126518404	1178613393	467736984	1433586741	599985827	68440689
	12CI	1487308948	1495881846	497453990	1388543853	774629123	80552361
	30CI	1113011371	1356393524	471534662	1426143159	599320891	51347438
	60 CI	1242100935	1155599683	481357366	1508473782	907401458	81609550
	240CI	923058396	721802035	374818048	1248211694	1314490828	59674030
	480CI	610329591	562317006	240081145	972532545	2931884807	16583874
	1440CI	613706149	215972337	265258266	1041277163	2971041631	20074900
Heart 4	Control	1.66E+09	8.39E+09	1.15E+09	1.19E+09	5.44E+08	9.58E+07
	6WI	1.32E+09	3.19E+09	1.11E+09	1.09E+09	1.07E+09	7.62E+07
	12WI	1.79E+09	3.83E+09	1.24E+09	1.11E+09	1.66E+09	8.41E+07
	30WI	2.03E+09	3.60E+09	1.24E+09	1.12E+09	1.85E+09	8.10E+07
	60WI	2.19E+09	1.88E+09	1.12E+09	9.39E+08	9.02E+08	8.95E+07
	240WI	5.79E+09	4.16E+09	1.97E+09	1.22E+09	5.81E+08	1.08E+08
	6CI	1.08E+09	4.22E+09	9.57E+08	9.63E+08	5.19E+08	8.01E+07
	12CI	1.18E+09	5.95E+09	1.15E+09	1.05E+09	7.93E+08	7.61E+07
	30CI	9.29E+08	4.37E+09	8.59E+08	9.76E+08	4.32E+08	7.68E+07
	60 CI	1.08E+09	4.11E+09	1.06E+09	9.96E+08	4.61E+08	7.49E+07
	240CI	7.51E+08	2.59E+09	6.55E+08	6.95E+08	1.56E+09	4.91E+07
	480CI	3.42E+08	1.45E+09	2.31E+08	3.64E+08	1.05E+09	1.00E+07
	1440CI	4.13E+08	5.46E+08	2.72E+08	3.26E+08	9.88E+07	7.62E+06

Appendix 3: Human LC-MS data

	sample	glyceryl phosphorylcholine	CMP	asparagine	serine	adenine	glycine
Heart 1	Control	1362466489		236984042	1383621171	1041623	653891050
	6WI	1330162281		242969790	1501799845	125611211	756633860
	12WI	1426026271		233461288	1414542096	252593983	967012736
	30WI	1110418554		208514663	1187852051	401762839	820626152
	60WI	1329195909		241327886	1551409618	380128078	1051023089
	240WI	919809940		253748187	1540264462	87069590	1052078214
	6CI	858284773		127503119	861256019	25573651	444198113
	12CI	1394939421		164496955	1183563049	134724536	705818159
	30CI	1245200155		148090351	935322106	59161744	530357106
	60 CI	1146068592		176908423	1193061286	130949854	680801401
	240CI	1323478642		162976268	1103308347	129124878	596491067
	480CI	1098746740		131448627	910172695	207645677	539013502
Heart 2	Control	2.26E+09	0.00E+00	1.56E+08	5.75E+08	1.41E+07	4.17E+08
	6WI	1.88E+09	4.21E+06	1.38E+08	4.34E+08	9.68E+07	3.32E+08
	12WI	2.34E+09	4.12E+06	1.47E+08	6.20E+08	1.59E+08	4.05E+08
	30WI	2.26E+09	2.00E+06	1.51E+08	4.50E+08	2.10E+08	3.32E+08
	60WI	2.53E+09	4.86E+05	1.45E+08	6.31E+08	3.30E+08	4.90E+08
	240WI	1.96E+09	1.08E+06	1.91E+08	9.20E+08	1.58E+08	6.33E+08
	6CI	2.20E+09	6.12E+05	8.88E+07	3.70E+08	2.43E+07	2.93E+08
	12CI	2.46E+09	2.67E+05	1.40E+08	4.32E+08	1.69E+07	2.74E+08
	30CI	1.74E+09	0.00E+00	4.50E+07	2.55E+08	4.55E+07	1.71E+08
	60 CI	1.72E+09	2.52E+05	1.65E+07	1.57E+08	1.11E+08	1.38E+08
	240CI	1.60E+09	2.00E+06	4.49E+07	2.32E+08	1.44E+08	1.46E+08
	480CI	1.14E+09	0.00E+00	7.57E+06	6.24E+07	3.50E+08	6.42E+07
	1440CI	1.04E+09	4.04E+05	7.38E+06	9.08E+07	3.52E+08	9.56E+07
Heart 3	Control	4526940268	5370719	218832375	694142319		248438822
	6WI	5823236702	11418459	213879747	1011448356		404058273
	12WI	5204830988	12056877	231736694	860051052		368500246
	30WI	4576251374	9401726	244044151	929870343		394046375
	60WI	4974754274	8381024	232543218	1005483457		464397169
	240WI	5485593359	2602731	324851496	1773536132		840979488
	6CI	4859626174	4053012	120312129	513710278		197333730
	12CI	4926359456	4085209	185401544	691413447		256203023
	30CI	5391864806	2828426	98518348	476269332		201853351
	60 CI	4936872011	2324932	145926725	530024022		191643091
	240CI	4362039730	2463595	92036663	371352913		148667620
	480CI	4616820882	1752502	29746291	200460565		127110962
	1440CI	4791303687	1898622	29587916	194137272		90130665
Heart 4	Control	4.15E+09	1.97E+06	3.03E+08	9.00E+08	1.46E+07	5.89E+08
	6WI	3.36E+09	4.26E+06	2.46E+08	7.02E+08	1.78E+08	4.97E+08
	12WI	3.57E+09	3.45E+06	2.75E+08	8.21E+08	3.24E+08	6.02E+08
	30WI	3.38E+09	2.61E+06	2.56E+08	7.97E+08	3.07E+08	6.29E+08
	60WI	1.90E+09	1.81E+06	3.08E+08	8.54E+08	2.92E+08	7.56E+08
	240WI	2.78E+09	3.66E+05	4.74E+08	1.53E+09	2.09E+08	1.89E+09
	6CI	2.88E+09	1.04E+06	1.76E+08	5.46E+08	3.73E+07	3.58E+08
	12CI	3.53E+09	1.39E+06	1.88E+08	5.96E+08	5.39E+07	3.99E+08
	30CI	2.87E+09	7.91E+05	1.68E+08	4.97E+08	7.36E+07	2.97E+08
	60 CI	3.18E+09	4.17E+05	1.82E+08	5.66E+08	5.80E+07	3.73E+08
	240CI	2.47E+09	2.39E+06	8.29E+07	3.15E+08	1.80E+08	2.39E+08
	480CI	1.84E+09	NF	1.61E+07	1.37E+08	1.73E+08	1.08E+08
	1440CI	5.69E+08	5.16E+05	1.44E+07	1.49E+08	2.42E+08	1.51E+08

Appendix 3: Human LC-MS data

	sample	GSSG	carnitine	citrulline	creatinine	choline	cytidine
Heart 1	Control	1556387	15011529074	49070268	2098671169	795490570	
	6WI	0	12238048193	52785719	853258292	5238061530	
	12WI	2791496	10590461574	46139005	788856363	4392604560	
	30WI	0	10805783106	29338660	545454706	4549537746	
	60WI	40102588	13403477324	53567423	724907121	5927475169	
	240WI	0	13055850297	37034497	803656320	14589068689	
	6CI	18999382	9632101676	25643861	532529171	1166933715	
	12CI	64298238	13215542832	37592742	731910470	3473459070	
	30CI	18145426	12889800452	29286626	700915872	1448705167	
	60 CI	50142452	11982519684	40442860	613581261	6278169357	
	240CI	63623340	12120609386	39843022	596321992	3791633348	
	480CI	53197626	9874037725	32898001	450286402	3033473143	
Heart 2	Control	2.26E+07	2.89E+10	6.18E+07	1.08E+10	2.38E+09	0.00E+00
	6WI	1.30E+06	2.03E+10	3.13E+07	1.79E+09	5.08E+09	2.85E+07
	12WI	5.71E+05	2.12E+10	5.61E+07	1.66E+09	5.52E+09	4.06E+07
	30WI	4.32E+06	2.40E+10	3.76E+07	1.48E+09	5.47E+09	3.02E+07
	60WI	5.23E+06	2.63E+10	5.46E+07	1.91E+09	6.57E+09	1.96E+07
	240WI	2.59E+06	2.68E+10	2.54E+07	1.62E+09	6.70E+09	1.78E+07
	6CI	2.04E+07	2.53E+10	2.08E+07	7.42E+09	2.61E+09	5.79E+05
	12CI	7.82E+06	3.17E+10	4.81E+07	8.09E+09	1.99E+09	0.00E+00
	30CI	1.91E+07	2.07E+10	3.74E+07	4.49E+09	1.51E+09	0.00E+00
	60 CI	2.46E+07	1.86E+10	3.09E+07	3.06E+09	2.18E+09	7.87E+05
	240CI	8.31E+06	1.98E+10	2.70E+07	1.11E+09	2.06E+09	4.66E+06
	480CI	2.73E+07	1.19E+10	9.43E+06	9.96E+08	1.48E+09	3.38E+06
	1440CI	3.21E+07	8.71E+09	7.03E+06	6.05E+08	1.26E+09	3.43E+05
Heart 3	Control	121631627	28292644750	34013552	1991817029	3765936971	2095404
	6WI	192947514	28388328571	79329875	1689864041	8308363135	38508148
	12WI	101805666	25668927818	42124873	1370753927	8957608937	55838330
	30WI	60594214	28121863740	40707294	1191135426	9782036132	15781463
	60WI	75763130	27779264706	45263272	1374672090	7694042487	17025364
	240WI	38040384	33856648050	41567991	1853243691	10737214734	28795353
	6CI	89879898	22802689435	28347038	1753051868	2590004811	4006691
	12CI	87986809	27247521981	51332308	2650206687	2885082624	3583842
	30CI	97187607	24305280077	26584851	2113247320	2476995166	5414015
	60 CI	62527442	24787898143	33970093	3452493528	3178383305	5395532
	240CI	62480754	19936427465	20356566	1395322766	2702757547	9538657
	480CI	79391891	14704511173	9462113	1879875127	2087147771	2106182
	1440CI	66082976	13436781907	17106305	1245785649	2287321860	1062545
Heart 4	Control	5.04E+07	2.61E+10	1.14E+08	2.93E+09	2.40E+09	5.70E+05
	6WI	4.52E+06	1.93E+10	4.82E+07	1.09E+09	5.95E+09	2.00E+07
	12WI	1.07E+07	2.07E+10	5.96E+07	1.25E+09	8.90E+09	2.75E+07
	30WI	4.22E+05	2.07E+10	3.79E+07	1.19E+09	1.03E+10	1.18E+07
	60WI	1.07E+06	1.91E+10	5.58E+07	9.12E+08	2.37E+10	1.98E+07
	240WI	3.64E+06	2.32E+10	1.09E+08	1.58E+09	4.28E+10	1.39E+07
	6CI	1.21E+07	1.84E+10	4.19E+07	1.02E+09	1.11E+09	5.95E+06
	12CI	1.16E+07	2.06E+10	6.40E+07	1.78E+09	1.14E+09	2.47E+06
	30CI	6.17E+06	2.27E+10	7.17E+07	1.64E+09	1.35E+09	2.43E+06
	60 CI	1.34E+07	2.04E+10	2.93E+07	4.02E+09	9.22E+08	1.23E+06
	240CI	8.29E+06	1.53E+10	3.54E+07	7.34E+08	3.26E+09	8.06E+06
	480CI	1.18E+07	1.33E+10	2.52E+07	4.01E+08	1.93E+09	4.60E+06
	1440CI	6.28E+06	1.18E+10	5.84E+06	1.94E+08	1.18E+10	4.80E+06

Appendix 3: Human LC-MS data

	sample	aminolevulinic acid	phosphoryl-choline	valine and betaine	cystine	arginino-succinate	histidine
Heart 1	Control	239428197	3972978	2167019016			186197442
	6WI	296605342	5034074	2472925088			199055973
	12WI	315563309	2599218	2321772655			160558641
	30WI	237202783	1346749	1348386221			134533689
	60WI	285006117	4697166	3004799391			213478576
	240WI	221543524	4256969	3259374363			220066553
	6CI	151979812	2028842	2124212893			103180030
	12CI	239058344	2623372	3188480142			155176400
	30CI	203305389	4937908	2672523751			126356069
	60 CI	199347089	4536466	2973648688			166131811
	240CI	210160114	4677193	2771218727			157500820
	480CI	182616984	2307649	2641265660			126221897
Heart 2	Control	5.33E+08	9.83E+06	2.40E+09	1.85E+07	2.49E+05	2.36E+08
	6WI	4.29E+08	7.13E+06	1.85E+09	7.53E+05	9.12E+04	1.90E+08
	12WI	5.23E+08	6.40E+06	2.36E+09	0.00E+00	8.33E+05	2.50E+08
	30WI	3.83E+08	1.35E+07	2.89E+09	1.99E+06	1.34E+06	2.25E+08
	60WI	5.67E+08	1.29E+07	2.89E+09	0.00E+00	1.44E+06	3.29E+08
	240WI	4.20E+08	1.13E+07	5.26E+09	3.27E+06	8.14E+06	3.86E+08
	6CI	4.77E+08	8.74E+06	2.05E+09	4.14E+06	2.60E+05	1.59E+08
	12CI	4.67E+08	8.93E+06	2.47E+09	2.82E+06	3.80E+05	2.34E+08
	30CI	3.53E+08	2.49E+06	1.82E+09	0.00E+00	1.21E+05	1.43E+08
	60 CI	3.08E+08	2.94E+06	1.94E+09	1.16E+06	1.46E+05	1.36E+08
	240CI	2.61E+08	2.83E+06	1.83E+09	2.96E+05	1.28E+05	1.27E+08
	480CI	1.17E+08	7.27E+05	2.20E+09	5.66E+05	3.44E+05	5.80E+07
	1440CI	1.37E+08	0.00E+00	2.07E+09	0.00E+00	1.11E+05	5.50E+07
Heart 3	Control	44449827	29396612	1177792831	237999	3062432	408008824
	6WI	52227903	36792215	1606184736	5138325	4697019	584696967
	12WI	52972187	36835358	1000958914	3730061	5695303	521960328
	30WI	40358973	30651597	1651321781	8186367	6260869	538512649
	60WI	52392154	34086793	1734331187	7810935	6405880	588948092
	240WI	39962764	32168822	6597234006	68477782	17923078	1054969994
	6CI	54391893	21388571	927679866	1527352	3481320	295457606
	12CI	47208357	26451785	1217767017	6334924	3141629	376758595
	30CI	58137350	20113587	977295570	512714	3063287	283574761
	60 CI	58150150	24356248	969525680	3159136	3328264	375516540
	240CI	46205982	19205029	910414441	1636166	2415867	239744601
	480CI	37455491	15268243	694472789	127463	3015448	157747438
	1440CI	30803601	10949074	791171219	1257564	2874036	173597258
Heart 4	Control	2.03E+08		8.55E+08	3.54E+06	2.65E+06	2.74E+08
	6WI	1.81E+08		5.98E+08	1.53E+06	1.75E+06	1.61E+08
	12WI	1.90E+08		1.30E+09	2.42E+06	2.98E+06	1.94E+08
	30WI	1.85E+08		1.85E+09	2.98E+06	4.04E+06	1.54E+08
	60WI	1.48E+08		1.73E+09	1.48E+07	2.74E+06	1.78E+08
	240WI	2.17E+08		4.10E+09	8.63E+07	1.48E+07	3.00E+08
	6CI	1.56E+08		7.23E+08	2.06E+06	1.52E+06	1.34E+08
	12CI	1.65E+08		5.63E+08	2.77E+06	8.73E+05	1.71E+08
	30CI	1.45E+08		4.48E+08	5.72E+05	8.79E+05	1.49E+08
	60 CI	1.68E+08		6.76E+08	6.30E+05	1.14E+06	1.45E+08
	240CI	1.01E+08		4.11E+08	1.23E+06	8.82E+05	9.47E+07
	480CI	4.53E+07		9.83E+08	4.67E+05	1.19E+05	4.40E+07
	1440CI	3.54E+07		9.56E+08	1.11E+07	NF	3.42E+07

Appendix 3: Human LC-MS data

	sample	hypotaurine	lysine	ornithine	arginine	histamine	thymine
Heart 1	Control	15911248	406560635	175505432	246764958	269907042	3583784
	6WI	10232432	491893838	190249635	322685350	251583000	2915852
	12WI	13656571	444965315	197229301	327279565	313706062	3473158
	30WI	20479584	359400047	156183568	307887368	226271848	3162354
	60WI	3358650	589604858	189703387	503273052	336617702	2355973
	240WI	9090677	986662496	171710678	1026392553	255837184	1532170
	6CI	2549070	238497036	148252231	156718992	161128101	839205
	12CI	2975978	382726300	167410729	283152454	303414526	1389499
	30CI	8716195	309041598	170793181	213532258	274577338	738720
	60 CI	4435111	444238770	177839772	358307348	222973897	1453171
	240CI	2170504	420459448	185325131	319146855	279971927	2014583
	480CI	2428133	294510673	159596347	226324495	287261220	972344
Heart 2	Control	2.55E+07	5.61E+08	1.22E+08	4.57E+08	3.25E+08	3.92E+06
	6WI	3.74E+07	4.31E+08	8.16E+07	3.87E+08	3.41E+08	3.26E+06
	12WI	2.24E+07	5.48E+08	1.04E+08	4.91E+08	3.04E+08	1.96E+06
	30WI	2.46E+07	4.83E+08	8.58E+07	4.78E+08	2.26E+08	4.39E+06
	60WI	2.89E+07	8.44E+08	1.32E+08	8.76E+08	3.40E+08	3.89E+06
	240WI	3.94E+07	1.56E+09	9.27E+07	2.10E+09	4.04E+08	4.22E+06
	6CI	4.63E+07	4.05E+08	7.77E+07	3.88E+08	2.90E+08	1.53E+06
	12CI	2.80E+07	4.87E+08	9.88E+07	4.30E+08	2.22E+08	3.99E+06
	30CI	2.75E+07	3.43E+08	7.56E+07	3.62E+08	1.87E+08	5.69E+05
	60 CI	2.60E+07	3.81E+08	8.04E+07	4.16E+08	2.71E+08	0.00E+00
	240CI	2.04E+07	2.88E+08	5.50E+07	2.90E+08	2.38E+08	1.04E+06
	480CI	1.42E+07	1.46E+08	3.13E+07	1.53E+08	1.88E+08	0.00E+00
	1440CI	1.77E+07	1.48E+08	3.32E+07	1.97E+08	3.00E+08	0.00E+00
Heart 3	Control	3511500	1016101673	171370272	1132215498	416042598	7016033.793
	6WI	2078610	1660332284	236422187	2012499358	648387410	7698672.572
	12WI	2396480	1398281072	211055248	1709076237	665192513	5610407.019
	30WI	2122224	1535668198	182598885	2268084899	536216189	5580629.125
	60WI	4659467	1696519091	209530978	2412560831	629073377	5100844.893
	240WI	2316889	4263849085	223447807	6607057637	590857833	4511132.27
	6CI	9377066	966071330	169865017	1200373762	481417156	4350952.094
	12CI	5441605	1138010565	178385921	1381217014	459050656	5990036.865
	30CI	8593019	899213815	144281369	1125426054	606275806	3090051.985
	60 CI	6991803	1102293314	166466659	1391641508	494011707	5042155.068
	240CI	12444521	804065770	122042277	1075859894	465695026	4103795.794
	480CI	17372855	574896226	84999217.6	768698732	614937107	171217.2608
	1440CI	9627826	637608175	86257458.4	900776133	474145530	204108.6418
Heart 4	Control	6.18E+07	1.14E+09	2.97E+08	7.04E+08	2.39E+08	4.68E+06
	6WI	7.32E+07	8.44E+08	2.22E+08	5.41E+08	2.00E+08	3.27E+06
	12WI	7.08E+07	1.11E+09	2.70E+08	7.83E+08	2.33E+08	3.92E+06
	30WI	7.81E+07	1.01E+09	2.12E+08	8.00E+08	2.38E+08	3.50E+06
	60WI	6.67E+07	1.12E+09	2.27E+08	9.76E+08	2.83E+08	4.99E+06
	240WI	7.12E+07	2.61E+09	3.79E+08	2.63E+09	3.63E+08	5.88E+06
	6CI	5.80E+07	7.63E+08	2.09E+08	4.83E+08	2.01E+08	2.09E+06
	12CI	6.22E+07	8.61E+08	2.15E+08	5.73E+08	3.45E+08	2.77E+06
	30CI	4.70E+07	7.84E+08	2.01E+08	4.86E+08	2.48E+08	3.02E+06
	60 CI	7.86E+07	7.66E+08	2.01E+08	5.08E+08	2.94E+08	3.32E+06
	240CI	4.90E+07	5.78E+08	1.54E+08	4.00E+08	2.57E+08	1.85E+06
	480CI	2.65E+07	3.12E+08	8.40E+07	2.16E+08	2.43E+08	NF
	1440CI	1.99E+07	3.16E+08	7.23E+07	3.13E+08	2.14E+08	NF

Appendix 3: Human LC-MS data

	sample	betaine	putrescine	ammonium and isovalerate	spermidine	pantothenic acid
Heart 1	Control		6780155	25020854	0	
	6WI		6597757	26186702	0	
	12WI		17186980	25977719	7930126	
	30WI		12789377	26797484	4239142	
	60WI		10109623	26488961	729224	
	240WI		7670426	51666965	0	
	6CI		3381827	27830496	8496384	
	12CI		7666326	29315557	83685020	
	30CI		8998706	24881420	0	
	60 CI		1485259	44407001	65118622	
	240CI		4475128	33027755	3421371	
	480CI		4940618	33060355	27448356	
Heart 2	Control		0.00E+00	5.38E+06	0.00E+00	9.43E+07
	6WI		1.83E+06	6.97E+06	0.00E+00	1.14E+08
	12WI		0.00E+00	1.04E+07	0.00E+00	1.35E+08
	30WI		0.00E+00	1.36E+07	0.00E+00	1.78E+08
	60WI		1.56E+06	1.06E+07	0.00E+00	2.43E+08
	240WI		2.77E+06	5.52E+06	4.82E+06	3.00E+08
	6CI		2.24E+06	5.90E+06	0.00E+00	1.03E+08
	12CI		4.43E+05	5.67E+06	2.36E+06	1.22E+08
	30CI		0.00E+00	6.69E+06	0.00E+00	7.24E+07
	60 CI		0.00E+00	7.35E+06	0.00E+00	7.89E+07
	240CI		0.00E+00	7.67E+06	0.00E+00	6.92E+07
	480CI		0.00E+00	1.01E+07	0.00E+00	3.81E+07
	1440CI		0.00E+00	4.99E+06	0.00E+00	3.42E+07
Heart 3	Control	2003178894	1282918	7619877		94877657
	6WI	1759582977	3109877	8355680		146902520
	12WI	2052944013	12473007	5233221		144567481
	30WI	1554443110	4270209	5225312		114581671
	60WI	2032104424	7598447	5350518		165447176
	240WI	1494761582	4292569	2774036		400341832
	6CI	2578729750	6706298	3453560		79326196
	12CI	1956858213	1890340	3638483		101627431
	30CI	2460402786	4409466	2801482		90495357
	60 CI	2605688366	3629452	4814751		103991160
	240CI	2733262028	4016346	2915588		77304442
	480CI	2413509976	896296	2401507		63754870
	1440CI	2596175691	537265	2450089		64962508
Heart 4	Control			2.26E+06	2.53E+07	1.99E+08
	6WI			5.38E+05	1.50E+07	1.69E+08
	12WI			1.73E+06	3.46E+07	2.37E+08
	30WI			1.60E+06	NF	2.19E+08
	60WI			3.84E+06	NF	2.86E+08
	240WI			7.75E+06	1.47E+05	1.04E+09
	6CI			7.68E+05	NF	1.25E+08
	12CI			5.55E+05	4.08E+06	1.57E+08
	30CI			1.26E+06	5.30E+05	1.27E+08
	60 CI			7.76E+05	7.25E+05	1.38E+08
	240CI			7.74E+05	2.36E+07	1.06E+08
	480CI			2.21E+06	NF	5.38E+07
	1440CI			NF	NF	9.19E+07

Appendix 3: Human LC-MS data

	sample	cytosine	dihydro-orotate	2-HG	2-succinyl cysteine	malate
Heart 1	Control	0		132267400		1.16E+09
	6WI	7505289		146929476		2.50E+09
	12WI	22981288		158963137		2.14E+09
	30WI	6065123		98166017		7.08E+08
	60WI	3232887		148211541		1.52E+09
	240WI	1491982		56257068		1.74E+09
	6CI	657626		88374959		8.58E+08
	12CI	623368		150481857		2.11E+09
	30CI	1312228		108895812		1.80E+09
	60 CI	1457525		111623464		2.28E+09
	240CI	1298461		146715643		3.52E+09
	480CI	4905190		119391825		1.36E+09
Heart 2	Control					
	6WI					
	12WI					
	30WI					
	60WI					
	240WI					
	6CI					
	12CI					
	30CI					
	60 CI					
	240CI					
	480CI					
	1440CI					
Heart 3	Control	6767533			3221800	
	6WI	24222438			2729268	
	12WI	35235959			2969629	
	30WI	14554036			2749603	
	60WI	12322305			1801893	
	240WI	16868650			3154628	
	6CI	6071483			3445758	
	12CI	5616832			2828020	
	30CI	6912572			4901090	
	60 CI	5109636			2454966	
	240CI	8969093			2297073	
	480CI	1995060			2026617	
	1440CI	1601347			2330184	
Heart 4	Control	1.42E+06	NF	1.42E+08	9.91E+05	
	6WI	8.53E+06	NF	1.05E+08	6.05E+05	
	12WI	8.99E+06	NF	1.05E+08	4.28E+05	
	30WI	3.27E+06	NF	1.06E+08	9.70E+05	
	60WI	4.34E+06	4.81E+05	6.66E+07	NF	
	240WI	1.23E+06	5.49E+06	8.03E+07	4.78E+06	
	6CI	1.76E+06	NF	1.21E+08	6.81E+05	
	12CI	3.98E+05	NF	1.11E+08	7.81E+05	
	30CI	7.90E+05	NF	1.06E+08	3.48E+05	
	60 CI	7.72E+05	NF	1.15E+08	7.97E+05	
	240CI	2.70E+06	NF	7.30E+07	3.04E+05	
	480CI	9.09E+05	NF	3.58E+07	2.15E+05	
	1440CI	9.01E+05	NF	3.18E+07	2.20E+05	